Université d'Ottawa · University of Ottawa

Université d'Ottawa · University of Ottawa

FACULTÉ DE ÉTUDES SUPÉRIEURES ET POSTDOCTORALES

FACULTY OF GRADUATE AND POSTDOCTORAL STUDIES

Patrick BAZINET

AUTEUR DE LA THÈSE - AUTHOR OF THESIS

Ph.D. (Chemistry)

GRADE - DEGREE

Department of Chemistry

FACULTÉ, ÉCOLE, DÉPARTEMENT - FACULTY, SCHOOL, DEPARTMENT

TITRE DE LA THÈSE - TITLE OF THE THESIS

Diaminonaphthalene and Guanidine as Scaffolds for ∏-Conjugated Amido Ligands : Versatile Supporting Frameworks for Transition and Main group Element

D. Richeson

DIRECTEUR DE LA THÈSE - THESIS SUPERVISOR

CO-DIRECTEUR DE LA THÈSE - THESIS CO-SUPERVISOR

EXAMINATEURS DE LA THÈSE - THESIS EXAMINERS

S. Barry

K. Fagnou

D. Fogg

P. Power

J.-M. De Koninck, Ph.D.

LE DOYEN DE LA FACULTÉ DES ÉTUDES SUPÉRIEURES ET POSTDOCTORALES

DEAN OF THE FACULTY OF GRADUATE AND POSTDOCTORAL STUDIES

Diaminonaphthalene and Guanidine as Scaffolds for π-Conjugated Amido Ligands: Versatile Supporting Frameworks for Transition and Main Group Elements

Patrick R. Bazinet

Thesis submitted to the
Faculty of Graduate and Postdoctoral Studies
in partial fulfillment of the requirements for the degree of

Doctorate in Philosophy
in
Chemistry

Ottawa-Carleton Chemistry Institute
University of Ottawa

Candidate
Patrick R. Bazinet

Supervisor
Professor Darrin Richeson

Your file Votre référence
ISBN: 0-494-01671-X
Our file Notre référence
ISBN: 0-494-01671-X

Dedicated to my Parents

From day one their love and support has been a constant force I knew would be with me no matter where, when or what. I am forever grateful for all of their hard work, sacrifices and dedication.

Acknowledgements

For the longest time my career plan was equivalent to sitting in a sailboat in the middle of an ocean and waiting for a gust of wind to push it in a random direction. The winds of fate conspired to provide me with an opportunity to join the Richeson group and I have never looked back. The passion and enthusiasm for scientific research which Darrin Richeson displays on a daily basis provides ample motivation to keep a graduate student going for his many years ahead. From him I have learnt not only a large cross-section of chemistry but also a way to think, learn, teach and inspire. I have truly loved every minute of my journey through the seas of graduate school and have him to thank for making it so. I now embark on a quest to show him, and the world, the enormous worth of his guidance.

The successful navigation of graduate school requires more than a supervisor and a fumehood. Many thanks to the great profs which have taught me the basics of this science, and to the administrative team for having lead me through the piles of red tape. I would like to thank Glenn Facey for helping me make sense of pulse sequences and time delays. And most of all, I am indebted to Glenn Yap for not only having solved, with great enthusiasm, the crystal structures contained within this work, but also for having the patience to teach me the basics in the art of crystallography. This thesis would surely not be the same without his many contributions.

Research is a team effort and I am enormously grateful for having worked with so many great individuals. My sincere gratitude goes out to all the post-docs, graduate and undergraduate students with whom I have spent varied lengths of time with over the years. I would specifically like to thank Steve Foley who showed me that it was possible to be a geek and a punk at the same time, Gan Ong for being such a great teammate and motivator and Jingning Shan for being the never quit competitor.

Maybe above all, I would like to thank my many friends and family who have always supported me, kept my spirits high, and with whom I have shared so many fantastic moments. From playing in my first hockey game to running my last race, every moment has been cherished and will remain with me forever.

Abstract

This work was launched with a desire to develop novel versatile amido ligands for transition and main group metals. Of utmost importance was building ligands capable of forming strong and robust metal-ligand interactions. Bidentate mono- and di-anionic amido ligands were targeted due to the advantageous effects of chelation. 1,8-Diaminonaphthalene (1,8-DAN) and guanidines were identified as target ligand platforms. The majority of this work deals with the preparation and use of 1,8-DAN based dianionic ligands for transition (Ta, Zn) and main group (B, Al, C, Ge, Sn) metals. The synthesis and reactivity of half-sandwich zirconium guanidinato compounds is also presented.

Chapter 1 presents the fundamental concepts surrounding ligand design and presents our rationale for choosing to investigate diamidonaphthalene and guanidinate ligands.

Chapter 2 discusses the synthetic routes utilized for the preparation of both classes of ligands used further in this work. Reductive alkylation was used to introduce bulky secondary alkyl groups on the 1,8-DAN frame. The preparation of a guanidine ligand tethered to a silsesquioxane is also reported.

Chapter 3 presents our efforts in preparing high-valent Ta(V) complexes supported by 1,8-DAN based ligands. Prevalent in this work is the tendency for Ta alkyl groups to further react with the ligand via C-H activation forming a metallaaziridine. The resulting trianionic tridentate binding motif of the ligand displays remarkable robustness towards a variety of metal functional groups.

Chapter 4 deals with the 1,8-DAN framework's ability to stabilize singlet carbenes. This new class of N-Heterocyclic Carbene (NHC) possessing a perimidine core demonstrates spectroscopic and reactive characteristics resembling those of the more reactive imidazolidine based NHCs. Linking two carbenes with a *para*-xylylene bridging unit enabled the formation of a dicarbene. However, irreversible dimerization and formation of an enetetramine resulted when *ortho*-xylylene was used as a bridging unit.

Chapter 5 describes the preparation of heavier group 14 analogues of perimidine based carbenes. The solid-state structure of the stannylene analogue indicated the presence of intermolecular Sn···arene interactions which were investigated using DFT calculations.

Chapter 6 investigates the Lewis basic character of carbenes and germylenes supported by diamidonaphthalene and their potential as ligands for late transition metals. An infrared study on a carbene-rhodiumdicarbonyl compound allowed us to compare its electron-donor strength to other diaminocarbenes.

Chapter 7 discusses the use of diisopropyl-1,8-DAN as a ligand for the stabilization of coordinatively unsaturated group 13 elements. Formation of a diamidonaphthalene bridged dinuclear species was also observed.

Chapter 8 presents a spectroscopic and structural study of mono(cyclopentadienyl)zirconium guanidinato species. The ability of the guanidinate, through its flexible electronic configuration, to satisfy the electrophilicity of the metal is discussed. Reactivity towards olefins revealed that these compounds produced 1-hexene oligomers only.

Chapter 9 summarizes the work presented in this thesis and discusses how the work reveals but a sliver of the enormous potential of diamidonaphthalene ligands.

Contents

Stabilization of Low-Coordinate Metals 7

Zirconium Guanidinates 8

Denouement 9

List of Common Abbreviations

1. Chemicals and Ligands

Ar	aromatic group
Bu	butyl (^{t}Bu, *tertiary*-butyl)
Bn	benzyl
Cp	cyclopentadienyl, C_5H_5
Cp*	pentamethylcyclopentadienyl, C_5Me_5
Cp''	1,3-bis(trimethylsilyl)cyclopentadienyl, 1,3-$(Me_3Si)_2C_5H_3$
c-Hex	cyclohexyl
1,8-DAN	1,8-diaminonaphthalene, 1,8-$(NH_2)_2C_{10}H_6$
E	element
Et	ethyl
^{i}Pr	*iso*-propyl
L	ligand
M	central atom (usually a metal) in a compound
Me	methyl
NHC	N-heterocyclic carbene
PDA	*o*-phenylenediamine, 1,2-$(NH_2)_2C_6H_4$
Ph	phenyl, C_6H_5
R	alkyl or aryl group
THF	tetrahydrofuran
X	halogen

2. Miscellaneous

Å	angstrom unit, 10^{-10}m
Hz	hertz
IR	infrared
m.p.	melting point
NMR	nuclear magnetic resonance
ppm	parts per million

List of Figures

List of Tables

1 *Introduction to Ligands and Design Concepts*

I. Ligand Design

Some are of the opinion that science is over.[1] The belief being that all of the major fundamental breakthroughs and discoveries have already been made (i.e. solar system, evolution, general relativity, etc.) and all there is left to do is fill in the details. However, knowing all the details can be invaluable. For example, it is not enough to simply know that mass is a form of energy. Building a nuclear power plant that doesn't spontaneously meltdown requires some pretty detailed understanding of the process. As for chemistry it's all about control. Maybe there aren't many new ground-breaking transformations left to be discovered. However gaining fine control over reactions in order to maximize such things as chemoselectivity, atom efficiency, rates, stereochemical selectivity and other various aspects is crucial to the usefulness or practicality of a process.

---

[1] For two opposite views on the subject see (a) Horgan, J. *The End of Science: Facing the Limits of Knowledge in the Twilight of the Scientific Age*; New York: Broadway Books, 1997. (b) Maddox, J. R. *What Remains to Be Discovered: Mapping the Secrets of the Universe, the Origins of Life, and the Future of the Human Race*; New York: Martin Kessler Books, 1998.

Metal-based catalysis has taken an important role in many fields of chemistry. Its goals are to provide routes to reactions, which if un-catalyzed are inaccessible, or to render existing processes easier, faster and more selective. A basic approach to achieving these goals is to exert some control over the structure of the reactive site at the metal centre. The ability to alter the electronic properties of the metal can also provide some control over the reactivity of the metal complex.

Ligand design is the construction and utilization of organic fragments that, when bound to a particular metal, will influence the reactivity of interest in a specific manner to achieve a pre-defined goal. As a general rule, the greater the need for control, the more specific are the required metal-ligand interactions. The implication is that every unique process has an ideal ligand set of unique composition and structure, or conversely that there is no all-purpose ligand perfect for positively influencing every reaction.

Be that as it may, there are specific examples of ligands which stand out for being particularly useful throughout a wide cross-section of inorganic chemistry. Carbon monoxide (CO) is a neutral ligand that forms strong bonds particularly with late transition metals. The strength of the metal-ligand interaction stems from CO being a moderate σ-donor and an exceptional π-acid. Thus electron rich metals capable of back-donation into the CO anti-bonding orbital essentially form double bonds with CO. This explains the propensity for CO to bond to late metals possessing several d-electrons.

Olefins are also good ligands for late transition metals, showing weaker but similar σ-donor and π-acid behaviours. Ligands possessing more than one olefin available for metal binding, such as 1,5-cyclooctadiene (cod), benefit from the combined interactions of both binding moieties, termed the chelate effect.

The cyclopentadienyl anion (Cp) has demonstrated an unparalleled capacity for binding to transition metals. It possesses the carbanion's pair of electrons in addition to two neutral olefins which are all available for donation to a metal. There is also a set of empty anti-bonding orbitals with appropriate geometry for participating in back-bonding interactions. However, on its own the very electron donating nature of the Cp ligand results in extremely strong metal-ligand bonding and Cp ligands are found throughout all of the

transition metals regardless of their capacity to engage in back-bonding. The discovery[2] and characterization[3] of the unprecedented bonding of the Cp ligand in ferrocene (Cp_2Fe) generated a groundswell of interest catapulting inorganic chemistry into a growth phase that has yet to show signs of stalling.

Understanding that there is not one perfect ligand for every situation fuels the continual efforts to find new ligands. The underlying goal of this thesis project is to develop new ligand scaffolds that would be appropriate for making strong bonding interactions with a wide selection of metals and to explore their coordination chemistry. Considering that there are a limited number of possible metal-ligand interactions, the new ligand should possess some unique structural or electronic trait thereby generating novel metal complexes with distinctive properties.

When contemplating possible candidates for new ligand scaffolds, we would be remiss to neglect common features found amongst the most useful ligands. Lewis basicity allows ligands to be good electron donors, resulting in strong stable bonds. Chemical stability minimizes unwanted side reactions with substrates, permitting the ligand to perform an ancillary or spectator role. Variability of the structure within a ligand class provides opportunity for small adjustments, leading to optimization of the ligand's influence on the metal complex.

The Cp ligand possesses all of these properties partly explaining its overwhelming presence in organometallic chemistry. Alkyl anions are very basic and interact with many metals to make strong bonds. The delocalized nature of the Cp anion reduces the localized charge, tempering its capacity to get involved in subsequent transformations. This contrasts with the reactivity of typical alkyl ligands whose propensity to undergo transformation forms the cornerstone of insertion polymerization. Conjugation also introduces additional binding opportunities for Cp ligands and allows it to take advantage of chelation effects. Also, Cp can be easily derivatized to yield Cp ligands with almost limitless structural variations. The

---

[2] (a) Kealy, T. J.; Pauson, P. L. *Nature* **1951**, *168*, 1039-1040. (b) Miller, S. A.; Tebboth, J. A.; Tremaine, J. F. *J. Chem. Soc.* **1952**, 632-635.

[3] (a) Fischer, E. O.; Pfab, W. *Z. Naturforschung* **1952**, *7 b*, 377-379. (b) Wilkinson, G.; Rosenblum, M.; Whiting, M. C.; Woodward, R. B. *J. Am. Chem. Soc.* **1952**, *74*, 2125-2126. Note, E. O. Fischer and G. Wilkinson won the chemistry Nobel prize in 1973 for their work on sandwich compounds. See http://www.nobel.se/chemistry/laureates/1973/index.html for more details.

pentamethyl derivative (Cp*) is one particularly noteworthy example. It is substantially larger in size, it is more electron donating, and methyl groups replace the somewhat reactive aromatic protons.

Carboxylates have been used as ligands throughout the periodic table. The delocalized anionic charge makes them very stable. The presence of superfluous lone-pairs offers flexibility in the electronic configuration permitting carboxylates to exhibit many different binding modes such as monodentate, bidentate, and bridging. Carboxylates suffer however from the lack of variability in their electron donating properties and the lack of steric bulk near the donor atoms limits the structural influence of the ligands.

Related to carboxylates, the β-diketonate ligands (commonly referred to as acetylacetonates (acac) are oxygen based ligands with a conjugated framework allowing for charge delocalization between two donating atoms. As well, they show varied bonding modes and form strong bonding interactions with metals across the entire periodic table. They also suffer from the same disadvantages in that the sterics are removed from the donating atom and the donating power of the ligand is difficult to alter.

Chart 1.1

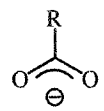

Carboxylate

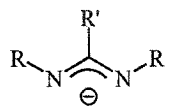

Amidinate

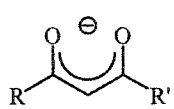

Acetylacetonate

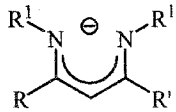

β-Diketiminate

Inorganic chemists in a perpetual search for useful ligands have not failed to notice the advantages of the aforementioned ligands. Seeing an opportunity for improvement, nitrogen analogues of the carboxylates and β-diketonates were investigated as ligands. Amidinates[4] and β-diketiminates[5] have been relatively recent examples of useful ligands for a variety of applications. Exchanging the oxygen atom for nitrogen introduces a second substituent group directly on the donor atom. The second group is not integrated in the conjugated framework and thus can easily be modified, introducing an opportunity for structural variability. The proximity of the substituent to the metal is also very beneficial as it

[4] See recent reviews: (a) Barker, J.; Kilner, M. *Coord. Chem. Rev.* **1994**, *133*, 219-300. (b) Edelmann, F. T. *Coord. Chem. Rev.* **1994**, *137*, 403-481. and references therein.
[5] See recent review: Bourget-Merle, L.; Lappert, M. F.; Severn, J. R. *Chem. Rev.* **2002**, *102*, 3031-3065. and references therein.

maximizes the influence the ligand structure has on the geometry of the metal centre. Nitrogen anions are more basic than their O-analogues making them stronger electron donors (for both σ- and π-donation). They are also generally more reactive but charge delocalization within the ligand framework can help minimize unwanted transformations of the N-based ligands.

Understanding all of the advantages and deficiencies of the previously discussed examples helped to lay out certain guidelines for the design of new ligands. Nitrogen based ligands offer more control over the steric impact of the ligand than do oxygen based species. The presence of at least two donating atoms presents the opportunity for chelation which increases the overall strength of the metal-ligand interaction. Incorporating a π-system for charge delocalization is essential for tempering the reactivity of amido ligands. Choosing a rigid backbone can help impart a very specific structure providing more control over the steric influences.

A. 1,8-diamidonapthalenes as ligands

Chart 1.2

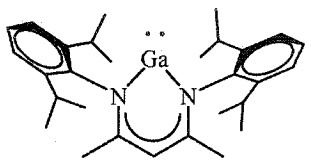

The β-diketiminate class of ligands (NacNac) have been key players in some very interesting and recent chemistry.[5] An elegant example is the use of a bulky β-diketiminate as a supporting ligand for low-valent group 13 compounds. Preparation of the intriguing Ga^{I} carbene analogue (Chart 1.2) demonstrates the impact of the ligand features discussed earlier.[6] The anionic charge is completely delocalized resulting in symmetric bonding of both nitrogens to gallium. The large aromatic substituents are oriented towards the metal, providing sufficient steric protection and preventing the aggregation of the molecule, enabling the structural characterization of such heretofore unknown species.

Inspired by the apparent success of β-diketiminates we undertook the design of a ligand which would be similar in structure and electronic configuration but would instead carry a dianionic charge. The additional negative charge would allow us to extend the existing NacNac chemistry to metals possessing higher oxidation states, and would provide the opportunity to explore applications inaccessible to monoanions.

---

[6] Hardman, N. J.; Eichler, B. E.; Power, P. P. *Chem. Commun.* **2000**, 1991-1992.

Amongst easily available diamines of appropriate composition for satisfying the above-mentioned criteria, 1,8-diaminonaphthalene (1,8-DAN) stands out as a prime candidate. Its amino groups are aligned in a manner favouring chelation to a metal centre. The fused aromatic backbone provides both rigidity and a π-system capable of charge delocalization. The orientation of the N-substituents is favourable for steric protection of a chelated metal centre, and the size and shape of the substituents can be varied providing an opportunity for optimization. Upon chelation the N lone-pairs would be aligned for π-donation to the metal and allow for a fluxional electronic interaction.

Chart 1.3

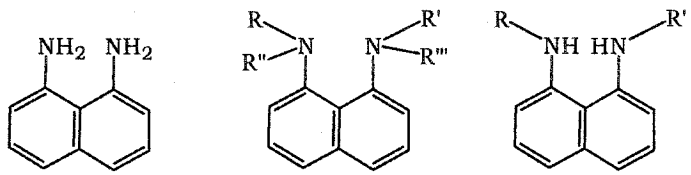

A **B** **C**

Of course the use of 1,8-DAN as a ligand platform has not completely eluded chemists and there are precedents for its use in coordination chemistry. However the number of examples where 1,8-DAN functions as a dianionic ligand seems inappropriately scant. The unsubstituted diamine 1,8-DAN can obviously, in its own right, be used as a ligand. Recent examples of this include the formation of diamidonaphthalene bridged diiridium complexes,[7] a bridged trimetallic magnesium cage,[8] chelated ruthenium[9] and platinum[10] complexes, bridged dinuclear rhodium complexes,[11] ligated osmium carbonyl clusters,[12] and some chelated boron complexes.[13]

---

[7] (a) Jiménez, M. V.; Sola, E.; Francisco, A. C.; Oro, L. A.; Lahoz, F. J.; Martínez, A. P. *Inorg. Chim. Acta* **2003**, *350*, 266-351. (b) Jiménez, M. V.; Sola, E.; Egea, M. A.; Huet, A.; Francisco, A. C.; Lahoz, F. J.; Oro, L. A. *Inorg. Chem.* **2000**, *39*, 4868-4878.

[8] Clegg, W.; Horsburgh, L.; Mulvey, R. E.; Rowlings, R. *Chem. Commun.* **1996**, 1739-1740.

[9] Nachtigal, C.; Al-Gharabli, S.; Eichele, K.; Lindner, E.; Mayer, H. A. *Organometallics* **2002**, *21*, 105-112

[10] Umapathy, P.; Harnesswala, R. A.; Dorai, C. S. *Polyhedron*, **1985**, *4*, 1595-1602.

[11] Matsuzaka, H.; Kamura, T.; Ariga, K.; Watanabe, Y.; Okubo, T.; Ishii, T.; Yamashita, M.; Kondo, M.; Kitagawa, S. *Organometallics* **2000**, *19*, 216-218.

[12] Cabeza, J. A.; Nöth, H.; Rasales-Hoz, M. de J.; Sánchez-Cabrera, G. *Eur. J. Inorg. Chem.* **2000**, 2327-2332.

[13] (a) Maruyama, S.; Kawanishi, Y. *J. Mater. Chem.* **2002**, *12*, 2245-2249. (b) Kaupp, G.; Naimi-Jamal, M. R.; Stepanenko, V. *Chem. Eur. J.* **2003**, *9*, 4156-4160. (c) Caserio, Jr., F. F.; Cavallo, J. J.; Wagner, R. I. *J. Org. Chem.* **1961**, *26*, 2157-2158. (d) Chissick, S. S.; Dewar, M. J. S.; Maitlis, P. M. *J. Am. Chem. Soc.* **1961**, *83*, 2708-2711.

Chart 1.4

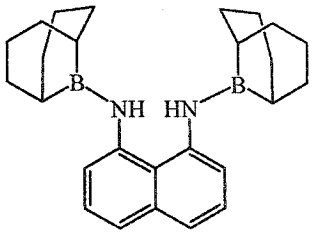

D

The fully substituted 1,8-DAN derivatives, especially 1,8-bis(dimethylamino)naphthalene ("proton sponge"), have displayed a unique ability to accept protons, and demonstrate unusually strong basicity for diamines.[14] They have also been employed as neutral chelating diamines for metals[15] but the lack of anionic charge limits their use.

More appealing is the use of N,N'-disubstituted 1,8-DAN (**C**) as a dianionic ligand. At the onset of this work there were very few examples of metal complexes incorporating dianionic ligands **C** (Chart 1.3). The bis(silyl) derivative (R = R' = $SiMe_3$) was first used to prepare a Sn^{II} compound in the mid-seventies,[16] and only very recently began to receive attention as an ancillary dianionic ligand.[17] A more exotic version is the bis(borylated) derivative **D** (R = R' = 9-borabicyclo[3.3.1]nonane (9-BBN), Chart 1.4) which was used to prepare a Ti complex.[18] However, the borylated derivative suffers from unwanted side-reactions involving the transformation of the ligand due to a labile B-N bond.

The importance of having a robust ligand structure cannot be overstated. The ideal N-substituent would be carbon based providing a sturdy C-N linkage preventing unfavourable rearrangements. To our knowledge, prior to 1999 (the birth date of this project), there were no reports using bis(alkyl) or bis(aryl) 1,8-DAN as dianionic ligands for

---

[14] Alder, R. W. *Chem. Rev.* **1989**, *89*, 1215-1223.

[15] (a) A lithium complex is reported in: Lucht, B. L.; Bernstein, M. P.; Remenar, J. F.; Collum, D. B. *J. Am. Chem. Soc.* **1996**, *118*, 10707-10718. (b) a Mn(II) complex reported in: Farzaneh, F.; Majidian, M.; Ghandi, M. *J. Mol. Catal. A* **1999**, *148*, 227-233. (c) Cu(II) complexes reported in: Collman, J. P.; Zhong, M.; Zhang, C.; Costanzo, S. *J. Org. Chem.* **2001**, *66*, 7892-7897. (d) A few B(III) complexes have been prepared and will be covered in more detail in Chapter 7.

[16] Schaeffer, Jr., C. D.; Zuckerman, J. J. *J. Am. Chem. Soc.* **1974**, *96*, 7160-7162.

[17] For Ti and Zr compounds see: (a) Lee, C. H.; La, Y.-H; Park, S. J.; Park, J. W. *Organometallics* **1998**, *17*, 3648-3655. (b) Lee, C. H.; La, Y.-H; Park, J. W. *Organometallics* **2000**, *19*, 344-351. (c) Nomura, K.; Naga, N.; Takaoki, K.; Imai, A. *J. Mol. Catal. A: Chem.* **1998**, *130*, L209-L213. (d) Nomura, K.; Naga, N.; Takaoki, K. *Macromolecules* **1998**, *31*, 8009-8015. (e) Nomura, K.; Oya, K.; Imanishi, Y. *Polymer* **2000**, *41*, 2755-2764. For Ta see: Decams, J. M.; Daniele, S.; Hubert-Pfalzgraf, L. G.; Vaissermann, J.; Lecocq, S. *Polyhedron* **2001**, *20*, 2405-2414. For Tl and In see: (f) Hellmann, K. W.; Galka, C.; Gade, L. H.; Steiner, A.; Wright, D. S.; Kottke, T.; Stalke, D. *Chem. Commun.* **1998**, 546-550. (g) Hellmann, K. W.; Galka, C. H.; Rüdenauer, I.; Gade, L. H.; Scowen, I. J.; McPartin, M. *Angew. Chem., Int. Ed.* **1998**, *37*, 1948-1951. (h) Gade, L. H.; Galka, C. H.; Hellmann, K. W.; Williams, R. M.; De Cola, L.; Scowen, I. J.; McPartlin, M. *Chem. Eur. J.* **2002**, *8*, 3732-3746. For Mg see: Galka, C. H.; Trösch, D. J. M.; Rüdenauer, I.; Gade, L. H.; Scowen, I.; Partlin, M. *Inorg. Chem.* **2000**, *39*, 4615-4620.

[18] Bar-Haim, G.; Shach, R.; Kol, M. *Chem. Commun.* **1997**, 229-230.

main-group or transition metals.[19] Considering its anticipated potential as a versatile ligand platform, we set forth with the goal of developing the coordination chemistry of diamido ligands derived from 1,8-diaminonaphthalene, with a particular focus on using derivatives possessing robust N-substituent groups.

B. Mono- and Di-anionic Guanidinates as Ligands

There exists a substantial body of work on utilizing amidinates as ancillary ligands and the early reports mainly consist of formamidinate ($[RNC(H)NR']^-$) and benzamidinate ($[RNC(C_6H_5)CR']^-$) ligand derivatives.[4] Improvements in the preparative routes to amidines has led to some more intricate and diverse examples such as chiral *trans*-cyclohexane-linked bis(amidinates)[20] and very bulky terphenyl derivatives.[21] Particularly, amidinates have enjoyed success as ancillary ligands for olefin polymerization catalysts. Transition-metal-free polymerization of ethylene was achieved with the use of aluminum monoamidinate precatalysts[22] and half-sandwich group 4 amidinate complexes show an impressive capability for the stereospecific living Ziegler-Natta polymerization of various α-olefins.[23]

Although guanidinates are structurally analogous, they have received substantially less attention as ancillary ligands.[24] Like amidinates, they are carboxylate analogues. They are bidentate ligands possessing a π-system capable of delocalizing an anionic charge. However, the presence of the additional amine functionality provides the opportunity for added bonding motifs and the possibility for carrying an extra anionic charge (R' or R'' = H). The possibility of all three nitrogens assuming an sp^2-hybridization and participating in the π-system of the ligand also introduces novel electronic configurations inaccessible to amidinates.

---

[19] Shortly after the commencement of the project a Sn(II) compound was reported, and will be discussed in Chapter 5.

[20] (a) Hagadorn, J. R.; Arnold, J. *Angew. Chem., Int. Ed.* **1998**, *37*, 1729. (b) Whitener, G. D.; Hagadorn, J. R.; Arnold, J. *J. Chem. Soc., Dalton Trans.* **1999**, 1249-1255.

[21] (a) Schmidt, J. A. R.; Arnold, J. *Chem. Commun.* **1999**, 2149-2150. (b) Abeysekera, D.; Robertson, K. N.; Cameron, T. S.; Clyburne, J. A. C. *Organometallics* **2001**, *20*, 5532-5536.

[22] Jordan, R. F.; Coles, M. P. *J. Am. Chem. Soc.* **1997**, *119*, 8125-8126.

[23] Jayaratne, K. C.; Sita, L. R. *J. Am. Chem. Soc.* **2000**, *122*, 958-959.

[24] See recent review: Bailey, P. J.; Pace, S. *Coord. Chem. Rev.* **2001**, *214*, 91-14. and references therein.

Our general interest in rigid chelating N-based ligands possessing conjugated π-orbitals attracted our attention to guanidinates. Our main interests lie in the possibility of exploiting the flexible electron donating properties of guanidinates as ancillary ligands. More precisely we desired to investigate the electronic effects of guanidinate ligands on the reactivity of group 4 transition metals. This work targeted the preparation of group 4 guanidinate complexes and characterization of the reactive properties of such compounds.

Chart 1.5

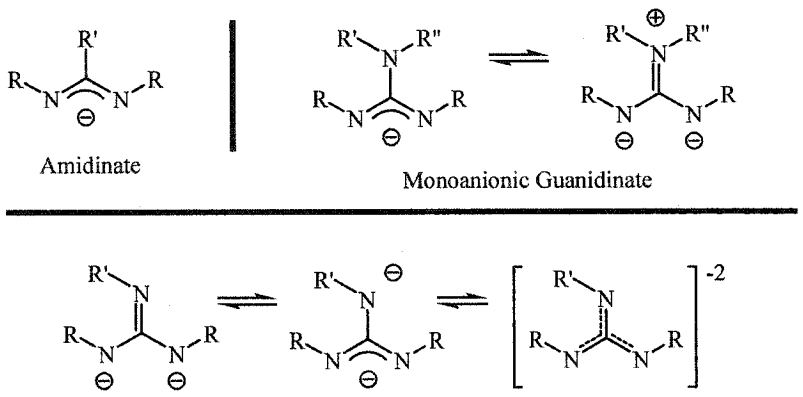

Guanidinato complexes of the group 4 metals have been reported previously. Examples include bis(guanidinate) metal alkyls which show some activity towards the polymerization of olefins,[25] and guanidinate supported metal imides showing the ability to catalyze the hydroamination of alkynes and carbodiimides, as well as the metathesis of C=N bonds.[26] Also bis(guanidinate) Ti(IV) compounds have been reduced to intermediate d^2 species which subsequently activate dinitrogen.[27]

Despite the successes, guanidinate ligands have also been shown to undergo spontaneous transformations.[26b,28] Our approach was to blend the properties of the stabilizing Cp ligands commonplace in group 4 chemistry, with the more fluxional donating properties of guanidinates. We set out to synthesize metal complexes containing two

[25] Duncan, A. P.; Mullins, S. M.; Arnold, J.; Bergman, R. G. *Organometallics* **2001**, *20*, 1808-1819.
[26] (a) Ong, T.-G.; Yap, G. P. A.; Richeson, D. S. *Organometallics* **2002**, *21*, 2839-2841. (b) Ong, T.-G.; Yap, G. P. A.; Richeson, D. S. *J. Am. Chem. Soc.* **2003**, *125*, 8100-8102. (c) Ong, T.-G.; Yap, G. P. A.; Richeson, D. S. *Chem. Commun.*, **2003**, 2612-2613.
[27] Mullins, S. M.; Duncan, A. P.; Bergman, R. G.; Arnold, J. *Inorg. Chem.* **2001**, *40*, 6952-6963.
[28] Thirupathi, N.; Yap, G. P. A.; Richeson, D. S. *Chem. Commun.*, **1999**, 2483-2484.

ancillary ligands, one being a Cp (or derivative) and the other a guanidinate, and to investigate the structural features and chemical properties of such compounds.

II. Prelude to Thesis Results

The goals of this thesis project can be divided into two broad categories. The primary goal focused on the preparation and development of N,N'-disubstituted-1,8-diaminonaphthalene as a potentially versatile novel ligand platform. The secondary goal was to extend transition metal guanidinate chemistry by preparing group 4 metal complexes containing both cyclopentadienyl and guanidinate ligands.

The lack of existing synthetic procedures for the preparation of disubstituted 1,8-DAN ligands demanded that useful preparative methods for this class of compounds be developed. In order to simplify the subsequent chapters, the methodology for preparing N,N'-dialkyl derivatives of 1,8-DAN will be presented in Chapter 2. Also contained in this chapter is an overview of synthetic routes to guanidine and guanidinates, which are used for the preparation of the targeted group 4 compounds (discussed further along in the work (Chapter 8)).

Chapter 3 describes the reaction of the parent diamine ligand or the dilithium salt of N,N'-diisopropyl-1,8-DAN with an organometallic Ta(V) species. The characterization of the synthesized compounds and further reactivity towards various substrates are presented. The work is intended to be an exploration of the use of 1,8-DAN ligands with early transition metals.

In Chapter 4 we show how the 1,8-DAN scaffold can be used to prepare stable singlet carbenes. Several derivatives of mono- and di-carbenes are prepared and studied. The formation of α-diaminoethers and an enetetramine demonstrates the reactive characteristics of this class of carbenes. This work highlights the structural and electronic differences between 1,8-DAN and other diamine frames for the stabilization of carbenes.

The use of 1,8-diamidonaphthalene ligands for the stabilization of heavier group 14 carbene analogues is presented in Chapter 5. Stable diamidogermylenes are synthesized and some preliminary reactivity for these compounds is presented. The observation of Sn···arene

interactions in the solid-state structure of the prepared diamidostannylene is investigated using theoretical calculations.

Chapter 6 contains examples where the aforementioned carbene, and the heavier Ge analogue, are utilized as neutral Lewis basic ligands for late transition metals. The prepared complexes show signs of significant steric strain and an IR study of Rh carbonyl stretching frequencies allows us to quantify the electron donating properties of the novel carbene ligands. This work illustrates the key structural and electronic properties of 1,8-DAN stabilized carbenes and the Ge analogue.

In Chapter 7 we extend the preparation of low-valent, low-coordinate compounds to group 13 elements. These compounds show a variety of structures and 1,8-diamidonaphthalene bridged bimetallic species are observed.

Chapter 8 discusses the synthetic routes to mono-cyclopentadienyl zirconium guanidinate species. The fluxional ligating behaviour of the guanidinates is investigated through variable-temperature NMR experiments. Dialkyl derivatives are screened for the polymerization of α-olefins.

The thesis project taken as a whole serves to show how rigid N-based chelating amido ligands are useful, versatile ligands capable of contributing to fields ranging from high-valent early transition metal amido chemistry to stabilization of low-valent carbon atoms as nucleophilic carbenes.

2 Ligand Syntheses

I. Introduction

The rational design of new dianionic ligands based on 1,8-DAN requires the preparation of disubstituted derivatives of the diamine (**C**). At the onset of this project, there were only a few examples of such compounds used as ligands in the literature. All of the reports presented 1,8-diamidonaphthalene ligands possessing heteroatom based substituents on the nitrogen atoms.[1] A silylated derivative (**C**; R = R' = $SiMe_3$) was first reported three decades ago[2] and only a few subsequent examples have followed. The lack of examples using this ligand is somewhat surprising and suggests that its chemistry might not be as straightforward as anticipated. Precedent for unwanted reactions with a similar related ligand, N,N'-bis(trimethylsilyl)-*o*-phenylenediamine which undergoes N-$SiMe_3$ bond cleavage,[3] suggests that ligand rearrangements might have been responsible for the limited applications of bis(silylated) 1,8-DAN derivatives.

---

[1] Chapter 1 presents a thorough summary of 1,8-DAN used for ligation.
[2] Schaeffer, C. D., Jr.; Zuckerman J. J. *J. Am. Chem. Soc.* **1974**, *96*, 7160.
[3] (a) Cameron, T. M.; Ortiz, C. G.; Ghiviriga, I.; Abboud, K. A.; Boncella, J. M. *J. Am. Chem. Soc.* **2002**, *124*, 922-923. (b) Decams, J. M.; Daniele, S.; Hubert-Pfalzgraf, L. G.; Vaissermann, J.; Lecocq, S. *Polyhedron* **2001**, *20*, 2405-2414.

More recently boryl substituents were introduced onto the DAN framework (**D**; Chart 1.4) and a few coordination compounds were prepared.[4] However the presence of a coordinatively unsaturated boron atom and a labile B-N bond leads again to unwanted transformations of the ligand, leading to B-N bond cleavage. Ideally, the ligand would possess substituents that are robust and inert to substitution or cleavage. Carbon-based substituents would provide strong, stable C-N bonds to the diamine frame minimizing ligand rearrangements. Dialkyl- and diaryl-1,8-DAN were therefore identified as target ligands (**C**; R, R' = alkyl, aryl).

Chart 2.1

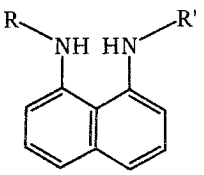

C

A literature search failed to locate any examples where dialkyl- or diaryl-1,8-DAN was prepared and used as a ligand. One reported synthesis for the preparation of dialkylated 1,8-DAN was found, however the substituents were limited to primary alkyl groups.[5] Wanting substituent groups which would provide maximum steric protection we set out to develop a synthetic methodology which would allow the preparation of ligands with at least secondary if not tertiary alkyl substituents. It was also essential that the synthetic route allow some means for varying the substituents thereby introducing some flexibility and control over the ligand structure.

II. Results

A. Substituted 1,8-Diaminonaphthalene

Initial attempts for the alkylation of 1,8-DAN using 3° or 2° alkyl halides proved unsuccessful. We attribute this to a weakly nucleophilic lone-pair on the aromatic nitrogen. The lone-pair can be partially delocalized within the extended aromatic ring, or possibly involved in intramolecular hydrogen bonding with the neighbouring amine, reducing its nucleophilic character.

---

[4] Bar-Haim, G.; Shach, R.; Kol, M. *Chem. Commun.* **1997**, 229-230.
[5] Bar-Haim, G.; Kol, M. *J. Org. Chem.* **1997**, *62*, 6682-6683.

Reductive amination is a common method for the alkylation of amines.[6] The process involves the formation of an imine, via the condensation of an amine with a carbonyl group, followed by reduction yielding a monoalkylated amine. The reaction between 1,8-DAN and ketones and aldehydes, however, does not give the anticipated diimine **E** (Scheme 2.1). Instead the product formed from this reaction is the aminal **1** (or diazaacetal). For example, reacting 1,8-DAN with a large excess of acetone yields the aminal **1a** quantitatively (Scheme

Scheme 2.1

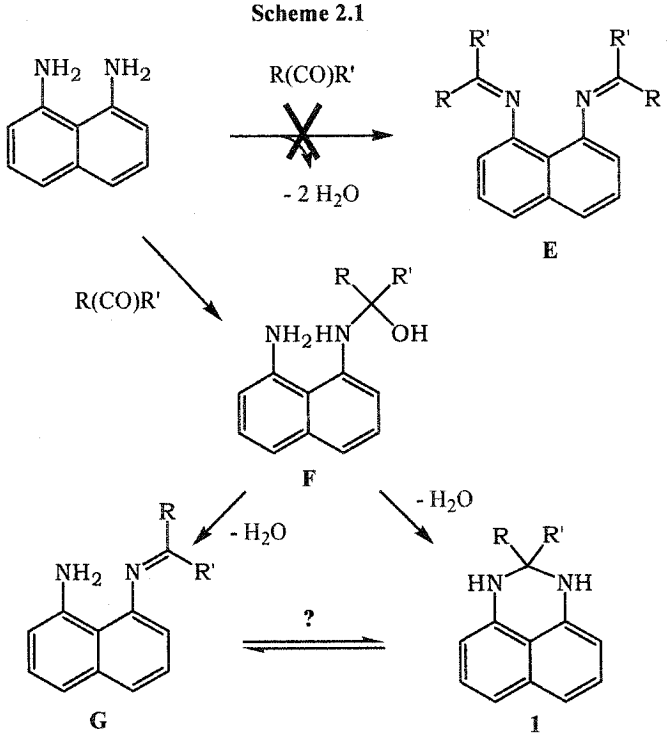

2.1). The formulation of **1a** as an aminal is based specifically on ^{13}C NMR spectroscopy and X-ray diffraction studies. The ^{1}H NMR spectrum of **1a** reveals that 1,8-DAN and acetone reacted in a 1:1 ratio and that the resulting molecule is symmetric, evidenced by a single resonance for both the *ortho* protons on the naphthyl rings, and the methyl groups. The lack of a downfield signal appropriate for an imine in the ^{13}C NMR along with the observation of a resonance for a quaternary carbon at 64.3 ppm supports the assignment of **1a** as an aminal.

An X-ray diffraction study on single crystals of compound **1a** (Table 2.1) provides definitive evidence. The molecular structure obtained from the study revealed two crystallographically unique but chemically equivalent molecules. One of the molecules is

[6] *Vogel's Textbook of Practical Organic Chemistry* 5th Ed.; Furniss, B. S., Hannaford, A. J., Smith, P. W. G., Tatchell, A. R., Eds.; Wiley: New York, 1989.

illustrated in Figure 2.1 and a list of selected bond lengths and angles is provided in Table 2.2. The most significant structural feature of **1a** is the formation of the six-membered heterocyclic ring. The CMe_2 moiety lies to one side of the naphthyl ring, rendering the methyl groups inequivalent in the solid-state structure, however the observation of a single peak in the proton NMR suggests that this structure is fluxional in solution.

The formation of aminal **1** can either arise from an isomerization of the monoimine **G**, or directly from the condensation intermediate **F** (Scheme 2.1). The existence of an equilibrium between **1** and the imine **G** can be ruled out on the basis that under reaction conditions, the imine should continue to react with acetone to yield the diimine **E**. Additionally, the ^1H NMR spectra do not show any indications of there being an isomer present.

Scheme 2.2

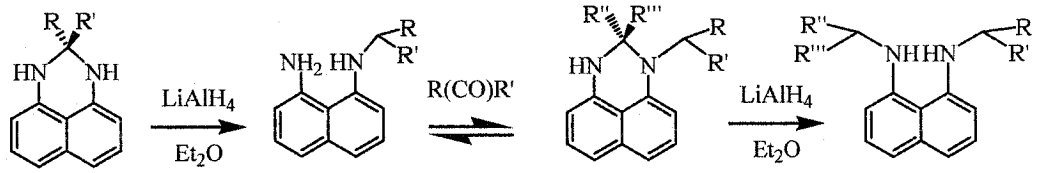

1a) R = R' = Me
1b) R-R' = C_6H_{12}

2a) R = R' = Me
2b) R-R' = C_6H_{12}

3a) R = R' = R'' = R''' = Me
3c) R = R' = Me, R''-R''' = C_4H_8

4a) R = R' = R'' = R''' = Me
4c) R = R' = Me, R''-R''' = C_4H_8

A scan of reducing agents revealed that using a large excess of $LiAlH_4$ can transform the aminal **1** into the monoalkyl-1,8-DAN derivative **2** (Scheme 2.2). This rather unusual transformation formally invokes the breaking of a C-N single bond. Alternatively, any imine generated through an isomerization, would readily react with excess reducing reagent. The exact mechanism for this reaction is not yet understood. However, it is logical to believe that the strongly basic $LiAlH_4$ reagent would deprotonate the aminal (**1**) to form an anionic intermediate. The localized negative charge could drive a rearrangement generating an imine derivative, which would be readily reduced by excess $LiAlH_4$ (Scheme 2.3).

Subsequent reaction of **2** with ketones leads again to an aminal (**3**) instead of an imine. Fortunately, the same reducing conditions that are used to transform **1** to **2**, can not only generate the dialkyl derivative, but yields exclusively the N,N'-dialkyl-1,8-DAN compound **4**. We have never observed the formation of the N,N-dialkyl-1,8-DAN isomers. At this time we do not know the exact mechanism for this transformation, however our

earlier proposed pathway is consistent with the generation of N,N'-substituted compounds. Deprotonation of aminal **3**, would drive the isomerization to an imine intermediate, which could then be reduced by excess $LiAlH_4$, generating the N,N'-substituted products exclusively. Despite the uncertainty in the mechanistic details, the developed method involves sequential addition of alkyl substituents via condensation followed by reduction, and allows for the preparation of the desired ligands with moderate to good overall yields.

Scheme 2.3

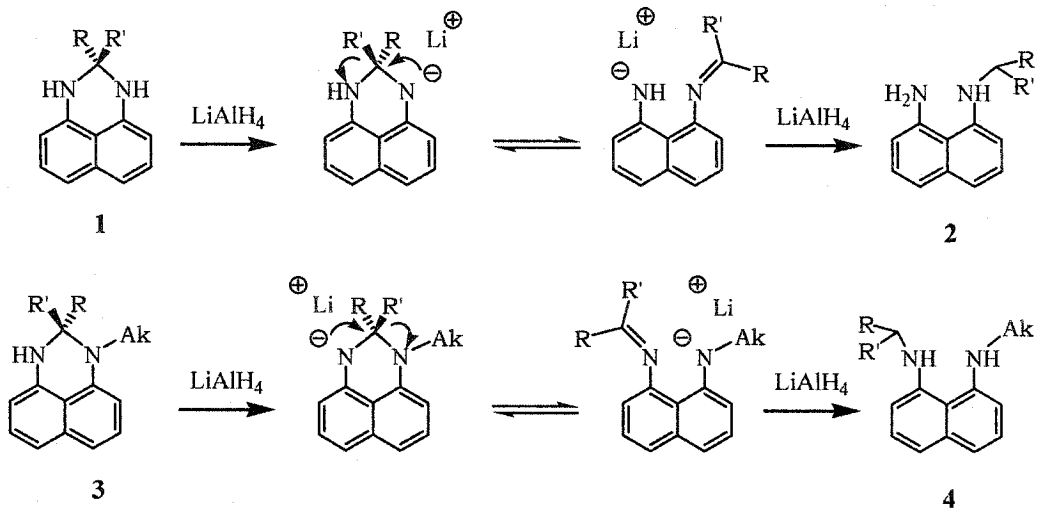

1 **2** **3** **4**

Although lengthy, the sequential nature of the method does enable us to introduce two different substituents in a very controlled manner. This prevents formation of mixtures of products, which would be difficult to separate, and leads to the desired N,N'-substituted diamines exclusively. The method also allows for the facile modification of the ligand structure in an almost limitless way due to the large variety of carbonyl compounds available. Use of a non-symmetric ketone would lead to a chiral centre after reduction, thus allowing access to chiral ligands. The preparation of chiral enantiomerically pure diamine ligands is a future goal of the research project which should allow for the preparation of chiral metal complexes and possibly catalysts for asymmetric synthesis.

B. Tri- and Tetra-Substituted Guanidines

Compared to 1,8-DAN, guanidinate ligands have received significant attention and many variations of guanidinate ligands are present in literature. The preparative methods for most of the guanidinate ligands used in this work have been reported previously, however a

general description of the synthetic routes to guanidines or guanidinates is included here to provide a more comprehensive overview of the ligand syntheses and to render the description of the organometallic chemistry of guanidinate compounds more succinct.

There are two basic variations of guanidinate ligands utilized in this project, trisubstituted and tetrasubstituted guanidinates, **H** and **I** respectively in Chart 2.2. The primary building block used in the preparation of guanidinates is a carbodiimide. The guanidine framework is constructed by either adding a neutral amine to a carbodiimide, which in return gives a neutral guanidine **5**, or by adding a deprotonated amine generating an anionic guanidinate **6** (Scheme 2.4). Addition of neutral amines to carbodiimides requires a fair amount of heating to give good yields, and the use of secondary or aromatic amines rarely gives acceptable yields of the desired products. These results are consistent with a mechanism which proceeds via nucleophilic attack of the amine on the electrophilic carbon of the carbodiimide. The increased bulk of a secondary amine or the reduced nucleophilicity of an aromatic amine would lead to much slower reactions and explains the poor yields.

Chart 2.2

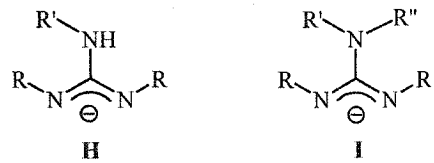

H **I**

Scheme 2.4

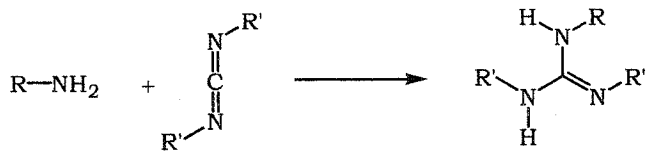

5a) R = R' = ^{i}Pr
5b) R = R' = *c*-Hex
5c) R = $CH_2CH{=}CH_2$, R' = ^{i}Pr

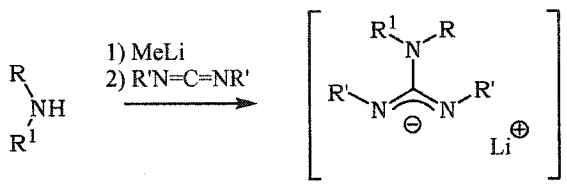

6a) R = R^1 = Me, R' = ^{i}Pr
6b) R = R^1 = $SiMe_3$, R' = ^{i}Pr
6c) R = $CH_2C_6H_5$, R^1 = ^{i}Pr , R' = ^{i}Pr

In order to circumvent this difficulty, deprotonation of a secondary amine generates a basic species which is a much stronger nucleophile. This strategy is successful in generating

tetrasubstituted guanidinates. As well, the amide base can be prepared *in situ,* eliminating the need to isolate the salt, and addition of the carbodiimide leads directly to the guanidinate salts **6**. The guanidinate salts can then be used for introducing the ligand into the coordination sphere of a main group or transition metal via salt-metathesis directly without need for isolation or purification.

Our work with guanidinate-based polymerization catalysts led us to contemplate the preparation of supported (heterogeneous) compounds. Wanting to prepare models of such compounds, we investigated tethering a guanidine to a functionalized silsesquioxane which serves as a soluble substitute for silica. The modified support features a benzyl chloride function which contains both an electrophilic carbon, and a good leaving group. Substitution of the chloride with a trisubstituted guanidinate salt yields a tetrasubstituted guanidine anchored onto the silsesquioxane, compound **5d** (Scheme 2.5). This is a somewhat rare example of guanidine alkylation. The scope of this method was not further investigated, but it does present the very interesting possibility of modifying guanidine ligands via simple S_n2 reactions.

Scheme 2.5

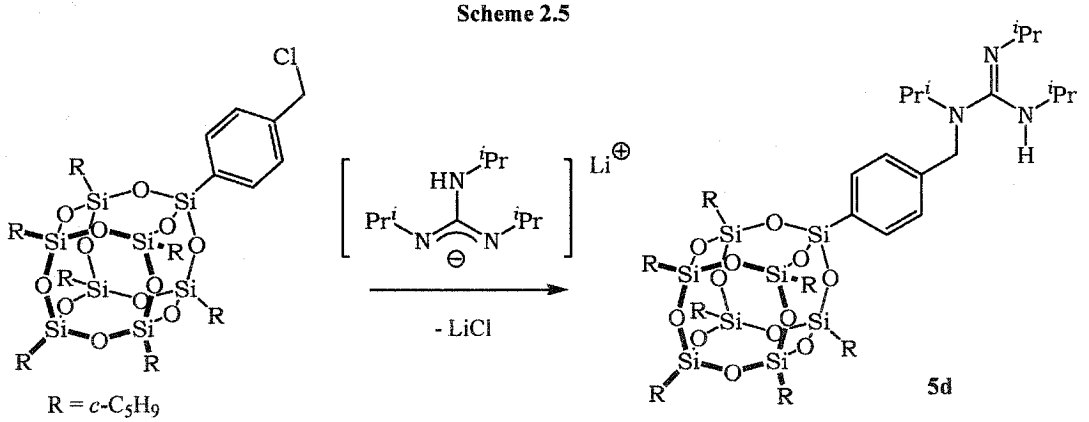

The existing methodologies for the preparation of guanidines and guanidinates enable us to prepare ligands that vary in structure, which ultimately influences the metal binding and electron donating properties of the ligands.

Experimental Section

General: All reduction reactions using $LiAlH_4$ were carried out either under nitrogen using standard Schlenk techniques or in a nitrogen filled dry box. For these reactions the solvents

used were sparged with nitrogen then dried by passage through column of activated alumina using an apparatus purchased from Anhydrous Engineering. Deuterated chloroform and benzene were purchased from Aldrich Chemical Company and in the case of C_6D_6 was dried by vacuum transfer from potassium. 1,8-diaminonapthalene and acetone, cyclopentanone, cycloheptanone, MeLi, and $LiAlH_4$ were purchased from Aldrich Chemical Company and used without further purification. The preparation of guanidines **5a** and **5b** were previously reported.[7] The silsesquioxane $(c\text{-}C_5H_9)_7Si_8O_{12}C_6H_4CH_2Cl$ was prepared by literature methods.[8] The lithium guanidinates **6a**[9a] and **6b**[9b] were previously reported, and compound **6c** was always prepared *in situ* and never characterized. ^1H and ^{13}C NMR spectra were run on a Varian Gemini-200, a Bruker 300 MHz or a Bruker 500MHz spectrometer using the residual protons of the deuterated solvent for reference. Exclusively for guanidines **5c** and **5d** NMR spectra were run on Varian Mercury 400 (^1H, 400 MHz; ^{13}C, 100.5 MHz) and Varian Indigo 500 (^{29}Si, 100 MHz) Spectrometers.

General Procedure for the reductive amination of 1,8-diaminonaphthalene:

The synthetic approach used to alkylate 1,8-DAN was roughly the same for all of the prepared compounds. The condensations were performed by reacting the diamine with an excess of the ketones, eliminating the need for solvent, at refluxing temperatures or 100°C whichever is lowest. The addition of approximately 1 g of activated molecular sieves (type 4A) per 0.1 g of water generated helped to drive the reactions to completion. The isolation of the products depended somewhat on the volatility of the ketones. The sieves were removed by suction filtration and washed with ether. The volatile products were removed under vacuum. When volatile ketones such as acetone were used no further purification was required. Non-volatile ketones were be partially removed by vacuum distillation and flash chromatography was used to isolate the pure product.

The reduction reactions were all carried out under nitrogen. The $LiAlH_4$ powder was weighed out in a Schlenk flask, and dry ether was added slowly. The suspension was stirred for 10-20 minutes to allow for the solvation heat released to subside. To this suspension was

---

[7] Thesis: Tin, M. University of Ottawa, **1997**.
[8] Leu, C.-M.; Chang, Y.-T.; Wei, K.-H. *Macromolecules* **2003**, *36*, 9122-9127.
[9] (a) although not isolated this reagent appears in Aeilts, S. L.; Coles, M. P.; Swenson, D. C.; Jordan, R. F.; Young Jr., V. G. *Organometallics* **1998**, *17*, 3265. (b) Wood, D.; Yap, G. P. A.; Richeson, D. S. *Inorg. Chem.* **1999**, *38*, 5788-5794.

added dropwise the aminals pre-dissolved or suspended in ether. The rate of addition was varied in order to control the vigorous reaction between the hydride reagent and the amine protons generating molecular hydrogen. The reactions were monitored via thin-layer chromatography by extracting small aliquots and quenching with water. In the case of reactions that did not proceed to completion after one day, an extra quantity of $LiAlH_4$ was added and the reaction was stirred for an additional day.

The reduction reactions were quenched by dropwise addition of isopropanol to the reaction mixture, followed by addition of water, with all of these steps being performed at 0°C. In order to maintain proper stirring in large-scale reactions an overhead stirrer was required. Alternatively, a three-neck round bottom flask, containing the isopropanol and equipped with an overhead stirrer and a nitrogen inlet was prepared and the reduction reaction was subsequently transferred to the isopropanol via pipette through the open neck under a continuous outflow of nitrogen. After complete transfer the stirring was stopped and water was added very slowly with occasional swirling of the flask. This step helped minimize the formation of an emulsion layer between the aqueous and organic phase. Large quantities of isopropanol can hinder phase separation, in such cases both ether and water are added until the phase boundary is clearly visible. The organic fraction is collected and combined with additional ether fractions used to wash the aqueous phase. Magnesium sulfate was used as a desiccant and the product isolated by filtration followed by evaporation of all volatiles.

Preparation of 2,2-dimethyl-2,3-dihydroperimidine, (1a)

Following the general procedures, 1,8-DAN (5.0g, 31.6 mmol) was reacted with acetone (18.5g, 319 mmol) and refluxed overnight. The product was isolated as a red/purple solid (5.87g, 94%).

^{1}H NMR ($CDCl_3$, 200 MHz): δ 7.17-7.32 (m, 4H, C*H*), 6.45 (d, 2H, C*H*), 4.18 (br, 2H, N*H*), 1.40 (s, 6H, CH_3). ^{13}C NMR ($CDCl_3$, 200 MHz): δ 140.3 (*C*), 134.4 (*C*), 126.9 (*C*H), 116.6 (*C*H), 112.6 (*C*), 105.6 (*C*H), 64.3 ($CHMe_2$), 28.4 ($CH(CH_3)_2$).

Preparation of 1,3-dihydro-spiro[perimidine-2,1'-cycloheptane], (1b)

Following the general procedures, 1,8-DAN (10.0g, 63.3 mmol) was reacted with cycloheptanone (28g, 250 mmol) and heated to 100°C overnight. The product was isolated after flash chromatography (using hexane, followed by ether) as a purple solid (15.3g, 96%). The product was used as obtained for the reduction reaction to form the monoalkyl **2b** and not characterized further.

Preparation of 1-(^{i}PrNH)-8-(NH_2)$C_{10}H_6$, (2a)

Following the general procedures, the aminal **1a** (5.0g, 25.2 mmol) was reacted with $LiAlH_4$ (2.9g, 76 mmol) and stirred overnight. The product was isolated as a purple oil (4.12g, 82%).

^{1}H NMR ($CDCl_3$, 300 MHz): δ 7.12-7.26 (m, 4H, C*H*), 6.55-6.59 (m, 2H, C*H*), 4.89 (br, 3H, N*H*), 3.60 (sept, 1H, C*H*Me$_2$), 1.26 (d, 6H, CH_3). ^{13}C NMR ($CDCl_3$, 300 MHz): δ 145.3 (*C*), 144.1 (*C*), 137.1 (*C*), 126.2 (*C*H), 125.9 (*C*H), 119.9 (*C*H), 118.7 (*C*H), 117.3 (*C*), 112.1 (*C*H), 108.5 (*C*H), 45.8 (*C*HMe$_2$), 22.7(*C*H$_3$).

Preparation of 1-(*c*-C_7H_{13}NH)-8-(NH_2)$C_{10}H_6$, (2b)

Following the general procedures, the aminal **1b** (15.0g, 59.5 mmol) was reacted with $LiAlH_4$ (6.78g, 178 mmol) and stirred overnight. The product was isolated as a purple solid (14.5g, 96%). The product can be further purified by column chromatography using 3:1 hexane/ether.

^{1}H NMR ($CDCl_3$, 200 MHz): δ 7.10-7.28 (m, 4H, C*H*), 6.58 (dd, 1H, C*H*), 6.46 (d, 1H, C*H*), 4.89 (br, 3H, N*H*), 3.48 (m, 1H, C*H*), 1.98-2.15 (m, 2H, CH_2), 1.50-1.80 (m, 10H, CH_2). ^{13}C NMR ($CDCl_3$, 200 MHz): δ 145.3 (*C*), 143.9 (*C*), 137.1 (*C*), 126.3 (*C*H), 125.8 (*C*H), 120.2 (*C*H), 117.9 (*C*H), 117.2 (*C*), 112.2 (*C*H), 107.3 (*C*H), 54.6 (*C*H), 34.3 (*C*H$_2$), 28.4 (*C*H$_2$), 24.5 (*C*H$_2$).

Preparation of 1-isopropyl-2,2-dimethyl-2,3-dihydroperimidine, (3a)

Following the general procedures, the diamine **2a** (1.0g, 5 mmol) was reacted with acetone (5.8g, 100 mmol) and refluxed overnight. The product was isolated as a purple oil (0.83g, 70%).

^{1}H NMR ($CDCl_3$, 500 MHz): δ 7.19-7.31 (m, 3H, C*H*), 7.14 (d, 1H, C*H*), 6.83 (d, 1H, C*H*), 6.42 (d, 1H, C*H*), 4.15 (br, 1H, N*H*), 4.00 (sept, 1H, C*H*Me_2), 1.50 (s, 6H, CH_3), 1.27 (d, 6H, CH_3). ^{13}C NMR ($CDCl_3$, 500 MHz): δ 140.9 (*C*), 140.1 (*C*), 134.5 (*C*), 126.3 (*C*H), 126.1 (*C*H), 118.7 (*C*H), 117.4 (*C*), 116.9 (*C*H), 112.9 (*C*H), 105.5 (*C*H), 68.9 (N_2CC_2), 48.0 (*C*HMe_2), 28.3 (*C*H_3), 21.6 (*C*H_3).

Preparation of 1-isopropyl-1,3-dihydro-spiro[perimidine-2,1'-cyclopentane], (3c)

Following the general procedures, the diamine **2a** (1.0g, 5 mmol) was reacted with cyclopentanone (4.2g, 50 mmol) and heated to 100°C overnight. The product was isolated by flash chromatography as a yellow oil (1.26g, 95%).

^{1}H NMR ($CDCl_3$, 300 MHz): δ 7.48 (d, 1H, C*H*), 7.35 (t, 1H, C*H*), 7.20-7.29 (m, 2H, C*H*), 6.98 (d, 1H, C*H*), 6.52 (d, 1H, C*H*), 4.40 (br, 1H, N*H*), 3.69 (sept, 1H, C*H*Me_2), 1.71-1.96 (m, 8H, CH_2), 1.04 (d, 6H, CH_3). ^{13}C NMR ($CDCl_3$, 300 MHz): δ 142.1 (*C*), 141.9 (*C*), 134.3 (*C*), 126.2 (*C*H), 125.7 (*C*H), 122.2 (*C*H), 120.4 (*C*), 118.7 (*C*H), 116.9 (*C*H), 106.6 (*C*H), 81.2 (N_2CC_2), 51.3 (*C*HMe_2), 38.3 (*C*H_2), 23.0 (4C, overlapping *C*H_2 and *C*H_3 determined by HMQC).

Preparation of 1,8-(^{i}PrNH)$_2$C$_{10}$H$_6$, (4a)

Following the general procedures, the aminal **3a** (3.0g, 12.5 mmol) was reacted with $LiAlH_4$ (1.2g, 32 mmol) and stirred overnight. The product was isolated as a purple oil (2.1g, 70%).

^{1}H NMR ($CDCl_3$, 500 MHz): δ 7.19-7.24 (m, 4H, C*H*), 6.58 (m, 2H, C*H*), 5.63, (br, 2H, N*H*), 3.58 (sept, 2H, C*H*Me_2), 1.24 (d, 12H, CH_3). ^{13}C NMR ($CDCl_3$, 500 MHz): δ 145.0 (*C*), 137.3 (*C*), 125.9 (*C*H), 119.3 (*C*H), 117.9 (*C*), 110.3 (*C*H), 46.4 (*C*HMe_2), 22.6 (*C*H_3).

Preparation of 1-(^{i}PrNH)-8-(*c*-C$_5$H$_9$NH)C$_{10}$H$_6$, (4c)

Following the general procedures, the aminal **3c** (1.15g, 4.3 mmol) was reacted with $LiAlH_4$ (0.5g, 13.1 mmol) and stirred overnight. The product was isolated as a purple oil (1.01g, 87%).

^{1}H NMR ($CDCl_3$, 200 MHz): δ 7.17-7.27 (m, 4H, C*H*), 6.57-6.65 (m, 2H, C*H*), 5.63, (br, 2H, N*H*), 3.84 (m, 1H, C*H*), 3.59 (sept, 1H, C*H*Me_2), 2.02 (m, 2H, CH_2), 1.63-1.82 (m, 6H, CH_2), 1.26 (d, 6H, CH_3). ^{13}C NMR ($CDCl_3$, 200 MHz): δ 145.9 (*C*), 144.9 (*C*), 137.1 (*C*),

126.1 (*C*H), 125.7 (*C*H), 119.9 (*C*H), 118.2 (*C*H), 117.6 (*C*), 111.0 (*C*H), 108.0 (*C*H), 55.9 (*C*HC$_4$H$_8$), 46.5 (*C*HMe$_2$), 33.0 (*C*H$_2$), 24.1 (*C*H$_3$), 22.6 (*C*H$_2$).

Preparation of N,N'-diisopropyl-N''-allyl-guanidine, (5c)

In a glass ampule, allylamine (4.52g, 79 mmol) and diisopropylcarbodiimide (5.0g, 40 mmol) were dissolved in approximately 20 ml of hexane. The solution was degassed and flame sealed under vacuum. The reaction was heated to 90°C for 3 days. The product was isolated by removing all volatiles under vacuum (14g, 97%).

^{1}H NMR ($CDCl_3$): δ 5.81 (m, 1H, C*H*), 5.07 (d, J = 17.0Hz, 1H, terminal C*H*$_2$), 4.95 (d, J = 10.2Hz, 1H, terminal C*H*$_2$), 3.62 (d, 2H, C*H*$_2$), 3.6 (br, 2H, C*H*Me$_2$), 1.04 (d, 12H, C*H*$_3$). ^{13}C NMR ($CDCl_3$): δ 152.6 (*C*N$_3$), 138.6 (*C*H), 114.8 (terminal *C*H$_2$), 49.1 (*C*H$_2$), 44.2 (*C*HMe$_2$), 24.5 (*C*H$_3$).

Preparation of (c-C$_5$H$_9$)$_7$Si$_8$O$_{12}$C$_6$H$_4$CH$_2$(^{i}Pr)NC(N^{i}Pr)NH^{i}Pr, (5d)

In a round bottom flask triisopropyl guanidine, **5a** (2.00g, 10.8 mmol), was dissolved in THF and an ether solution of MeLi (6.75 ml, 1.6M, 10.8 mmol) was added dropwise. The solution was stirred for one hour, followed by addition of solid (c-C$_5$H$_9$)$_7$Si$_8$O$_{12}$C$_6$H$_4$CH$_2$Cl (5.0g, 4.88 mmol). The reaction was stirred for 5 days at room temperature then all volatiles were removed under vacuum. The product was extracted using toluene and filtered. The solution was concentrated and acetonitrile was added to precipitate the product. The product (a white powder) was isolated by filtration and dried under vacuum to give 4.45g (3.79 mmol, 78%).

^{1}H NMR (C_6D_6): δ 7.94 (d, 2H, C*H*$_{Bn}$), 7.53 (d, 2H, C*H*$_{Bn}$), 4.15 (s, 2H, C*H*$_2$-Bn), 3.87 (sept, 1H, C*H*Me$_2$), 3.42 (br, 1H, C*H*Me$_2$), 3.19 (br, 1H, C*H*Me$_2$), 1.40-2.00 (m, 56H, C*H*$_2$-cC$_5$H$_9$), 1.18 (m, 7H, C*H*-cC$_5$H$_9$), 1.06 (d, 6H, C*H*$_3$-^{i}Pr), 0.82 (br, 12H, C*H*$_3$-^{i}Pr). ^{13}C NMR (C_6D_6): δ 152.6 (*C*N$_3$), 144.4 (*C*), 133.8 (*C*H$_{Bn}$), 129.3 (*C*), 128.7 (*C*H$_{Bn}$), 50.5 (*C*H$_2$-Bn), 45.3 (br, 3C, *C*HMe$_2$), 27.86, 27.80, 27.47, 27.36 (*C*H$_2$-cC$_5$H$_9$), 24.1 (br, *C*H$_3$-^{i}Pr), 22.79, 22.71 (*C*H-cC$_5$H$_9$), 19.8 (s, C*H*$_3$-^{i}Pr). ^{29}Si NMR (C_6D_6, 500, d1=8 sec): δ -65.6, -65.9, -78.2 ((≡O)$_3$*Si*C$_5$H$_9$, 3:4:1).

Crystal Structure Determination of Compound 1a.

Suitable crystal was selected, mounted on thin glass fibre using viscous oil and cooled to the data collection temperature. Data were collected on a Bruker AX SMART 1k CCD diffractometer using 0.3° ω-scans at 0, 90, and 180° in ϕ. Unit-cell parameters were determined from 60 data frames collected at different sections of the Ewald sphere. Semi-empirical absorption corrections based on equivalent reflections were applied (Blessing, R., *Acta Cryst.*, **1995,** A51, 33-38).

Systematic absences in the diffraction data and unit-cell parameters were uniquely consistent for the reported space group for **1a**. The structure was solved by direct methods, completed with difference Fourier syntheses and refined with full-matrix least-squares procedures based on F^2. All non-hydrogen atoms were refined with anisotropic displacement parameters. All hydrogen atoms were treated as idealized contributions. All scattering factors are contained in the SHEXTL 5.10 program library (Sheldrick, G. M., Bruker AXS, Madison, WI, 1997).

Figure 2.1 Thermal ellipsoid plot showing the molecular structure and atom numbering scheme for one of the two symmetry unique molecules of the aminal **1a**. Carbon bound hydrogen atoms have been omitted for clarity. Thermal ellipsoids are drawn at 30% probability.

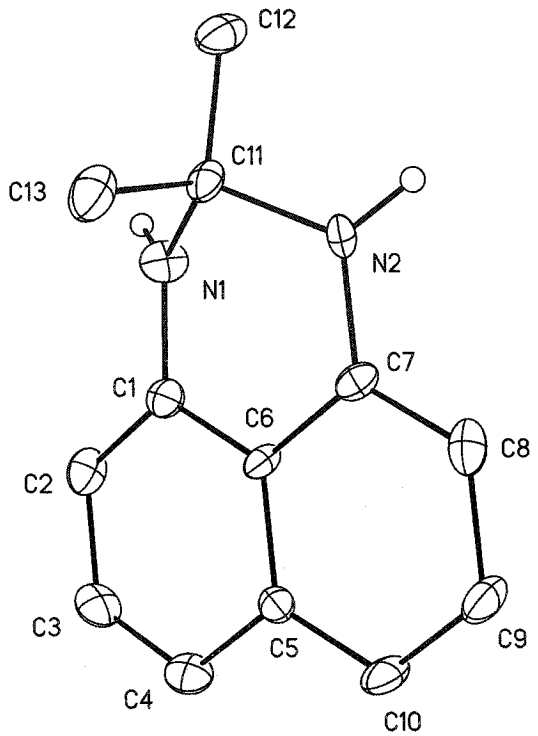

Table 2.1. Selected Crystal Data and Data Collection Parameters for **1a**

	dr253a
$C_{13}H_{14}N_2$	$C_{13}H_{14}N_2$
formula weight	198.26
T (K)	203(2)
wavelength (Å)	0.71073
crystal system	monoclinic
space group	$P2_1/c$
a (Å)	16.328(3)
b (Å)	7.688(3)
c (Å)	17.675(7)
α (deg)	90
β (deg)	105.67(2)
γ (deg)	90
V (Å^3)	2136(1)
Z	8
abs coeff (mm^{-1})	0.074
final R indices	R1 = 0.0698
	wR2 = 0.1025

Table 2.2. Selected Bond Distances and Angles for **1a**.

	Bond Distances (Å)		
N(1)-C(11)	1.474(4)	N(2)-C(11)	1.465(5)
N(1)-C(1)	1.406(5)	N(2)-C(7)	1.400(5)
C(11)-C(12)	1.531(5)	C(11)-C(13)	1.543(5)
	Bond Angles (deg)		
C(1)-N(1)-C(11)	116.3(3)	N(2)-C(11)-N(1)	107.0(3)
C(7)-N(2)-C(11)	118.5(4)	C(12)-C(11)-C(13)	111.6(4)

3 Tantalum Amido Alkyls

I. Introduction

Organometallic complexes containing metals with a d^0 configuration have been involved in a multitude of small molecule activation reactions such as insertions, polymerizations, and hydrometallations.[1] Notably, metallocenes are quite versatile and display a diverse assortment of transformations.[2] Accordingly, a host of analogous non-metallocene complexes have been prepared and studied in an attempt to understand the underlying principles which affect reactivity, and to map out the scope and generality of the reactions.[3] This approach has propelled a movement towards the design of new and interesting ligands capable of controlling the structure and reactivity of d^0 metal centres.

---

[1] For selected reviews see: (a) Arndtsen, B. A.; Bergman, R. G.; Mobley, T. A.; Peterson, T. H. *Acc. Chem. Res.* **1995**, *28*, 154 and references therein. (b) Berresford, D. J.; Bolm, C.; Sharpless, K. B. *Angew. Chem., Int. Ed. Engl.* **1995**, *34*, 1059 and references therein. (c) Tilley, T. D. *Acc. Chem. Res.* **1993**, *26*, 22 and references therein.

[2] (a) Bochmann, M. *J. Chem. Soc. , Dalton Trans.* **1996**, *3*, 255. (b) Negishi, E.; Takahashi, T. *Acc. Chem. Res.* **1994**, *27*, 124. (c) Green, J. C. *Chem. Soc. Rev.* **1998**, *27*, 263-270.

[3] See recent review: Gibson, V. C.; Spitzmesser, S. K. *Chem. Rev.* **2003**, *103*, 283-315 and references therein.

The highly reactive nature of this class of compounds arises from the electronic configuration of the metals. Having no d electrons, the metal centres can only access electron density from the coordinated ligands. The size and nature of these ligands usually sets an upper limit for the maximum coordination number of the metal. The maximum number of ligands is almost always less than 9, which means that rarely are these complexes electronically saturated species (18 electron rule). For example, a typical octahedral compound of Zr(IV) where the ligands donate 2 e^- each would have 12 electrons in its valence shell. This resulting compound would have a high degree of Lewis acidity and concomitantly high reactivity with electron density of a substrate molecule. A strategy for controlling and directing this reactivity is to use very bulky sterically demanding ligands that form very stable bonds to the metal. This restricts the reactivity of a metal complex by limiting intermolecular interactions, and reducing the number of reactive functionalities on a metal centre. The ultimate goal is to design a ligand framework which allows the metal centre access to specific substrates without any interference or unwanted side reactions with the ligand or other molecules.

Chart 3.1

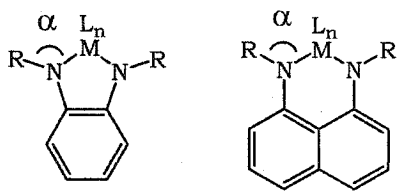

N,N'-R_2PDA **N,N'-R_2DAN**

We are particularly interested in investigating the use of N-based anionic ligands possessing π-systems capable of stabilizing the negative charges. Specifically we wanted to explore the use of N,N'-disubstituted-1,8-diaminonaphthalenes (1,8-DAN) as ancillary ligands with early transition metals (Chart 3.1). Probably the most closely related ligand that has been used for similar goals with early transition metals are ligands based on *o*-phenylenediamine (PDA)[4] (Chart 3.1). The DAN based ligands should provide increased steric protection because the geometry of the six-membered ring, formed upon chelation to a metal, will force the N-substituents closer to the metal centre. This should produce smaller angles, between the substituents and the metal (α angle), compared to those found for similar PDA ligands.

[4] For example (a) hydroamination Y catalyst; Kim, Y. K.; Livinghouse, T.; Bercaw, J. E. *Tetrahedron Lett.* **2001**, *42*, 2933-2935. (b) ethylene polymerization Zr, Ti catalysts; Danièle, S.; Hitchcock, P. B.; Lappert, M. F.; Merle, P. G. *J. Chem. Soc., Dalton Trans.* **2001**, 13-19.

The dianionic nature of the chelating DAN ligand makes it useful for compensating the cationic charges of high-valent metals. With this in mind, we targeted tantalum compounds in the +5 oxidation state. Furthermore, we envisioned that replacement of a typical monoanionic ligand, such as Cp, with a dianionic DAN based ligand would reduce the metal coordination number of a typical Ta(V) species leading to novel reactivity. For example one could imagine replacing a Cp and an alkyl ligand of a Cp_2TaR_3 complex and generating a $Cp(L)TaR_2$ (L = N,N'-R_2DAN) complex that might possess reactive characteristics analogous to Group 4 metallocene compounds.

II. Results and Discussion

A. Protonolysis with Tantalum Alkyls

The reaction between the parent ligand **4a** and trimethyltantalum dichloride was anticipated to proceed by deprotonation of the diamine and release of two equivalents of methane to give a compound containing a dianionic ligand $[C_{10}H_6(^iPrN)]^{2-}$ bound to a Ta(V) centre possessing two chlorides and one methyl group. Instead compound **7** was isolated from the reaction in a 75% yield (Scheme 3.1). Initial spectroscopic characterization of **7** clearly indicated that it was not the anticipated product. The ^1H NMR spectrum does not contain signals appropriate for a Ta-Me group, and the appearance of a broad singlet in the aliphatic region integrating for two methyl groups suggested that one of the isopropyl groups had been modified. The ^{13}C NMR of **7** exhibited a resonance at 65.8 ppm. The spectroscopic data pointed to a product that had undergone a subsequent reaction which eliminated the Ta-Me group and had transformed one of the N-substituents.

Scheme 3.1

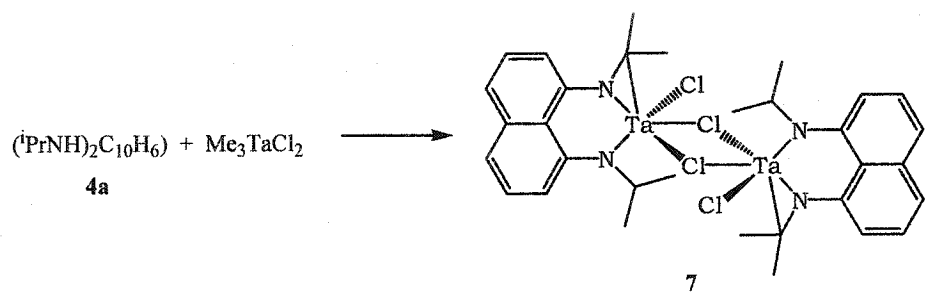

7

To establish the identity of compound **7** we obtained its molecular structure via X-ray crystallography (Figure 3.1). The data showed that one ^{i}Pr group had undergone C-H activation resulting in the formation of a metallaaziridine with elimination of a third equivalent of methane. This structure is consistent with the spectroscopic appearance of a quaternary carbon at 65.8 ppm and the singlet observed for the methyl signals in the ^{1}H NMR. It also explained the lack of a Ta-Me signal. The solid-state structure of compound **7** is a dinuclear species comprised of two equivalent moieties bridged by two chlorides. The structure clearly shows the trianionic tridentate nature of the ligand which binds in a planar fashion to Ta forming a bicyclic structure. An inversion centre lies between the Ta centres rendering the ligands equivalent, however each ligand is entirely asymmetric. In other words the methyl groups of the ^{i}Pr and the metallaaziridine are all inequivalent. The ^{1}H NMR spectrum contains only one signal for the methyl groups of the heterocycle and one for the methyl groups of the ^{i}Pr and both are broad. This observation suggests that the dimeric structure is either fluxional, or is not maintained in solution.

The structural parameters of **7** favour a formulation as a metallaaziridine rather than the η^2-imine isomer (side-on coordination). The internal angles within the three-membered heterocycle are consistent with the few related metallaaziridine complexes of Ta(V),[5] and the N(2)-C(14) distance of 1.413(7) Å is indicative of a single bond azametallacycle formulation.[6]

Related rigid chelating aromatic diamido ligands *N,N'*-bis(trialkylsilyl)-*o*-phenylenediamide (N,N'-$(SiMe_3)_2$PDA) have been employed in the preparation of high-valent group 4,[7] Ta,[8,9] Mo,[10] and W[11] species. A common structural feature of all but one of these PDA complexes is a distortion of the ligand from planarity. The folding of the ligand

---

[5] (a) Boncella, J. M.; Cajigal, M. L.; Abboud, K. A. *Organometallics* **1996**, *15*, 1905. (b) Takai, K.; Ishiyama, T.; Yasue, H.; Nobunaka, T.; Itoh, M.; Oshiki, T.; Mashima, K.; Tani, K. *Organometallics* **1998**, *17*, 5128. (c) Clark, J. R.; Fanwick, P. E.; Rothwell, I. P. *Organometallics* **1996**, *15*, 3232.
[6] Burke-Laing, M.; Laing, M. *Acta Crystallogr., Sect. B* **1976**, *32*, 3216.
[7] Aoyagi, K.; Gantzel, P. K.; Kalai, K.; Tilley, T. D. *Organometallics* **1996**, *15*, 923.
[8] Pindado, G. J.; Thornton-Pett, M.; Bochmann, M. *J. Chem. Soc., Dalton Trans.* **1998**, *393*.
[9] Aoyagi, K.; Gantzel, P. K.; Tilley, T. D. *Polyhedron* **1996**, *15*, 4299.
[10] (a) Cameron, T. M.; Abboud, K. A.; Boncella, J. M. *Chem. Commun.* **2001**, 1224. (b) Ortiz, C. G.; Abboud, K. A.; Boncella, J. M. *Organometallics* **1999**, *18*, 4253.
[11] (a) Cameron, T. M.; Ortiz, C. G.; Abboud, K. A.; Boncella, J. M.; Baker, R. T.; Scott, B. L. *Chem. Commun.* **2000**, 573. (b) Wang, S. Y. S.; Vanderlende, D. D.; Abboud, K. A.; Boncella, J. M. *Organometallics* **1998**, *17*, 2628. (c) Wang, S. Y. S.; Abboud, K. A.; Boncella, J. M. *J. Am. Chem. Soc.* **1997**, *119*, 11990. (d) VanderLende, D. D.; Abboud, K. A.; Boncella, J. M. *Organometallics* **1994**, *13*, 3378.

about the N-N vector has been attributed to the presence of an additional π-type bonding interaction of an empty metal d orbital with the lone electron pairs of the amido N centres (i.e., a 3c-4e interaction)[12]. This should quench the electrophilicity of the metal. These observations contrast with the structural details for the 1,8-DAN based system reported here. We attribute this difference to a combination of the geometric constraints of the metallaaziridine moiety and the naphthalene frame of the ligand.

Evidence that the dimeric structure may not persist in solution is provided by the easy displacement of the bridging chlorides by strong donor ligands. When **7** is recrystallized from pyridine, a mononuclear species is obtained with two solvent molecules bound to each tantalum atom, compound **7-py$_2$** (Figure 3.2). The molecular structure obtained from X-ray

Scheme 3.2

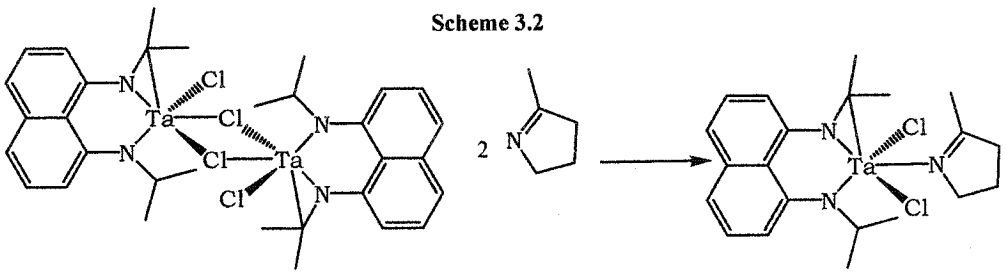

7 **8**

crystallography (Table 3.1) shows a monomeric species with a seven coordinate Ta atom. The three ligand donor atoms, along with the two pyridines all lie in a plane, with the two chlorides in pseudo-axial positions. The structure also clearly shows the unperturbed trianionic tridentate binding mode of the ligand.

We were interested in examining the robustness of the bicyclic tridentate binding mode of the ligand. Considering the potential for ring strain in the metallaaziridine, we anticipated that the Ta-C bond might be highly reactive. Addition of 2 equivalents of 2-methylpyrroline to compound **7** yielded mononuclear Ta complexes with one pyrroline bound to each metal via the N lone-pair, compound **8** (Scheme 3.2). The ^{1}H NMR spectrum showed similar ligand signals to compound **7**, and a symmetric environment was indicated by equivalent methyl signals. The spectrum also contained additional peaks due to the pyrroline.

[12] Galindo, A.; Ienco, A.; Mealli, C. *New J. Chem.* **2000**, *24*, 73-75.

Structural characterization confirmed the geometric features of **8** (Figure 3.3). These include the presence of an intact $[\eta^3\text{-}C_{10}H_6(Me_2CN)(^iPrN)]^{3-}$ ligand and the coordination of the pyrroline nitrogen. The Ta(V) coordination geometry is almost identical to that of **7**, with N(3) occupying the site formerly occupied by the bridging chloride ligand of the dimer. The bonding parameters within the $[\eta^3\text{-}C_{10}H_6(Me_2CN)(^iPrN)]Ta$ frame are similar to those observed in **7**. We chose the pyrroline derivative in part because it possesses enolizable protons which are relatively acidic, and a C-N double bond susceptible to insertion. The lack of reactivity demonstrates the robustness of the tridentate binding mode and the stability of the metallaaziridine.

The chloride ligands of compound **7** can be displaced via salt metathesis. One chloride per metal centre can be substituted with a pentamethyl cyclopentadienide by reacting **7** with two equivalents of LiCp* to produce a Ta complex bearing the DAN based ligand and one Cp* ligand, compound **9** (Scheme 3.3). The product can be clearly identified through ^1H NMR spectroscopy which shows once again the characteristic signals for a

Scheme 3.3

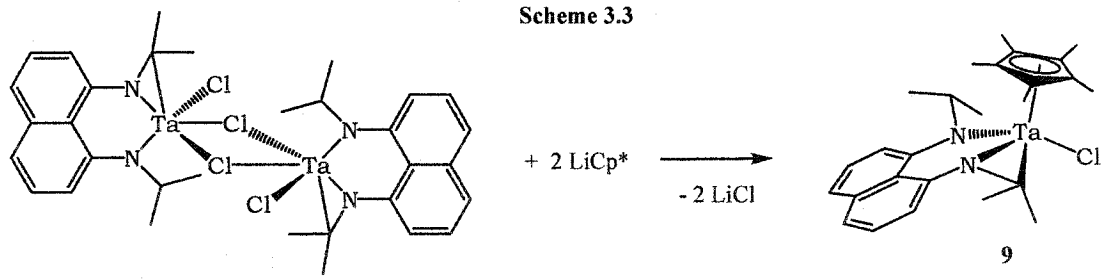

9

trianionic ligand and the additional singlet for the methyl groups of the Cp* ligand. The asymmetric environment of Ta is reflected in the NMR spectrum. The two ^{i}Pr methyls are diastereotopic as are the two metallaaziridine Me groups. The ^{13}C spectrum supports the structural assignment of compound **9**, the appropriate signals for the trianionic ligand along with those for the Cp* fragment are all clearly identifiable. The molecular structure was obtained via X-ray crystallography (Table 3.1) and confirms the formulation of compound **9**. Figure 3.4 illustrates the molecular structure and demonstrates the planar tricyclic metallaheterocycle. Selected bond lengths and angles are listed in Table 3.6 and indicate that very little has changed within the metallaaziridine function.

Both of the chlorides in **7** can be exchanged for alkyl ligands. Reacting **7** with four equivalents of BnMgCl gives the bis(benzyl) derivative **10** (Scheme 3.4). We decided to

Scheme 3.4

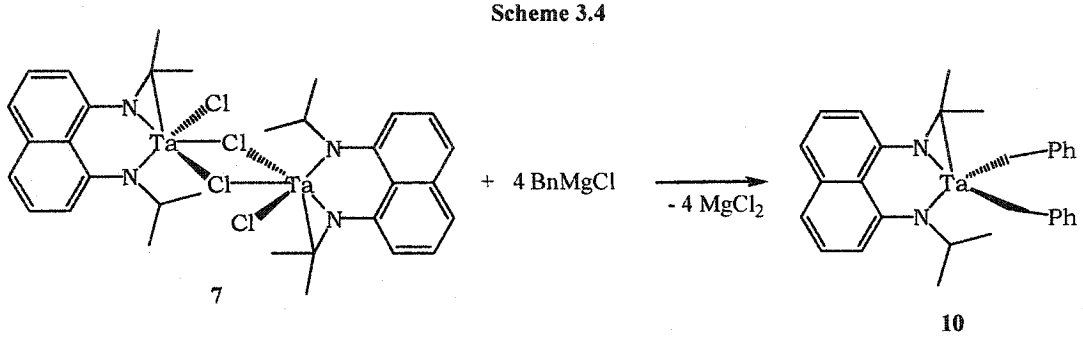

7 **10**

introduce benzyl ligands because their α-protons are known to be susceptible to activation, and we speculated that formation of a benzylidene function might be favoured over the bicyclic structure of the ligand. The envisioned transformation would effectively transfer a proton from the benzyl to the Ta-C bond of the metallaaziridine. However, the ^{1}H NMR spectrum of **10** clearly shows persistence of the signals for the trianionic ligand framework, with additional peaks due to the benzyl groups. Interestingly the methylene protons of the benzyl groups appear as an AB pattern (doublet of doublets) which indicates that both benzyls are equivalent, but that the protons are diastereotopic. This is consistent with the asymmetric binding of the tridentate ligand, with only one mirror plane coincident with the $C_{10}H_6$-N_2CTa plane. The lack of reactivity or rearrangement once again shows the stability of the binding mode.

B. Salt-Metathesis with Dilithio Diamidonaphthalene

Our attempts to obtain a Ta complex with a bidentate dianionic DAN ligand by reacting the diamine **4a** with Me_3TaCl_2 proved to be unsuccessful. Even our attempts to open the metallaaziridine by exposing the compounds to reagents that could potentially transfer a proton did not yield the desired structures, nor did it lead to any rearrangements whatsoever. We therefore decided to reverse the synthetic strategy and try to introduce the ligand from the dilithium salt, which could be reacted with an appropriate starting material already containing the alkyl ligands.

The dilithium salt of the ligand is easily obtained by reacting the diamine (**4a**) with two equivalents of MeLi. This can either be done *in situ* or stepwise with isolation and purification of the salt by crystallization from cold THF. The diamido salt was then reacted with Me_3TaCl_2 anticipating that the product would contain the diamido ligand $[C_{10}H_6(^iPrN)_2]^{-2}$ bound to Ta which would retain it's three methyl ligands. However, once

again the ^{i}Pr group undergoes C-H activation and the ligand assumes the same tridentate trianionic bicyclic binding mode (Scheme 3.5). This is easily verifiable by NMR spectroscopy of the product, compound **11**, which reveals the characteristic peaks for the ligand moiety and typical signals for Ta-Me groups. The NMR spectrum also indicates that a molecule of THF has been retained by the metal, expanding the coordination sphere. The

Scheme 3.5

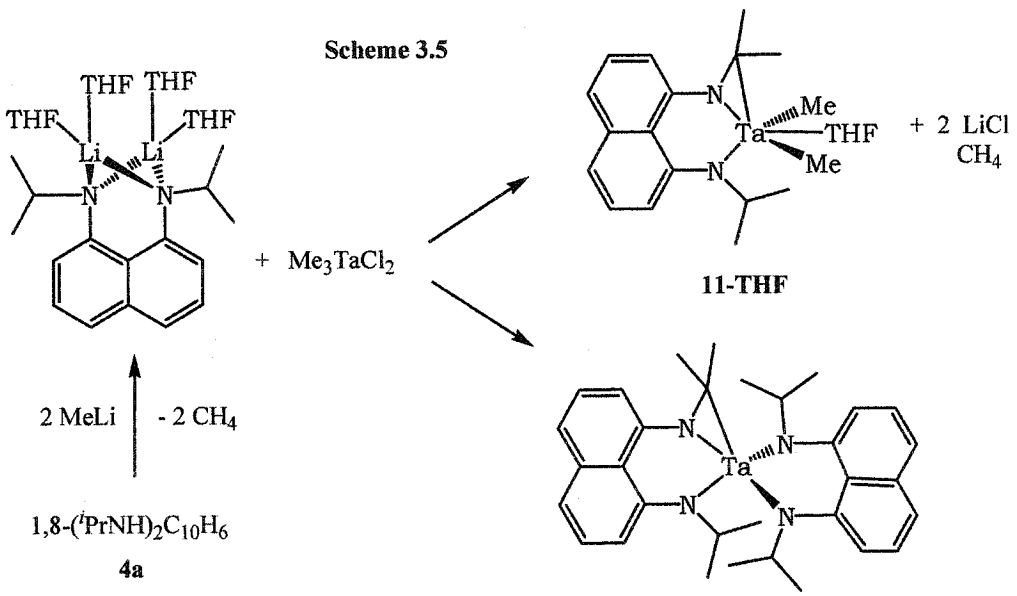

molecular structure of **11·THF** was determined, and shows the metallaaziridine function, along with the Ta-methyl groups and the coordinated THF (Figure 3.5). The X-Ray diffraction data suggests that the C(18) position is partially occupied by chloride. This disorder was modeled with a 25% chloride occupancy. This reveals that the product is not pure. Unfortunately, as this structure demonstrates, the co-crystallization of these two species prevents us from further purifying the compound via fractional crystallization. In an attempt to circumvent the purity problem, we performed the methylation of **7** with MeMgCl and obtained the same compound **11·THF**, which was again contaminated by the presence of a disordered chloride ligand.

During our investigations of the synthesis of **11·THF**, we observed the presence of a by-product. By exploiting the differences in solubility, we were able to separate a compound (**12**) from the reaction, in a low yield, which we identify as being [η^3-$C_{10}H_6(Me_2CN)(^{i}PrN)$]Ta[$(N^{i}Pr)_2C_{10}H_6$], best described as a spiro bis(ligand) complex. The

Scheme 3.6

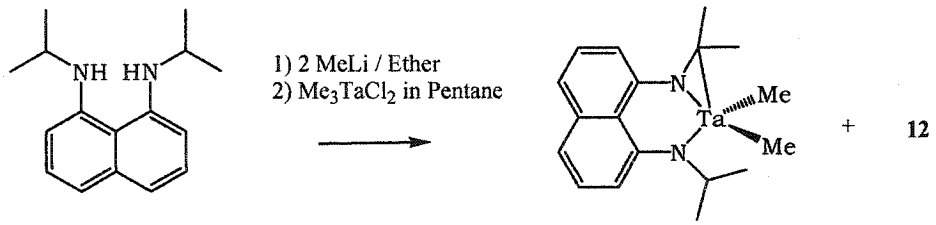

4a **11**

^1H and ^{13}C NMR spectra are consistent with the proposed composition of the compound. Specifically, the appearance of three distinct doublets for ^{i}Pr methyl groups, each integrating as 6H, along with a singlet integrating as two methyls supports the geometry for **12** proposed in Scheme 3.5. Consistent with this interpretation is the appearance of two methine multiplets in a ratio of 2:1. Both sides of the dianionic ligand are symmetrically equivalent, but the ^{i}Pr methyls are diastereotopic (one septet and two doublets). This is because the C-H activated ligand, which is presumably rotated 90° with respect to the second ligand, is not symmetric creating a complex that contains only one mirror plane which is co-planar with the $C_{10}H_6N_2C$-Ta plane of the C-H activated ligand and bisects the other ligand. Despite repeated attempts we were unable to obtain X-ray diffraction quality crystals of **12**.

Although compound **12** contains the sought after bidentate dianionic ligand, it is unclear as to how this complex is formed. It may be formed via an intermediate containing the bidentate ligand and three methyl groups, which can then undergo ligand exchange with one molecule of the major product. The low-yielding nature of the product suggests it is formed through some secondary reactions. Performing the salt metathesis reaction with *in situ* prepared dilithium diamido salt (excluding THF solvent) in pentane allowed us to isolate a solvent free version of compound **11**. However, the presence of the same spiro by-product **12** is observed (Scheme 3.6), and can be isolated cleanly in a 17 % yield due to the high solubility of THF free **11**.

III. Conclusion

In all of our attempts to prepare a high-valent tantalum species containing both, a bidentate dianionic 1,8-DAN ligand and alkyl (methyl) groups we observed C-H activation of the ipso proton of one of the isopropyl substituents. This activation leads to the formation

of a metallaaziridine function which is part of a trianionic tridentate binding mode of the ligand. This bicyclic structure is demonstrated to be quite robust, as evidenced by resistance to reactivity with the enolizable protons of an imine substrate, or with the α-protons of Ta-Bn groups. The structure also remains intact during subsequent metathesis reactions including ligand exchange processes.

Experimental Section

General: All manipulations were carried out in either a nitrogen filled dry box or under nitrogen using standard Schlenk techniques. Reaction solvents were sparged with nitrogen then dried by passage through column of activated alumina using an apparatus purchased from Anhydrous Engineering. Deuterated methylene chloride, benzene and toluene were purchased from Aldrich Chemical Company and in the case of C_6D_6 and C_7D_8 were dried by vacuum transfer from potassium. 1,8-diaminonapthalene and $PhCH_2MgCl$ were purchased from Aldrich Chemical Company and used without further purification. Me_3TaCl_2 was prepared by literature procedures.[13] ^1H and ^{13}C NMR spectra were run on a Varian Gemini-200, a Bruker 300 MHz or a Bruker 500MHz spectrometer by using the residual protons of the deuterated solvent for reference.

Preparation of $Li_2[1,8\text{-}(^iPrN)_2C_{10}H_6](THF)_4$

Addition of MeLi (2.5 ml, 1.4 M in ether, 3.5 mmol) to a dark red/purple solution of diamine **4a** (0.424 g, 1.7 mmol) in ether (ca. 30 ml) led to an immediate color change of the solution to green then brown with gas evolution. The reaction mixture was stirred for 4 h and then all volatiles were removed under vacuum. The crude product (0.440 g, 99%) was then purified by crystallization from THF at –35°C. The crystals were filtered and dried under vacuum. The product isolated by this method possessed four molecules of THF.

^1H NMR (C_6D_6,): δ 7.40 (t, 2H, Ar-*H*), 6.94 (d, 2H, Ar-*H*), 6.36 (m, 2H, Ar-*H*), 3.55 (sept, 2H, C*H*Me_2), 3.36 (t, 16H, THF) 1.28 – 1.18 (overlapping signals, 28H, CH_3 and THF).

[13] Schrock, R. R.; Parshall, G. W. *Chem. Rev.* **1976**, 76, 243.

^{13}C NMR ($C_7D_{8,}$): 127.1 (Ar *C*H), 110.9 (Ar *C*H), 101.3 (Ar *C*H), 68.0 (*C*H_2, THF), 47.3 (*C*HMe_2), 25.6 (*C*H_2, THF), 25.1 (*C*H_3).

Preparation of {[η^3-$C_{10}H_6$(Me_2CN)(Me_2CHN)]$TaCl_2$}$_2$, (7)

In a 50 ml round bottom flask equipped with a magnetic stir bar, diamine **4a** (0.485g, 0.002 mol) was dissolved in 20 ml of toluene. To this flask was added Me_3TaCl_2 (0.714g, 0.0024 mol) dissolved in 10 ml of toluene. The reaction mixture was stirred for 4 days at room temperature. Filtration yielded a fine red powder of **7** (0.745g, 75%). Single crystals of **7** could be obtained from benzene.

^{1}H NMR (C_7D_8, 500 MHz): δ 7.30 (br, 4H, Ar-*H*), 7.20 (br, 1H, Ar-*H*), 6.84 (br, 1H, Ar-*H*), 4.82 (br, mult. 1H, C*H*Me_2), 2.48 (br s, 6H, C*H*$_3$), 1.44 (br d, 6H, C*H*$_3$).

^{13}C NMR (C_7D_8, 500 MHz): 139.6 (Ar *C*), 136.7 (Ar *C*), 126.8 (Ar *C*H), 125.6 (Ar *C*H), 123.3 (Ar *C*H), 123.0 (Ar *C*H), 110.3 (Ar *C*H), 109.11 (Ar *C*H), 65.8 (Ta-*C*), 48.06 (*C*H(CH$_3$)$_2$), 26.2 (*C*H$_3$), 18.5 (*C*H$_3$). Note: two of the quaternary aromatic carbons were not observed. We attribute this to the low solubility of compound **7** and to the quadrupolar broadening from the nitrogen centres.

Preparation of [η^3-$C_{10}H_6$(Me_2CN)(Me_2CHN)]$TaCl_2$(NC_4H_3-2-CH_3), (8)

In a sealed NMR tube a suspension of complex **7** (0.030g, 0.03 mmol) in approximately 0.7 ml of C_6D_6 was prepared. To this was added 2-methyl-1-pyrroline (0.005g, 0.06mmol) that had been dissolved in 0.2 ml of C_6D_6. The tube was closed and agitated, to give an orange solution. The product was obtained as orange crystals from benzene at room temperature (0.012g, 35%).

^{1}H NMR (C_6D_6, 300 MHz): δ 7.5-7.25 (m, 5H, Ar-*H*), 7.14 (partially hidden d, 1H, Ar-*H*), 4.48 (br. 2H, imine C*H*$_2$), 4.2 (sept, 1H, C*H*Me_2), 2.55 (s, 6H, C*H*$_3$), 2.04 (s, 3H, imine C*H*$_3$) 1.72 (overlapping d and m, 8H, ^{i}Pr-(C*H*$_3$)$_2$ and imine C*H*$_2$), 1.38 (m, 2H, imine C*H*$_2$).

^{13}C NMR (C_6D_6, 300 MHz): 181.6 (imine *C*) 140.6 (Ar-*C*), 140.0 (Ar-*C*), 137.4 (Ar-*C*), 129.3 (Ar-*C*), 126.8 (Ar-*C*H), 126.5 (Ar-*C*H), 122.4 (Ar-*C*H), 120.7 (Ar-*C*H), 108.9 (Ar-*C*H), 107.4 (Ar-*C*H), 64.1 (imine *C*H$_2$) 61.0 (Ta-*C*Me_2), 44.9 (*C*HMe_2), 40.2 (imine *C*H$_2$), 26.6 (*C*H$_3$), 21.8 (imine *C*H$_2$) 20.5 (imine *C*H$_3$), 17.4 (*C*H$_3$).

Preparation of [η^3-$C_{10}H_6(Me_2CN)(Me_2CHN)$]Ta($\eta^5$-$C_5Me_5$)Cl, (9)

In a 50 ml round bottom flask equipped with a magnetic stir bar, compound **7** (0.260g, 0.26 mmol) was suspended in 30 ml of ether. To this suspension was added solid LiCp* (0.075g, 0.53 mmol). The reaction mixture turned from orange to dark red/purple within a few minutes and was stirred for 20 hours at room temperature. The solvent was removed under vacuum and the solid was extracted with pentane. Filtration followed by drying under vacuum yielded **9** as a purple powder (0.201g, 65%). The crude product can be purified by crystallization from pentane at -35°C.

^{1}H NMR (C_6D_6, 500MHz): δ 7.386 (dd, 1H, Ar-*H*), 7.34-7.316 (overlapping d and t, 2H, Ar-*H*), 7.284 (t, 1H, Ar-*H*), 7.201 (dd, 1H, Ar-*H*), 7.068 (d, 1H, Ar-*H*), 3.809 (sept., 1H, C*H*Me$_3$), 2.364 (s, 3H, C*H*$_3$), 2.134 (s, 3H, C*H*$_3$), 1.831 (s, 15H, C*H*$_3$), 1.563 (d, 3H, C*H*$_3$), 1.345 (d, 3H, C*H*$_3$)

^{13}C NMR (C_6D_6, 500MHz): 145.3 (Ar *C*), 142.9 (Ar *C*), 138.0 (Ar *C*), 126.50 (Ar *C*H), 126.45 (Ar *C*H), 126.14 (Ar *C*), 121.7 (Ar *C*H), 120.0 (Ar *C*H), 119.5 (Cp* *C*), 111.7 (Ar *C*H), 111.6 (Ar *C*H), 67.1 (Ta-*C*), 49.6 (*C*HMe$_3$), 29.3 (TaC(*C*H$_3$)$_2$), 29.1 (TaC(*C*H$_3$)$_2$), 24.2 (CH(*C*H$_3$)$_2$), 18.3 (CH(*C*H$_3$)$_2$), 12.1 (Cp* *C*H$_3$).

Preparation of [η^3-$C_{10}H_6(Me_2CN)(Me_2CHN)$]Ta($CH_2C_6H_5$)$_2$, (10)

In a 50 ml round bottom flask equipped with a magnetic stir bar, compound **7** (0.080g, 0.08 mmol) was added to 15 ml of ether. To this suspension was $C_6H_5CH_2MgCl$ (0.35ml, 0.35 mmol) in ether. The reaction was stirred for 20 hours at room temperature. The solvent was removed under vacuum and toluene was utilized to extract the product. Filtration followed by drying under vacuum yielded **10** as an orange powder (0.060g, 62%).

^{1}H NMR (CD_2Cl_2, 300 MHz): δ 7.46 (t, 1H, Ar-*H*), 7.38 (overlapping d, 2H, Ar-*H*), 7.33 (t, 1H, Ar-*H*), 7.20 (m, 6H, Ph-*H*), 7.09 (d, 1H, Ar-*H*), 6.97 (d, 1H, Ar-*H*), 6.84 (m, 4H, Ph-*H*), 3.13 (br mult. 1H, C*H*Me$_2$), 2.08 (s, 6H, C*H*$_3$), 1.45 (d, 6H, C*H*$_3$), 1.25 (d, 2H, diast. C*H*$_2$), 1.19 (d, 2H, diast. C*H*$_2$).

^{13}C NMR (CD_2Cl_2, 300 MHz): 141.5 (Ar *C*), 140.5 (Ar *C*), 138.7 (Ph *C*), 137.2 (Ar *C*), 130.0 (Ph *C*H), 129.3 (Ph *C*H), 128.5 (Ar *C*), 127.1 (Ar *C*H), 126.0 (Ph *C*H), 125.9 (Ar *CH*),

121.4 (Ar *C*H), 120.3 (Ar *C*H), 109.8 (Ar *C*H), 109.4 (Ar *C*H), 72.3 (Ta-*C*H_2), 64.5 (Ta-*C*Me_2), 40.2 (*C*HMe_2), 27.1 (*C*H_3), 20.7 (*C*H_3).

Preparation of [η^3-$C_{10}H_6$(Me_2CN)(Me_2CHN)]Ta(CH_3)$_2$•THF, (11·THF)

In a 50 ml round bottom flask equipped with a magnetic stir bar, Li_2[1,8-(^{i}PrN)$_2C_{10}H_6$](THF)$_4$ (0.310g, 0.57 mmol) was suspended in 20 ml of pentane. To this suspension was added Me_3TaCl_2 (0.170g, 0.54 mmol) pre-dissolved in pentane. The reaction was stirred overnight, and then filtered. The solvents were removed under vacuum and the dark orange product (0.193 g, 68 %) can be crystallized out of a toluene/pentane mixture at –30°C. The crystals used for X-ray diffraction contained half an equivalent of toluene as a co-crystallized solvent.

^{1}H NMR (C_6D_6, 500MHz): δ 7.35-7.45 (mult., 3H, Ar-*H*), 7.28 (t, 1H, Ar-*H*), 7.13 (obscured doublet, 1H, Ar-*H*), 6.85 (br, 1H, Ar-*H*), 4.41 (br, 1H, C*H*Me_2) 3.68 (mult, 4H, THF), 2.67 (s, 6H, Ta-C(C*H*$_3$)$_2$), 1.42 (d, 6H, CH(C*H*$_3$)$_2$), 1.39 (mult, 4H, THF), 0.13 (br, 6H, Ta-C*H*$_3$).

^{13}C NMR (C_6D_6, 500MHz): 142.0 (Ar *C*), 140.5 (Ar *C*), 137.6 (Ar *C*), 127.5 (Ar *C*H), 126.3 (Ar *C*), 125.5 (Ar *C*H), 121.5 (Ar *C*H), 120.4 (Ar *C*H), 109.5 (Ar *C*H), 109.1 (Ar *C*H), 69.1 (*C*H_2 THF), 66.9 (Ta-*C*(CH_3)$_2$), 61.5 (2 Ta-*C*H_3), 42.9 (*C*HMe_2), 25.8 (*C*H_2 THF), 25.3 (Ta-C(*C*H_3)$_2$), 20.6 (CH(*C*H_3)$_2$).

Preparation of [η^3-$C_{10}H_6$(Me_2CN)(Me_2CHN)]Ta(CH_3)$_2$, (11)

In a 50 ml round bottom flask equipped with a magnetic stir bar, diamine **4a** (0.170g, 0.7 mmol) was dissolved in 20 ml of ether. To this suspension was added a 1.4 M etheral solution of MeLi (1.0 ml, 1.4 mmol). The reaction was stirred for one and a half hours. All volatile compounds were removed under vacuum. To the flask containing the solid residue, 20 ml of pentane was added, and the suspension was stirred. To this suspension was added Me_3TaCl_2 (0.210g, 0.7 mmol) pre-dissolved in pentane. The reaction was stirred for 5 hours, and then filtered. The pentane was removed under vacuum to give 0.165g of product (52%).

^{1}H NMR (C_6D_6, 200MHz): δ 7.20-7.44 (m, 4H, Ar-*H*), 7.13 (obscured doublet, 1H, Ar-*H*), 6.8 (br d, 1H, Ar-*H*), 4.58 (br, 1H, C*H*Me_2), 2.31 (s, 6H, Ta-C(C*H*$_3$)$_2$), 1.37 (d, 6H, CH(C*H*$_3$)$_2$), 0.25 & 0.29 (overlapping s, 6H, Ta-C*H*$_3$).

^{13}C NMR (C_6D_6, 300MHz): 141.8 (Ar *C*), 139.9 (Ar *C*), 137.3 (Ar *C*), 128.3 (Ar *C*H), 127.2 (Ar *C*H), 125.4 (Ar *C*H), 122.0 (Ar *C*H), 120.7 (Ar *C*), 110.0 (Ar *C*H), 109.3 (Ar *C*H), 67.4 (Ta-*C*(CH_3)$_2$), 64.2 (2 Ta-*C*H_3), 42.7 (*C*HMe_2), 25.6 (Ta-C(*C*H_3)$_2$), 20.3 (CH(*C*H_3)$_2$).

Preparation of [η^3-$C_{10}H_6$(Me_2CN)(Me_2CHN)]Ta[1,8-(^{i}PrN)$_2$$C_{10}H_6$], (12)

Compound **12** was isolated by recovering the pentane insoluble precipitate from the reaction generating **11**. The product was obtained as dark orange/brown solid (0.080 g, 17 %).

^{1}H NMR (C_6D_6, 500 MHz): <u>symmetric ligand</u>: δ 7.310 (d, 2H, Ar-*H*), 7.250 (t, 2H, Ar-*H*), 6.771 (d, 2H, Ar-*H*), 4.088 (sept, 2H, C*H*Me_2), 0.905 (d, 6H, CH(C*H*$_3$)$_2$) 0.713 (d, 6H, CH(C*H*$_3$)$_2$). <u>non-symmetric ligand</u>: δ 7.466 (t, 1H, Ar-*H*), 7.396 (dd, 1H, Ar-*H*), 7.33-7.37 (overlapping d and t, 2H, Ar-*H*), 7.032, (dd, 1H, Ar-*H*), 6.897 (dd, 1H, Ar-*H*), 4.618 (sept, 1H, C*H*Me_2), 2.220 (s, 6H, Ta-C(C*H*$_3$)$_2$) 1.402 (d, 6H, CH(C*H*$_3$)$_2$).

^{13}C NMR (C_6D_6, 500 MHz): <u>symmetric ligand</u>: δ 144.9 (Ar *C*), 138.4 (Ar *C*), 126.3 (Ar-*C*H), 125.95 (Ar *C*), 123.4 (Ar *C*H), 114.7 (Ar *C*H), 52.8 (*C*H(CH$_3$)$_2$), 21.9 (CH(*C*H$_3$)$_2$), 21.4 (CH(*C*H$_3$)$_2$). <u>non-symmetric ligand</u>: δ 142.6 (Ar *C*), 137.3 (Ar *C*), 129.3 (Ar *C*), 126.7 (Ar-*C*H), 126.0 (Ar-*C*H), 125.6 (Ar *C*), 120.7 (Ar *C*H), 119.9 (Ar *C*H), 110.1 (Ar *C*H), 109.8 (Ar *C*H), 61.9 (Ta-*C*(CH$_3$)$_2$), 50.5 (*C*H(CH$_3$)$_2$), 27.4 (Ta-C(*C*H$_3$)$_2$), 20.0 (CH(*C*H$_3$)$_2$).

Structural determinations for 7, 7-py$_2$, 8, 9 and 11·THF:

Single crystals were mounted on thin glass fibres using viscous oil and then cooled to the data collection temperature. Crystal data and details of the measurements are summarized in Table 3.1and 3.2 for each of these compounds. Data were collected on a Bruker AX SMART 1k CCD diffractometer using 0.3° ω-scans at 0, 90, and 180° in ϕ. Unit-cell parameters were determined from 60 data frames collected at different sections of the Ewald sphere. Semi-empirical absorption corrections based on equivalent reflections were applied (Blessing, R., *Acta Cryst.*, **1995,** A51, 33-38).

The structures were solved by direct methods, completed with difference Fourier syntheses and refined with full-matrix least-squares procedures based on F^2. All non-hydrogen atoms were refined with anisotropic displacement parameters. All hydrogen atoms were treated as idealized contributions. All scattering factors and anomalous dispersion factors are

contained in the SHELXTL 5.1 program library (Sheldrick, G. M., Bruker AXS, Madison, WI, 1997).

Figure 3.1. Two views of the molecular structure for compound **7**. Hydrogen atoms, except methine hydrogens, have been omitted for clarity. Thermal ellipsoids are drawn at 30% probability. The bottom figure highlights the planarity of the ligand.

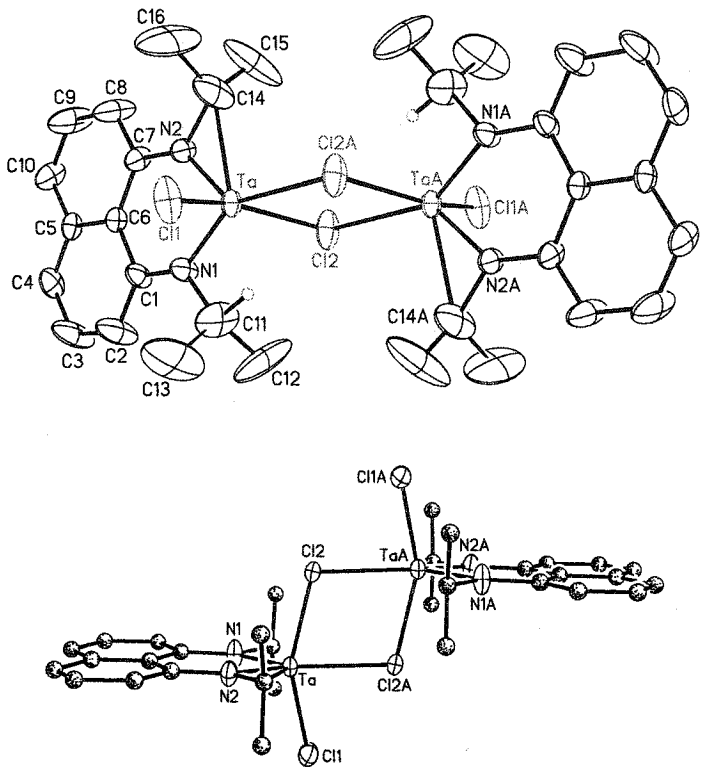

Figure 3.2. Molecular structure and atom numbering scheme for compound **7-py$_2$**. Hydrogen atoms have been omitted for clarity. Thermal ellipsoids are drawn at 30% probability.

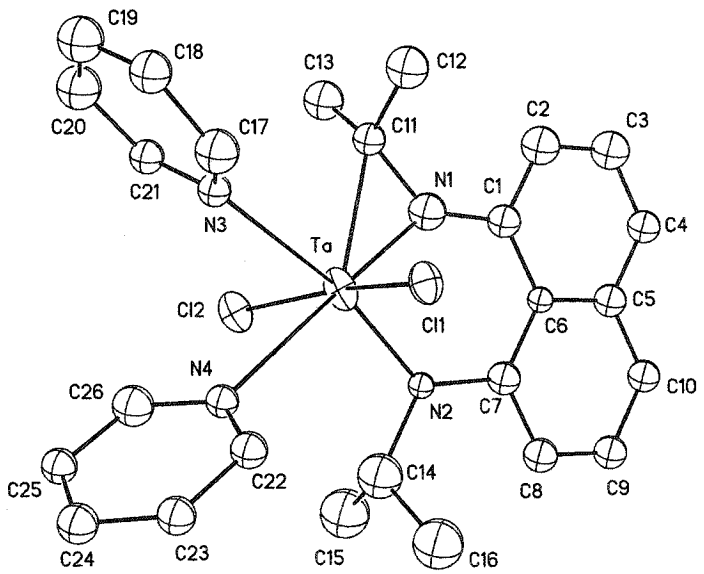

Figure 3.3. Molecular structure and atom numbering scheme for compound **8**. Hydrogen atoms have been omitted for clarity. Thermal ellipsoids are drawn at 30% probability.

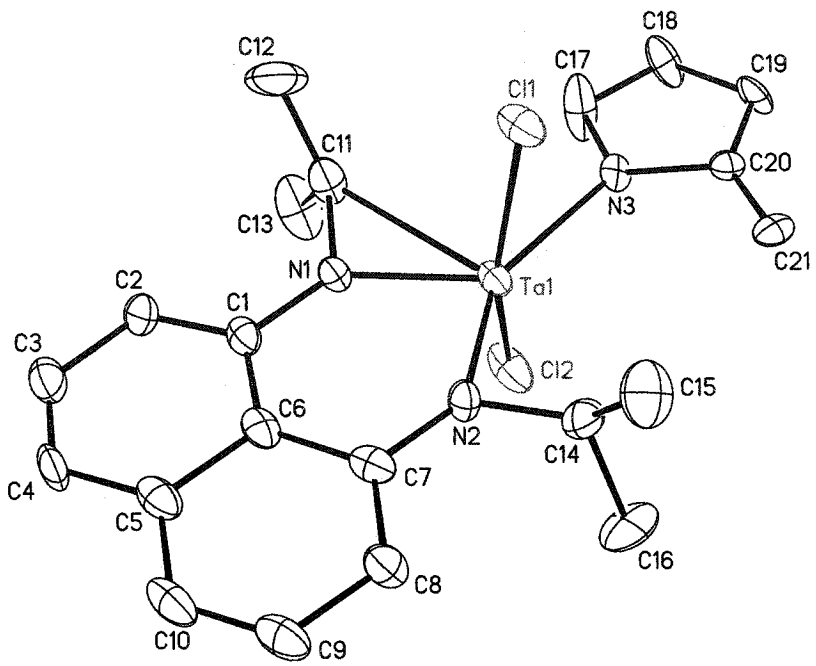

Figure 3.4. Two views of the molecular structure and atom numbering scheme for compound **9**. Hydrogen atoms have been omitted for clarity. Thermal ellipsoids are drawn at 30% probability.

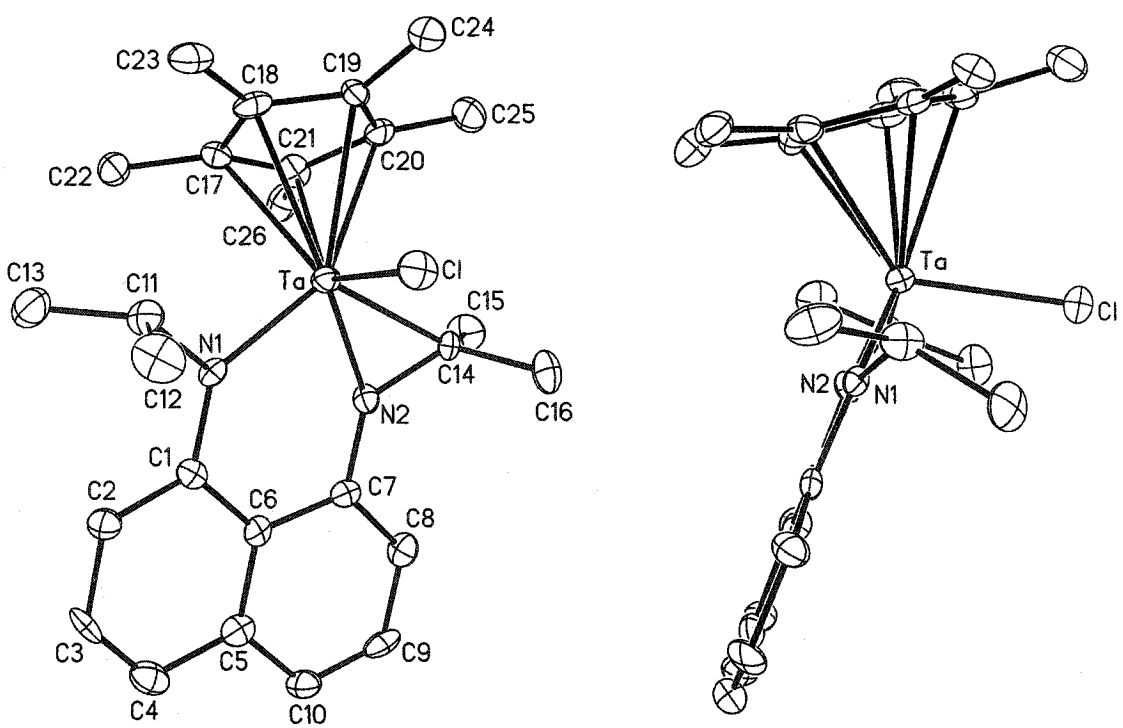

Figure 3.5. The molecular structure and atom numbering scheme for compound **11-THF**. Hydrogen atoms and co-crystallized toluene (0.5 eq.) have been omitted for clarity. Thermal ellipsoids are drawn at 30% probability. The C(18) position is modeled with a 25% chloride / 75% carbon occupancy.

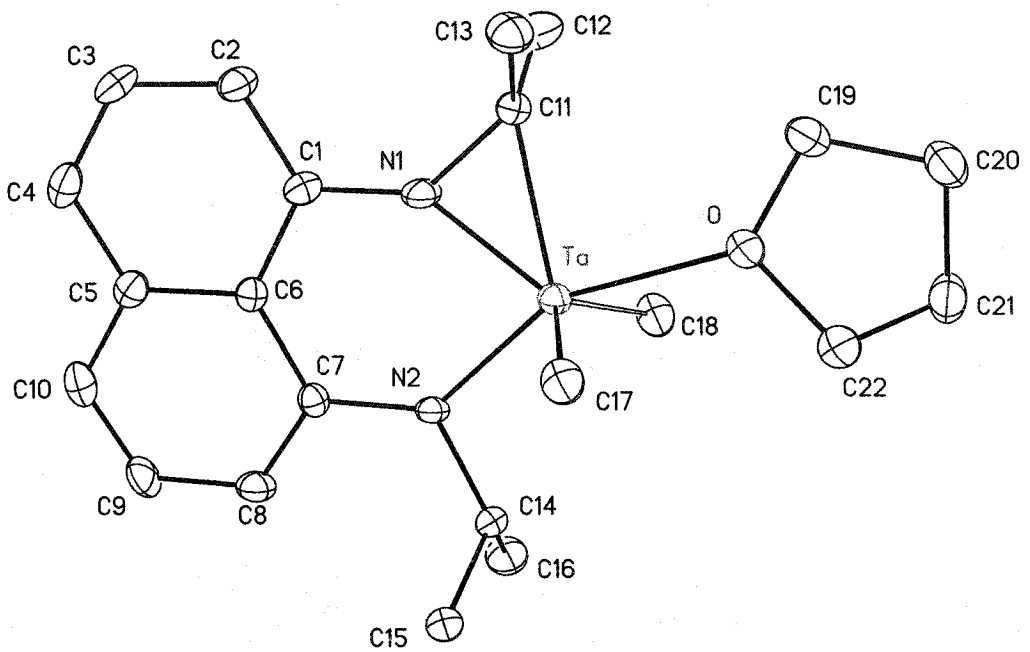

Table 3.1. Selected Crystal Data and Data Collection Parameters for **7**, **7-py2**, **8**, and **9**.

	7	**7-py$_2$**	**8**	**9**
empirical formula	$C_{44}H_{50}Cl_4N_4Ta_2$	$C_{26}H_{29}Cl_2N_4Ta$	$C_{30}H_{37}Cl_2N_3Ta$	$C_{26}H_{34}ClN_2Ta$
formula weight	1138.58	649.38	691.48	590.95
T (K)	203(2)	203(2)	203(2)	203(2)
wavelength (Å)	0.71073	0.71073	0.71073	0.71073
crystal system	Triclinic	Monoclinic	Triclinic	Orthorhombic
space group	P-1	$P2_1/n$	P-1	Pbcn
a (Å)	9.085(1)	9.156(4)	10.093(2)	23.328(2)
b (Å)	9.529(1)	17.591(7)	16.240(2)	10.1925(9)
c (Å)	13.481(2)	16.213(7)	19.669(3)	19.3464(17)
α (deg)	110.555(2)	90	70.143(2)	90
β (deg)	95.041(2)	104.466(7)	81.021(3)	90
γ (deg)	95.855(2)	90	80.977(3)	90
V (Å^3)	1077.4(2)	2529(2)	2976.4(8)	4599.9(7)
Z	1	4	4	8
abs coeff (mm^{-1})	5.358	4.580	3.895	4.911
final R indices	R1 = 0.0355	R1 = 0.0592	R1 = 0.0442	R1 = 0.0498
	wR2 = 0.0650	wR2 = 0.1169	wR2 = 0.0807	wR2 = 0.1090

Table 3.2. Selected Crystal Data and Data Collection Parameters for **11-THF**

	11-THF-(0.5 Toluene)
empirical formula	$C_{25.25}H_{36.25}Cl_{0.25}N_2OTa$
formula weight	573.68
T (K)	203(2)
wavelength (Å)	0.71073
crystal system	Monoclinic
space group	P2(1)/n
a (Å)	9.964(1)
b (Å)	14.195(2)
c (Å)	16.896(2)
α (deg)	90
β (deg)	93.453(2)
γ (deg)	90
V (Å^3)	2385.4(5)
Z	4
abs coeff (mm^{-1})	4.654
final R indices	R1 = 0.0359
	wR2 = 0.0623

Table 3.3. Selected Bond Distances and Angles for **7**

Bond Distances (Å)			
Ta-N(1)	1.911(3)	Ta-Cl(1)	2.347(3)
Ta-N(2)	1.918(3)	Ta-Cl(2)	2.446(3)
Ta-C(11)	2.418(6)	Ta-Cl(2)#1	2.617(3)
N(1)-C(11)	1.454(6)	N(2)-C(14)	1.413(7)
N(1)-C(1)	1.405(5)	N(2)-C(7)	1.411(5)
Bond Angles (deg)			
N(1)-Ta-N(2)	81.64(16)	Cl(1)-Ta-Cl(2)	151.9(4)
N(2)-Ta-C(14)	35.49(18)	Cl(1)-Ta-Cl(2)#1	82.1(3)
N(2)-C(14)-Ta	52.0(2)	Cl(2)-Ta-Cl(2)#1	75.39(11)
C(14)-N(2)-Ta	92.5(3)	C(11)-N(1)-Ta	90.9(3)
internal TaN(2)C(14) angles	179.99	C(1)-N(1)-C(11)	129.0(4)
C(14)-N(2)-C(7)	128.9(4)	C(1)-N(1)-Ta	140.1(3)
C(7)-N(2)-Ta	138.6(3)		

Table 3.4. Selected Bond Distances and Angles for **7-py$_2$**

Bond Distances (Å)			
Ta-N(1)	2.03(2)	Ta-N(3)	2.463(17)
Ta-N(2)	1.990(15)	Ta-N(4)	2.618(18)
Ta-C(11)	2.34(2)	Ta-Cl(1)	2.408(6)
N(1)-C(1)	1.33(2)	Ta-Cl(2)	2.361(6)
N(1)-C(11)	1.44(2)	N(2)-C(7)	1.543(17)
		N(2)-C(14)	1.48(3)
Bond Angles (deg)			
N(1)-Ta-N(2)	81.1(7)	Cl(2)-Ta-Cl(1)	163.3(2)
N(1)-Ta-C(11)	37.7(6)	N(1)-Ta-Cl(1)	97.3(5)
N(2)-Ta-N(4)	98.3(6)	N(1)-Ta-Cl(2)	99.0(5)
N(3)-Ta-N(4)	70.2(5)	N(2)-Ta-Cl(1)	93.5(5)
C(11)-Ta-N(3)	72.7(7)	N(2)-Ta-Cl(2)	92.4(5)
sum of equatorial angles	360.0	C(1)-N(1)-C(11)	138.3(18)
N(1)-C(11)-Ta	59.5(11)	C(1)-N(1)-Ta	137.4(14)
C(11)-N(1)-Ta	82.7(13)	C(14)-N(2)-C(7)	118.5(15)
internal TaN(1)C(11) angles	179.9	C(14)-N(2)-Ta	109.4(14)
		C(7)-N(2)-Ta	131.9(11)

Table 3.5. Selected Bond Distances and Angles for **8**

Bond Distances (Å)			
Ta(1)-N(1)	1.972(6)	Ta(1)-Cl(1)	2.378(2)
Ta(1)-N(2)	1.899(7)	Ta(1)-Cl(2)	2.363(3)
Ta(1)-N(3)	2.398(11)	Ta(1)-C(11)	2.620(9)
N(1)-C(1)	1.404(10)	Ta(1)-C(14)	2.349(10)
N(1)-C(11)	1.474(11)	N(2)-C(7)	1.387(11)
N(3)-C(20)	1.4200	N(2)-C(14)	1.418(9)
Bond Angles (deg)			
N(2)-Ta(1)-N(1)	81.0(3)	Cl(2)-Ta(1)-Cl(1)	157.56(9)
N(1)-Ta(1)-C(11)	33.9(3)	N(2)-Ta(1)-Cl(1)	100.1(2)
N(3)-Ta(1)-C(11)	94.8(4)	N(2)-Ta(1)-Cl(2)	100.5(2)
N(2)-Ta(1)-N(3)	150.4(4)	Cl(1)-Ta(1)-N(3)	79.9(4)
C(11)-N(1)-Ta(1)	97.9(5)	Cl(2)-Ta(1)-N(3)	77.8(4)
C(1)-N(1)-C(11)	124.2(7)	C(14)-N(2)-Ta(1)	88.9(5)
C(1)-N(1)-Ta(1)	137.9(6)	C(7)-N(2)-C(14)	129.4(8)
		C(7)-N(2)-Ta(1)	141.6(6)

Table 3.6. Selected Bond Distances and Angles for **9**

Bond Distances (Å)			
Ta-N(1)	2.036(7)	Ta-C(17)	2.472(9)
Ta-N(2)	1.935(8)	Ta-C(18)	2.560(9)
Ta-C(14)	2.248(9)	Ta-C(19)	2.551(10)
Ta-Cl	2.347(3)	Ta-C(20)	2.499(10)
N(2)-C(7)	1.372(11)	Ta-C(21)	2.408(10)
N(2)-C(14)	1.405(11)	N(1)-C(1)	1.416(11)
		N(1)-C(11)	1.501(11)
Bond Angles (deg)			
N(2)-Ta-N(1)	79.9(3)	N(1)-Ta-Cl	98.5(2)
N(2)-Ta-C(14)	38.3(3)	N(2)-Ta-Cl	106.1(2)
N(2)-C(14)-Ta	58.7(4)	C(14)-Ta-Cl	94.2(3)
C(14)-N(2)-Ta	83.0(5)	N(1)-Ta-C(17)	93.6(3)
internal TaN(2)C(14) angles	179.0	C(14)-Ta-C(20)	82.9(3)
C(7)-N(2)-Ta	144.2(6)	N(1)-Ta-C(21)	117.6(3)
C(7)-N(2)-C(14)	131.5(8)	N(2)-Ta-C(21)	106.7(3)
C(11)-N(1)-Ta	107.3(6)	C(1)-N(1)-C(11)	117.5(8)
C(1)-N(1)-Ta	134.2(6)		

Table 3.7. Selected Bond Distances and Angles for **11-THF-(0.5 Toluene)**

Bond Distances (Å)			
Ta-N(1)	1.923(5)	Ta-Cl	2.305(3)
Ta-N(2)	2.004(4)	Ta-O	2.272(4)
Ta-C(11)	2.189(5)	N(1)-C(1)	1.366(7)
Ta-C(17)	2.192(5)	N(1)-C(11)	1.426(6)
N(2)-C(7)	1.420(6)	N(2)-C(14)	1.477(6)
Bond Angles (deg)			
N(1)-Ta-N(2)	80.60(17)	N(1)-Ta-C(17)	107.2(2)
N(1)-Ta-C(11)	39.93(18)	N(2)-Ta-C(17)	93.01(18)
C(11)-Ta-O	85.97(17)	C(11)-Ta-C(17)	107.7(2)
N(2)-Ta-O	153.87(16)	C(17)-Ta-O	77.33(17)
C(11)-N(1)-Ta	80.1(3)	O-Ta-Cl	77.75(13)
C(1)-N(1)-C(11)	136.1(5)	C(17)-Ta-Cl	136.40(18)
C(1)-N(1)-Ta	143.8(4)	C(14)-N(2)-Ta	105.1(3)
		C(7)-N(2)-Ta	134.8(3)
		C(7)-N(2)-C(14)	120.1(4)

4 Stable Carbenes

I. Introduction

A carbene is best described as a neutral divalent carbon atom possessing only 6 electrons in its valence shell. The formation of two bonds with the substituents accounts for 4 electrons, leaving behind two non-bonding electrons. A disubstituted carbon can possess one of two limiting geometries, linear or bent. A linear arrangement leads to a carbon which has an approximate sp-hybridization leaving two remaining p-type orbitals, orthogonal to the axis of the molecule and to each other. Unless other factors are at play, the two orbitals would have degenerate energies, favouring an electronic configuration with one unpaired electron in each orbital (triplet state) as predicted by Hund's rule. However the substituents, through orbital interactions or by forcing the carbon into a bent geometry, can cause the energies of the empty orbitals to become inequivalent. A bent structure forces the carbon to adopt an sp^2-hybridization which causes the two orbitals to possess different shapes, orientations, and ultimately different energies. The size of the energy gap will determine

whether the singlet or the triplet state is energetically favourable.[1] In general if the energy gap is larger than the pairing energy for a doubly occupied orbital, then the singlet state should be the most stable.

Carbenes are such fascinating species because though they are electron deficient, the carbene can behave as a nucleophile. This can be rationalized if both remaining electrons choose to occupy the same orbital, effectively forming a lone-pair. Whether this is the preferred electronic arrangement depends on the nature of the two substituents on the carbon, and the resulting structure of the carbene.

Carbenes have long been known as reactive intermediates in organic transformations,[2] however substantial effort has been invested in the preparation of a stable species. A breakthrough came in the early 90's with the first report of a room-temperature stable carbene, 1,3-di-1-adamantylimidazol-2-ylidene[3] (**J**, R = Adamantyl). This represented the first example of what would turn out to be a class of carbenes termed N-heterocyclic carbenes (NHCs). Since this initial development, carbene chemistry has seen tremendous advances that have moved these fascinating species into the realm of isolable, commercial compounds.[4,5] The preparation of stable NHCs of type **J** and **K** (Chart 4.1) represents a synthetic milestone,[6] and their swift application as ligands for the stabilization of transition metal compounds has been particularly successful. They are rapidly usurping the role of ubiquitous donor ligands (e.g., phosphines) in transition metal catalyzed reactions.[7]

The ylidenes **J** and **K** represent the typical architectures of stable nucleophilic singlet carbenes. These species have been largely restricted to five-membered heterocyclic rings.[8]

---

[1] Hoffmann, R. *J. Am. Chem. Soc.* **1968**, *90*, 1475-1485.
[2] (a) *Advances in Carbene Chemistry*; Brinker, U. H., Ed.; Jai Press: Greenwich and Stamford, 1994 and 1998 and 2001; Vols. 1, 2 and 3. (b) *Carbenes*; Jones, M., Moss, R. A., Eds.; Wiley: New York, 1973 and 1975; Vols. 1 and 2.
[3] Arduengo, III, A. J.; Harlow, R. L; Kline, M. *J. Am. Chem. Soc.* **1991**, *113*, 361-363.
[4] *Carbene chemistry*: from fleeting intermediates to powerful reagents; Bertrand, G., Ed.; Marcel Dekker: New York, 2002.
[5] For reviews see (a) Bourissou, D.; Guerret, O.; Gabbaï, F. P.; Bertrand, G. *Chem. Rev.* **2000**, *100*, 39-91. (b) Herrmann, W. A.; Köcher, C. *Angew. Chem. Int. Ed.* **1997**, *36*, 2162-2187.
[6] For the first report of a saturated NHC (**B**) see: Arduengo, III, A. J.; Goerlich, J. R.; Marshall, W. J. *J. Am. Chem. Soc.* **1995**, *117*, 11027-11028.
[7] Herrmann, W. A. *Angew. Chem. Int. Ed.* **2002**, *41*, 1291-1309.
[8] Six-membered ring carbene are reported in: (a) Alder, R. W.; Blake, M. E.; Bortolotti, C.; Bufali, S.; Butts, C. P.; Linehan, E.; Oliva, J. M.; Orpen, A. G.; Quayle, M. J. *Chem. Commun.* **1999**, 241. (b) Guillen, F.; Winn, C. L.; Alexakis, A. *Tetrahedron: Asymmetry* **2001**, *12*, 2083.

The more stable species, those having an unsaturated structure of type **J**, possess the 6π electron structure expected for aromatic systems.[9,10] The stability of the diaminocarbenes stems from both the bent structure imposed by the heterocycle (breaks orbital degeneracy) and some degree of orbital overlap of the empty p_z orbital on the $C_{carbene}$ with the nitrogen lone-pairs. The sum of these factors determines whether the singlet state is the favoured electronic arrangement.

Chart 4.1

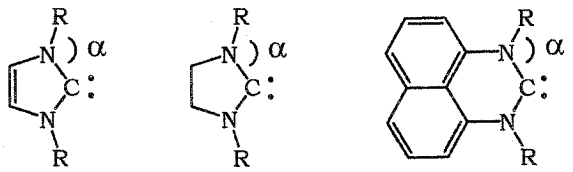

J **K** **L**

We desired to undertake the design and development of new stable singlet carbenes possessing different scaffolds and electronic structures. Realizing the structural similarities between the diamine scaffolds of carbenes **J** and **K** and the N,N'-disubstituted-1,8-DAN frame, we decided to use dialkyl 1,8-DAN ligands for the stabilization of novel carbenes, which ultimately would possess a perimidine core (**L**). Such carbenes will differ from the known examples in two respects. First the carbene centre will be part of a six-membered ring. This has significant implications on the steric impact of the N substituents (R), it effectively pushes them closer to the carbene atom, increasing the steric pressure on both the carbene and for a coordinated metal (smaller α angle, Chart 4.1). Second, the extended aromatic system of the perimidine places the divalent carbon in a formally seven π-electron, six-membered heterocyclic ring.[11] This could increase the nucleophilic character of the carbene, resulting in a more electron donating ligand.

---

[9] For the report of an annelated carbene (benzimidazol-2-ylidenes), see: (a) Liu, Y.; Lindner, P. E.; Lemal, D. M. *J. Am. Chem. Soc.* **1999**, *121*, 10626. (b) Hahn, F. E.; Wittenbecher, L.; Le Van, D.; Fröhlich, R. *Angew.* Chem., Int. Ed. **2000**, *39*, 541.

[10] (a) Heinemann, C.; Müller, T.; Apeloig, Y.; Schwarz, H. *J. Am. Chem. Soc.* **1996**, *118*, 2023. (b) Boehme, C.; Frenking, G. *J. Am. Chem. Soc.* **1996**, *118*, 2039.

[11] *Handbook of Heterocyclic Chemistry*, 2nd ed.; Katritzky, A. R., Pozharskii, A. F., Eds.; Pergamon: New York, 2000.

II. Results and Discussion

A. Perimidinium Salts

The decade or so of work on the preparation of stable carbenes has unveiled several synthetic routes to these interesting species. There are two basic approaches, deprotonation of a cationic carbene precursor or reduction of species such as thioureas. The simplicity of the acid-base reaction involved in the first method directed us to explore that route. Thus we established the perimidinium cation as the target precursor compound, from which could be prepared the desired carbene.

Our previous work on utilizing dialkyl 1,8-DAN ligands allowed us to prepare the desired perimidinium salt rather easily. The diamine **4a** reacts with an excess of triethyl orthoformate under acidic conditions leading to the formation the 1,3-diisopropylperimidinium salts (**13a** and **13b**) with a variety of counter anions depending on the acid that is employed (Scheme 4.1). In the case of the formate, which is often obtained with co-crystallized formic acid and THF, the counter anion can be exchanged for a chloride, by washing a methylene chloride solution of the perimidinium salt with a highly concentrated NaCl solution, containing an appropriate quantity of NaOH, leading to the perimidinium chloride **14**. The use of ammonium bromide as an acid to generate the

Scheme 4.1

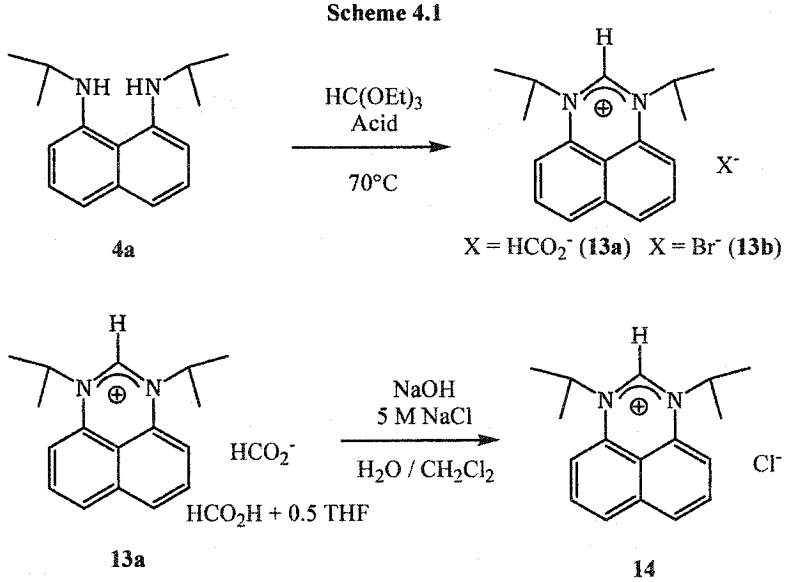

perimidinium bromide is hampered by difficulties in separating any unreacted NH_4Br salt from the product.

The molecular structure of the perimidinium salts **13a** and **14** were determined by single-crystal X-ray diffraction studies and the results are presented in Figure 4.1. Selected bond lengths and angles are listed in Tables 4.3 and 4.4. In both structures a delocalized cationic charge seems to be the best description of the bonding. This is supported by the fact that the both C-N bonds are equivalent in each structure. Their average value of 1.33 Å is indicative of a C-N bond order of 1.5.[12] The N-C-N angles are 125.7(8)° and 124.5(4)° for the formate and chloride structures respectively. The average α angle (Chart 4.1) is the same in both structures at 120°.

A more general approach to the preparation of perimidinium salts is to start from the unsubstituted or monosubstituted perimidine and then introduce the nitrogen substituents subsequently (Scheme 4.2). Varying slightly on a reported procedure, reaction of 1,8-DAN with triethyl orthoformate in the presence of a catalytic amount of formic acid results in the

Scheme 4.2

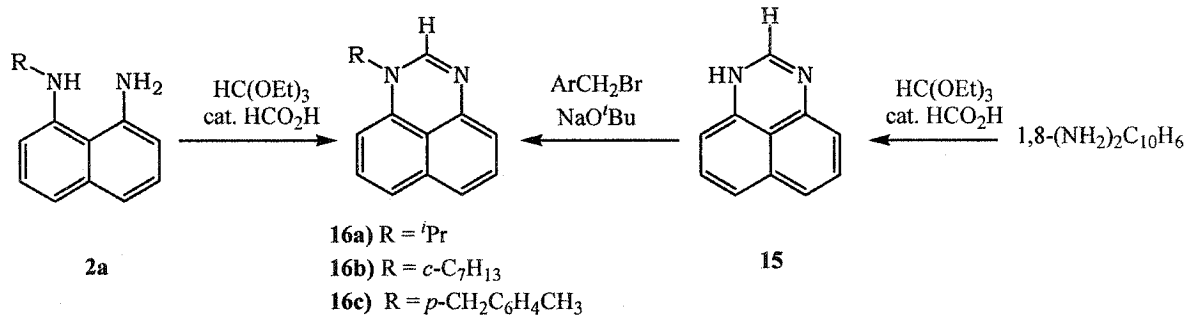

2a

16a) R = ^{i}Pr
16b) R = *c*-C_7H_{13}
16c) R = *p*-$CH_2C_6H_4CH_3$

15

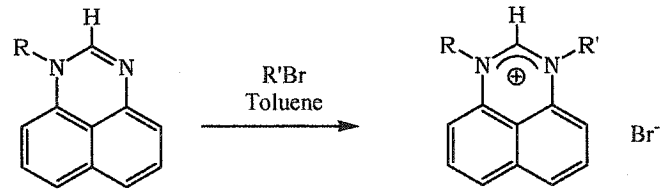

16a) R = ^{i}Pr
16b) R = *c*-C_7H_{13}
16c) R = *p*-$CH_2C_6H_4CH_3$

17a) R = ^{i}Pr R' = CH_2Ph
17b) R = ^{i}Pr R' = $CH_2C_6F_5$
17c) R = ^{i}Pr R' = *p*-$CH_2C_6H_4CH_3$
17d) R = *c*-C_7H_{13} R' = *p*-$CH_2C_6H_4CH_3$
17e) R = *c*-C_7H_{13} R' = $CH_2C_6F_5$
17f) R = R' = *p*-$CH_2C_6H_4CH_3$

[12] Burke-Laing, M; Laing, M. *Acta Crystallogr., Sect. B* **1976**, *32*, 3216-3223.

formation of 1H-perimidine (**15**).[13] Similarly, reacting mono-alkylated 1,8-DAN under the same conditions leads to the formation of 1-alkyl-perimidines (**16**). The unsubstituted perimidine (**15**) can be converted into a benzylated derivative via a substitution reaction with benzyl bromide in the presence of a base.[13] The nature of the base is somewhat arbitrary, NaOH works but NaO^{t}Bu is preferred due to it's solubility in toluene. The reaction is performed at room temperature in order to avoid the quaternization of the second nitrogen, which can happen at higher temperatures (see formation of **17**). This is avoided in order to allow for the isolation and purification of the 1-alkyl-perimidine, which is easily done via column chromatography. Starting with very pure 1-alkyl-perimidines makes the subsequent salt formation step high yielding and avoids the need for purification of the salts. However, thus far we have only explored using benzyl bromide derivatives for the alkylation of 1H-perimidine. This pathway was explored initially out of necessity because the preparation of N-benzyl-1,8-DAN was not possible via the reductive amination route utilized for the secondary alkyls.

Using a bifunctional electrophile allows us to prepare linked or bridged diperimidinium salts (Scheme 4.3). For instance the use of α,α'-dibromo-*o*-xylene gives *o*-xylyl bridged diperimidinium dibromide (**18a**). Likewise using α,α'-dibromo-*p*-xylene yields the *para*-bridged salt (**18b**). The diperimidinium salts are significantly less soluble than the monofunctional versions in organic solvents, and require very polar solvent such as

Scheme 4.3

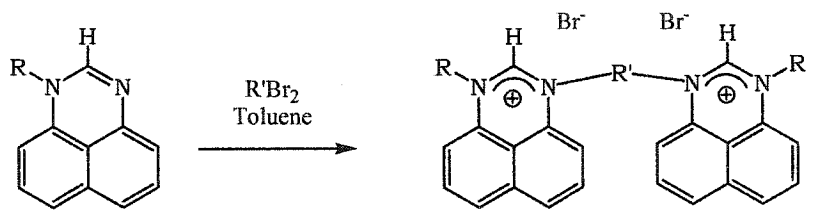

16

18a R = ^{i}Pr R' = *o*-$CH_2C_6H_5CH_2$,
18b R = ^{i}Pr R' = *p*-$CH_2C_6H_4CH_2$

DMSO or methanol to solubilize them for analytical purposes. Compound **18a** was crystallized by layering a DMF solution of the salt with hexane, and the crystals were used to obtain the molecular structure (Figure 4.2) via an X-ray diffraction study (Table 4.1). Selected bond lengths and angles are listed in Table 4.5. The general bonding within the

[13] Herbert, J. M.; Woodgate, P. D.; Denny, W. A. *J. Med. Chem.* **1987**, *30*, 2081-2086.

perimidinium moiety is essentially the same in the diperimidinium (**18a**) as it is for **13a** and **14**.

B. Free Carbenes

Generating stable carbenes from protonated precursors has proven to be a fairly general method for accessing these species. This has also allowed for the *in situ* preparation of carbenes, since many catalytic processes require a base which can serve as reagents and as a deprotonating agent for generating the carbene ligand. One of the most common bases used for this purpose is the *tert*-butoxide anion. However, reacting **14** with one equivalent of NaO^tBu does not yield the desired free carbene. The isolated product for this reaction is compound **19** (Scheme 4.4). The formation of this α-diamino ether (**19**) is intriguing because there is two distinct ways in which one can reasonably imagine the formation of the product. Instead of behaving like a base, the butoxide can add via nucleophilic addition to the carbocation, yielding compound **19** and NaCl. However, the steric encumbrance afforded by the *tert*-butyl group generally prohibits nucleophilic additions for this reagent, explaining its popularity as a non-nucleophilic base. Otherwise **19** could be formed in a two step process where first the free carbene is formed then reacts with the alcohol that is generated during the deprotonation.

Scheme 4.4

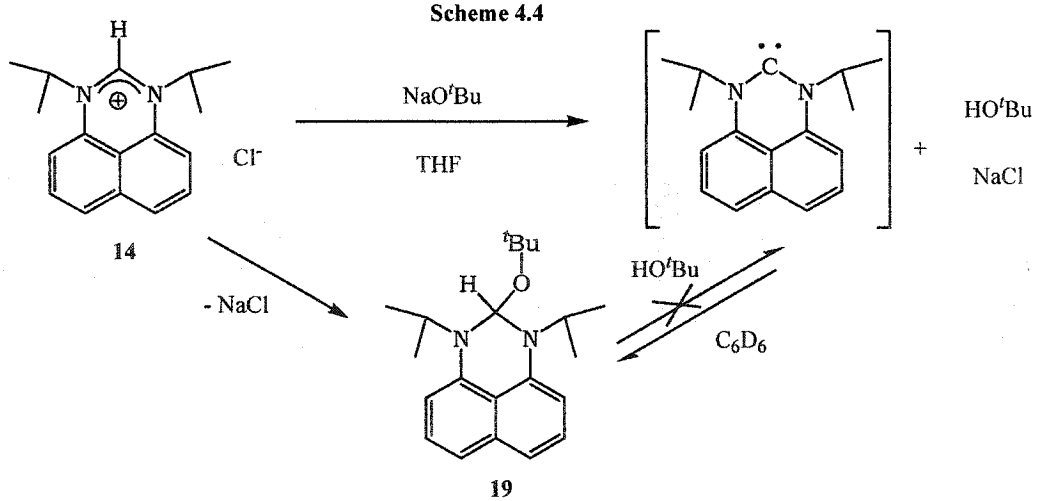

The ^1H NMR of **19** displays one septet signal for the ipso protons of both ^iPr groups, but two doublets for the methyl moieties. The appearance of diastereotopic methyl groups reveals that the central carbon does not interchange geometry, i.e. that the butoxy and hydrogen groups do not interchange positions on an NMR timescale. These observations

indicate that if **19** is formed by reaction of the carbene with the alcohol then the reaction is not reversible, at least not on an NMR timescale.

Encouraged by the evidence supporting a carbene intermediate, we decided to investigate the use of bulkier, less nucleophilic bases for the generation of the carbene. Reacting the perimidinium salt **14** with one equivalent of LiHMDS (lithium hexamethyldisilazide) leads to the formation of the desired carbene, compound **20** (Scheme 4.5). The solubility of the product of this reaction in non-polar solvents such as hexane and toluene immediately indicated that it was a neutral species rather than the ionic starting material. The ^{1}H NMR of the product revealed the disappearance of the downfield proton (C2 position in **14**) suggesting a successful deprotonation. However the most distinctive feature which characterizes the product as a free carbene is a ^{13}C NMR (C_6D_6) signal for the $C_{carbene}$ at δ 241.7 ppm. The extreme downfield chemical shift for this carbon signal indicates the highly deshielded, or electron poor, configuration for the $C_{carbene}$ atom. The position of the signal is reminiscent of the saturated species **K**, which generally appear in the range of 235-245 ppm compared to the $C_{carbene}$ signals of unsaturated carbenes of type **J** which appear further upfield in the 205-220 ppm region.[14] A symmetrical structure for **20** was supported by a single set of ^{1}H NMR signals for the N-^{i}Pr groups.

Scheme 4.5

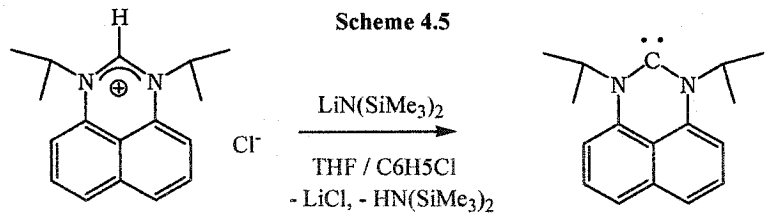

14 **20**

The formulation of compound **20** as a stable monomeric carbene, was supported by the NMR results, however there remained the possibility of the carbene existing as a dimer (enetetramine) at lower temperatures or in the solid state. Single-crystal X-ray diffraction analysis (Table 4.1) confirmed the monomeric structure of **20** (Figure 4.3). Selected bond distances and angles are listed in Table 4.6. In addition to the two-coordinate environment of C(1), several features of this structure, including the planar geometry around the N atoms, and the short N-$C_{carbene}$ distances with an average of 1.359(6) Å, are consistent with that of a

[14] For a summary of ^{13}C shifts for typical carbenes see: Herrmann, W. A.; Öfele, K.; Preysing, D. v.; Herdtweck, E. *J. Organomet. Chem.* **2003**, *684*, 235-248.

carbene structure. This value is slightly longer than for the cation precursors, which possess delocalized double bonds. The longer N-C_{ring} bond lengths (average = 1.414(6) Å) suggest that the N lone-pairs are more involved with bonding to $C_{carbene}$ than to the naphthyl ring. The N-$C_{carbene}$-N angle in **20** of 115.3° is considerably larger than the analogous angles observed for isolated carbenes of type **J** and **K**, which fall in the 100-110° range. We anticipated a decrease in the α angle upon moving from the five-membered ring to the six-membered ring geometry. Typical values of α for structures of type **J/K** are 122-123°.[3,6,15] As predicted the observed α values in **20** average 115.5° and are the smallest of the three angles around the N centres. Interestingly the α angle in **20** is smaller than in the cationic precursor. The result is an increased steric impact of the nitrogen substituents on the $C_{carbene}$ centre and this will have a concomitant effect of the reactivity of this centre and of metal complexes of **20**.

In order to shed some light on the results of our earlier attempts at generating the carbene using NaO^{t}Bu, we reacted the free carbene (**20**) with ^{t}BuOH. The NMR experiment showed that the alcohol reacted immediately (faster then we could get the sample to the NMR spectrometer, <5 minutes) to cleanly generate the same product **19** (Scheme 4.4). Again the presence of diastereotopic methyls for the ^{i}Pr group implies that there is either no equilibrium with the carbene, or that it does not occur under these conditions.

Unsaturated carbenes of type **J** can usually be generated by deprotonation with a butoxide base, but when trying to generate saturated carbene analogues, type **K**, alkoxides also sometimes yield α-diamino ethers.[16] However it is unclear as to whether the alkoxides add directly to the cationic precursors, or if an intermediate carbene is generated which then reacts with the alcohol that is produced. Considering α-diamino ethers are sometimes used as carbene precursors for transferring a carbene moiety to a transition metal upon heating, it is logical to assume that the α-diamino ethers of type **K** are in equilibrium with the carbene and alcohol. Our result suggests that the reactive properties of **20** are closer to those of saturated carbenes, than the more stable unsaturated analogues. However, saturated NHCs are well known to dimerize irreversibly unless the $C_{carbene}$ centre is extremely well protected by very large N substituents and compound **20** shows no signs of dimerizing.

---

[15] Denk, M. K.; Thadani, A.; Hatano, K.; Lough, A. J. *Angew. Chem. Int. Ed. Engl.* **1997**, *36*, 2607-2609.
[16] Scholl, M.; Ding, S.; Lee, C. W.; Grubbs, R. H. *Org. Lett.* **1999**, *1*, 953-956.

The kinetic stabilization of carbenes, via the steric protection afforded by the bulky substituents is a well established factor in the generation of stable carbenes.[15] Although not impressive in size, the ^{i}Pr groups on the N centres are secondary alkyl groups and could be an important factor that prevents further reactivity (e.g. dimerization) of the carbene. The benzylated perimidiniums (**17a-f**) on the other hand possess at least one primary alkyl substituent. It can be envisioned that the phenyl ring of the benzyl substituent can easily rotate to one side of the naphthyl plane and allow substrates, like a second carbene molecule, to approach and react with the $C_{carbene}$ atom.

Despite the reduction in sterics, the benzyl perimidinium derivatives **17a**, **17c**, and **17d** can be deprotonated with one equivalent of LiHMDS to cleanly generate the free carbenes **21a**, **21b**, and **21d** (Scheme 4.6). The monomeric nature of the products is evinced by the ^{13}C NMR of the compounds which all contain a $C_{carbene}$ signal at similar chemical shifts as compound **20** (**21a** = 245.3, **21a** = 245.1, **21d** = 246.6 ppm). The only significant difference in the NMR spectra of the benzyl derivatives compared to **20** is that the aromatic

Scheme 4.6

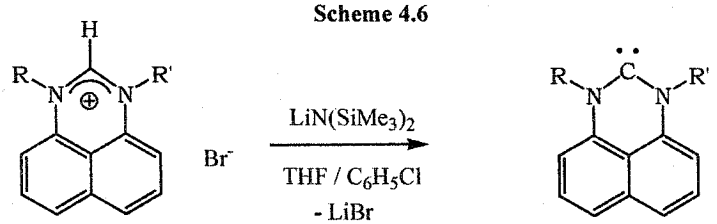

17a) R = ^{i}Pr R' = CH_2Ph
17c) R = ^{i}Pr R' = *p*-$CH_2C_6H_4CH_3$
17d) R = *c*-C_7H_{13} R' = *p*-$CH_2C_6H_4CH_3$

21a) R = ^{i}Pr, R' = $CH_2C_6H_5$
21c) R = ^{i}Pr, R' = *p*-$CH_2C_6H_4CH_3$
21d) R = *c*-C_7H_{13}, R' = *p*-$CH_2C_6H_4CH_3$

protons for the naphthalene backbone generate six signals instead of three, which is indicative of the unsymmetric nature of the compounds. However, as with **20** the methyls of the ^{i}Pr substituents in **21a**, **21c**, and **21d** are equivalent, signifying there is a mirror plane coincident with the naphthyl-$NC_{car}N$ plane within the molecule.

Steric protection may however still play an important role in the stabilization of the carbenes **21a**, **21c**, and **21d** . It has been demonstrated that the presence of at least one bulky substituent can be enough to prevent unwanted reactions with the $C_{carbene}$ centre such as

dimerization.[17] On the other hand one can argue that the carbenes are stable due to a large singlet-triplet gap which is imposed by the stabilization of the lone-pair via the σ-withdrawing nitrogens, and the partial occupancy of the empty p-type orbital through π-donation from the nitrogen lone-pairs.

Convinced that monobenzyl derivatives are kinetically stable enough for isolation, we attempted to generate carbenes starting from the pentafluorobenzyl derivatives. Reaction of the perimidinium bromides **17b** and **17e** with one equivalent of LiHMDS did not proceed in the same manner as observed for the non-fluorinated derivatives. Specifically, when compound **17b** is mixed with LiHMDS base, one observes the persistence of a yellow colour typical for perimidinium salts. Initially, this was interpreted as a lack of reaction with the base. However upon typical work-up a yellow toluene soluble product was isolated which suggested that some transformation generating a neutral organic product had occurred. The ^{1}H NMR of the compound contained typical signals for an ^{i}Pr group (septet and doublet) but lacked the expected signal for the methylene protons of the pentafluorobenzyl group. The only other observed signals were in the aromatic region, and included a singlet at 6.86 ppm. The ^{19}F NMR spectra for compound **25e** showed four distinct signals, this being inconsistent with a C_6F_5 ring.

To elucidate the nature of **25b** and **25e**, a single-crystal X-ray diffraction study was performed on **25b** (Table 4.2). The molecular structure is depicted in Figure 4.4 and selected bond lengths and angles are listed in Table 4.7. The structural study revealed that the product is a tetracyclic compound that was apparently generated by the substitution of an *ortho* C-F bond of the pentafluorophenyl by the *in situ* generated carbene. A close look at the results also shows that one of the methylene protons has been eliminated resulting in a sp^2-hybridized configuration for what was originally the benzylic methylene carbon (C14). This explains the lack of signals in the aliphatic region for the substituent, and is also consistent with there being a singlet in the aromatic region since the proton on C14 is not coupled to any other proton in the molecule.

We propose that the overall reaction proceeds in the following manner. A transient carbene species (**22**) is generated upon deprotonation of the perimidinium cation and

[17] Hahn, F. E.; Paas, M.; Le Van, D.; Lügger, T. *Angew. Chem. Int. Ed. Engl.* **2003**, *42*, 5243-5246.

Scheme 4.7

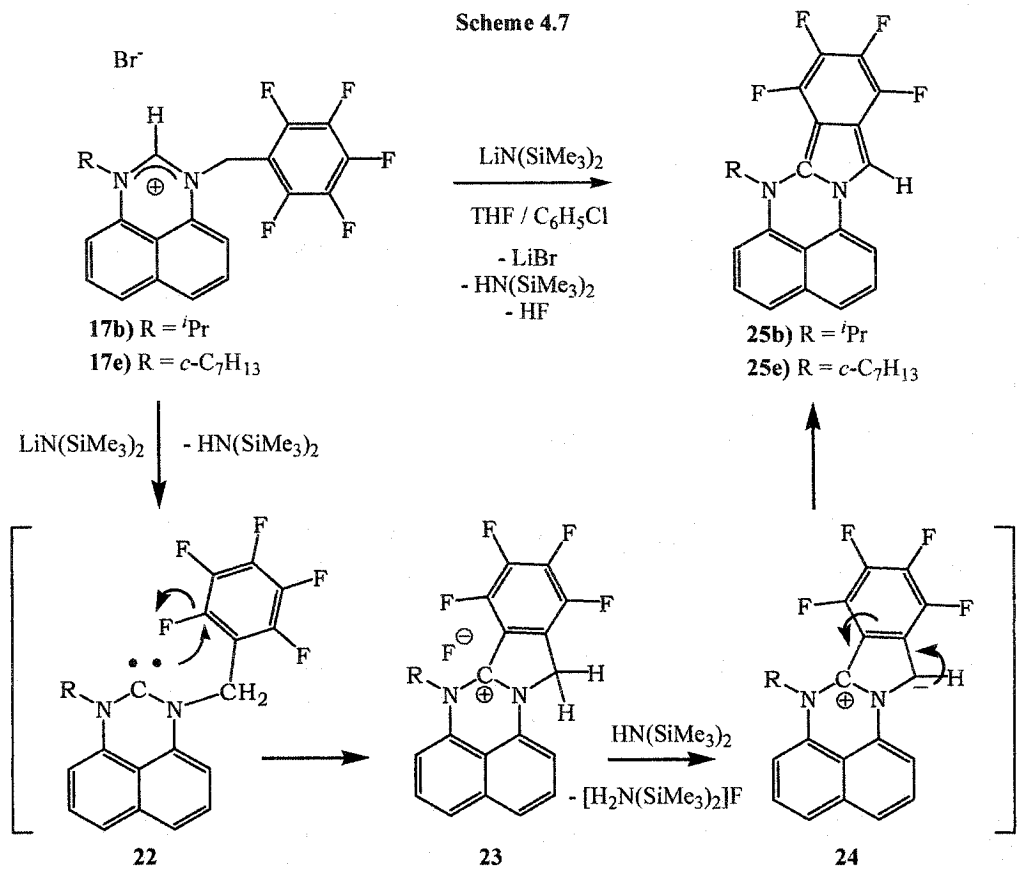

immediately attacks the electrophilic *ortho*-carbon, possibly via a nucleophilic aromatic substitution, to give an intermediate product (**23**). This intermediate then eliminates HF, perhaps as the ammonium salt ($H_2N(SiMe_3)_2F$) via deprotonation by the amine base $HN(SiMe_3)_2$, to yield the polyaromatic compound **25** (Scheme 4.7).

Unlike reactive transient carbenes, stable NHCs do not typically react with C-H or C-X bonds. To our knowledge this is the first report of an NHC activating, or displacing, a fluoride group. However it should be noted that there are no reports of pentafluorobenzyl substituted carbenes of type **J** and **K** and therefore the possibility that these carbenes also react in this manner still exists. This unusual transformation, taken in conjunction with the fact that the free carbene **20** irreversibly adds alcohol suggests that carbenes of type **L** possess properties similar to the more reactive saturated carbenes, than the unsaturated versions.

Interestingly, we had observed that the deprotonation reaction, which yields **20**, commonly generates a small amount of a by-product, which we eventually isolated,

characterized spectroscopically and structurally (Figure 4.5), and identified as being a bis(α-diamino ether) **26** (Scheme 4.8). Table 4.8 lists selected bond lengths and angles. Unique spectroscopic features for compound **26** are observed in the ^{1}H NMR spectrum such as a highly deshielded aliphatic signal for the proton on the triheteroatom-substituted carbon, and two doublets for the diastereotopic methyl groups. The lack of such by-products when preparing the unsymmetrically substituted carbenes suggested that the liquid-liquid anion exchange step in the route to the perimidinium salt **14,** likely introduces a trace of water which is not be completely removed. This adventitious water can react with two carbene species generated during the deprotonation and yield compound **26**. NHCs are known to undergo hydrolysis of N-C bonds in the presence of water to generate formamides.[18] Therefore generation of compound **26** via the addition of water would represent an unusual transformation.

Scheme 4.8

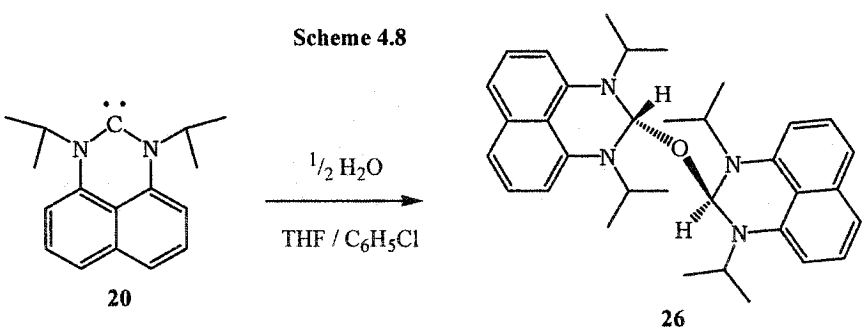

20 **26**

C. Dicarbenes

Our synthetic methodology allowed us to easily extend the preparation of perimidinium cations to that of diperimidinium salts, thus we decided to investigate the synthesis of xylyl bridged dicarbenes. Using the same conditions developed for the preparation of monomeric carbenes **20** and **21**, we attempted the preparation of dicarbenes from diperimidinium salts **18**. Reacting the *para*-xylyl bridged diperimidinium salt with LiHMDS proceeded in a very similar manner to that of the monomeric analogue. The yellow colour of the salt disappeared quickly, and an orange solid was extracted from the dried reaction mixture using toluene, indicating the product was most likely a neutral organic species. The nearly identical N-substituents for the dicarbene **27,** compared to the unsymmetric monocarbenes **21**, and the rigid structure of the linking group would prevent

[18] Denk, M. K.; Rodezne, J. M.; Gupta, S.; Lough, A. J. *J. Organomet. Chem.* **2001**, *617-618*, 242-253.

any intra- or inter-molecular interactions between carbene centres. We therefore assume that

Scheme 4.9

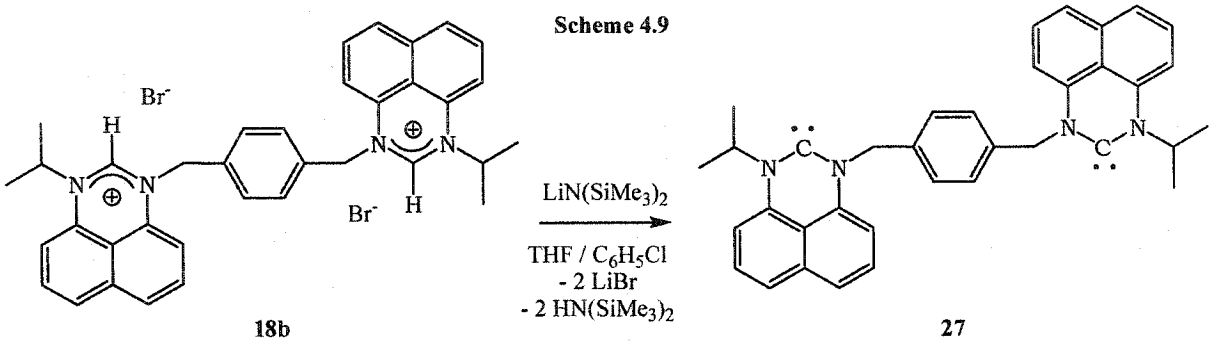

18b **27**

the product of the reaction is the desired dicarbene **27** (Scheme 4.9). The poor solubility of compound **27** in common non-polar solvents and difficulties in recrystallizing the compound from polar solvents prevented us from obtaining pure samples of the dicarbene. However, the lone and distinct $C_{carbene}$ signal in the ^{13}C NMR at 245.2 ppm leaves little question as to its identity.

Reacting the *o*-xylyl bridged diperimidinium bromide **18a** with two equivalents of LiHMDS also proceeded in a typical manner. The off-white product extracted from the reaction mixture with toluene indicated the likelihood of the product being a neutral species. However, ^{1}H NMR spectroscopy indicated that the structure of the product wasn't that of the anticipated dicarbene. The downfield signal for the proton on C2 in **18a** had disappeared, indicating deprotonation had occurred. However the presence of two doublets and one septet for the ^{i}Pr groups and an AB pattern for the xylyl methylene protons suggested that the

Scheme 4.10

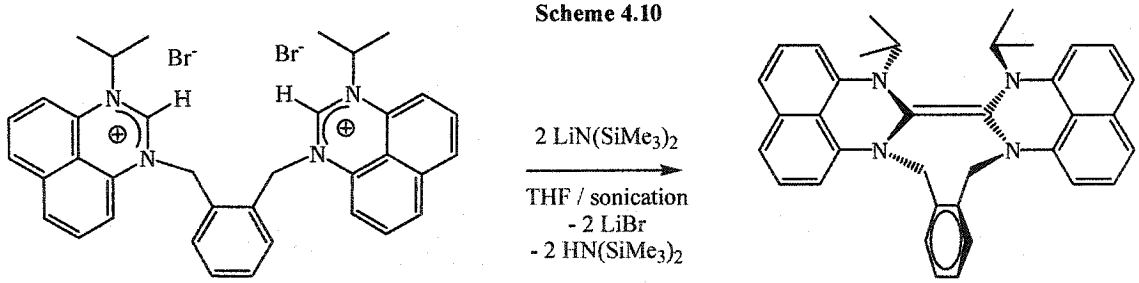

18a **28**

product did not possess the anticipated symmetry for the dicarbene. The ^{13}C NMR confirmed our suspicions since the characteristic signal for a carbene in the δ 230-250 ppm range was absent. The most downfield signal in the spectrum of this compound was at δ 144.5 ppm. Initially we suspected the presence of adventitious water which could have reacted with the two carbene moieties and generated a bis(α-diamino ether) similar to

compound **26**. However, the proton NMR spectrum was void of a signal appropriate for a strongly deshielded aliphatic proton.

A molecular structure for **28** (Scheme 4.10) was obtained via X-ray diffraction in order to determine the nature and structure of the product. The results are illustrated in Figure 4.6 and a list of selected bond lengths and angles is provided in Table 4.9. Compound **28** turned out to be formally a dimerized dicarbene, or in other words an enetetramine. The molecule possesses two perimidine moieties that are linked to each other through the C2 carbon. The nitrogens of each perimidine unit are on opposite sides of the bridging phenyl plane, and the dimerized $C_{carbene}$ atoms meet each other in the middle. The net effect is that the molecule possesses a C_2 axis leading to inequivalent methyls for the ^{i}Pr groups and diastereotopic benzylic protons. The root for the chirality in compound **28** stems from its inability to invert its conformation, and is analogous to atropisomers such as BINAP and BINOL. The C6-C6$^{\#}$1 bond length of 1.346(5) implies is in line with that of a typical double bond.[12] The C6-N bond lengths are longer (1.412(3) and 1.426(3) Å) compared to those of the free carbene **20** (avg 1.359(6) Å), suggesting that the N lone-pairs are less involved in π bonding with the C=C carbon atoms than to the carbenic centre. Another interesting feature of the structure of **28** is that one of the nitrogens (N(5)) has planar geometry whereas the other (N(7)) is pyramidal. This is reflected in the sum of the angles around N(5) and N(7) (Table 4.9). Our current explanation for this structural feature is that the steric repulsion between the two ^{i}Pr groups on N(7) and N(7)# prohibit these centres from achieving a planar configuration.

Chart 4.2

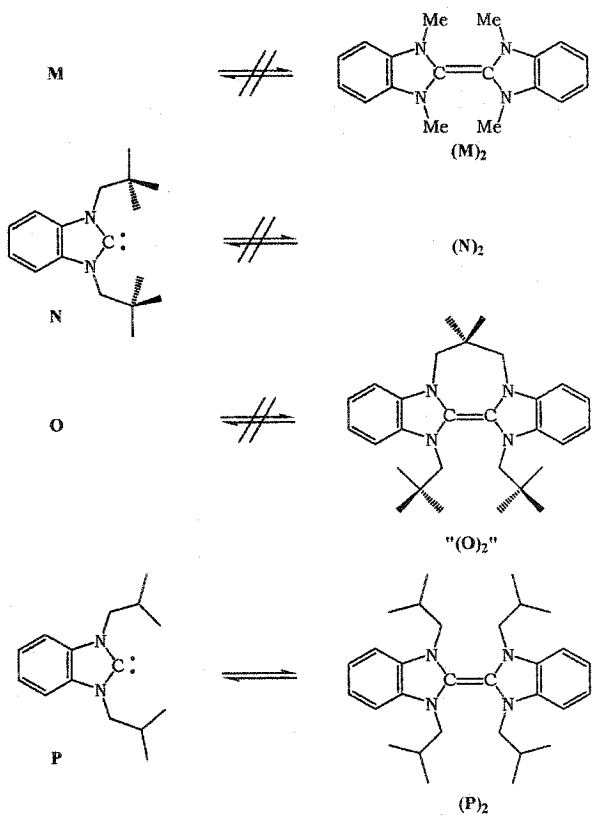

Dimerization of NHCs has been observed, and readily occurs for saturated type **K** derivatives, but is rare for the more stable unsaturated type **J** structures.[19] Dimerization of annelated carbene analogues derived from *o*-phenylenediamines (PDA) has been observed, and studies revealed that olefin formation is highly dependant on the steric bulk of the N-substituents (Chart 4.2).[20] Small N-substituents such as methyl groups lead to the enetetramine **(M)$_2$**, whereas bulky neopentyl groups prevent dimerization **N**. The isobutyl N-substituents are intermediate in size and this results in there being an equilibrium between the carbene **P**, and the dimer **(P)$_2$** at room temperature. Crystallization of the mixture always yields the dimer exclusively. The linked dicarbene **O**, despite possessing large neopentyl groups, is exclusively obtained as the enetetramine **"(O)$_2$"**.

The presence of diastereotopic signals for the methyl groups of **28** rules out the possibility for the dimer to be in equilibrium with the monomers at room temperature. Additionally all of our attempts to cleave the C=C bond of **28** or to generate a dicarbene from **18a** have failed, suggesting that the dimerization is effectively irreversible.

The driving force for carbene dimerization is thought to be thermodynamic in nature and a method for predicting the C=C bond energies was developed by Goddard III and Carter.[21] In summary, the energy gained by the formation of a C=C double bond, which is approximated to that of the bond in ethylene at 172 kcalmol^{-1}, must be larger than the sum of the singlet-triplet gap for both carbene moieties. The singlet-triplet gap for type **J** carbenes has been calculated to be approximately 85 kcalmol^{-1}[22] explaining why they do not form dimers ((2 x 85) -172 = -2 kcalmol^{-1}). On the other hand, type **K** carbenes always dimerize unless sterically protected with bulky N-substituents implying that they possess smaller singlet-triplet gaps. Our results which show that monocarbenes are stable (**20** and **21**), but linked dicarbene **28** dimerizes, suggest that the singlet-triplet gap for perimidine based carbenes is closer in value to those of saturated (**K**) or annelated (PDA) carbenes than to the unsaturated versions. The fact that with the same N-substituents, linked dicarbene **28**

---

[19] Doubly bridged dicarbenes of type **J** have been reported to dimerize: Taton, T. A.; Chen, P. *Angew. Chem. Int. Ed. Engl.* **1996**, *35*, 1011-1013.
[20] Hahn, F. E.; Wittenbecher, L.; Le Van, D.; Fröhlich, R. *Angew. Chem. Int. Ed.* **2000**, *39*, 541-544.
[21] Carter, E. A.; Goddard III., W. A. *J. Phys. Chem.* **1986**, *90*, 998-1001.
[22] (a) Dixon, D. A.; Arduengo, III, A. J. *J. Phys. Chem.* **1991**, *95*, 4180-4182. (b) Heinemann, C.; Thiel, W. *Chem. Phys. Lett.* **1994**, *217*, 11-16.

dimerizes indicates that the difference in entropy, which is not accounted for in the approximation, becomes the dominant factor in the thermodynamics.

III. Conclusion

The use of dialkyl-1,8-DAN as a framework for the stabilization of a low-valent carbon centre led to the preparation of a novel class of stable carbenes. These perimidine based carbenes all display characteristic ^{13}C NMR resonances for the carbene C at approximately 245 ppm. This chemical shift range is upfield from acyclic diamino carbenes, but downfield compared to typical imidazole and imidazolidine based NHCs. The reaction of carbene **20** with alcohol and water generated α-diaminoethers. Intramolecular C-F bond activation was observed when pentafluorobenzyl was used as an N-substituent. A dicarbene was observed when *para*-xylylene was used as a linking unit, however irreversible dimerization and formation of an enetetramine occurs for the carbenes linked by *ortho*-xylylene. The perimidine scaffold of the stable carbenes is responsible for imparting these coordinatively unsaturated species with unique structural and electronic features. Further investigations into their reactive properties and their characteristics as Lewis basic ligands are needed before one can fully assess their potential applications.

Experimental Section

General: All manipulations concerning the preparation of carbenes were carried out in either a nitrogen filled dry box or under nitrogen using standard Schlenk techniques. For these reactions, solvents were sparged with nitrogen then dried by passage through column of activated alumina using an apparatus purchased from Anhydrous Engineering. Deuterated dimethyl sulfoxide, chloroform, and benzene were purchased from Aldrich Chemical Company and in the case of C_6D_6 was dried by vacuum transfer from potassium. 1,8-diaminonapthalene, triethyl orthoformate, formic acid, benzyl bromide, α-bromo-*p*-xylene, α,α'-dibromo-*p*-xylene, pentafluorobenzyl bromide and sodium butoxide were purchased from Aldrich Chemical Company and used without further purification. LiHMDS was also purchased from Aldrich, but purified by crystallization from cold hexane. *O*-xylylene

dibromide was purchased from Lancaster Synthesis LTD and used without further purification. ^{1}H and ^{13}C NMR spectra were run on a Varian Gemini-200, a Bruker 300 MHz or a Bruker 500MHz spectrometer using the residual protons of the deuterated solvent for reference.

Preparation of 1,3-diisopropylperimidinium formate, (13a)

Under nitrogen in a Teflon screw-top stoppered Schlenk flask equipped with a stir-bar was added the diamine **4a** (1.452g, 6 mmol) and approximately 50 ml of dry, deoxygenated toluene. To this solution was added triethyl orthoformate (8.00 g, 54 mmol) followed by formic acid (4.08 g, 77 mmol). The solution was then degassed (freeze/pump/thaw) and then stirred at 80°C overnight (note that over-heating causes the formation of a by-product believed to be the $C_{10}H_6(^{i}PrN)_2CH_2$ derivative). All volatiles were removed under vacuum and the yellow solid was dissolved in THF and cooled to 4°C. The crystallized product was then filtered and washed with diethyl ether then dried under vacuum (2.25 g). ^{1}H NMR revealed that the salt had co-crystallized with two equivalents of formic acid (FW = 390 g/n, yield 96 % yield). ^{1}H NMR (300 MHz, $CDCl_3$): δ 14.67 (s, 2H, CO_2H), 8.72 (s, 1H, HCN_2), 8.37 (s, 3H, HCO_2), 7.49 (d, 2H, *H*Ar), 7.41 (t, 2H, *H*Ar), 6.93 (d, 2H, *H*Ar), 4.60 (sept, 2H, $HCMe_2$), 1.65 (d, 12H, $CH3$). ^{13}C NMR (300 MHz, $CDCl_3$): δ 166.0 (s, HCO_2), 148.2 (s, N_2CH), 135.4 (s, C_{Ar}), 131.2 (s, C_{Ar}), 128.0 (s, CH_{Ar}), 124.6 (s, CH_{Ar}), 122.2 (s, C_{Ar}), 108.1 (s, CH_{Ar}), 55.1 (s, $CHMe_2$), 19.8 (s, CH_3).

Preparation of 1,3-diisopropylperimidinium bromide, (13b)

Under nitrogen in a round bottom flask equipped with a stir-bar and a condenser were mixed diamine **4a** (0.485g, 2.0 mmol), ammonium bromide (0.196g, 2.0 mmol), triethyl orthoformate (7.0g, 47 mmol) and ethanol (10 g). The reaction heated to 80°C and let reflux for 2 hours. The reaction was stirred for an additional 12 hours. All volatiles were removed under vacuum and the product was washed with ether and dried under vacuum. The product was isolated as a yellow powder (0.51g, 77%).

^{1}H NMR (200 MHz, $CDCl_3$): δ 8.40 (s, 1H, HCN_2), 7.50 (d, 2H, *H*Ar), 7.41 (t, 2H, *H*Ar), 6.96 (d, 2H, *H*Ar), 4.53 (sept, 2H, $HCMe_2$), 1.74 (d, 12H, CH_3).

Preparation of 1,3-diisopropylperimidinium chloride, (14)

Compound **13a** (1.0 g, 2.6 mmol) was added to 10 ml of a NaOH/NaCl solution (0.51 M and 5.0 M respectively) in a separatory funnel. The aqueous layer was extracted repeatedly with 10 ml aliquots of CH_2Cl_2 until the organic layer showed very little yellow colour. The crude product obtained by removal of solvent under vacuum was purified by crystallization from a CH_2Cl_2 solution layered with diethyl ether (0.50 g, 65 % yield).

^{1}H NMR (300 MHz, $CDCl_3$): δ 9.89 (s, 1H, *H*CN_2), 7.46 (dd, 2H, *H*Ar), 7.38 (t, 2H, *H*Ar), 6. 92 (dd, 2H, *H*Ar), 4.81 (sept, 2H, *H*CMe_2), 1.82 (d, 12H, C*H*$_3$). ^{13}C NMR (300 MHz, $CDCl_3$): δ 149.9 (s, N_2*C*H), 128.0 (s, *C*H_{Ar}), 124.3 (s, *C*H_{Ar}), 108.0 (s, *C*H_{Ar}), 55.7 (s, *C*HMe_2), 19.8 (s, *C*H_3). Note, the quaternary C atoms were not observed due to low concentration.

Preparation of 1-isopropylperimidine, (16a)

To a 250ml round bottom flask was added N-isopropyl-1,8-diaminonaphthalene **2a** (4.0g, 20 mmol), triethyl orthoformate (29.6g, 200 mmol) and formic acid (0.04 ml, 1 mmol). The reaction was heated to 100°C under nitrogen for 4 hours and monitored by TLC. The product was purified by column chromatography using silica gel and a 1 to 1 ether dichloromethane solvent mixture 3.5g (83%) of a brown solid was obtained.

^{1}H NMR ($CDCl_3$, 300 MHz): δ 7.40 (s, 1H), 7.21 (t, 1H), 7.04-7.13 (m, 3H), 6.80 (d, 1H), 6.21 (d, 1H), 4.02 (sept, 1H), 1.42 (d, 6H). ^{13}C NMR ($CDCl_3$, 300 MHz): δ 144.5 (*C*H), 143.3 (C), 137.7 (*C*), 135.6 (*C*), 128.7 (*C*H), 127.3 (*C*H), 123.2 (*C*), 120.2 (*C*H), 119.1 (*C*H), 114.8 (*C*H), 100.2 (*C*H), 47.8 (*C*HMe_2), 20.8 (2C, *C*H_3).

Preparation of 1-cycloheptylperimidine, (16b)

Prepared in the same manner as **16a**. Reacted N-cycloheptyl-1,8-diaminonaphthalene **2b** (2.0g, 7.9 mmol), triethyl orthoformate (11.7 g, 79 mmol) and formic acid (0.015 ml, .4 mmol), obtained 1.2 g (58%) of a brown solid.

^{1}H NMR ($CDCl_3$, 200 MHz): δ 7.36 (s, 1H), 7.21 (t, 1H), 7.02-7.15 (m, 3H), 6.79 (dd, 1H), 6.18 (dd, 1H), 3.71 (m, 1H), 1.95-2.16 (m, 2H), 1.41-1.94 (m, 10H). ^{13}C NMR ($CDCl_3$, 200 MHz): δ 145.4 (*C*H), 143.3 (C), 137.7 (*C*), 135.7 (*C*), 128.6 (*C*H), 127.2 (*C*H), 123.3 (*C*),

120.1 (*C*H), 119.0 (*C*H), 114.7 (*C*H), 100.0 (*C*H), 57.8 (*C*H), 33.7 (2C, CH_2), 27.1 (2C, CH_2) 25.2 (2C, CH_2).

Preparation of 1-(4-MeBn) perimidine, (16c)

In a round bottom flask equipped with a magnetic stir bar a suspension of 1-H perimidine (10.00 g, 59 mmol), in toluene (250 mL) was prepared. To the reaction mixture was added α-bromo-*p*-xylene (16.52 g, 89 mmol) and KO^{t}Bu (26.66 g, 238 mmol). The reaction was stirred for 24 hours, filtered through Celite, and the solution was dried under vacuum. The product was purified by column chromatography using silica and a 2:1 misture of ether and dichloromethane (2.83 g, 17 %).

^{1}H NMR ($CDCl_3$, 200 MHz): δ 7.40 (s, 1H, N_2CH), 7.11 (m, 8H, C*H*), 6.21 (dd, 2H, C*H*), 4.68 (s, 2H, CH_2), 2.31 (s, 3H, CH_3). ^{13}C NMR ($CDCl_3$, 200 MHz): δ 148.8 (*C*H), 140.5 (*C*), 137.9 (*C*), 135.2 (*C*), 132.3 (*C*), 131.2 (*C*), 129.8 (2C, *C*H), 128.7 (*C*H), 127.3 (*C*H), 126.5 (2C, *C*H), 122.1 (*C*), 120.8 (*C*H), 119.8 (*C*H), 115.2 (*C*H), 102.2 (*C*H), 68.0 (CH_2), 21.1 (CH_3).

Preparation of 1-^{i}Pr-3-Bn perimidinium Bromide, (17a)

In a round bottom flask equipped with a magnetic stir-bar and a reflux condenser was mixed 1-^{i}Pr-perimidine **16a** (1.0g, 4.76 mmol), benzyl bromide (1.6g, 9.36 mmol) and approximately 100 ml of toluene. The reaction was heated at 100°C overnight. A yellow product precipitated from the reaction mixture and was isolated by filtration and drying under vacuum and determined to be pure **17a** (1.64g, 90%).

^{1}H NMR ($CDCl_3$, 500 MHz): *δ* 10.21 (s, 1H), 7.37-7.44 (m, 5H), 7.28-7.32 (m, 2H), 7.22-7.26 (m, 2H), 6.96 (d, 1H), 6.75 (d, 1H), 5.77 (s, 2H), 4.62 (m, 1H), 1.83 (d, 6H). ^{13}C NMR ($CDCl_3$, 500 MHz): *δ* 150.9 (C^+H), 135.1 (*C*), 132.2 (*C*), 131.6 (*C*), 131.4 (*C*), 129.2 (2C, *C*H), 128.6 (1C, *C*H), 128.08 (1C, *C*H), 128.07 (1C, *C*H), 127.1 (2C, *C*H), 124.5 (1C, *C*H), 124.3 (1C, *C*H), 121.8 (*C*), 108.8 (1C, *C*H), 107.9 (1C, *C*H), 54.9 (CH_2), 54.3 (*C*H), 20.6 (2C, CH_3).

Preparation of 1-^{i}Pr-3-$CH_2C_6F_5$ perimidinium Bromide, (17b)

Prepared in the same manner as **17a**. The perimidine **16a** (0.44g, 2.1 mmol) and pentafluorobenzyl bromide (0.6g, 2.3 mmol) were refluxed in about 20 ml of toluene. The product, a yellow powder, was isolated by filtration and dried under vacuum (0.91g, 92%).

^{1}H NMR ($CDCl_3$, 300 MHz): δ 10.34 (s, 1H), 7.40-7.50 (m, 3H), 7.31 (t, 1H), 7.02 (d, 1H), 6.63 (d, 1H), 6.08 (s, 2H), 4.62 (sept, 1H), 1.83 (d, 6H). ^{13}C NMR ($CDCl_3$, 300 MHz): δ 152.0 (C^+H), 135.2 (*C*), 130.83 (*C*), 130.77 (*C*), 128.4 (*C*H), 128.2 (*C*H), 125.1 (*C*H),124.8 (*C*H), 121.4 (*C*), 108.4 (*C*H), 106.3 (*C*H), 54.3 (*C*H), 44.1 (CH_2), 20.8 (CH_3).

Preparation of 1-^{i}Pr-3-*p*-$CH_2C_6H_4CH_3$ perimidinium Bromide, (17c)

Prepared in the same manner as **17a**. Compound **16a** and (1.0g, 4.76 mmol) and α-bromo-*p*-xylene (1.78g, 9.6 mmol) were reacted together. A yellow powder was obtained as pure product (1.6g, 85 %).

^{1}H NMR ($CDCl_3$, 500 MHz): δ 10.18 (s, 1H), 7.41 (d, 1H), 7.34-7.37 (m, 2H), 7.26 (d, 2H), 7.21-7.24 (m, 1H), 7.08 (d, 2H), 6.91 (d, 1H), 6.75 (d, 1H), 5.69 (s, 2H), 4.58 (sept, 1H), 2.23 (s, 3H), 1.82 (d, 6H). ^{13}C NMR ($CDCl_3$, 500 MHz): δ 150.9 (C^+H), 138.5 (*C*), 135.1 (*C*), 131.6 (*C*), 131.5 (*C*), 129.9 (2C, *C*H), 129.1 (*C*), 128.1 (1C, *C*H), 128.0 (1C, *C*H), 127.2 (2C, *C*H), 124.5 (1C, *C*H), 124.3 (1C, *C*H), 121.9 (*C*), 108.8 (1C, *C*H), 107.8 (1C, *C*H), 54.9 (CH_2), 54.3 (*C*H), 21.1 (1C, CH_3), 20.6 (2C, CH_3).

1-^{c}Hep-3-*p*-$CH_2C_6H_4CH_3$ perimidinium Bromide, (17d)

Prepared in the same manner as **17a**. Compound **16b** and (1.0g, 3.8 mmol) and α-bromo-*p*-xylene (1.40g, 7.6 mmol) were reacted together. The product, a yellow powder, was isolated by filtration and dried under vacuum (1.5g, 93 %).

^{1}H NMR ($CDCl_3$, 500 MHz): δ 10.26 (br, 1H), 7.35-7,45 (m, 3H), 7.28 (d, 2H), 7.23 (t. 1H), 7.08 (d, 2H), 6.87 (br d, 1H), 6.75 (d, 1H), 5.68 (br, 2H), 4.14 (br, 1H), 2.66 (br, 2H), 2.22 (s, 3H), 2.12 (br, 2H), 1.91 (br, 2H), 1.50-1.80 (br m, 6H). ^{13}C NMR ($CDCl_3$, 500 MHz): δ 151.4 (C^+H), 138.4 (*C*), 135.1 (*C*), 131.5 (*C*), 129.8 (2C, *C*H), 129.1 (*C*), 128.9 (*C*), 128.1 (1C, *C*H), 127.9 (1C, *C*H), 127.2 (2C, *C*H), 124.4 (1C, *C*H), 124.2 (1C, *C*H), 121.9 (*C*), 108.7 (1C, *C*H), 107.4 (br, 1C, *C*H), 63.3 (br, *C*H), 54.6 (CH_2), 33.0 (br 2C, CH_2), 26.3 (br 2C, CH_2), 24.8 (br 2C, CH_2), 21.0 (1C, CH_3).

Preparation of 1-^{c}Hep-3-$CH_2C_6F_5$ perimidinium Bromide, (17e)

Prepared in the same manner as **17a**. Compound **16b** and (0.46g, 1.7 mmol) and α-bromo-*p*-xylene (0.67g, 2.6 mmol) were reacted together. The product, a yellow powder, was isolated by filtration and dried under vacuum (0.80g, 90 %).

^{1}H NMR ($CDCl_3$, 500 MHz): δ 10.41 (br, 1H), 7.40-7.49 (m, 3H), 7.30 (t. 1H), 6.94 (d, 1H), 6.60 (d, 1H), 6.09 (br, 2H), 4.19 (br, 1H), 2.59 (br, 2H), 2.15 (br, 2H), 1.94 (br, 2H), 1.76 (br, 2H), 1.66 (br, 2H), 1.53 (br, 2H). ^{13}C NMR ($CDCl_3$, 500 MHz): δ 152.6 (C^+H), 136.8 (*C*), 130.9 (2C, *C*), 128.4 (*C*H), 128.1 (*C*H), 125.0 (*C*H), 124.8 (*C*H), 121.4 (*C*), 108.0 (br, *C*H), 106.3 (*C*H), 63.5 (br, *C*H), 44.0 (CH_2), 33.4 (br 2C, CH_2), 26.2 (br 2C, CH_2), 24.6 (br 2C, CH_2).

Preparation of [α,α'-di(1-^{i}Pr perimidinium) *ortho*-xylene]dibromide, (18a)

The ^{i}Pr perimidine **16a** (2.0g, 9.5 mmol) and *O*-xylene dibromide (1.26g, 4.8 mmol) were dissolved in approximately 30 ml of toluene and refluxed for 8 hours. The product, a yellow powder, was isolated by filtration and dried under vacuum (3.2g, 98%).

^{1}H NMR (DMSO-d_6, 300 MHz): δ 9.24 (s, 2H), 7.10-7.72 (m, 14H), 6.89 (d, 2H), 5.83 (s, 4H), 4.76 (sept, 2H), 1.60 (d, 12H). ^{13}C NMR (DMSO-d_6, 300 MHz): δ 151.3 (C^+H), 134.5 (*C*), 132.0 (2C, *C*), 130.4 (*C*), 128.4 (*C*H), 128.1 (*C*H), 128.0 (*C*H), 125.7 (*C*H), 123.9 (*C*H), 123.7 (*C*H), 121.4 (*C*), 108.6 (*C*H), 108.4 (*C*H), 52.9 (*C*H), 52.1 (CH_2), 20.2 (CH_3).

Preparation of [α,α'-di(1-^{i}Pr perimidinium) *para*-xylene]dibromide, (18b)

The ^{i}Pr perimidine **16a** (0.6g, 2.9 mmol) and α,α'-dibromo-*p*-xylene (0.378g, 1.4 mmol) were dissolved in approximately 30 ml of toluene and refluxed for 6 hours. The product, a yellow powder, was isolated by filtration and dried under vacuum (0.86g, 90%).

^{1}H NMR (DMSO-d_6, 200 MHz): δ 9.12 (s, 2H), 7.64 (s, 4H), 7.48-7.60 (m, 6H), 7.28-7.37 (m, 4H), 6.76 (d, 2H), 5.44 (s, 4H), 4.70 (sept, 2H), 1.56 (d, 12H). ^{13}C NMR (DMSO-d_6, 200 MHz): δ 151.2, 134.4, 133.2, 132.0, 131.7, 128.5, 128.0, 127.7, 123.8, 123.6, 121.6, 108.5, 108.3, 54.1, 52.7, 20.2.

Preparation of ^{t}BuO(H)C(N^{i}Pr)$_2$-1,8-$C_{10}H_6$, (19)

The diisopropyl perimidinium chloride **14** (0.20g, 0.69 mmol) was reacted with sodium *tert*-butoxide (0.072g, 0.75 mmol) in approximately 20 ml of THF. The reaction was stirred overnight, and all volatiles were removed under vacuum. The product was extracted with toluene and filtered through Celite. Removal of all volatiles under vacuum yielded the product as a greenish oil (0.216g, 96%).

^{1}H NMR (300 MHz, C_6D_6): δ 7.30 (m, 4H, *H*Ar), 6.68 (m, 2H, *H*Ar), 5.54 (s, 1H, N_2CHO), 3.64 (sept, 2H, $CHMe_2$), 1.15 (m two overlapping doublets and singlet, 21H, CH_3 from ^{i}Pr and ^{t}Bu). ^{13}C NMR (300 MHz, C_6D_6): δ 140.7 (s, C_{Ar}), 135.3 (s, C_{Ar}), 126.7 (s, CH_{Ar}), 120.4 (s, C_{Ar}), 119.4 (s, CH_{Ar}), 110.3 (s, CH_{Ar}), 87.5 (s, N_2CHO), 73.7 (s, $OCMe_3$), 51.3 (s, $CHMe_2$), 29.4 (s, $C(CH_3)_3$), 22.4 (s, $CH(CH_3)_2$), 19.6 (s, $CH(CH_3)_2$).

Preparation of 1,3-(^{i}Pr)$_2$-perimidin-2-ylidene, (20)

Under a nitrogen atmosphere in a dry-box, lithium bis(trimethylsilyl)amide (LiHMDS) (0.232 g, 1.4 mmol) was added to a round bottom flask equipped with a stir-bar and dissolved in 4 ml of 1:1 chlorobenzene and THF. To this solution was added dropwise a suspension of compound **14** (0.40 g, 1.4 mmol) in 20 ml of the 1:1 solvent mixture. The reaction was stirred overnight. All volatiles were removed under vacuum and the product extracted with toluene and filtered through Celite. Removal of the volatiles afforded the crude product which was purified by crystallizing from an ether solution at –25°C (0.160 g, 46 % yield). ^{1}H NMR (300 MHz, C_6D_6): δ 7.12 (m, 4H, *H*Ar), 6.29 (dd, 2H, *H*Ar), 4.08 (sept, 2H, $HCMe_2$), 1.41 (d, 12H, CH_3). ^{13}C NMR (300 MHz, C_6D_6): δ 241.7 (s, NCN), 136.0 (s, C_{Ar}), 133.7 (s, C_{Ar}), 128.0 (s, CH_{Ar}), 122.7 (s, C_{Ar}), 119.4 (s, CH_{Ar}), 102.9(s, CH_{Ar}), 51.5 (s, $CHMe_2$), 22.3 (s, CH_3).

Preparation of 1-^{i}Pr-3-*p*-$CH_2C_6H_5$-perimidin-2-ylidene, (21a)

Perimidinium bromide **17a** (1.0g, 2.6 mmol) was added to LiHMDS (0.43g, 2.6 mmol) in a total of about 60 ml of solvent mixture (THF/PhCl). The product, a pale brown viscous liquid, was isolated by extraction with toluene and drying under vacuum (0.76g, 2.5 mmol, 96%).

^{1}H NMR (C_6D_6, 200 MHz): δ 7.28 (d, 2H), 6.98-7.14 (m, 6H), 6.87 (t, 1H), 6.34-6.39 (m, 1H), 6.28 (dd, 1H), 5.27 (s, 2H), 4.12 (sept, 1H), 1.49 (d, 6H). ^{13}C NMR (C_6D_6, 200 MHz): δ 245.3 (C_{carb}), 137.8 (*C*), 135.7 (*C*), 133.6 (*C*), 133.3 (*C*), 128.8 (2C, *C*H), 128.0 (2C, *C*H), 127.4 (1C, *C*H), 126.8 (1C, *C*H), 122.5 (*C*), 120.0 (1C, *C*H) 119.8 (1C, *C*H), 105.2 (1C, *C*H), 103.5 (1C, *C*H), 61.0 (CH_2), 51.4 (*C*H), 22.6 (CH_3).

Preparation of 1-^{i}Pr-3-*p*-$CH_2C_6H_4CH_3$-perimidin-2-ylidene, (21c)

Perimidinium bromide **17c** (0.74g, 1.9 mmol) was added to LiHMDS (0.31g, 1.9 mmol) in a total of about 60 ml of solvent mixture (THF/PhCl). The product, a viscous liquid, was isolated by extraction and drying under vacuum (0.52g, 1.7 mmol, 87%).

^{1}H NMR (C_6D_6, 300 MHz): δ 7.25 (d, 2H), 7.09-7.15 (m, 2H), 7.05 (d, 1H), 6.88-6.95 (m, 3H), 6.32-6.39 (m, 2H), 5.29 (s, 2H), 4.13 (sept, 1H), 2.02 (s, 3H) 1.51 (d, 6H). ^{13}C NMR (C_6D_6, 300 MHz): δ 245.1 (C_{carb}), 136.7 (*C*), 135.7 (*C*), 134.7 (*C*), 133.7 (*C*), 133.3 (*C*), 129.6 (2C, *C*H), 128.0 (2C, *C*H), 126.9 (2C, *C*H), 125.6 (*C*), 120.0 (1C, *C*H) 119.8 (1C, *C*H), 105.2 (1C, *C*H), 103.6(1C, *C*H), 60.8 (CH_2), 51.4 (br, *C*H), 22.5 (CH_3), 21.0 (CH_3).

Preparation of 1-^{c}Hep-3-*p*-$CH_2C_6H_4CH_3$ perimidin-2-ylidene, (21d)

Perimidinium bromide **17d** (0.535g, 1.2 mmol) was added to LiHMDS (0.20g, 1.2 mmol) in a total of about 25 ml of solvent mixture (THF/PhCl). The product, an off-white solid, was isolated by extraction with hexane and drying under vacuum (0.408g, 92 %).

^{1}H NMR (C_6D_6, 500 MHz): δ 7.26 (d, 2H), 7.11-7.17 (m, 2H), 7.04 (d, 1H), 6.91-6.94 (m, 3H), 6.51 (br, 1H), 6.34 (d, 1H), 5.29 (s, 2H), 4.05 (br, 1H), 2.38 (m, 2H), 2.19 (br, 2H), 2.03 (s, 3H), 1.77 (br, 2H), 1.56 (br, 2H), 1.42 (br, 2H). ^{13}C NMR (C_6D_6, 500 MHz): δ 246.6 (C_{carb}), 136.7 (*C*), 135.8 (*C*), 134.8 (*C*), 133.8 (*C*), 133.3 (*C*), 129.8 (2C, *C*H), 128.4 (1C, *C*H), 127.8 (1C, *C*H), 126.9 (2C, *C*H), 122.7 (*C*), 119.9 (1C, *C*H), 119.8 (1C, *C*H), 105.1 (1C, *C*H), 103.3 (br, 1C, *C*H), 61.25 (*C*H), 60.8 (CH_2), 35.5 (br 2C, CH_2), 28.2 (br 2C, CH_2), 25.4 (br 2C, CH_2), 21.0 (CH_3).

Preparation of Compound 25b.

Perimidinium bromide **17b** (0.367g, 0.78 mmol) was reacted with LiHMDS (0.130g, 0.78 mmol) in a total of about 25 ml of solvent mixture (THF/PhCl). The product, a yellow solid, was isolated by extraction with toluene and drying under vacuum. The product was crystallized out of toluene at -25°C (0.102g, 35%).

^{1}H NMR (C_6D_6, 200 MHz): δ 7.26 (d, 1H), 7.10-7.22 (m, 2H), 7.00 (t, 1H), 6.86 (overlapping d and s, 2H), 6.53 (d, 1H), 4.21 (sept, 1H), 1.15 (d, 6H).

Preparation of Compound 25e.

Perimidinium bromide **17e** (0.400g, 0.76 mmol) was reacted with LiHMDS (0.127g, 0.76 mmol) in a total of about 25 ml of solvent mixture (THF/PhCl). The product, a yellow solid, was isolated by extraction with toluene and drying under vacuum (0.158g, 49%).

^{1}H NMR (C_6D_6, 300 MHz): δ 7.25 (d, 1H), 7.13-7.23 (m, 2H), 7.02 (t, 1H), 6.96 (dd, 1H), 6.86 (d, J = 1.6 Hz, 1H), 6.52 (d, 1H), 4.12 (sept, 1H), 1.80-1.96 (m, 4H), 1.27-1.50 (m, 8H). ^{13}C NMR (C_6D_6, 300 MHz): δ 136.7 (*C*), 135.3 (*C*), 131.3 (*C*), 127.2 (*C*H), 126.7 (*C*H), 124.0 (*C*H), 119.0 (*C*H), 118.7 (*C*), 111.2 (*C*H), 106.4 (*C*H), 95.6 (d, J = 10.9 Hz, *C*H), 71.5 (d, J = 6.49 Hz, *C*H), 33.8 (d, J = 1.74 Hz, CH_2), 27.7 (s, CH_2), 26.1 (d, J = 1.06 Hz, CH_2).

Note, seven quaternary carbons were not observed presumably due to the strong coupling to the fluorine nuclei. The unexpected coupling to some of the observed carbon signals was confirmed by comparing coupling constants for the same sample run at 500 MHz.

^{13}C NMR (C_6D_6, 500 MHz): δ 136.8 (*C*), 135.4 (*C*), 131.4 (*C*), 127.3 (*C*H), 126.7 (*C*H), 124.0 (*C*H), 119.1 (*C*H), 118.8 (*C*), 111.3 (*C*H), 106.4 (*C*H), 95.7 (d, J = 9.8 Hz, *C*H), 71.3 (d, J = 6.56 Hz, *C*H), 33.9 (d, J = 1.63 Hz, CH_2), 27.8 (s, CH_2), 26.1 (CH_2). ^{19}F NMR (C_6D_6, 300 MHz, referenced to an internal capillary of CF_3CO_2H): δ -67.7 (t, J = 17.9 Hz, 1F), -76.1 (t, J = 17.9 Hz, 1F), -87.5 (t, J = 16.8 Hz, 1F), -92.6 (t, J = 16.7 Hz, 1F).

Preparation of [$C_{10}H_6$-1,8-(^{i}PrN)$_2$C(H)]$_2$O, (26)

Usually is present in approximately 1:8 ratio (α-diamino ether : carbene), i.e. 20 % of the starting material is converted to the ether **26**. Can be purified by fractional crystallization from hexane as colourless blocks.

^{1}H NMR (C_6D_6, 300 MHz): δ 7.31 (d, 4H), 7.24 (t, 4H), 6.55 (d, 4H), 5.90 (s, 2H), 3.57 (sept, 4H), 1.10 (d, 12H), 0.68 (d, 12H). ^{13}C NMR (C_6D_6, 300 MHz): δ 140.4 (*C*), 135.2 (*C*), 126.7 (*C*H), 120.3 (*C*), 119.3 (*C*H), 110.3 (*C*H), 86.4 (N_2C(H)O), 50.8 (*C*HMe$_2$), 22.0 (*C*H$_3$), 18.8 (*C*H$_3$).

Preparation of the dicarbene, (27)

A suspension of the diperimidinium dibromide **18b** was (0.50g, 0.73 mmol) was added to pre-dissolved LiHMDS (0.465g, 1.9 mmol) using a total of approximately 30 ml of solvents. All volatiles were removed under vacuum and the product was extracted with toluene,

filtered through Celite and dried under vacuum. The poor solubility of the dicarbene in non-polar solvents prohibited the further purification of the product.

^{1}H NMR (C_6D_6, 200 MHz): δ 6.8-7.4 (m), 6.41 (m), 6.24 (d), 5.22 (s), 4.18 (m), 1.55 (d). ^{13}C NMR (C_6D_6, 200 MHz): δ 245.2 ($C_{carbene}$), 136.7, 135.7, 133.6, 133.4, 129.4, 127.2, 126.3, 120.0, 119.9, 105.2, 103.6, 60.7, 51.5, 21.5.

Preparation of the enetetramine, (28)

A suspension of the diperimidinium dibromide **18a** (0.60g, 0.87 mmol) was added to pre-dissolved [LiHMDS·Et_2O]$_2$[23] (0.465g, 1.9 mmol) using a total of approximately 30 ml of solvents. All volatiles were removed under vacuum and the product was extracted with toluene, filtered through Celite and dried under vacuum. Crystallization from an ether solution at -25°C yielded two crops of crystal from which X-ray quality crystals were obtained (total 0.20g, 44%).

^{1}H NMR (C_6D_6, 300 MHz): δ 7.29-7.41 (m, 4H), 6.95-7.15 (m, 10H), 6.36 (d, 2H), 4.30 (d, 2H), 4.21 (d, 2H), 3.65 (sept, 2H), 1.24 (d, 6H), 1.01 (d, 6H). ^{13}C NMR (C_6D_6, 300 MHz): δ 144.5 (C_{olefin}), 140.8 (*C*), 137.5 (*C*), 135.4 (*C*), 130.8 (*C*), 129.3 (*C*H), 128.3 (*C*H), 127.1 (*C*H), 127.0 (*C*H), 121.5 (*C*H), 119.6 (*C*), 117.6 (*C*H), 115.6 (*C*H), 103.0 (*C*H), 60.7 (*C*H), 55.4 (CH_2), 22.0 (CH_3), 21.4 (CH_3).

Crystal Structure Determination of Compounds 13a, 14, 18a, 20, 25b, 26, and 28.

Suitable crystals were selected, mounted on thin glass fibres using viscous oil and cooled to the data collection temperature. Data were collected on a Bruker AX SMART 1k CCD diffractometer using 0.3° ω-scans at 0, 90, and 180° in ϕ. Unit-cell parameters were determined from 60 data frames collected at different sections of the Ewald sphere. Semi-empirical absorption corrections based on equivalent reflections were applied (Blessing, R., *Acta Cryst.*, **1995,** A51, 33-38).

The structures were solved by direct methods, completed with difference Fourier syntheses and refined with full-matrix least-squares procedures based on F^2. All non-hydrogen atoms were refined with anisotropic displacement parameters. All hydrogen atoms were treated as

[23] Commercial LiHMDS crystallized out of ether, see a) Lappert, M. F.; Slade, M. J.; Singh, A. *J. Am. Chem. Soc.* **1983,** *105*, 302-304 b) Engelhardt, L. M.; May, A. S.; Raston, C. L.; White, A. H. *J. Chem. Soc., Dalton Trans.* **1983**, 1671-1673.

idealized contributions. All scattering factors are contained in the SHEXTL 5.10 program library (Sheldrick, G. M., Bruker AXS, Madison, WI, 1997).

Figure 4.1. (a) Molecular structure showing one of the two symmetry unique molecules of perimidinium formate **13a**. (b) Molecular structure for perimidinium chloride **14**. Counter anions, solvent molecules for **13a** (formic acid and THF) and most hydrogen atoms have been omitted for clarity. Thermal ellipsoids are drawn at 30% probability.

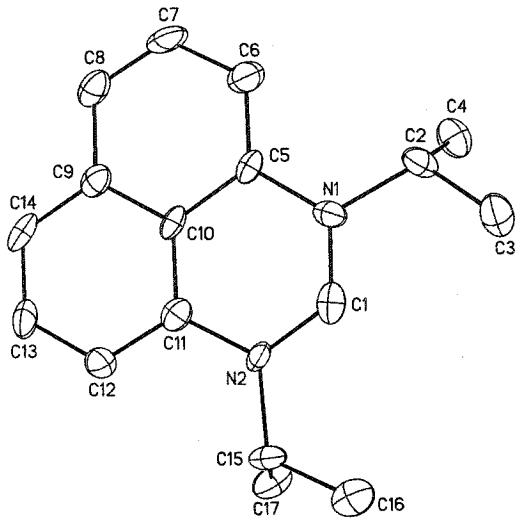

(a) Compound **13a**.

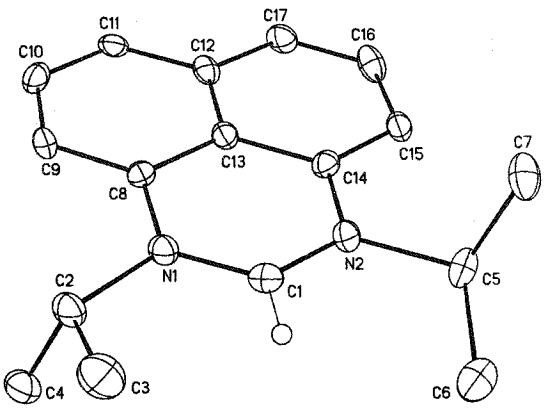

(b) Compound **14**.

Figure 4.2. Molecular structure showing the diperimidinium bromide **18a**. Counter anions, solvent molecules (H_2O and DMF) and hydrogen atoms have been omitted for clarity. Thermal ellipsoids are drawn at 30% probability.

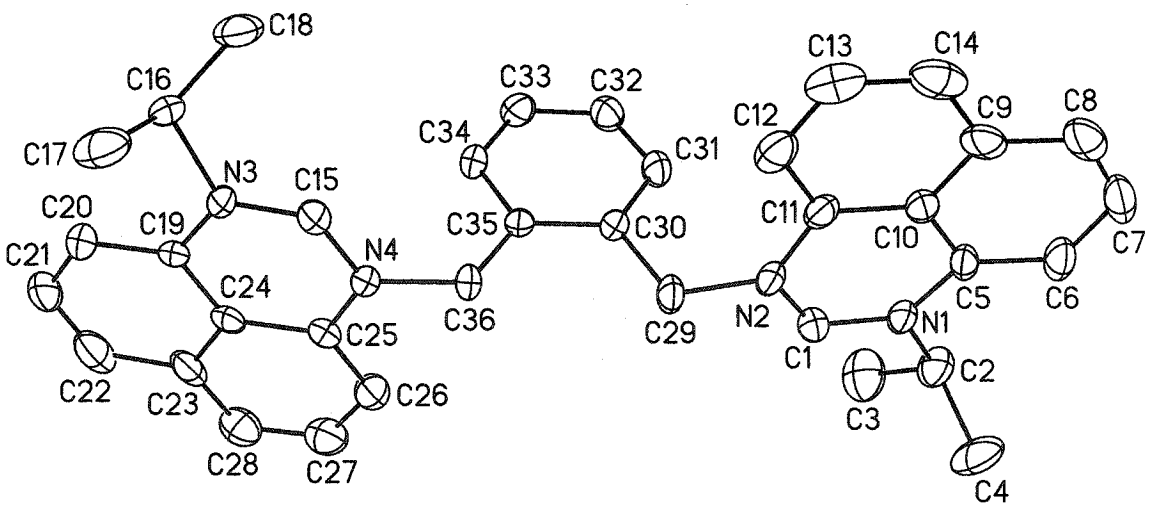

Figure 4.3. Molecular structure of carbene **20**. Hydrogen atoms have been omitted for clarity. Thermal ellipsoids are drawn at 30% probability.

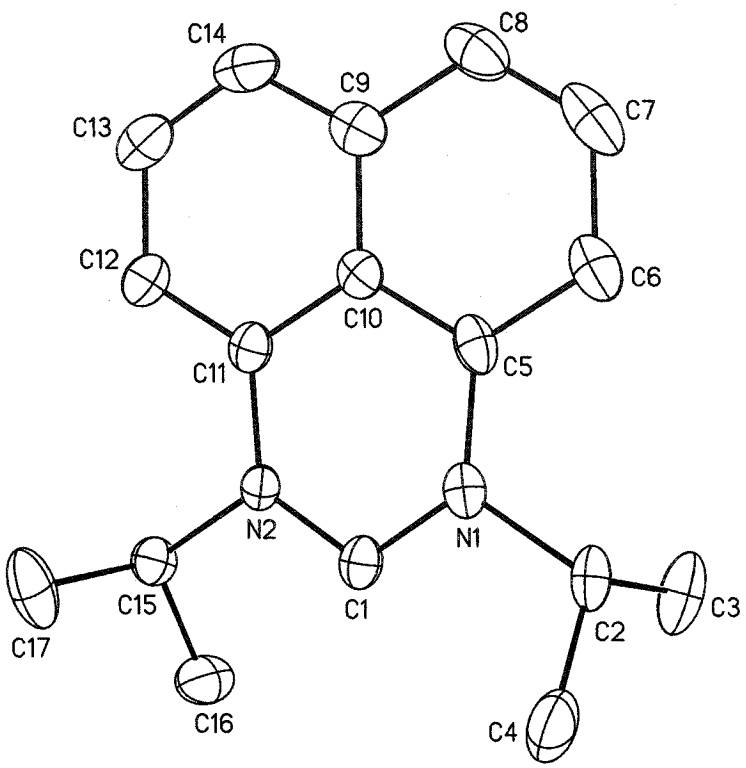

Figure 4.4. Molecular structure of compound **25b**. Hydrogen atoms have been omitted for clarity. Thermal ellipsoids are drawn at 30% probability.

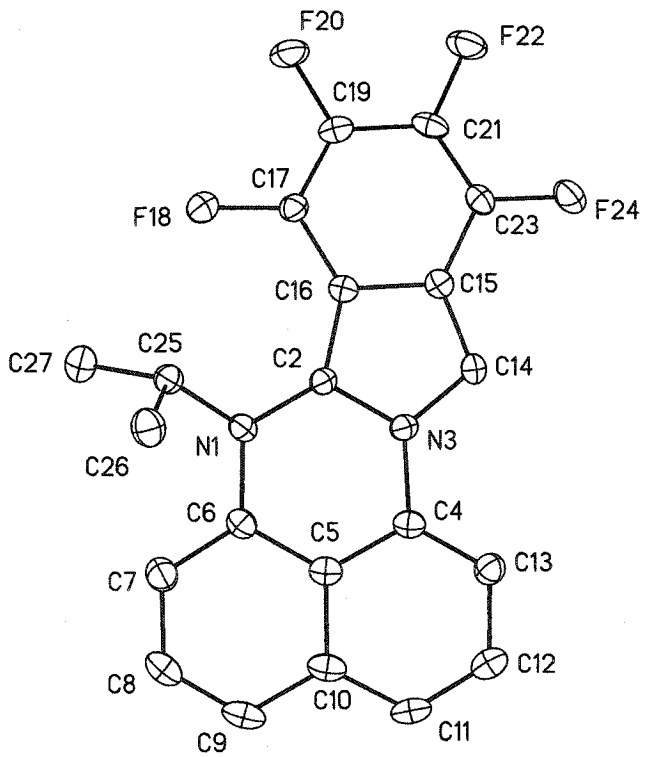

Figure 4.5. Molecular structure of compound **26**. Hydrogen atoms have been omitted for clarity. Thermal ellipsoids are drawn at 30% probability.

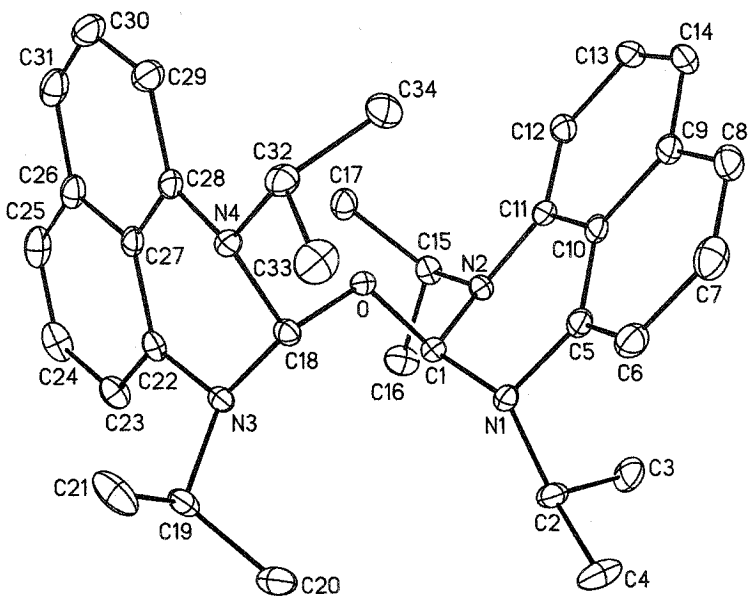

Figure 4.6. Two views of the molecular structure and atom numbering scheme for compound **28**. Hydrogen atoms and co-crystallized diethyl ether have been omitted for clarity. Thermal ellipsoids are drawn at 30% probability.

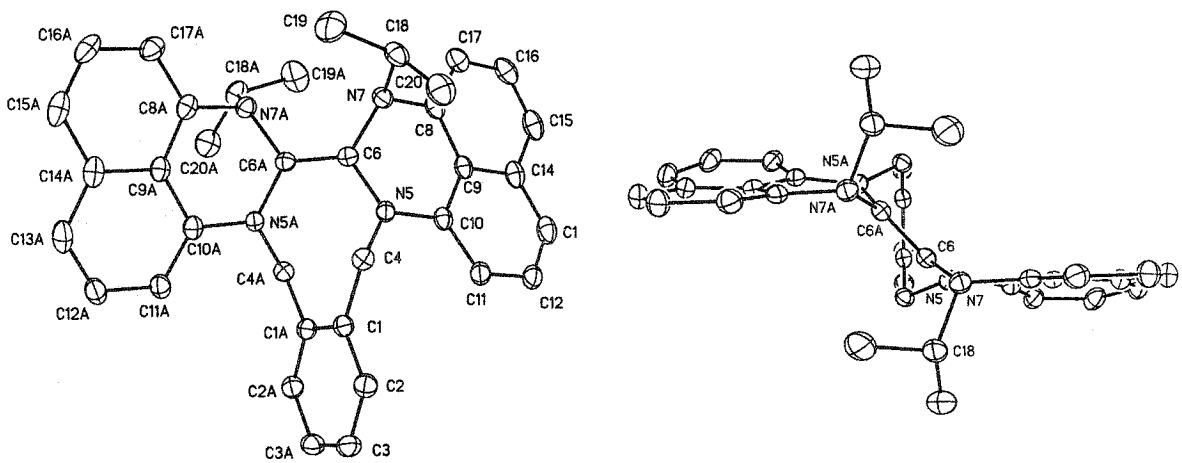

Table 4.1. Selected Crystal Data and Data Collection Parameters for **13a**, **14**, **18a**, and **20**.

	13a-(HCO_2H + 0.5 THF)	**14**	**18a-(H_2O + DMF)**	**20**
empirical formula	$C_{21}H_{28}N_2O_{4.50}$	$C_{17}H_{21}ClN_2$	$C_{39}H_{45}Br_2N_5O_2$	$C_{17}H_{20}N_2$
formula weight	380.45	288.81	775.62	252.35
T (K)	203(2)	233(2)	298(2)	223(2)
wavelength (Å)	0.71073	0.71073	0.71073	0.71073
crystal system	Triclinic	Hexagonal	Monoclinic	Monoclinic
space group	P-1	$P6_5$	$P2_1/n$	$P2_1$
a (Å)	12.969(6)	11.6131(18)	15.553(4)	9.223(4)
b (Å)	14.064(6)	11.6131(18)	12.622(3)	8.553(4)
c (Å)	14.585(7)	20.469(7)	19.236(4)	10.143(5)
α (deg)	115.767(6)	90	90	90
β (deg)	90.768(6)	90	92.794(4)	117.04(4)
γ (deg)	90.768(6)	120	90	90
V (Å^3)	2056.1(16)	2390.7(9)	3771.8(15)	712.6(6)
Z	4	6	4	2
abs coeff (mm^{-1})	0.086	0.232	2.189	0.069
final R indices	R1 = 0.0948	R1 = 0.0604	R1 = 0.0665	R1 = 0.0759
	wR2 = 0.2213	wR2 = 0.1274	wR2 = 0.1781	wR2 = 0.2471

Table 4.2. Selected Crystal Data and Data Collection Parameters for **25b**, **26**, **28**.

	25b	**26**	**28-(0.95 Et_2O)**
empirical formula	$C_{21}H_{14}F_4N_2$	$C_{34}H_{42}N_4O$	$C_{39.75}H_{43.50}N_4O$
formula weight	370.34	522.72	593.29
T (K)	208(2)	150(2)	208(2)
wavelength (Å)	0.71073	0.71073	0.71073
crystal system	Triclinic	Monoclinic	Orthorhombic
space group	P-1	$P2_1/c$	Fdd2
a (Å)	9.023(4)	8.690(4)	17.395(4)
b (Å)	9.391(4)	18.893(8)	22.900(5)
c (Å)	11.352(5)	17.825(7)	16.709(3)
α (deg)	68.161(7)	90	90
β (deg)	79.077(7)	96.126(6)	90
γ (deg)	62.512(6)	90	90
V (Å^3)	791.8(6)	2910(2)	6656(2)
Z	2	4	8
abs coeff (mm^{-1})	0.125	0.073	0.072
final R indices	R1 = 0.0695	R1 = 0.0698	R1 = 0.0532
	wR2 = 0.1613	wR2 = 0.1523	wR2 = 0.1283

Table 4.3. Selected Bond Distances and Angles for **13a-(HCO_2H + 0.5 THF).**

	Bond Distances (Å)		
C(1)-N(1)	1.314(10)	C(1)-N(2)	1.350(9)
N(1)-C(5)	1.430(9)	N(1)-C(2)	1.515(9)
N(2)-C(11)	1.420(9)	N(2)-C(15)	1.492(9)
	Bond Angles (deg)		
N(1)-C(1)-N(2)	125.7(8)	C(1)-N(1)-C(5)	120.8(7)
C(1)-N(1)-C(2)	118.6(7)	C(5)-N(1)-C(2)	120.5(7)
C(1)-N(2)-C(15)	121.2(7)	C(1)-N(2)-C(11)	118.1(7)
C(11)-N(2)-C(15)	120.6(7)		

Table 4.4. Selected Bond Distances and Angles for **14.**

	Bond Distances (Å)		
C(1)-N(1)	1.328(6)	C(1)-N(2)	1.338(6)
N(1)-C(8)	1.434(5)	N(1)-C(2)	1.511(6)
N(2)-C(14)	1.432(5)	N(2)-C(5)	1.528(6)
	Bond Angles (deg)		
N(1)-C(1)-N(2)	124.5(4)	C(1)-N(1)-C(2)	119.9(4)
C(1)-N(1)-C(8)	120.7(4)	C(8)-N(1)-C(2)	119.3(4)
C(1)-N(2)-C(14)	120.4(4)	C(1)-N(2)-C(5)	120.0(4)
C(14)-N(2)-C(5)	119.5(4)		

Table 4.5. Selected Bond Distances and Angles for **18a-(H_2O + DMF)**describing only one of the crystallographically independent perimidinium moieties.

	Bond Distances (Å)		
C(1)-N(1)	1.335(8)	C(1)-N(2)	1.313(8)
C(15)-N(3)	1.315(9)	C(15)-N(4)	1.335(8)
N(1)-C(5)	1.426(9)	C(2)-N(1)	1.499(9)
	Bond Angles (deg)		
N(1)-C(1)-N(2)	124.4(7)	C(1)-N(1)-C(2)	118.9(6)
C(1)-N(1)-C(5)	119.5(6)	C(5)-N(1)-C(2)	121.6(5)
C(1)-N(2)-C(11)	120.7(6)	C(1)-N(2)-C(29)	117.2(6)
C(11)-N(2)-C(29)	122.1(6)		

Table 4.6. Selected Bond Distances and Angles for **20**.

	Bond Distances (Å)		
C(1)-N(1)	1.355(6)	C(1)-N(2)	1.362(6)
C(5)-N(1)	1.410(6)	C(11)-N(2)	1.418(6)
C(2)-N(1)	1.509(6)	C(15)-N(2)	1.495(5)
	Bond Angles (deg)		
N(1)-C(1)-N(2)	115.3(4)		
C(1)-N(1)-C(2) α	115.0(4)	C(1)-N(2)-C(15) α	116.1(3)
C(1)-N(1)-C(5)	125.9(4)	C(11)-N(2)-C(15)	118.9(3)
C(5)-N(1)-C(2)	118.7(4)	C(1)-N(2)-C(11)	124.9(4)

Table 4.7. Selected Bond Distances and Angles for **25b**.

	Bond Distances (Å)		
N(1)-C(2)	1.383(4)	C(2)-N(3)	1.378(4)
N(1)-C(6)	1.402(4)	N(3)-C(14)	1.373(4)
N(1)-C(25)	1.491(4)	N(3)-C(4)	1.419(4)
C(2)-C(16)	1.408(4)	C(14)-C(15)	1.364(4)
C(15)-C(16)	1.440(4)	C(16)-C(17)	1.422(4)
C(17)-C(19)	1.350(5)	C(19)-C(21)	1.417(5)
C(21)-C(23)	1.345(5)	C(15)-C(23)	1.422(4)
	Bond Angles (deg)		
C(2)-N(1)-C(6)	118.7(3)	N(3)-C(2)-N(1)	120.9(3)
C(2)-N(1)-C(25)	117.2(3)	N(1)-C(2)-C(16)	132.6(3)
C(6)-N(1)-C(25)	121.1(2)	N(3)-C(2)-C(16)	106.5(3)
C(2)-N(3)-C(4)	122.5(3)	C(15)-C(14)-N(3)	107.2(3)
C(14)-N(3)-C(4)	126.0(3)	C(2)-C(16)-C(15)	106.2(3)
C(14)-N(3)-C(2)	111.3(3)	C(14)-C(15)-C(16)	108.6(3)

Table 4.8. Selected Bond Distances and Angles for **26**.

	Bond Distances (Å)		
O-C(1)	1.425(3)	O-C(18)	1.433(3)
N(1)-C(5)	1.430(3)	N(1)-C(1)	1.444(3)
N(1)-C(2)	1.493(3)		
	Bond Angles (deg)		
C(1)-O-C(18)	116.51(17)	O-C(1)-N(1)	109.80(18)
O-C(1)-N(2)	105.49(18)	N(1)-C(1)-N(2)	113.44(19)
C(5)-N(1)-C(1)	112.31(19)	C(5)-N(1)-C(2)	117.18(19)
C(1)-N(1)-C(2)	112.95(18)		
Sum at C(1)	328.73	Sum at N(1)	342.44

Table 4.9. Selected Bond Distances and Angles for **28-(0.95 Et_2O)**.

Bond Distances (Å)			
C(6)-C(6)#1	1.346(5)	N(5)-C(6)	1.412(3)
N(7)- C(6)	1.426(3)	N(5)-C(4)	1.462(3)
N(7)-C(8)	1.418(4)	N(5)-C(10)	1.387(3)
N(7)-C(18)	1.508(4)		
Bond Angles (deg)			
C(6)#1-C(6)-N(5)	121.32(14)	C(10)-N(5)-C(6)	118.0(2)
C(6)#1-C(6)-N(7)	122.04(14)	C(10)-N(5)-C(4)	121.5(2)
N(5)-C(6)-N(7)	116.3(2)	C(6)-N(5)-C(4)	120.4(2)
Sum at C(6)	359.7	Sum at N(5)	359.9
C(8)-N(7)-C(6)	112.1(2)	C(8)-N(7)-C(18)	114.1(2)
C(6)-N(7)-C(18)	115.7(2)	Sum at N(5)	341.9

5 *Heavier Carbene Analogues*

I. Introduction

The discovery of stable carbenes and their very rapid application to catalysis has generated a surge of interest in this novel type of ligand for transition metals. An obvious similarity exists between carbenes and the heavier analogues. Therefore silylenes, germylenes and stannylenes are now sought after in order to explore their potential as ligands and as possible synthetic precursors for materials.

As one moves a the column of the periodic table, the stability of lower oxidation-states increases, and it becomes easier to isolate compounds possessing only two substituents and one lone-pair. Therefore it is not surprising to find that these compounds were discovered and investigated long before it was known that stable carbenes could be isolated. In fact it is probably fair to say that the work done with the heavier elements led to an understanding of the stabilizing electronic factors for carbene-like structures and provided future researchers a solid foundation for their work.

For instance nitrogen-based ligands, presumably due to the σ-inductive effect of the electronegative N, have played a pivotal role in the successful isolation of these species with

the archetypes being $M[N(SiMe_3)_2]_2$[1] (M = Ge, Sn). Also theoretical and experimental results indicate that ligands exhibiting delocalized heterocyclic π-systems lend improved stability to these compounds.[2,3,4,5,6] For example, (^{t}BuNCHCHN^{t}Bu)Ge (**R**) is significantly more stable than (^{t}BuNCH$_2$CH$_2$N^{t}Bu)Ge (**S**).[7] The phenylenediamine-derived compound *o*-$C_6H_4(NSiMe_3)_2Ge$ (**T**)[8] and the aminotroponiminate species [1,2-$C_7H_5(N^iPr)_2$]Ge^+ (**U**)[9] have been prepared and their stability attributed to their 10-π electron systems. In addition to π delocalization, the presence of sterically demanding substituents on the metal-bonded N centres undoubtedly plays an essential role in preventing aggregation of these species.[10] For example, while (^{t}BuNCH$_2$CH$_2$N^{t}Bu)Ge (**S**) is monomeric, the isopropyl derivative forms dimers in the solid state.[11] A common feature for the reported compounds in this family is the dominance of five-membered heterocyclic ring systems. However, the recently reported cationic germylene compound [Ge{N(C_6H_3-2,6-^{i}Pr$_2$)CMe}$_2$CH]$^+$ (**V**) which is supported by a β-diketonate ligand, is an example of a six-membered metallaheterocycle.[12] The large N-substituents and the geometric arrangement of the ligand efficiently protect the metal centre,

Chart 5.1

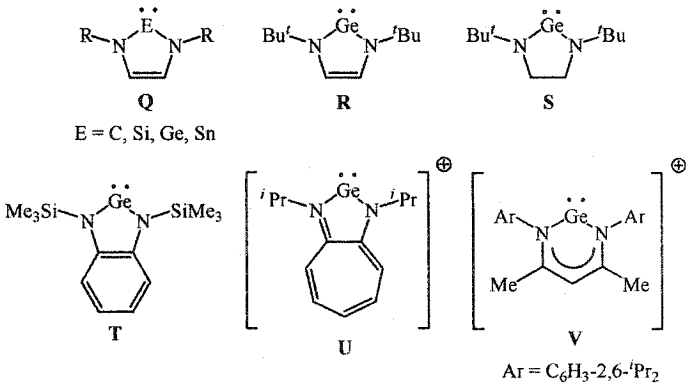

[1] (a) Schaeffer, Jr., C. D.; Zuckerman, J. J. *J. Am. Chem. Soc.* **1974**, *96*, 7160-7162. (b) Harris, D. H.; Lappert, M. F. *J. Chem. Soc., Chem. Comm.***1974**, 895-896. (c) Gynane, M. J. S.; Harris, D. H.; Lappert, M. F.; Power, P. P.; Rivière, P.; Rivière-Baudet, M. *J. Chem. Soc., Dalton Trans.* **1977**, 2004-2009. (d) Chorley, R. W.; Hitchcock, P. B.; Lappert, M. F.; Leung, W.-P.; Power, P. P.; Olmstead, M. M. *Inorg. Chim. Acta* **1992**, *198-200*, 203-209. (e) Fjeldberg, T.; Hope, H.; Lappert, M. F.; Power, P. P.; Thorne, A. J. *J. Chem. Soc., Chem. Commun.* **1983**, 639-641.

[2] Driess, M.; Grützmacher, H. *Angew. Chem. Int. Ed. Engl.* **1996**, *35*, 828-856.

[3] Boehme, C.; Frenking, G. *J. Am. Chem. Soc.* **1996**, *118*, 2039-2046.

[4] Heinemann, C.; Herrmann, W. A.; Thiel, W. *J. Organomet. Chem.* **1994**, *475*, 73-84.

[5] Heinemann, C.; Müller, T.; Apeloig, Y.; Schwarz, H. *J. Am. Chem. Soc.* **1996**, *118*, 2023-2038.

[6] Lehmann, J. F.; Urquhart, S. G.; Ennis, L. E.; Hitchcock, A. P.; Hatano, K.; Gupta, S.; Denk, M. K. *Organometallics* **1999**, *18*, 1862-1872.

[7] Herrmann, W. A.; Denk, M.; Behm, J.; Scherer, W.; Klingan, F.-R.; Bock, H.; Solouki, B.; Wagner, M. *Angew. Chem. Int. Ed. Engl.* **1992**, *31*, 1485-1488.

[8] Pfeiffer, J.; Maringgele, W.; Noltemeyer, M.; Meller, A. *Chem. Ber.* **1989**, *122*, 245-252.

[9] Dias, H. V. R.; Wang, Z. *J. Am. Chem. Soc.* **1997**, *119*, 4650-4655.

[10] Denk, M. K.; Thadani, A.; Hatano, K.; Lough, A. J. *Angew. Chem. Int. Ed. Engl.* **1997**, *36*, 2607-2609.

[11] Veprek, S.; Prokop, J.; Glatz, F.; Mercia, R.; Klingan, F. R.; Herrmann, W. A. *Chem. Mater.* **1996**, *8*, 825.

[12] Stender, M.; Phillips, A. D.; Power, P. P. *Inorg. Chem.* **2001**, *40*, 5314-5315.

which does not display any interactions with its counter ion $[HO\{B(C_6F_5)_3\}_2]^-$ in the solid state.

Our general interests in the design and implementation of rigid chelating ligands with delocalized π-electrons, led us to the preparation of a novel diamido ligand, based on 1,8-diaminonaphthalene, that yields a six-membered metallaheterocycle system when coordinated to a metal centre. We anticipated that the steric impact exerted by the nitrogen substituents of this ligand would be greater than the five-membered-ring systems of Chart 5.1 due to the relative geometric constraints of the two cycles. The diamido ligand seemed appealing for stabilization of neutral Ge(II) and Sn(II) species.[13] This chapter presents the synthetic and structural details for new germylene and stannylene compounds supported by 1,8-DAN ligands $M[1,8\text{-}(RN)_2C_{10}H_6]$ (for M = Ge, R = R^1 and R^2; for M = Sn, R = R^1; R^1 = ^{i}Pr, R^2=3,5-$Me_2C_6H_3$). We also report subsequent redox chemistry of the germanium species.

II. Results and Discussion

A. Diamido Germylenes

The metathetical reaction between an equimolar ratio of $Li_2[1,8\text{-}(^i PrN)_2C_{10}H_6]$ and $GeCl_2$(dioxane) in Et_2O successfully provided $Ge[1,8\text{-}(^i PrN)_2C_{10}H_6]$ (**29**) as an orange solid in excellent yield (Scheme 5.1). Alternatively a transamination reaction between $Ge[N(SiMe_3)_2]_2$ and $[1,8\text{-}(^i PrNH)_2C_{10}H_6]$ also yields **29**. The first pathway is preferable for isolation of the product.

Compound **29** is soluble in a variety of organic solvents, exhibits a sharp, reversible melting point, and was characterized by NMR spectroscopy, elemental analysis, and X-ray diffraction studies. ^{1}H and ^{13}C NMR spectroscopy indicates a symmetrical solution structure for **29** with a single set of resonances for the ^{i}Pr substituents and symmetrical naphthalene

Scheme 5.1

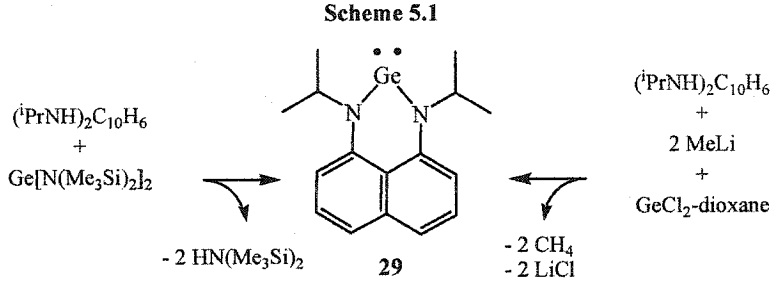

skeleton. Single-crystal X-ray diffraction provided details for the level of aggregation and revealed the structural features of **29** (Table 5.1). Results of this study are displayed in Figure 5.1 with selected bond distances and angles in Table 5.2. A clearly distinguishing feature of **29** is that it is a mononuclear species exhibiting a planar six-membered metallaheterocycle. The deviation of the Ge centre from the mean plane defined by N(1), C(1), C(6), C(7), and N(2) is only 0.042 Å. Although not present crystallographically, an approximate molecular mirror plane of symmetry passing through the Ge centre and bisecting the C(6) and C(5) atoms is consistent with the symmetrical structure deduced from NMR.

The two Ge-N bond lengths in **29** are equivalent within experimental error (1.84 Å) and comparable to those observed for **T** (range = 1.845(9)-1.868(9) Å)[8] but shorter than those reported for **U** (Ge-N = 1.901-1.92 Å).[9] Further comparison of Ge-N distances can be made with $Ge[N(SiMe_3]_2$ (1.878(5), 1.873(5) Å),[1d] **R** (1.856(1) Å),[7] and **S** (1.833(2) Å).[7] Like the related 1,2 phenylenediamine complex (**T**) the Ge bonded N atoms (N(1), N(2)) are planar with their lone-pairs of electrons aligned for π overlap with the atoms in the six-membered metallacycle. Calculations suggest that a true single Ge^{II}-N bond distance for a diaminogermylene should be approximately 1.88 Å and that $p\pi$-$p\pi$ interactions would shorten the Ge^{II}-N bond by 0.06-0.07 Å.[4] These results suggest some π-stabilizing interaction in **29**.

Except for the N(1)-Ge-N(2) angle of 97.28(7)°, the other angles within the six-membered heterocycle range from 121.00(18)° to 127.53(13)° and approach the ideal angle of 120°. As might be expected, this N-Ge-N angle is smaller than the acyclic species $Ge[N(SiMe_3]_2$ (N-Ge-N 107.1(2)°)[1d] but larger than those of the five-membered ring compounds shown in Chart 5.1 (e.g.: **R**, N-Ge-N = 84.8(1)°;[7] **S**, N-Ge-N = 88.0(1)°;[7] **T**, N-Ge-N = 87.2(4)°,[8]).

As anticipated, the steric impact of the nitrogen substituents is more pronounced in **29** than for the five-membered metallaheterocycles (**R-U**). This is demonstrated by the observation that the smallest angle around each of the nitrogen atoms is the α angle, the angle defined by the ^{i}Pr substituent and the Ge(II) (termed α see Chart 4.1). For example, C(11)-N(1)-Ge and C(14)-N(2)-Ge exhibit values of 115.63(13)° and 115.46(13)°,

---

[13] A Sn complex with a related ligand $(1,8\text{-}(Me_3SiN)_2C_{10}H_6)^{-2}$ is reported in 1a)

respectively. For comparison, the analogous angles (Ge-N-Si) for **T** fall in the range 123.3(5)-124.4(5)°.[8]

Examination of the packing of germylene **29** reveals an ordered anti-parallel arrangement between two adjacent molecules (Figure 5.2) and prompts consideration of intermolecular interactions. A similar packing arrangement was observed for Sn{*o*-$C_6H_4[N(CH_2{}^tBu)]_2$}, which crystallized in bimolecular aggregates due to a weak η^6-C_6···Sn interaction.[14] However, unlike this species, the closest approach between adjacent molecules of **29** is 3.719 Å (Ge and C(7)), a distance that is well beyond any bonding interaction.[15] The absence of extended interactions for compound **29** in the solid state contrasts with the cationic *N*-alkyl-2-(alkylamino)troponiminate derivatives (**U**) which clearly display interactions between the Ge and the counterions.[9]

Concurrent developments within the research group led to the preparation of diarylated versions of 1,8-DAN ligands via Goldberg coupling reactions.[16] Utilization of 1,8-$[(3,5\text{-}Me_2C_6H_3)NH]_2C_{10}H_6$ ligand in an analogous metathetical reaction provided once again a stable germylene Ge{1,8-$[(3,5\text{-}Me_2C_6H_3)NH]_2C_{10}H_6$} **30,** also an orange solid (Scheme 5.2).

Compound **30,** which is less soluble in organic solvents than **29**, presumably due to its rigid aromatic structure, was characterized by NMR spectroscopy and X-ray diffraction. ^1H and ^{13}C NMR spectra indicate a symmetrical structure for **30** with only one signal for the Me groups and a symmetrical naphthalene pattern.

Scheme 5.2

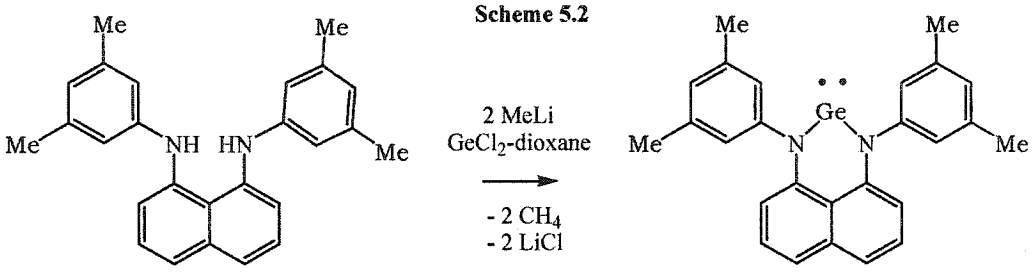

30

Single-crystal X-ray diffraction provided structural details for germylene **30** (Table 5.1) and the results of this study are displayed in Figure 5.3 with selected bond distances and

[14] Braunschweig, H.; Gehrhus, B.; Hitchcock, P. B. Lappert, M. F. *Z. anorg. allg. Chem.* **1995**, *621*, 1922-1928.
[15] Glocking, F. In *Encyclopedia of Inorganic Chemistry*; King, R. B., Ed.; Wiley: New York, 1994; Vol. 3, p 1282.
[16] Liu, J.; Primeau, L.; Richeson, D. S. unpublished results.

angles in Table 5.3. The structure of **30** reveals a mononuclear germylene species being supported by the diaryl 1,8-DAN ligand. Interestingly, the Ge atom is co-planar with the naphthyl backbone, but the nitrogen centres, which possess planar geometries, deviate and lie on opposite sides of this plane. This small twisting of the ligand is probably the result of packing forces which favour having the molecules stacked flat against its neighbours in an anti-parallel manner (Figure 5.4) similar to **29**. However, planarity cannot be achieved because the aromatic rings resist being co-planar with the naphthyl rings due to the steric repulsion between the two *ortho* protons of the aromatic N-substituents and the protons of the naphthyl backbone (2 and 7 positions).

The Ge-N bond lengths averaging out to be 1.876 Å are equivalent within error, and significantly longer than in **29** and equal to the calculated value for diaminogermylenes without $p\pi$-$p\pi$ interactions.[4] This implies that there is little or no π overlap between the N lone-pairs and the Ge empty orbital. The N-C_{naph} distances of **30** are also slightly longer (0.013 Å) than for **29**. Substituting N-isopropyls for N-aryl substituents results in competition for overlap with the N lone-pairs and effectively reduces the bond order to the other atoms. However the N-C_{Ar} distances (average 1.45 Å) are longer than the N-C_{naph} bonds, suggesting that the lone-pairs are still contributing to the π system of the metallaheterocycle, and that the observed elongation of the N-Ge bonds is the result of other factors.

As with germylene **29**, the geometric constraints of the six-membered-ring imposed by the ligand result in crowding of the Ge centre from the N substituents. The very modest α angle of 113° is smaller than in **29** and other germylenes (**R-U**) and demonstrates the steric protection afforded by the large aromatic substituents. This crowding may also account for the smaller bite-angle N(1)-Ge-N(2) of 94.58(19)° which is almost three degrees smaller than in **29**.

B. Diamido Stannylene

Employing the same reaction paths as outlined for germylene **29**, substituting with the appropriate Sn reagents, the Sn analogue can be prepared. A metathetical reaction between *in situ generated* $Li_2[1,8\text{-}(^iPrN)_2C_{10}H_6]$ and $SnCl_2$ provides the stannylene $Sn[1,8\text{-}(^iPrN)_2C_{10}H_6]$ (**31**) in good yield. Once again, **31** can be prepared by a transamination reaction between $1,8\text{-}(^iPrNH)_2C_{10}H_6$ and $Sn[N(SiMe_3)_2]_2$ with the release $HN(SiMe_3)_2$

(Scheme 5.3). The dark orange/brown compound is considerably less soluble in organic solvents than the Ge derivative. The lower electronegativity of Sn might be responsible for a more ionic bonding, explaining the lower solubility in non-polar solvents. ^{1}H and ^{13}C NMR spectroscopy reveals a symmetric bonding environment for the ligand, suggesting an identical structure to that of the germanium analogue (**29**). ^{119}Sn NMR spectroscopy revealed a broad peak at 330 ppm.

Scheme 5.3

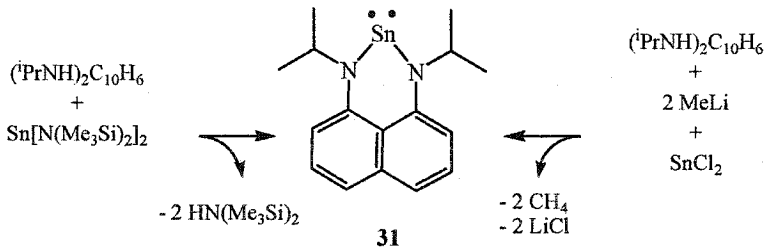

An X-ray diffraction study performed to determine the molecular structure of compound **31** (Table 5.1) revealed, however, that the solid-state structure of the stannylene is quite different than the Ge derivatives. The molecular structure is illustrated in Figure 5.5, and Table 5.4 lists values for selected bond distances and angles. The major structural difference for compound **31** is the deviation of the Sn atom out of the ligand plane ($C_{10}H_6N_2$) by 0.7688 Å. Additionally the chelating N atoms are spread apart resulting in the opening of the internal angles of the metallacycle at the C_{naph} junctions (C(6)-C(1)-N(1) = 126.9(4)° and N(2)-C(7)-C(6) = 129.8(5)°). Due to its larger size the Sn-N bond lengths, averaging 2.07 Å, are considerably longer (0.23Å) than the Ge-N bonds, but are comparable with the Sn-N bond lengths observed for $Sn(N(SiMe_3)_2)_2$ (2.096(1)Å, 2.088(6)Å)[1e]. The longer bonds allow for a smaller bite-angle of 85.6(3)Å for N(1)-Sn-N(2) compared to the germylenes **29** and **30** (97.28(7)° and 94.58(19)° respectively). Despite the non-planar metallaheterocycle, the N atoms remain planar (sum of angles are 358.7° and 359.6°) indicating an sp^2 hybridization for these centres. A related dialkyl-1,8-DAN supported stannylene compound (**X**, Chart 5.2) has been recently reported but is not crystallographically characterized.[17] Interestingly, the Lewis base adduct (**Y**) of compound **X** is structurally characterized. Although not directly comparable to the structure of **31**, there is a resemblance between the structural features of the Sn(dialkyl-1,8-DAN) portion of **Y** and compound **31**.

[17] Drost, C.; Hitchcock, P. B.; Lappert, M. F. *Angew. Chem. Int. Ed.* **1999**, *38*, 1113-1116.

The origin for the non-planar structure of **31** compared to the Ge analogue might be partially attributed to the ionic radius of the Sn atom which could prevent it from lying flat within the constrained cavity imposed by the ligand. However a closer look at the extended 3-dimensional structure revealed an intermolecular interaction between the Sn atom and the π electrons of the naphthalene ring of an adjacent molecule in the crystal structure (Figure 5.6). The interaction does not appear to be symmetrical with respect to the ring, with the shortest intermolecular interactions being observed between Sn and the C(3), C(4), and C(5) carbons of the naphthyl rings of an a neighbouring molecule with distances of 3.022, 2.803 and 3.217Å respectively. These distances all fall well within the sum of the van der Waals radii of Sn and C of 3.90 Å. The Sn-C bond in $[Sn(CHTMS_2)_2]_2$ is 2.22Å.[18]

Despite the intermolecular interactions between stannylene molecules observed in the solid-state, the NMR spectroscopy suggests a symmetric structure in solution. We questioned whether the Sn atom really is too big to fit in between the amido groups and always lies to one side of the ligand plane, or if in solution it lies perfectly flat forming a symmetric species consistent with the NMR results. Fluxional exchange of the Sn position would generate a symmetric pattern in the NMR spectra, however poor solubility of **31** prevented us from performing variable temperature experiments which could have provided evidence for the dynamic exchange.

Chart 5.2

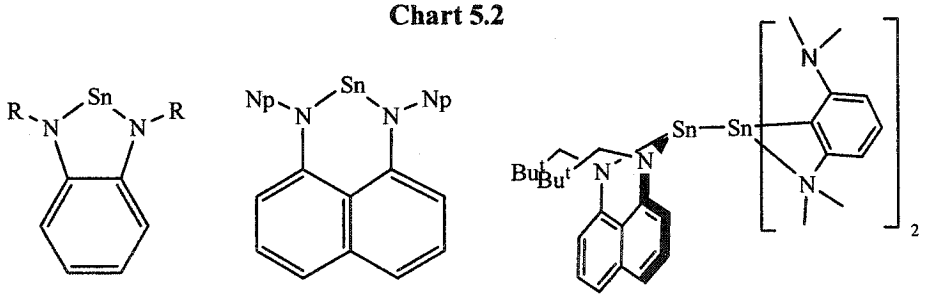

W **X** **Y**

The only directly comparable crystallographically characterized example in the literature is reported for the PDA supported stannylene $Sn(C_6H_4(NR)_2)$ (**W**, R = Np).[14] Examination of the packing diagram of this species revealed an ordered antiparallel arrangement between adjacent molecules. A short distance between the Sn centre of one monomer with the phenylene ring of an adjacent monomeric unit was described as a weak η^6

[18] Goldberg, D. E.; Hitchcock, P. B.; Lappert, M. F.; Thomas, K. M.; Thorne, A. J.; Fjeldberg, T.; Haaland, A.; Schilling, B. E. R. *J. Chem. Soc., Dalton Trans.*. **1986**, 2387-2394.

interaction. In this case, support for an $[\eta^6\text{-}C_6H_4\cdots Sn]_2$ interaction comes from the close contact between the Sn and the centroid of the phenylene ring of 3.23 Å.

There are some literature examples documenting the ability of diamido Sn(II) complexes to function as Lewis acid acceptors. Two of the most interesting are the TMEDA adduct (TMEDA)[Sn{1,2-$(Me_3SiN)_2C_6H_4$}]$_2$[14] (TMEDA[**W**]$_2$) in which each nitrogen of the TMEDA coordinates to a Sn(II) center, and complex **Y** which was characterized as a donor-acceptor complex between an Sn[1,8-$(NCH_2{}^tBu)_2C_{10}H_6$] (**X**) acceptor and a $SnAr_2$ (Ar = 2,5-$(Me_2N)_2C_6H_3$) donor.[17]

C. Theoretical Study

We have examined compound **31** computationally.[19] Beginning with the crystallographic atomic positions, both a single point energy and an energy optimization were carried out on compound **31**. The Hartree-Fock (HF) and Density Functional Theory (DFT/B3LYP) methods were used for these calculations, which employed the two effective core potential basis sets, LANL2DZ and SDD.[20,21,22] The LANL2DZ basis set was used for single point and optimization calculations with both the HF and DFT/B3LYP methods. An additional set

Figure 5.7. Calculated optimized structure and numbering scheme for stannylene **31**.

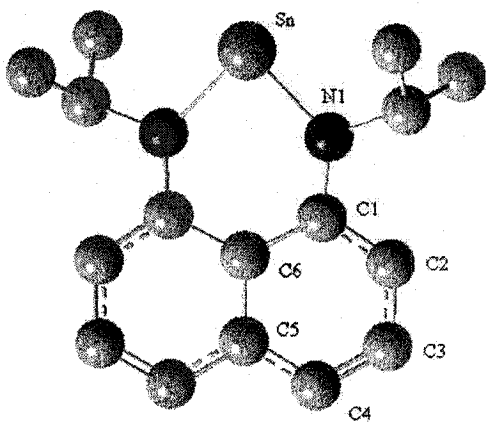

[19] Gaussian 03, Revision A.1, M. J. Frisch, G. W. Trucks, H. B. Schlegel, G. E. Scuseria, M. A. Robb, J. R. Cheeseman, J. A. Montgomery, Jr., T. Vreven, K. N. Kudin, J. C. Burant, J. M. Millam, S. S. Iyengar, J. Tomasi, V. Barone, B. Mennucci, M. Cossi, G. Scalmani, N. Rega, G. A. Petersson, H. Nakatsuji, M. Hada, M. Ehara, K. Toyota, R. Fukuda, J. Hasegawa, M. Ishida, T. Nakajima, Y. Honda, O. Kitao, H. Nakai, M. Klene, X. Li, J. E. Knox, H. P. Hratchian, J. B. Cross, C. Adamo, J. Jaramillo, R. Gomperts, R. E. Stratmann, O. Yazyev, A. J. Austin, R. Cammi, C. Pomelli, J. W. Ochterski, P. Y. Ayala, K. Morokuma, G. A. Voth, P. Salvador, J. J. Dannenberg, V. G. Zakrzewski, S. Dapprich, A. D. Daniels, M. C. Strain, O. Farkas, D. K. Malick, A. D. Rabuck, K. Raghavachari, J. B. Foresman, J. V. Ortiz, Q. Cui, A. G. Baboul, S. Clifford, J. Cioslowski, B. B. Stefanov, G. Liu, A. Liashenko, P. Piskorz, I. Komaromi, R. L. Martin, D. J. Fox, T. Keith, M. A. Al-Laham, C. Y. Peng, A. Nanayakkara, M. Challacombe, P. M. W. Gill, B. Johnson, W. Chen, M. W. Wong, C. Gonzalez, and J. A. Pople, Gaussian, Inc., Pittsburgh PA, 2003.

[20] T. H. Dunning Jr. and P. J. Hay, in *Modern Theoretical Chemistry*, Ed. H. F. Schaefer III, Vol. 3 (Plenum, New York, 1976) 1-28.

[21] P. J. Hay and W. R. Wadt, *J. Chem. Phys.* **1985**, *82*, 270.

[22] (a) X. Y. Cao and M. Dolg, *J. Mol. Struct. (Theochem)* **2002**, *581*, 139. (b) X. Y. Cao and M. Dolg, *J. Chem. Phys.* **2001**, *115*, 7348.

of DFT/B3LYP calculations was carried out using the SDD basis set. The results from these calculations are summarized in Figure 5.7 and Tables 5.5-5.7.

All three optimizations yielded nearly planar molecular structures with the Sn center lying in the same plane as the naphthyl group and with only a slight twist in the metallaheterocycle (Figure 5.7). The structures derived from the calculations are quite similar to each other, and to the structures observed for compounds **29** and **30**, and exhibit symmetrical features as suggested by the NMR spectroscopic measurements. However, the calculated structures differ considerably from the solid state crystallographic data. The most obvious difference between the experimental and calculated structures is the position of the Sn center relative to the plane of the ligand. This comparison can be quantified by the values of the dihedral angles N-Sn-N-C_{naph} and Sn-C(1)-C(6)-C(7) reported in Table 5.5. Accompanying the change in the relative position of Sn in the optimized structures is an increase in the N-Sn-N and the Sn-N(1)-C(1) angles. The N(1) center remains planar (Σ of angles = 360°) but the geometry around N(1) changes slightly with the C(1)-N(1)-C(11) angle decreasing in concert with an increase in the Sn-N(1)-C(1) angle.

The changes that are observed in the optimized structures lead to calculated energy values that are approximately 50 kcal/mole lower than the calculated single point energies for the pyramidal structure that is observed experimentally. The overall similarity of the results obtained from two different theoretical models and different basis sets, supports the validity of comparing of these results with experimental data. The lower energies obtained for the optimized structures suggest that they may be a more accurate description of the solution structure of **31** and that the structure obtained from the X-ray study is an artifact of intermolecular interactions and crystal packing forces.

In order to gain insight on the intermolecular interactions between stannylene **31** molecules, we performed an energy calculation (LANL2DZ basis set in a DFT/B3LYP) on two adjacent molecular units (a dimer) taken from the crystal structure. Our goal was to gain some measure of the energy of the intermolecular Sn-$C_{naphthyl}$ interaction. The calculated single point energy of the bimolecular unit gave a value (-1468.97428229 au) that was slightly lower than twice the value (-734.47894044 au) of a single molecule of **31**. This energy difference corresponds to 10.3 kcal/mole for the stabilization energy of the dinuclear

species relative to two isolated molecules of **31** and provides an estimate for the energy of the Sn-naphthyl interaction.

The remaining 40 kcal/mole energy difference between the optimized, planar structure and the pyramidal, experimental structure may be due to crystal packing forces. The calculated dipole moments and some selected Mulliken charges for the two structures are summarized in Table 5.7. The higher dipole obtained for the experimental structure is consistent with the less symmetrical nature and will lead to additional stability in the solid state (lattice energy). Finally, consistent with the observation that the shortest intermolecular distance is between Sn and C(4) (2.803Å) is the fact that the highest negative charge in the naphthyl moiety is localized on C(4).

To summarize, our calculations show that a planar metallaheterocyclic structure is favoured by approximately 50 kcal/mol. The Sn-naphthyl interaction was determined to be 10.3 kcal/mol compensating only partially for the energy cost associated with the pyramidal experimental structure. The remaining stabilizing energy must therefore come from other interactions within the extended 3-dimensional solid-state structure.

Table 5.5. Selected calculated structural parameters and energies for optimized Sn[1,8-(^{i}PrN)$_2$C$_{10}$H$_6$] (**31**). For ease of comparison with crystallographic data a consistent atom numbering scheme is employed.

Model Basis Set	DFT/B3LYP LANL2DZ	DFT/B3LYP SDD	HF LANL2DZ	Average from Experimental Structure
Sn-N(1)[a]	2.03180	2.07139/42	2.00316	2.07
N(1)-C(1)	1.42540	1.42493/4	1.41912	1.39
N(2)-Sn-N(1)[b]	91.305	90.239	92.141	85.6(3)
C(1)-N(1)-C(11)	117.033	117.245	116.960/2	120.4
C(1)-N(1)-Sn	126.160	125.898/92	125.167	122.1
C(11)-N(1)-Sn	116.429	116.402/4	117.706/4	116.8
C(2)-C(1)-N(1)	119.715	119.528/9	120.134/6	111.6
C(6)-C(1)-N(1)	121.610	121.791	125.167	128.4
C(1)-C(6)-C(7)	125.445	125.623	124.905	120
Dihedral				
N-Sn-N-C(1)	13.2	14.0	14.9	35.6
Sn-C(1)-C(6)-C(7)	0.000	0.012	0.000	16.0

[a] Distances are in Å units. [b] Angles are in degrees. [c] The single point energy values for crystallographic structure are given in parenthesis.

Table 5.6. Energy differences between the optimized structure of Sn[1,8-(^{i}PrN)$_2$C$_{10}$H$_6$] (**31**) and the solid state structure from single crystal X-ray analysis.

Calculated Energy Difference for the Optimized Structures of **31** and the Experimental Structure (kcal/mole)			
Method Basis Set	DFT/B3LYP LANL2DZ	DFT/B3LYP SDD	HF LANL2DZ
Optimized structure	49.67	51.07	51.70

Table 5.7. Calculated Dipole Moment and selected Mulliken Charges for the Experimental and Optimized Structures of Sn[1,8-(^{i}PrN)$_2$C$_{10}$H$_6$] (**31**). For ease of comparison with crystallographic data a consistent atom numbering scheme is employed.

Method Basis Set	DFT/B3LYP LANL2DZ	DFT/B3LYP LANL2DZ	DFT/B3LYP SDD	DFT/B3LYP SDD	HF/ LANL2DZ	HF/ LANL2DZ
	Exp	Opt	Exp	Opt	Exp	Opt
Dipole moment (D)	3.8571	3.0201	3.8182	3.1973	4.4513	2.8391
Mulliken Charges						
Sn	0.775	0.793	0.722	0.742	1.125	1.128
N	-0.69	-0.69	-0.65	-0.636	-1.03	-1.046
C(2)	-0.35	-0.376	-0.36	-0.377	-0.35	-0.385
C(3)	-0.31	-0.262	-0.31	-0.257	-0.27	-0.229
C(4)	-0.49	-0.475	-0.49	-0.472	-0.45	-0.424
C(5)	0.566	0.481	0.565	0.474	0.482	0.374

D. Germanium Chalcogenido Compounds

Carbenes and their heavier analogues typically exist in the +2 oxidation state and are accordingly susceptible to oxidation. Elemental chalcogens are well-known oxidants for low-valent group 14 compounds and have been used for the preparation of interesting terminal chalcogenido compounds.[23] Germylene **29** is susceptible to oxidation by chalcogens to yield Ge(IV) chalcogenido species (Scheme 5.4). Reaction of **29** with elemental sulfur or selenium proceeds smoothly with complete conversion (monitored by NMR) to yield species that display ^{1}H and ^{13}C NMR spectra that are similar to each other and consistent with the formulation of compounds **32a** and **32b**. However, **29** did not react with the milder oxidizing agent tellurium even after 6 days in the presence of excess reagent.

[23] For examples of amidinate group 14 terminal chalcogenido species see: (a) Zhou, Y.; Richeson, D. S. *J. Am. Chem. Soc.* **1996**, *118*, 10850-10852. (b) Foley, S. R.; Bensimon, C.; Richeson, D. S. *J. Am. Chem. Soc.* **1997**, *119*, 10359-10363. (c) Foley, S. R.; Richeson, D. S. *Chem. Commun.* **2000**, 1391-1392.

Scheme 5.4

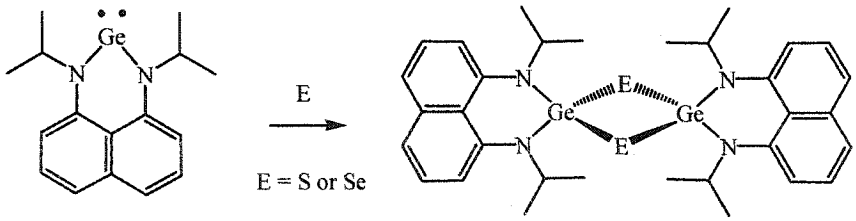

32a) E = S, **32b)** E = Se

Germanium chalcogenido complexes exhibit a range of aggregation levels that depend on the steric contributions of the supporting ligands and on the presence of other bases that can coordinate to the metal centre. Therefore, the structural features of **32a** were investigated by single-crystal X-ray diffraction (Table 5.1). Figure 5.8 displays the results of this analysis with selected bond distances and angles presented in Table 5.8. These results show that **32a** has a dinuclear structure with bridging sulfide ligands generating a planar $[Ge(\mu\text{-}S)]_2$ unit situated on a crystallographic inversion centre. The distorted tetrahedral coordination of the Ge(IV) centre is completed by the original diamidonaphthalene ligand. One molecule of THF co-crystallized in the lattice but displays no interaction with **32a**. The Ge atom in **32a** deviates to one side of the ligand plane (N(1), C(4), C(9), C(10), N(2)) by 0.251 Å while the methine carbons of the ^{i}Pr groups lie 0.016 Å on the opposite side of this plane. The Ge^{IV}-N bond lengths in **32a** of 1.800(3) Å are slightly shorter than those observed for **29**. Other than the N(1)-Ge-N(2) angle, which has increased substantially to 103.91(12)°, the internal angles of the metallaheterocycle are quite similar to those observed in the starting material **29**. The bond lengths and the internal angles for the germanium sulfido core of **32a** are similar to the few reported species exhibiting a $[Ge^{IV}(\mu\text{-}S)]_2$ arrangement which exhibited Ge-S bond lengths in the range 2.226(2)-2.243(8) Å, S-Ge-S angles from 95.2 to 96.7°, and Ge-S-Ge angles from 83.2 to 84.7°.[24,25]

---

[24] For examples of structurally characterized dimeric μ-sulfido complexes see: (a) Wojnowska, M.; Noltemeyer, M.; Füllgrabe, H.-J.; Meller, A. *J. Organomet. Chem.* **1982**, *228*, 229. (b) Hitchcock, P. B.; Jasim, H. A.; Kelley, R. E.; Lappert, M. F. *J. Chem. Soc., Chem. Commun.* **1985**, 1776. (c) Puff, H.; Braun, K.; Franken, S.; Kök, T. R.; Schuh *J. Organomet. Chem.* **1987**, *335*, 167. (d) Veith, M.; Nötzel, M.; Stahl, L.; Huch, V. *Z. Anorg. Allg. Chem.* **1994**, *620*, 1264.

[25] For examples of structurally characterized sesquisulfides possessing [Ge(μ-S)]2 units see: (a) Ando, W.; Kadowaki, T.; Kabe, Y.; Ishii, M. *Angew. Chem., Int. Ed. Engl.* **1992**, *31*, 59. (b) Unno, M.; Kawai, Y.; Shioyama, H.; Matsumoto, H. *Organometallics* **1997**, *16*, 4428.

III. Conclusion

The use of chelating diamido ligands based on dialkyl- and diaryl-1,8-DAN successfully led to the isolation of low-valent group 14 carbene analogues. In the case of the germylenes (**29** and **30**), the newly formed metallaheterocycles are planar, or very slightly twisted in the solid-state. The stannylene (**31**) despite exhibiting spectroscopic features consistent with a planar metallaheterocycle, assumes pyramidally distorted geometry in the solid-state. The presence of an intermolecular Sn···arene interaction was observed in the extended molecular structure. Calculations revealed that the planar heterocyclic geometry should be favoured by approximately 50 kcal/mol, and that the Sn···arene interactions only account for 10.3 kcal/mol of the energy cost associated with the pyramidal distortion. Reactions with chalcogens demonstrated the facile oxidation of the germylenes to yield bridging chalcogenido species. The apparent ambivalence of this group of species for displaying both Lewis-acidic (π-coordination) and Lewis-basic (facile oxidation) behaviours should lead to interesting and unanticipated applications.

Experimental Section

General: All manipulations were carried out in either a nitrogen filled dry box or under nitrogen using standard Schlenk-line techniques. Unless otherwise noted, solvents were purged with nitrogen then dried by passage through column of activated alumina using an apparatus purchased from Anhydrous Engineering. Deuterated benzene and toluene were dried by vacuum transfer from potassium. $SnCl_2$, 1,8-diaminonapthalene, S_8, Se, Te, MeLi (1.4 M in ether, were purchased from Aldrich Chemical Company and used without further purification. $Ge[N(SiMe_3)_2]_2$,[1b] $Sn[N(SiMe_3)_2]_2$,[1b] $GeCl_2$·dioxane[26] were prepared according to literature procedures. All elemental analyses were run on a Perkin Elmer PE CHN 4000 elemental analysis system. ^1H and ^{13}C NMR spectra were run on Varian Gemini-200, a Bruker 300MHz or a Bruker 500MHz using the residual protons of the deuterated solvent for reference unless otherwise specified.

[26] Fjeldberg, T.; Haaland, A.; Schilling, B. E. R.; Lappert, M. F.; Thorne, A. J. *J. Chem. Soc., Dalton Trans.* **1986**, 1551-1556.

Preparation of $Li_2[1,8\text{-}(^iPrN)_2C_{10}H_6](THF)_4$

Addition of MeLi (2.5 ml, 1.4 M in ether, 3.5 mmol) to a dark red/purple solution of diamine **4a** (0.424 g, 1.7 mmol) in ether (ca. 30 ml) led to an immediate color change of the solution to green then brown with gas evolution. The reaction mixture was stirred for 4 h and then all volatiles were removed under vacuum. The crude product (0.440 g, 99%) was then purified by crystallization from THF at –35°C. The crystals were filtered and dried under vacuum. Product isolated by this method possessed four molecules of THF.

^{1}H NMR (C_6D_6,): δ 7.40 (t, 2H, Ar-H), 6.94 (d, 2H, Ar-H), 6.36 (m, 2H, Ar-H), 3.55 (sept, 2H, $CH(Me)_2$), 3.36 (t, 16H THF) 1.28 – 1.18 (overlapping signals, 28H, CH_3 and THF).

^{13}C NMR (C_7D_8,): 127.1 (Ar *C*H), 110.9 (Ar *C*H), 101.3 (Ar *C*H), 68.0 (*C*H_2, THF), 47.3 (*C*HMe_2), 25.6 (*C*H_2, THF), 25.1 (*C*H_3). Anal Calcd for $C_{32}H_{52}N_2O_4Li_2$: C, 70.83; H, 9.66; N, 5.16. Found: C, 70.48; H, 9.29; N, 5.60.

Preparation of $Ge[1,8\text{-}(^iPrN)_2C_{10}H_6]$, (29)

From $GeCl_2$(dioxane) and $Li_2[1,8\text{-}(^iPrN)_2C_{10}H_6]$

Addition of MeLi (2.86 ml, 1.4 M in ether, 4.0 mmol) to a dark red/purple solution of diamine **4a** (0.485 g, 2.0 mmol) in ether (ca. 30 ml) led to a color change to green, then brown with gas evolution. The mixture was stirred for 1 h and solid $GeCl_2$•dioxane (0.466 g, 2.0 mmol) was then added. The reaction mixture quickly became orange in color and a precipitate was formed. After 18 h of stirring the solvent was removed under vacuum and the product was extracted with hexane (ca. 50 ml). Filtration followed by removal of the volatiles yielded **29** (0.50 g, 80 %). Compound **29** could be further purified by recrystallization from hexane or ether. ^{1}H NMR (C_6D_6,): δ 7.25 (s, 2H, Ar-H), 7.22 (s, 2H, Ar-H), 6.33 (m, 2H, Ar-H), 3.81 (sept, 2H, $CH(Me)_2$), 1.28 (d, 12H, CH_3). ^{13}C NMR (C_6D_6,): 144.7 (Ar *C*), 138.6 (Ar *C*), 126.8 (Ar *C*H), 123.9 (Ar *C*), 119.4 (Ar *C*H), 104.5 (Ar *C*H), 51.0 (*C*HMe_2), 26.2 (*C*H_3). Anal Calcd for $C_{16}H_{20}N_2Ge$: C, 61.4; H, 6.44; N, 8.95. Found: C, 61.06; H, 6.78; N, 8.75. m.p. 103-105°C

From $Ge[N(SiMe_3)_2]_2$ and $[1,8\text{-}(^iPrNH)_2C_{10}H_6]$

In a 50 ml round bottom flask equipped with a magnetic stir bar, $Ge[N(SiMe_3)_2]_2$ (0.316 g, 0.80 mmol) previously dissolved in 30 ml of hexane was added a hexane solution of diamine

4a (0.195 g, 0.80 mmol). The color of the solution turned from purple to brownish with concomitant formation of precipitate. After stirring for 18 hrs the reaction mixture was filtered. The hexane solution was then allowed to stand for one week. An NMR spectrum of the reaction mixture was prepared by removing an aliquot of the mixture, evaporating to dryness and dissolving in C_6D_6. This indicated that compound **29** along with a small amount of $HN(SiMe_3)_2$ and unreacted diamine **4a** were the only constituents. Further purification of **29** from this solution was troublesome due to the high solubility of both products in hexane.

Preparation of Ge[1,8-(3,5-$Me_2C_6H_3N)_2C_{10}H_6$], (30)

In a round bottom flask equipped with a stir-bar was dissolved the diamine ligand 1,8-((3,5-$Me_2C_6H_3$)NH)$_2C_{10}H_6$ (0.210g, 0.57 mmol) in approximately 25 ml of ether. To this solution was added an ether solution of MeLi (0.82 ml, 1.4 M, 1.15 mmol) dropwise and the reaction was stirred for one hour. Solid $GeCl_2$·dioxane (0.132g, 0.57 mmol) was added to the reaction. The solution turned orange/yellow and a precipitate started forming. The reaction was stirred overnight then all volatiles were removed under vacuum. The yellow powder was tritrated with toluene twice and the product was extracted with 20 ml of toluene and the insoluble precipitate was removed by filtration. The volatiles were removed under vacuum and pure product was obtained as a orange/yellow solid (0.24g, 0.55 mmol, 96 %). The product can be recrystallized from an ether/toluene solution at -25°C.

^{1}H NMR (C_6D_6, 300 MHz): δ 7.12 (d, 2H, C*H*), 7.00 (t, 2H, C*H*), 6.78 (s, 4H, C*H*), 6.72 (s, 2H, C*H*), 6.36 (d, 2H, C*H*), 2.10 (s, 12H, CH_3).

^{13}C NMR (C_6D_6, 300 MHz): δ 147.2 (*C*), 145.5 (*C*), 140.2 (*C*), 138.6 (*C*), 128.6 (2C, C_{Ar}H), 127.2 (4C, C_{Ar}H), 127.1 (*C*H), 122.3 (*C*), 119.8 (*C*H), 108.3 (*C*H), 21.2 (CH_3).

Preparation of Sn[1,8-(^{i}PrN)$_2C_{10}H_6$], (31)

Following a procedure similar to the preparation of **29**. The diamine ligand **4a** (0.485g, 2.0 mmol) was reacted with MeLi (2.86 ml, 1.4 M) and $SnCl_2$ (0.378g, 2.0 mmol) and yield the product **31** (0.561g, 78 %) after extraction of the evaporated reaction mixture with toluene. The product could be further purified by recrystallization from hot toluene.

^{1}H NMR (C_7D_8, 500 MHz): δ 7.24 (t, 2H, C*H*), 7.15 (d, 2H, C*H*), 6.32 (d, 2H, C*H*), 4.05 (sept, 2H, C*H*Me_2), 1.27 (d, 12H, CH_3),

^{13}C NMR (C_7D_8, 500 MHz): δ 149.1 (*C*), 139.0 (*C*), 126.3 (*C*H), 118.7 (*C*H), 116.8 (*C*), 105.3 (*C*H), 51.8 (*C*HMe$_2$), 27.8 (*C*H).

^{119}Sn NMR (C_7D_8, 500 MHz): δ 330 (br)

Anal Calcd for $C_{16}H_{20}N_2Sn$: C, 53.52; H, 5.61; N, 7.80. Found: C, 53.87; H, 5.62; N, 7.73.

Preparation of {[1,8-(^{i}PrN)$_2$C$_{10}$H$_6$]Ge(μ-S)}$_2$, (32a)

To a pale orange solution of **29** (0.117 g, 0.36 mmol) in ether (ca. 30 ml) was added solid S_8 (0.047 g, 0.18 mmol). The solution became pale yellow and some unreacted sulfur remained. After 18 h of stirring the reaction mixture was filtered and the solvent was removed under vacuum. The product was recrystallized from THF (0.040g, 31%).

^1H NMR (C_6D_6,): δ 7.26 (dd, 2H), 7.18 (t, 2H), 6.88 (dd, 2H), 4.90 (sept, 2H, CH(Me)$_2$), 1.57 (d, 12H, CH_3).

^{13}C NMR (C_6D_6,): 143.0 (Ar *C*), 138.4 (Ar *C*), 126.2 (Ar *C*), 125.7 (Ar *C*H), 120.3 (Ar *C*H), 110.9 (Ar *C*H), 50.6 (*C*HMe$_2$), 20.9 (*C*H$_3$).

Anal Calcd for $C_{16}H_{20}N_2GeS$: C, 55.70; H, 5.84; N, 8.11. Found: C, 55.85; H, 5.88; N, 8.16. m.p. 228°C decomp.

Preparation of {[1,8-(^{i}PrN)$_2$C$_{10}$H$_6$]Ge(μ-Se)}$_2$, (32b)

In a Teflon sealed NMR tube, **29** (0.020 g, 63 μmol) was dissolved in approximately 1 ml of C_6D_6. To this pale orange solution was added an excess of solid Se (0.030 g). The solution turned slightly reddish and there remained some solid selenium in the tube. After six days the NMR spectra showed complete conversion of the starting material to **32b**. ^1H NMR (200 MHz, C_6D_6,): δ 7.24 (dd, 2H), 7.19 (t, 2H), 6.87 (dd, 2H), 5.0 (sept, 2H), 1.62 (d, 12H). ^{13}C NMR (200 MHz, C_6D_6,): 125.7 (2 C), 120.0 (2 C), 110.3 (2 C), 50.9 (2 C), 20.7 (4 C). m.p. 237°C decomp.

Structural determinations for 29, 30, 31 and 32a:

Single crystals were mounted on thin glass fibres using viscous oil and then cooled to the data collection temperature. Crystal data and details of the measurements are summarized in Table 5.1. Data were collected on a Bruker AX SMART 1k CCD diffractometer using 0.3° ω-scans at 0, 90, and 180° in ϕ. Unit-cell parameters were determined from 60 data frames

collected at different sections of the Ewald sphere. Semi-empirical absorption corrections based on equivalent reflections were applied (Blessing, R., *Acta Cryst.*, **1995,** A51, 33-38).

The structures were solved by direct methods, completed with difference Fourier syntheses and refined with full-matrix least-squares procedures based on F^2. All non-hydrogen atoms were refined with anisotropic displacement parameters. All hydrogen atoms were treated as idealized contributions. All scattering factors and anomalous dispersion factors are contained in the SHELXTL 5.1 program library (Sheldrick, G. M., Bruker AXS, Madison, WI, 1997).

Figure 5.1. Molecular structure of germylene **29**. Hydrogen atoms have been omitted for clarity. Thermal ellipsoids are drawn at 30% probability.

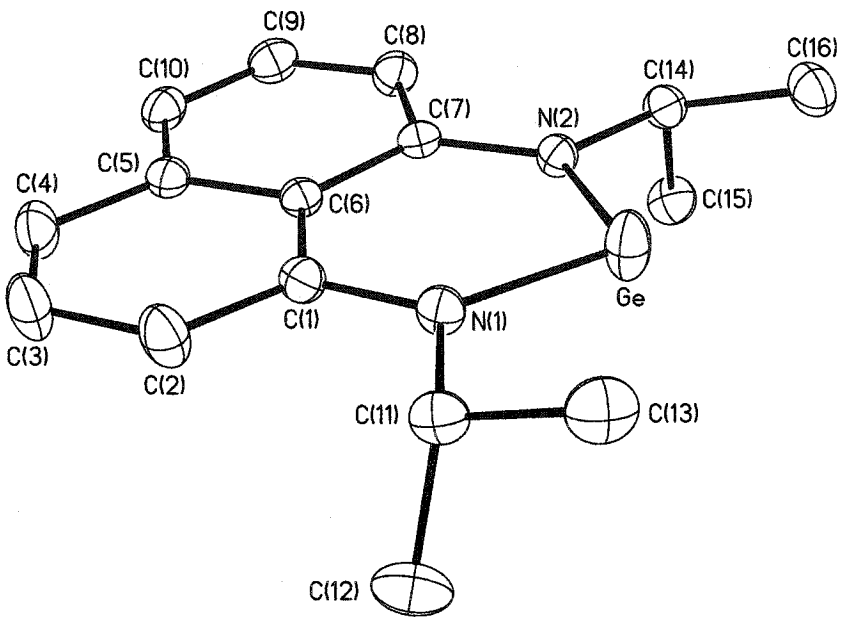

Figure 5.2. Packing arrangement of germylene **29** showing the relationship between adjacent molecules in the structure.

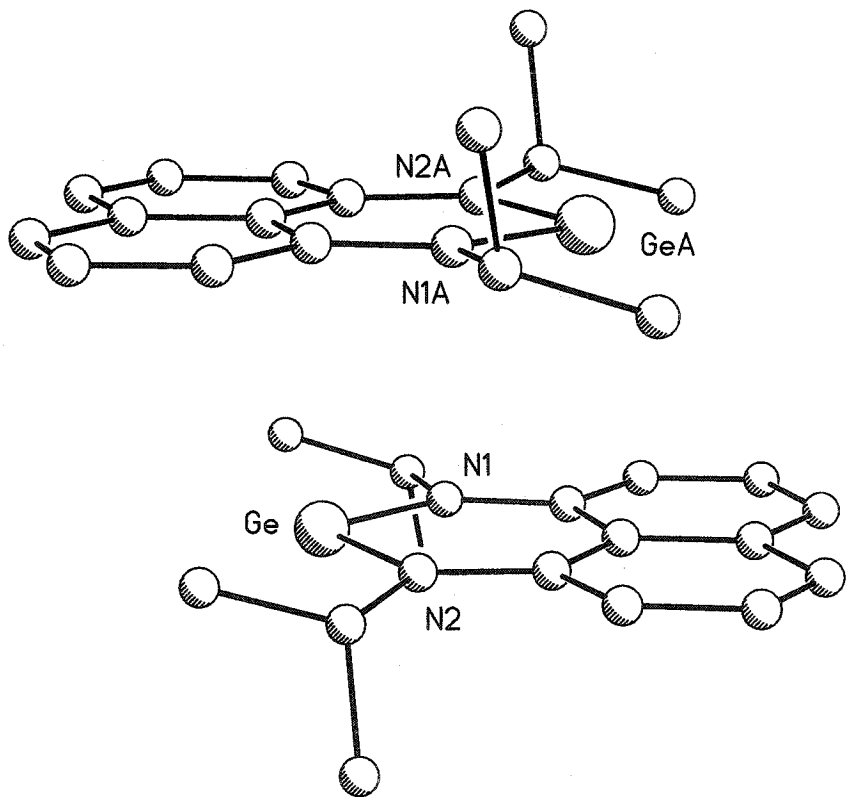

Figure 5.3. Molecular structure of germylene **30**. Hydrogen atoms and CH_2Cl_2 have been omitted for clarity. Thermal ellipsoids are drawn at 30% probability.

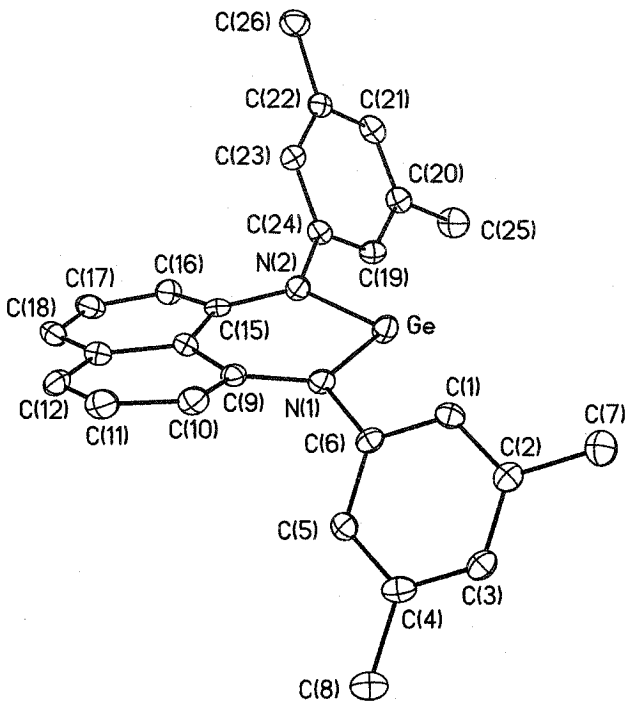

Figure 5.4. Packing arrangement of germylene **30** showing the relationship between adjacent molecules in the structure.

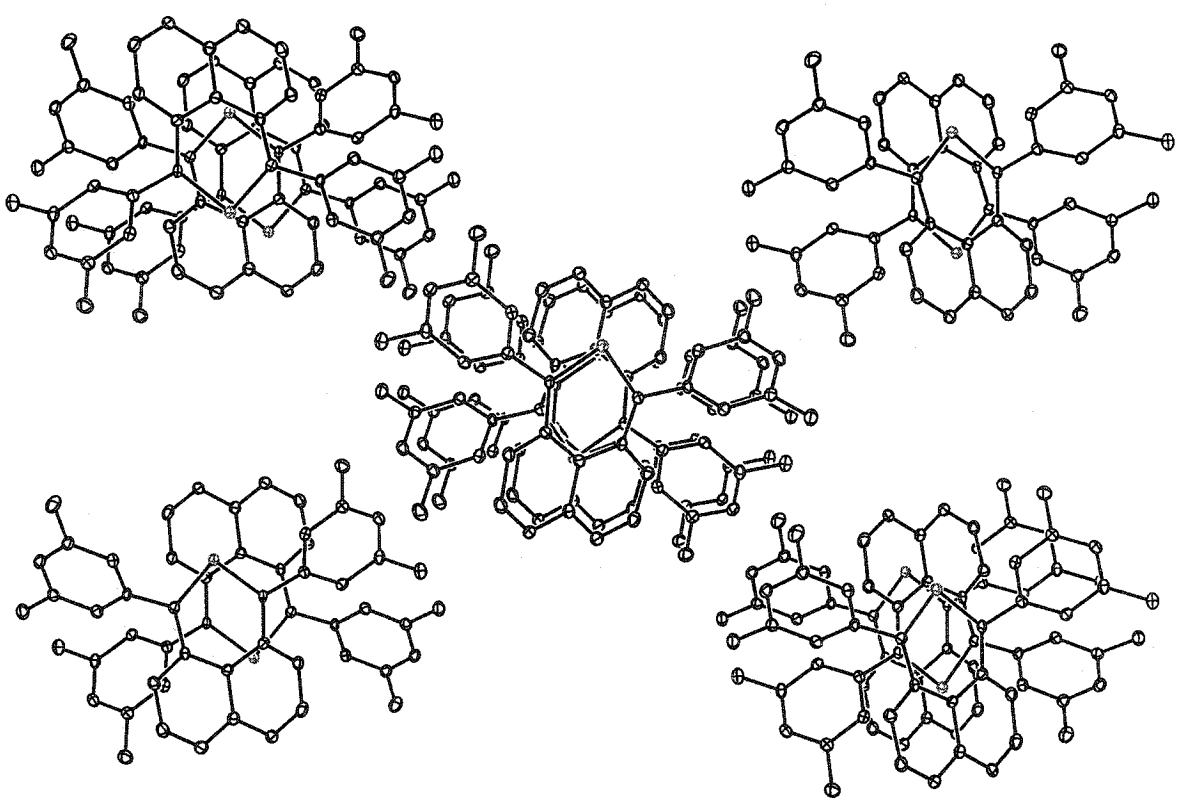

Figure 5.5. Molecular structure of stannylene **31**. Hydrogen atoms have been omitted for clarity. Thermal ellipsoids are drawn at 30% probability.

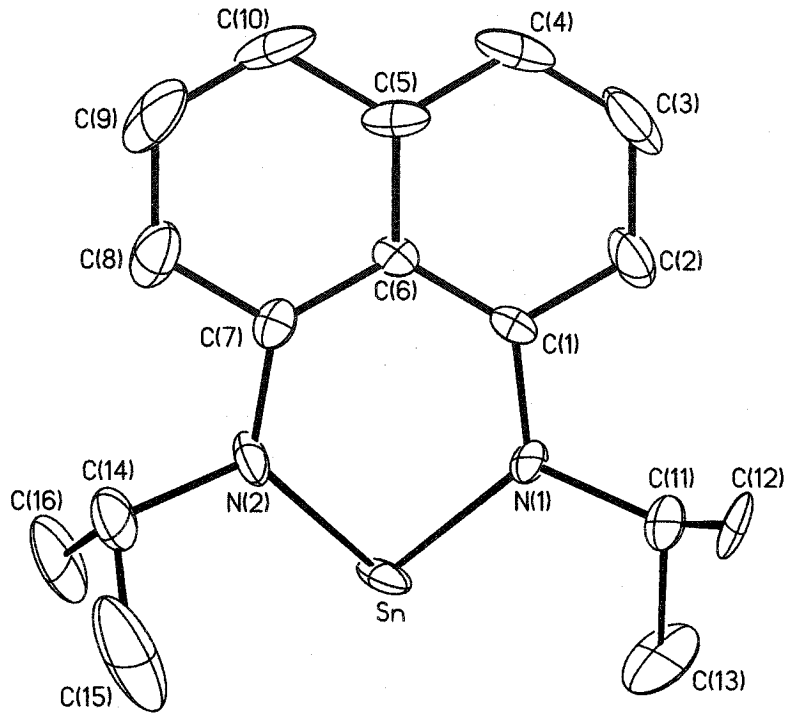

Figure 5.6. Packing arrangement of stannylene **31** showing the relationship between two adjacent molecules in the structure.

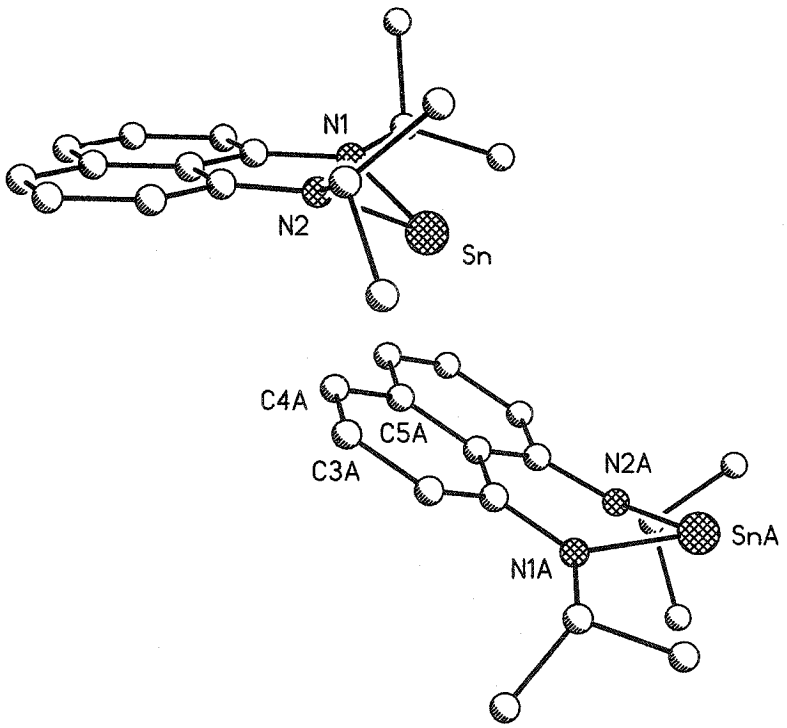

Figure 5.8. Molecular structure of germanium sulfido **32a**. All hydrogen atoms and two co-crystallized THF molecules have been omitted for clarity. Thermal ellipsoids are drawn at 30% probability.

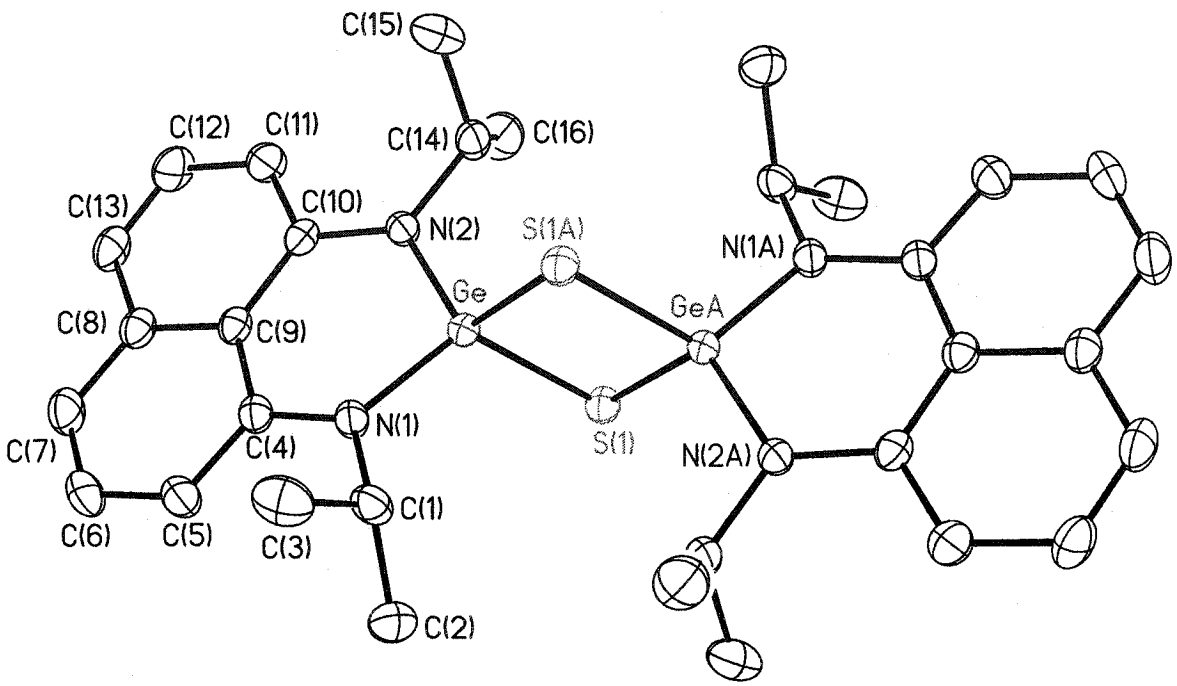

Table 5.1. Selected Crystal Data and Data Collection Parameters for **29**, **30**, **31**, and **32a**.

	29	**30**	**31**	**32a-(2 THF)**
empirical formula	$C_{16}H_{20}GeN_2$	$C_{27}H_{26}Cl_2GeN_2$	$C_{16}H_{20}N_2Sn$	$C_{40}H_{56}Ge_2N_4O_2S_2$
formula weight	312.93	521.99	359.03	834.19
T (K)	236(2)	203(2)	238(2)	238(2)
wavelength (Å)	0.71073	0.71073	0.71073	0.71073
crystal system	Orthorhombic	Monoclinic	Orthorhombic	Monoclinic
space group	Pbca	$P2_1/c$	$P2_12_12_1$	$P2_1/c$
a (Å)	16.191(4)	8.4211(13)	9.646(3)	15.881(2)
b (Å)	10.877(3)	13.515(2)	9.685(3)	14.853(2)
c (Å)	16.398(4)	21.598(3)	15.689(5)	8.597(1)
α (deg)	90	90	90	90
β (deg)	90	94.363(3)	90	98.974(3)
γ (deg)	90	90	90	90
V (Å^3)	2888(1)	2451.0(6)	1465.7(8)	2002.9(5)
Z	8	4	4	2
abs coeff (mm^{-1})	2.110	1.485	1.732	1.644
final R indices	R1 = 0.0342	R1 = 0.0677	R1 = 0.0596	R1 = 0.0405
	wR2 = 0.0732	wR2 = 0.1318	wR2 = 0.1088	wR2 = 0.0870

Table 5.2. Selected Bond Distances and Angles for **29**

Bond Distances (Å)			
Ge-N(1)	1.8417(17)	Ge-N(2)	1.8420(16)
N(1)-C(1)	1.410(3)	N(2)-C(7)	1.402(2)
N(1)-C(11)	1.487(3)	N(2)-C(14)	1.494(3)
Bond Angles (deg)			
N(1)-Ge-N(2)	97.28(7)	C(7)-N(2)-C(14)	116.95(16)
C(1)-N(1)-Ge	127.22(14)	C(7)-N(2)-Ge	127.53(13)
C(11)-N(1)-Ge α	115.63(13)	C(14)-N(2)-Ge α	115.46(13)
C(1)-N(1)-C(11)	117.14(16)	Sum at N(2)	359.94
Sum at N(1)	359.99		

Table 5.3. Selected Bond Distances and Angles for **30**

Bond Distances (Å)			
Ge-N(1)	1.879(4)	N(1)-C(9)	1.424(7)
Ge-N(2)	1.873(5)	N(2)-C(24)	1.450(6)
N(1)-C(6)	1.441(6)	N(2)-C(15)	1.414(7)
Bond Angles (deg)			
N(2)-Ge-N(1)	94.58(19)	C(15)-N(2)-C(24)	118.9(4)
C(6)-N(1)-Ge α	112.7(3)	C(24)-N(2)-Ge α	113.2(3)
C(9)-N(1)-Ge	127.8(4)	C(15)-N(2)-Ge	127.9(4)
C(9)-N(1)-C(6)	119.3(4)	Sum at N(2)	360.0
Sum at N(1)	359.8		

Table 5.4. Selected Bond Distances and Angles for **31**

	Bond Distances (Å)		
Sn-N(1)	2.074(8)	Sn-N(2)	2.066(8)
N(1)-C(1)	1.402(8)	N(2)-C(7)	1.382(9)
N(1)-C(11)	1.509(14)	N(2)-C(14)	1.526(14)
	Bond Angles (deg)		
N(2)-Sn-N(1)	85.6(3)	C(7)-N(2)-Sn	121.2(5)
C(11)-N(1)-Sn	116.1(7)	C(14)-N(2)-Sn	117.4(7)
C(1)-N(1)-Sn	122.9(5)	C(7)-N(2)-C(14)	121.0(8)
C(1)-N(1)-C(11)	119.7(8)	Sum at N(2)	359.6
Sum at N(1)	358.7		
C(6)-C(1)-N(1)	126.9(4)	N(2)-C(7)-C(6)	129.8(5)

Table 5.8. Selected Bond Distances and Angles for **32a-(2 THF)**

	Bond Distances (Å)		
Ge-N(1)	1.800(3)	Ge-S(1)	2.2457(9)
Ge-N(2)	1.800(3)	Ge-S(1)#1	2.2230(9)
N(1)-C(4)	1.409(4)	N(2)-C(10)	1.398(4)
N(1)-C(1)	1.479(4)	N(2)-C(14)	1.487(4)
	Bond Angles (deg)		
N(2)-Ge-N(1)	103.91(12)	S(1)#1-Ge-S(1)	95.05(3)
N(1)-Ge-S(1)#1	114.58(10)	N(2)-Ge-S(1)#1	114.23(9)
N(1)-Ge-S(1)	115.78(9)	N(2)-Ge-S(1)	113.77(10)
Ge#1-S(1)-Ge	84.95(3)	C(10)-N(2)-C(14)	123.6(3)
C(4)-N(1)-C(1)	123.1(3)	C(10)-N(2)-Ge	122.7(2)
C(4)-N(1)-Ge	121.5(2)	C(14)-N(2)-Ge	113.8(2)
C(1)-N(1)-Ge	115.3(2)	Sum at N(2)	360.1
Sum at N(1)	359.9		

6 *Metal Complexes of Carbenes and Analogues*

I. Introduction

Intimately linked to the efforts in ligand design is the realization that the electronic and structural properties of a ligand have a powerful impact on the rates, turnover numbers and selectivity of metal-based catalytic reactions. There are two opposite, yet converging approaches to ligand design for practical catalytic processes. The first method is to take an existing catalytic system, and to use ligand design in order to improve certain desired aspects of the system, such as selectivity, catalyst loading, or any other targeted attribute. The other is to design a ligand which possesses unique electronic and structural properties, and to exploit these properties in an appropriate catalytic system.

The synthetic breakthrough which permitted the isolation of stable carbenes had a profound, and unexpected, effect in the field of homogeneous catalysis. Metal carbene complexes have been known for many decades and were, until the advent of the stable

carbene, classified in two distinct categories; Fischer carbenes, and Schrock carbenes.[1] The Schrock carbene is best described as an alkylidene, or an $M=CR_2$ fragment where the carbene moiety would be assigned a formal charge of -2.[2] Fischer carbenes on the other hand, are characterized by the presence of at least one stabilizing heteroatom, M=C(ER)R (E = O, N, etc.), and are viewed as neutral ligands or lone-pair donors with a formal charge of 0.[3]

The two types of carbenes however, were considered as reactive functional groups, not as ancillary ligands capable of affecting the reactivity of other functionalities. Additionally, the synthetic approaches which generated metal carbene complexes were fairly limited: carbenes were known to be stable only as coordinated metal fragments. An important point to realize is that diaminocarbenes had been observed as metal carbene fragments and justly considered as Fischer type carbenes. However, the diaminocarbene complexes were exclusively obtained from enetetramines, which served as carbene synthons.[4]

Shortly after realizing that stable carbenes could be isolated and purified, researchers began to explore their properties as ligands. It quickly became apparent that these carbenes were adept at making strong metal-ligand bonds and the possibility of using carbenes as supporting ligands to replace other lone-pair donors such as amines and phosphines began to surface. This has led to the exploitation of the unique properties of nucleophilic carbenes for various catalytic systems.

One of the early, and perhaps the most significant, impacts of stable carbenes was in the field of Ru-based olefin metathesis. Grubbs and co-workers had been developing phosphine based ruthenium alkylidene complexes that were capable of catalyzing olefin metathesis reactions (ring-closing, ring-opening, cross-metathesis). Replacement of one phosphine ligand by a stable nucleophilic N-Heterocyclic Carbene (NHC) greatly improved

---

[1] For a brief description of these two ligand types see: *The Organmetallic Chemistry of the Transition Metals*; Crabtree, R. H.; Wiley: New York, 1994; 2nd ed.
[2] Schrock, R. R. *J. Am. Chem. Soc.* **1974**, *96*, 6796-6797.
[3] Fischer, E. O.; Maasböl, A. *Angew. Chem. Int. Ed. Engl.* **1964**, *3*, 580-581.
[4] For a review on the coordination chemistry of enetetramines see: Lappert, M. F. *J. Organomet. Chem.* **1988**, *358*, 185-214.

the rates and robustness of the catalysts.[5] The remarkable usefulness of these catalysts began to be explored by researchers in fields ranging from materials chemistry to natural product synthesis. In some respects, the advent of such practical olefin metathesis catalysts has changed organic chemistry as a whole.[6]

The conclusions drawn from the studies on Ru olefin metathesis catalysts suggested that NHCs are very electron donating ligands that tend to form strong metal-ligand bonds which seemingly do not undergo dissociation or exchange. These are very appealing properties to be found in a ligand, and stable carbenes were subsequently explored as potential ligands for a myriad of catalytic systems. Stable carbene ligands are now regarded as a staple in homogeneous catalysis.

Our interest in developing rigid chelating diamido ligands which possessed delocalized π-systems directed us to the utilization of 1,8-DAN based ligands for transition and main group metals. This novel ligand platform proved to be excellent for the stabilization of low-valent low-coordinate group 14 compounds. A series of stable carbenes, along with Ge and Sn analogues were synthesized. This new class of carbene, and the heavier analogues, possesses two non-bonding electrons which, in a ground-state singlet configuration, form a lone pair. As a result, these molecules function as Lewis bases and, like typical NHCs, are potential ligands for transition metals.

We decided to explore the possibility of using the carbenes, and carbene analogues, described earlier in this work as ligands for late-transition metals in an attempt to gain an understanding for their electronic properties. This chapter will show that indeed dialkyl-1,8-DAN supported carbenes and germylenes can function as ligands. We will also present some spectroscopic experiments which indicate that the perimidine-based carbenes are among the most electron-donating nucleophilic carbenes.

---

[5] (a) Scholl, M.; Trnka, T. M.; Morgan, J. P.; Grubbs, R. H. *Tetrahedron Lett.* **1999**, *40*, 2247-2250. (b) Ackermann, L.; Fürstner, A.; Weskamp, T.; Kohl, F. J.; Herrmann, W. A. *Tetrahedron Lett.* **1999**, *40*, 4787-4790. (c) Huang, J.; Stevens, E. D.; Nolan, S. P.; Peterson, J. L. *J. Am. Chem. Soc.* **1999**, *121*, 2674-2678. (d) Scholl, M.; Ding, S.; Lee, C. W.; Grubbs, R. H. *Org. Lett.* **1999**, *1*, 953-956. (e) Morgan, J. P.; Grubbs, R. H. *Org. Lett.*, **2000**, *2*, 3153-3155.

[6] For a review on Ru olefin metathesis catalysts see Trnka, T. M.; Grubbs, R. H. *Acc. Chem. Res.* **2001**, *34*18-29.

II. Results

A. Metal Germylene Complexes

Germylenes have been employed as ligands in metal complexes and are most commonly used with middle to late transition metals.[7] Germylene complexes of Ni have received particular attention and have shown interesting catalytic and photochemical properties.[8] The routes taken to obtain the Ni bound germylene complexes typically utilize nickel phosphine, or olefin complexes which undergo ligand exchange with the germylenes.

Reaction of germylene **29** with bis(1,5-cyclooctadiene)nickel ($Ni(COD)_2$) was investigated. When monitored by ^1H NMR spectroscopy in C_6D_6 the reaction between **29** and $Ni(COD)_2$ in a ratio of 4:1 appeared complete and free 1,5-cyclooctadiene was the sole by-product (Scheme 6.1). The NMR spectroscopic characterization of **33** supports the formation of a single germylene containing product with a single naphthalene environment. These results point to the assignment of a homoleptic germylene complex as the identity of **33**.

Scheme 6.1

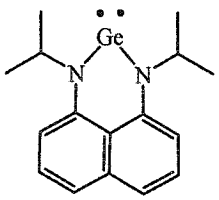

29

$Ni[COD]_2$

- 2 COD

$[C_{10}H_6(^iPrN)_2]_4Ni$

33

The only other reported homoleptic germylene nickel complex, Ni(germylene)$_3$ (germylene = **S**, Chart 5.1, Chapter 5), is not structurally characterized.[9,10] Structurally characterized Ni germylene complexes are limited to the bis(germylene) complex $L_2Ni(CO)_2$ (**Z**, L = **S**), the mono(germylene) species $LNi(PPh_3)_2$ (L = $Ge[N(SiMe_3)_2]$ (**AA**) or Ge(2,4,6-

[7] For a review on transtion metal MX_2 componds (M = Ge, Sn, Pb; X = anionic ligand) see Lappert, M. F.; Rowe, R. S. *Coord. Chem. Rev.* **1990**, *100*, 267-292.

[8] (a) Litz, K. E.; Bender IV, J. E.; Kampf, J. W.; Banaszak Holl, M. M. *Angew. Chem. Int. Ed. Engl.* **1997**, *36*, 496-497. (b) Bender, J. E.; Banaszak Holl, M. M.; Mitchell, A.; Wells, N. J.; Kampf, J. W. *Organometallics* **1998**, *17*, 5166-5171. (c) Bender, J. E.; Shustermann, A. J.; Banaszak Holl, M. M.; Kampf, J. W. *Organometallics* **1999**, *18*, 1547-1552. (d) Litz, K. E.; Bender, J. E.; Sweeder, R. D.; Banaszak Holl, M. M.; Kampf, J. W. *Organometallics* **2000**, *19*, 1186-1189.

[9] Herrmann, W. A.; Denk, M.; Behm, J.; Scherer, W.; Klingan, F.-R.; Bock, H.; Solouki, B.; Wagner, M. *Angew. Chem. Int. Ed. Engl.* **1992**, *31*, 1485-1488.

[10] Related homoleptic Pd(0) and Pt(0) germylene ($Ge(N(SiMe_3)_2)$ compounds are reported in Hitchcock, P. B.; Lappert, M. F.; Misra, M. C. *J. Chem. Soc., Chem. Commun.* **1985**, 863-864.

$(CF_3)_3C_6H_2)_2$ (**BB**)), and $\{[(^tBuO)(\mu\text{-}O^tBu)]GeNi\text{-}(CO)_3\}_2$ (**CC**).[9,11,12] Therefore, we chose to carry out a single-crystal X-ray structure determination on **33** (Table 6.1). This study revealed two independent molecules of the tetrakis(germylene)Ni(0) complex in the unit cell, $Ni\{Ge[(^iPrN)_2C_{10}H_6]\}_4$, with each exhibiting similar structural parameters. One of these is displayed in Figure 6.1 with selected bond distances and angles provided in Table 6.2. The Ni centre possesses a single crystallographically unique germylene ligand and a coordination environment that is distorted tetrahedral. The Ge-Ni bond length of 2.2400(16) Å is close to the sum of the covalent radii for these elements and similar to the Ge-Ni bond distances observed in **Y** and **CC**.[9,12] These distances are slightly longer than observed for $(Ph_3P)_2NiGe[N(SiMe_3)_2]_2$ (**AA**) with a Ni-Ge distance of 2.206(1) Å and for which some degree of multiple bonding was suggested.[11]

Within the germylene ligands, the Ge-N bond lengths and the N-Ge-N angle are slightly reduced from those of the parent germylene (**29**). Distinct from the planar structure observed for **29**, when bonded to the Ni centre the germylene exhibited a substantial twist (Figure 6.1) as evinced by the torsion angles C(11)-N(1)-C(1)-C(2) = 23.3(13)° and C(14)-N(2)- C(7)-C(8) = 10.4(14)°. This contrasts with the related species **Z** and the recently reported homoleptic Ni(silylene)$_3$ complexes.[13] The twisting of the germylene structure substantiates our thoughts that the geometric constraints of a six-membered ring forces the N-substituents close to the metal centre imposing strong steric pressure.

The cone angle observed for the germylene ligand in **33** provides a measure of the steric bulk of these ligands when bonded to Ni. Using the space filling diagram shown in Figure 6.2 a cone angle of 145° was measured for **29**. Although more planar, or 2-dimensional, than phosphines the large cone angle of **29** puts it in league with bulky ligands such as PPh_3.[14]

---

[11] (a) Litz, K. E.; Bender IV, J. E.; Kampf, J. W.; Banaszak Holl, M. M. *Angew. Chem. Int. Ed. Engl.* **1997**, *36*, 496-497. (b) Bender, J. E.; Shustermann, A. J.; Banaszak Holl, M. M.; Kampf, J. W. *Organometallics* **1999**, *18*, 1547-1552.
[12] Grenz, M.; Hahn, E.; du Mont, W.-W.; Pickardt, J. *Angew. Chem., Int. Ed. Engl.* **1984**, *23*, 61.
[13] Schmedake, T. A.; Haaf, M.; Paradise, B. J.; Powell, D.; West, R. *Organometallics* **2000**, *19*, 3263-3265.
[14] Tolman, C. A. *Chem. Rev.* **1977**, *77*, 313-348.

B. Six-Membered Carbene Complexes

Encouraged by the initial success with using germylene **29** as a ligand, we turned our attention to the new class of perimidine-based carbenes, whose preparation is described in Chapter 4. A handful of homoleptic Ni(0) NHC complexes have been reported in the literature and remarkably NHC ligands seem bulky enough to allow for the isolation of di-coordinate nickel species.[15,16]

Reaction of $Ni(COD)_2$ with only two equivalents of carbene **20** in C_6D_6 allows us to closely follow the reaction. Appearance of free 1,5-cyclooctadiene coupled with disappearance of the starting materials (**20** and $Ni(COD)_2$) is clearly observed in the ^1H NMR spectrum along with the formation of a single new carbene species. The most distinctive signature for the new species is the presence of a septet farther downfield (δ = 7.52 ppm) than all of the aromatic signals for the naphthalene skeleton. Also there are now two doublets which each integrate for 6 protons, instead of only one signal equating to 12 protons for **20**. The presence of only one septet but two doublets signifies diastereotopic methyl groups for the ^{i}Pr moieties. The ^{13}C NMR spectrum reveals a signal at 207 ppm, which is assigned to the Ni(0) bound $C_{carbene}$. This represents an upfield shift of 35 ppm from free carbene **20**.

Scheme 6.2

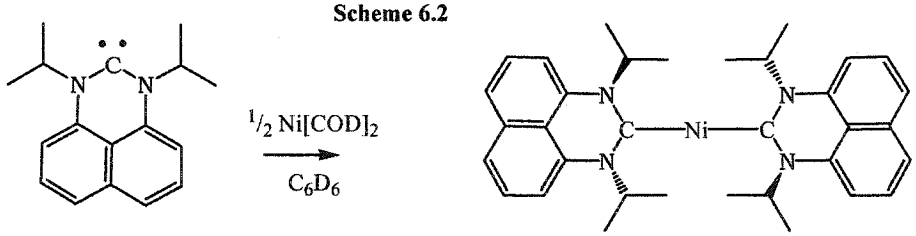

20 **34**

We propose that the product formed from this reaction is the bis(carbene) nickel **34** (Scheme 6.2). Compound **34** would be consistent with a species that contains only one set of ligand signals, and an upfield chemical shift for $C_{carbene}$ is anticipated upon binding to a metal. The drastic shift for the ^{i}Pr α-proton is somewhat unusual however we have seen that the geometric constraints of the ligand are such that the ^{i}Pr group is probably held quite close

[15] Arduengo, III, A. J.; Gamper, S. F.; Calabrese, J. C.; Davidson, F. *J. Am. Chem. Soc.* **1994**, *116*, 4391-4394.
[16] (a) Arnold, P. L.; Cloke, G. N.; Geldbach, T.; Hitchcock, P. B. *Organometallics* **1999**, *18*, 3228-3233. (b) Böhm, V. P. W.; Gstöttmayr, C. W. K.; Weskamp, T.; Herrmann, W. A. *Angew. Chem. Int. Ed.* **2001**, *40*, 3387-3389.

to the electron-rich metal centre, and the proximity of the proton could result in unexpected deshielding.

We would have anticipated a completely symmetric structure for **34** however the diastereotopic signals for the ^{i}Pr methyl groups indicate the contrary. The solid-state structure of the Ni-germylene analogue **33** reveals some ligand twisting due to the close proximity of the metal centre and the twisted C_{2v} conformation renders the methyls inequivalent. However in solution the geometry of **33** is either symmetric or fluxional as indicated by the appearance of only one doublet for the ^{i}Pr groups in the NMR spectra. NHCs are known to bind in a non-dissociative manner and if carbene **20** experiences a similar twist as the germylene **29** upon binding to Ni then the lack of reversibility could lead to diastereotopic signals. We were very interested in doing a structural study of compound **34** but were unsuccessful in obtaining X-ray quality crystals.

Our preliminary results with Ni encouraged us to continue to explore the possibilities for using perimidine-based carbenes as ligands. Rhodium is a very important metal in homogeneous catalysis and has been used to catalyze a variety of important organic transformations.[17] We decided to prepare Rh-carbene complexes with the goal of gaining further understanding of perimidine-based carbene ligands.

The reaction of one equivalent of **20** with $[(COD)Rh(\mu\text{-}Cl)]_2$ (COD = 1,5-cycloocatdiene) at room temperature yielded the yellow compound **35** (Scheme 6.3). NMR spectroscopy of **35** revealed the presence of a single set of new signals for the carbene along with the presence of a metal bound COD ligand. Upon coordination to the Rh(I) metal centre, several changes are observed in the NMR signatures for **20**. The ^{13}C NMR signal for $C_{carbene}$ shifts upfield to δ 213.3 ppm and appears as a doublet due to Rh coupling ($^{1}J_{RhC}$ = 48.3 Hz). This value is more than 30 ppm downfield from those observed for analogous Rh(I) complexes of the unsaturated type carbenes **J** (Chart 4.1, Chapter 4) and provides evidence for an unusual environment offered by our new carbene framework.[18]

---

[17] For examples, see reviews on; catalysis using trialkylphosphine Rh complexes (a) Simpson, M. C.; Cole-Hamilton, D. J. *Coord. Chem. Rev.* **1996**, *155*, 163-207. Rh catalysts in hydroformylation: (b) Trzeciak, A. M.; Ziółkowski, J. J. *Coord. Chem. Rev.* **1999**, *190-192*, 883-900. Rh catalyzed C-C bond formation: (c) Fagnou, K.; Lautens, M. *Chem. Rev.* **2003**, *103*, 169-196. Also see (d) Osborn, J. A.; Jardine, F. H.; Young, J. F.; Wilkinson, G. *J. Chem. Soc. (A)* **1966**, 1711-1732.

[18] Herrmann, W. A.; Köcher, C.; Goossen, L. K.; Artus, G. R. J. *Chem.- Eur. J.* **1996**, *2*, 1627.

The ^{1}H NMR spectrum reveals a dramatic change in the chemical shift for the α-protons of the N^{i}Pr groups. The methine septet moves from δ 4.08 ppm in free **20** to 7.97 ppm for **35**. This chemical shift is almost identical to that observed for the Ni(0) complex **34** and again we attribute this to the proximity of the α-proton to the electron-rich metal centre. This is a direct effect of the six-membered heterocyclic structure of **20** enforcing a close approach of the N-substituents to the metal centre.

Scheme 6.3

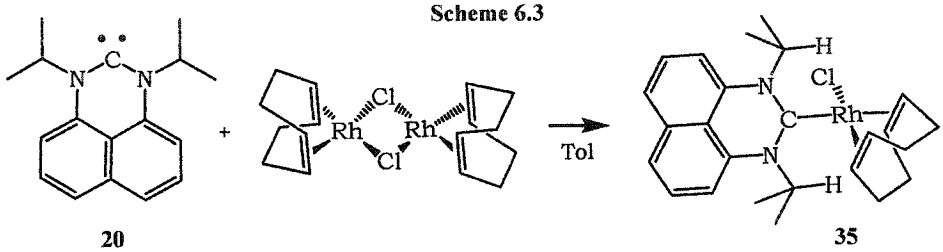

20 **35**

The ^{1}H NMR also reveals diastereotopic methyl groups for the ^{i}Pr substituents. Unlike the Ni compound however, the asymmetric nature of the Rh compound **35** should lead to two different environments for the methyl groups. The observation of the diastereotopic signals in this case suggests the hindered rotation of the Rh-$C_{carbene}$ bond in **35**. Similar effects have been previously observed for reported Rh-**J** complexes.[18] A twisting of the ligand structure along with a hindered rotation would in fact lead to four distinct signals for the methyl groups, but only two signals were observed in the room temperature NMR spectra.

We were successful in obtaining X-ray quality crystals of compound **35** and the molecular structure was determined (Table 6.1) and is illustrated in Figure 6.3. A list of selected bond lengths and angles is provided in Table 6.3. The coordination of **20** to the square planar rhodium(I) centre results in only very minor structural changes within the carbene group. Unlike the Ni-germylene compound **33** and the proposed Ni-carbene compound **34**, the carbene ligand in **35** is not distorted or twisted: it is completely planar. The larger radius for Rh could be responsible for a reduced steric pressure enforced on the ligand. The Rh-$C_{carbene}$ bond distance of 2.06(1) Å is considerably longer than those reported for (COD)RhCl(**J**)) (2.021(4) Å, 2.023(2) Å).[18,19] This reflects the steric congestion that was designed into **20**.

[19] Herrmann, W. A.; Elison, M.; Fischer, J.; Köcher, C. *Chem.-Eur. J.* **1996**, *2*, 772.

One of the fundamental chemical properties of diheteroatom stabilized carbenes is their strong electron-donor ability. In general, saturated **K**-type carbenes are more electron donating than their unsaturated analogues **J**, and both of these species are stronger donors than trialkylphosphines. To assess the electron-donating ability of carbene **20**, we prepared the Rh(I) dicarbonyl species **36** by the reaction of **20** with $[Rh(CO)_2(\mu\text{-}Cl]_2$ or by replacement of the COD ligand of **35** with CO (Scheme 6.4). The NMR spectra for **36** display a $C_{carbene}$ resonance at δ 200.1 ppm (d, $^1J_{RhC}$ = 40.8 Hz) and diastereotopic methyl groups for the ^{i}Pr moieties. The *cis*-geometry for **36** is supported by the appearance of two ^{13}C NMR signals for the CO carbons and by IR spectroscopy, which shows two CO stretching vibrations (ν_{CO}) of similar intensity at 1985 and 2073 cm^{-1}.

Scheme 6.4

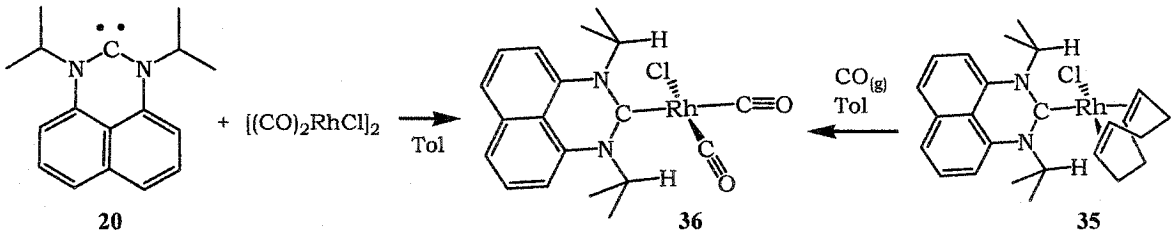

The donor ability of a ligand can be estimated by comparing its effect on the ν_{CO} for metal carbonyl complexes. Electron donation from the ligand to the metal via coordination, increases the electron density of the metal center, which in turn increases the amount of back-bonding from the metal d_π to the CO π^* orbitals. This results in the weakening of the CO bond, accompagnied by a shift of ν_{CO} to lower energies. By comparing ν_{CO} values for analogous complexes, one can obtain a relative measure of a ligands donating property. Comparison of the values obtained for **36** with the saturated carbene complexes *cis*-$(CO)_2RhCl(\mathbf{K})$[20] (R = Me; ν_{CO} = 2090, 2005, Et; ν_{CO} = 2094, 2003, Ph; ν_{CO} = 2085, 2004) and *cis*-$(CO)_2RhCl(C(N^iPr_2)_2)$[21] (ν_{CO} = 2057, 1984) indicates that **20** is a stronger electron donor than carbenes of type **K** but weaker than the acyclic carbene $C(N^iPr_2)_2$.

The appearance of diastereotopic methyl signals for the ^{i}Pr groups in the ^{1}H NMR spectrum of **36** again indicates hindered rotation around the Rh-$C_{carbene}$ bond.[22] For

[20] Doyle, M. J.; Lappert, M. F.; Pye, P. L.; Terreros, P. *J. Chem. Soc., Dalton Trans.* **1984**, 2355-2364.
[21] Denk, K.; Sirsch, P.; Herrmann, W. A. *J. Organomet. Chem.* **2002**, *649*, 219.
[22] Enders, D.; Gielen, H. *J. Organomet. Chem.* **2000**, *617*, 70.

$(CO)_2Rh(\mathbf{J})Cl$ (R = 4-$CH_2C_6H_4CH_3$)[23] and $(CO)Rh(\mathbf{K})_2Cl$ (R = CH_2CH_3),[24] the rotational activation energies are approximately 16 kcal/mol, and free rotation is observed above 55 °C. In the case of **36**, NMR spectra acquired at up to 90 °C in benzene-d_6 show no broadening for the doublets assigned to diastereotopic methyl peaks consistent with a $\Delta G^{\ddagger}$ of >20 kcal/mol for M-C bond rotation. This observation supports the greater steric congestion associated with the new structural features exhibited by **20**.

The molecular structure of **36** was determined by performing an X-ray diffraction study and results confirmed the *cis*-geometry for the CO ligands. The structure contains two crystallographically independent yet chemically equivalent molecules and one of them is illustrated in Figure 6.4. A list of selected bond lengths and angles is provided in Table 6.4. The Rh centre possesses a square planar geometry, once again perpendicular to the plane of the carbene (NCN-naph). The Rh-$C_{carbene}$ bond length of 2.090(3) Å is slightly longer than in the Rh(COD) complex **35** and the geometric parameters for the carbene are basically unchanged. The Rh-CO lengths are significantly different (Rh(1)-C(18) = 1.876(5), Rh(1)-C(19) = 1.899(3) Å) with the ligand *trans* to the carbene being longer. This is consistent with the carbene being a strong σ-donor. The same *trans* CO ligand however has a C≡O bond which is longer by 0.07 Å which implies that there is more back-bonding to it, compared to the *cis* ligand. This is contrary to the trend for the Rh-C bond lengths.

III. Conclusion

The 1,8-DAN scaffold can be used to prepare novel stable carbenes and germylenes which, due to the uniqueness of their structure, exhibit increased steric impact and electron-donating ability. The geometric constraints imposed by the ligands manifest themselves by yielding sterically encumbered metal-carbene complexes evidenced by distortions of the ligand framework, drastic chemical shifts in the ^1H NMR, and hindered metal-ligand rotation. The novel electronic framework gives rise to a nucleophilic carbene center capable of acting as a strong σ-donor ligand with properties comparable to the most donating NHCs. These features should enable the dialkyl-1,8-DAN-supported carbenes, and heavier

[23] Chianese, A. R.; Li, X.; Janzen, M. C.; Faller, J. W.; Crabtree, R. H. *Organometallics* **2003**, *22*, 1663-1667.
[24] Doyle, M. J.; Lappert, M. F. *J. Chem. Soc., Chem. Commun.* **1974**, 679-680.

analogues, to provide steric protection and electronic activation to coordinatively unsaturated metal complexes that are vital intermediates in a myriad of catalytic transformations.

Experimental Section

General: All manipulations were carried out in either a nitrogen filled dry box or under nitrogen using standard Schlenk techniques. Reaction solvents were sparged with nitrogen then dried by passage through column of activated alumina using an apparatus purchased from Anhydrous Engineering. Deuterated, benzene and toluene were purchased from Aldrich Chemical Company and were dried by vacuum transfer from potassium. $Ni(COD)_2$ and $[RhCl(CO)_2]_2$ were purchased from Aldrich Chemical Company and used without further purification. $[RhCl(COD)]_2$ was purchased from Strem Chemicals and used without further purification. ^1H and ^{13}C NMR spectra were run on a Varian Gemini-200, a Bruker 300 MHz or a Bruker 500MHz spectrometer using the residual protons of the deuterated solvent for reference.

Preparation of $\{[1,8\text{-}(^i PrN)_2C_{10}H_6]Ge\}_4Ni$, (33)

To a 50 ml round bottom flask equipped with a magnetic stir bar, bis(cyclooctadiene)nickel (0) (0.050 g, 0.18 mmol) was added to 15 ml of hexane. To the flask was added germylene **29** (0.227 g, 0.73 mmol). The pale yellow/green solution rapidly turns orange then, gradually over a few minutes, to a deep burgundy. Precipitation of a red solid was observed after approximately 30 minutes. The reaction was stirred for an additional 16 hours, and product is isolated by filtration (0.190 g, 0.145 mmol, 80%). The product can be further purified by crystallization out of THF at –35°C.

^1H NMR (C_7D_8,): δ 7.10 (br, 4H, Ar-*H*), 6.66 (dd, 2H, Ar-*H*), 5.17 (sept, 2H, C*H*Me_2), 1.41 (d, 12H, C*H*$_3$).

^{13}C NMR (C_7D_8,): 143.4 (Ar *C*), 139.0 (Ar *C*), 127.4 (Ar *C*), 125.8 (Ar *C*H), 120.3 (Ar *C*H), 109.5 (Ar *C*H), 51.5 (*C*HMe_2), 22.0 (*C*H$_3$).

Anal Calcd for $C_{64}H_{80}N_8Ge_4Ni$:. C, 58.66; H, 6.15; N, 8.55. Found: C, 59.02; H, 5.98; N, 8.26. m.p. 193°C decomp.

Preparation of {[1,8-(^{i}PrN)$_2$C$_{10}$H$_6$]C}$_2$Ni, (34)

To a Teflon valve sealed NMR tube was dissolved carbene **20** (0.033g, 0.13 mmol) and Ni(COD)$_2$ (0.18g, 0.065 mmol) in C_6D_6. After one day the ^{1}H NMR showed complete conversion of the carbene to the Ni complex.

^{1}H NMR (200 MHz, C_6D_6): δ 7.55 (sept, 2H, C*H*Me$_2$), 7.16 (m, 4H, H_{Ar}), 6.67 (m, 2H, H_{Ar}), 1.64 (d, 6H, CH_3), 1.34 (d, 6H, CH_3). ^{13}C NMR (200 MHz, C_6D_6): δ 207 (C_{carb}).

Preparation of {[1,8-(^{i}PrN)$_2$C$_{10}$H$_6$]C}Rh(COD)Cl, (35)

Under a nitrogen atmosphere in a dry-box, dichlorobis(1,5-cyclooctadiene)dirhodium (0.100 g, 0.2 mmol) was added to a round bottom flask equipped with a stir bar, and dissolved in about 10 ml of toluene. To this solution was added dropwise carbene **20** (0.104 g, 0.4 mmol) pre-dissolved in 10 ml of toluene. The solution turned from orange to yellow within minutes. The reaction was stirred for 1 hour then the volatiles were removed under vacuum. The crude product was washed with 2-4 ml of ether to remove any uncoordinated carbene, and then dried under vacuum (0.110 g, 55 % yield).

^{1}H NMR (300 MHz, C_6D_6): δ 7.97 (sept, 2H, *H*CMe$_2$), 7.04 (d, 2H, *H*Ar), 6.96 (t, 2H, *H*Ar), 6.62 (d, 2H, *H*Ar), 5.35 (m, 2H, CH_{cod}), 3.47 (m, 2H, CH_{cod}), 2.24 (m, 4H, (CH_2)$_{cod}$), 1.78 (m, 4H, (CH_2)$_{cod}$), 1.75 (d, 6H, CH_3), 1.54 (d, 6H, CH_3)

^{13}C NMR (300 MHz, C_6D_6): δ 213.3 (d, $^1J_{RhC}$ = 48.3 Hz, C_{carb}Rh), 136.1 (s, C_{Ar}), 132.4 (s, C_{Ar}), 127.0 (s, CH_{Ar}), 123.4 (s, C_{Ar}), 120.8 (s, CH_{Ar}), 107.4 (s, CH_{Ar}), 95.9 (d, $^1J_{RhC}$ = 7.2 Hz, CH_{cod}), 69.0 (d, $^1J_{RhC}$ = 14.1 Hz, CH_{cod}), 61.1 (s, $CHMe_2$), 32.9 (s, (CH_2)$_{cod}$), 29.2 (s, (CH_2)$_{cod}$), 20.4 (s, CH_3), 17.7 (s, CH_3).

Preparation of {[1,8-(^{i}PrN)$_2$C$_{10}$H$_6$]C}Rh(CO)$_2$Cl, (36)

Under a nitrogen atmosphere in a dry-box, dichlorotetracarbonyldirhodium (0.081 g, 0.208 mmol) was added to a round bottom flask equipped with a stir bar, and dissolved in about 10 ml of toluene. To this solution, carbene **20** (0.115 g, 0.456 mmol), pre-dissolved in 10 ml of toluene, was added dropwise. The solution turned to a slightly paler yellow. The reaction was stirred for 1 hour then all volatiles were removed under vacuum. The crude product was washed with 20 ml of hexanes to remove any uncoordinated carbene, and then dried under vacuum (0.135 g, 73 % yield).

^{1}H NMR (300 MHz, C_6D_6): δ 7.00 (d, 2H, H_{Ar}), 6.86 (t, 2H, H_{Ar}), 6.72 (sept, 2H, $HCMe_2$), 6.50 (d, 2H, H_{Ar}), 1.49 (d, 6H, CH_3), 1.25 (d, 6H, CH_3) ^{13}C NMR (300 MHz, C_6D_6): δ 200.1 (d, $^1J_{RhC}$ = 40.8 Hz, C_{carb}Rh), 187.1 (d, $^1J_{RhC}$ = 54.8 Hz, OCRh), 183.3 (d, $^1J_{RhC}$ = 74.0 Hz, OCRh), 136.0 (s, C_{Ar}), 131.8 (s, C_{Ar}), 127.0 (s, CH_{Ar}), 123.7 (s, C_{Ar}), 121.6 (s, CH_{Ar}), 108.4 (s, CH_{Ar}), 62.2 (s, $CHMe_2$), 17.7 (s, CH_3), 17.2 (s, CH_3).

Structural determinations for 33, 35, and 36:

Single crystals were mounted on thin glass fibres using viscous oil and then cooled to the data collection temperature. Crystal data and details of the measurements are summarized in Table 5.1. Data were collected on a Bruker AX SMART 1k CCD diffractometer using 0.3° ω-scans at 0, 90, and 180° in ϕ. Unit-cell parameters were determined from 60 data frames collected at different sections of the Ewald sphere. Semi-empirical absorption corrections based on equivalent reflections were applied (Blessing, R., *Acta Cryst.*, **1995,** A51, 33-38).

The structures were solved by direct methods, completed with difference Fourier syntheses and refined with full-matrix least-squares procedures based on F^2. All non-hydrogen atoms were refined with anisotropic displacement parameters. All hydrogen atoms were treated as idealized contributions. All scattering factors and anomalous dispersion factors are contained in the SHELXTL 5.1 program library (Sheldrick, G. M., Bruker AXS, Madison, WI, 1997).

Figure 6.1. Molecular structure showing one of the two symmetry unique molecules of germylene complex **33**. Hydrogen atoms and co-crystallized THF molecules have been omitted for clarity. Thermal ellipsoids are drawn at 30% probability.

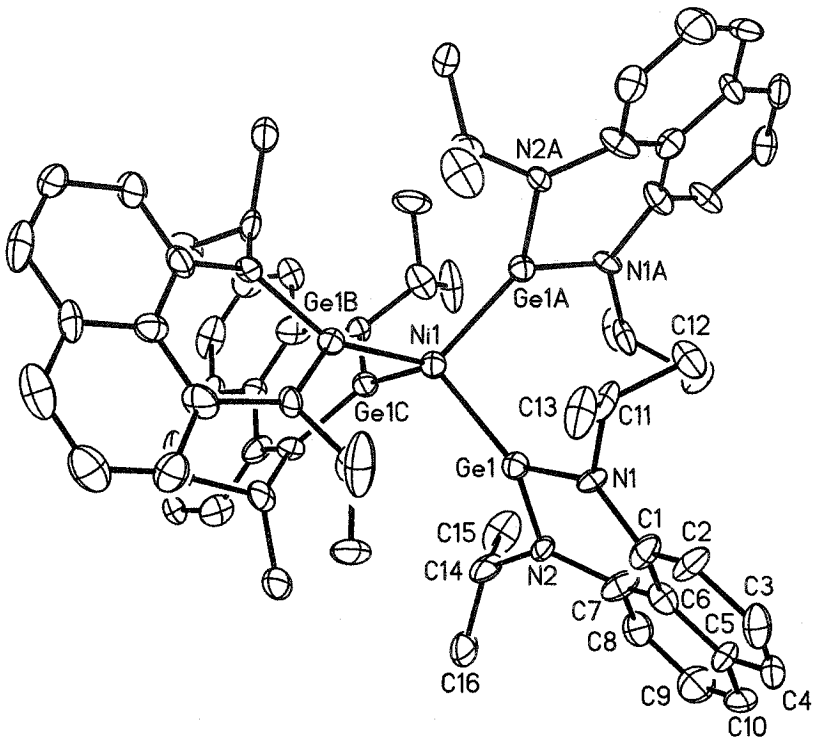

Figure 6.2. Space filling diagram for one of the two asymmetric units, $NiGe[(^{i}PrN)_2C_{10}H_6]$, of the structure of the nickel germylene complex **33**.

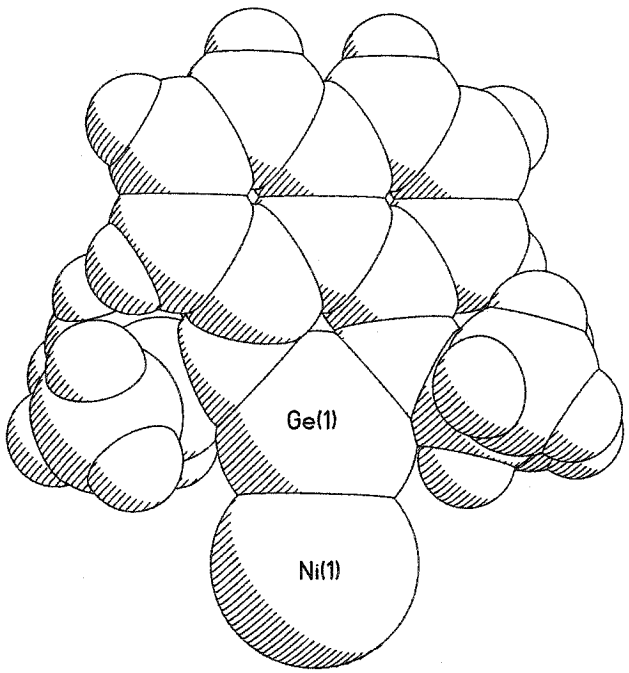

Figure 6.3. Thermal ellipsoid plot showing the molecular structure and atom numbering scheme for the carbene complex **35**. Hydrogen atoms have been omitted for clarity. Thermal ellipsoids are drawn at 30% probability.

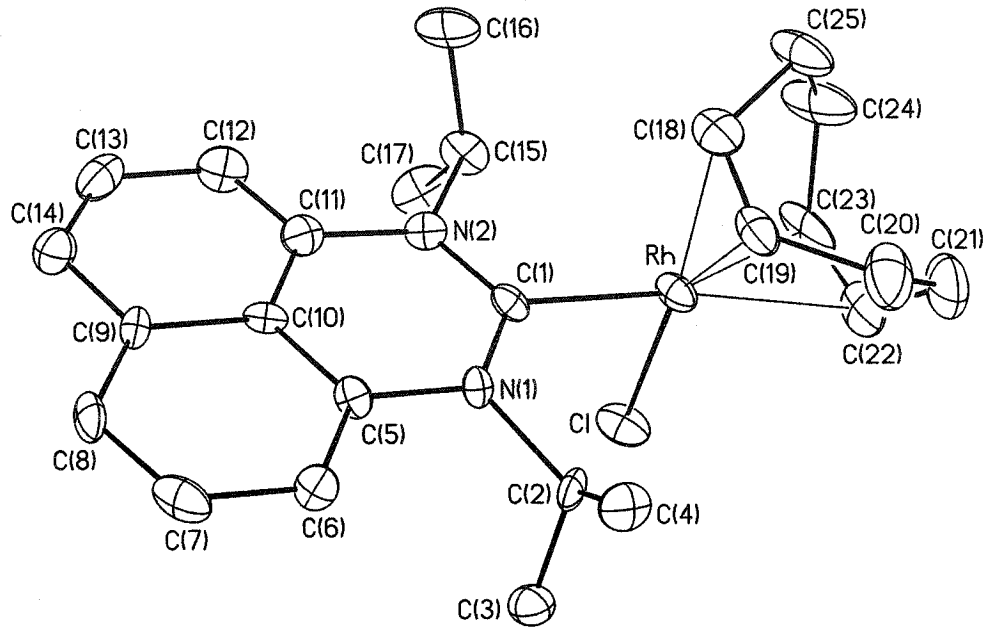

Figure 6.4. Thermal ellipsoid plot showing the molecular structure and atom numbering scheme for one of the two symmetry unique molecules the carbene complex **36**. Hydrogen atoms have been omitted for clarity. . Thermal ellipsoids are drawn at 30% probability.

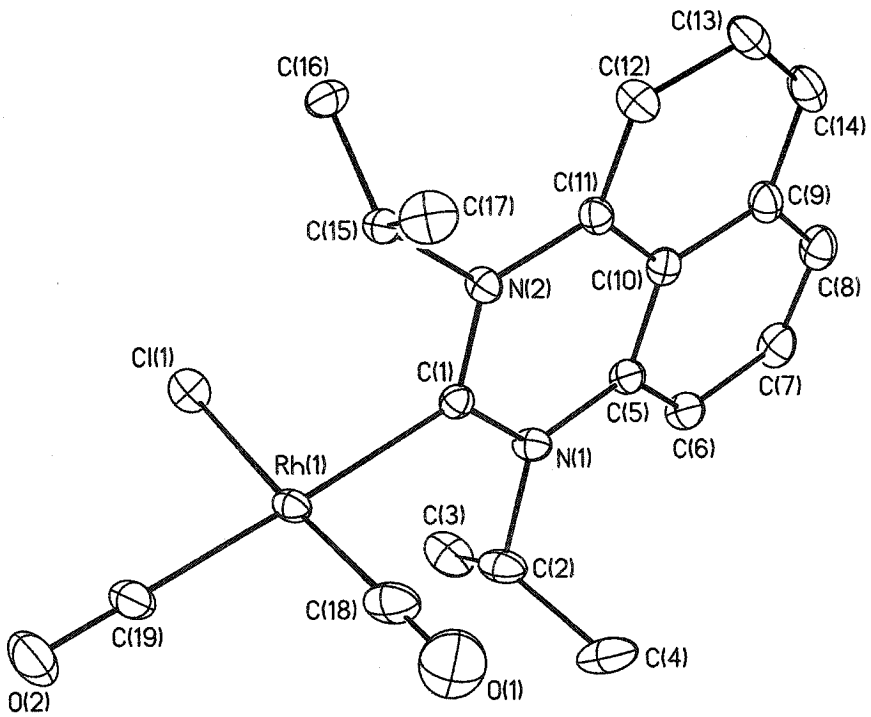

Table 6.1. Selected Crystal Data and Data Collection Parameters for **33**, **35** and **36**

	33-(THF)	**35**	**36-(0.5 Toluene)**
empirical formula	$C_{72}H_{96}Ge_4N_8NiO_2$	$C_{25}H_{32}ClN_2Rh$	$C_{22.50}H_{24}ClN_2O_2Rh$
formula weight	1454.64	498.89	492.80
T (K)	203(2)	213(2)	150(2)
wavelength (Å)	0.71073	0.71073	0.71073
crystal system	Tetragonal	Monoclinic	Triclinic
space group	I-4	$P2_1/n$	P-1
a (Å)	24.248(3)	10.241(2)	10.3248(16)
b (Å)	24.248(3)	16.129(3)	14.149(2)
c (Å)	11.514(2)	14.067(3)	16.339(3)
α (deg)	90	90	112.486(2)
β (deg)	90	104.722(4)	93.646(2)
γ (deg)	90	90	94.078(2)
V (Å^3)	6770.0(17)	2247.2(8)	2189.3(6)
Z	4	4	4
abs coeff (mm^{-1})	2.080	0.893	0.922
final R indices	R1 = 0.0731	R1 = 0.0724	R1 = 0.0399
	wR2 = 0.1700	wR2 = 0.1916	wR2 = 0.1107

Table 6.2. Selected Bond Distances and Angles for **33-(THF)**

	Bond Distances (Å)		
Ge(1)-Ni(1)	2.2400(16)	N(1)-C(1)	1.433(12)
Ge(1)-N(1)	1.812(11)	N(1)-C(11)	1.534(17)
Ge(1)-N(2)	1.794(10)	N(2)-C(7)	1.461(12)
		N(2)-C(14)	1.490(17)
	Bond Angles (deg)		
Ge(1)-Ni(1)-Ge(1)#1	114.82(5)	C(1)-N(1)-C(11)	122.3(10)
Ge(1)-Ni(1)-Ge(1)#2	99.23(8)	C(1)-N(1)-Ge(1)	124.5(7)
Ge(1)#1-Ni(1)-Ge(1)#2	114.82(5)	C(11)-N(1)-Ge(1) α	112.8(8)
Ge(1)-Ni(1)-Ge(1)#3	114.82(5)	Sum at N(1)	359.6
Ge(1)#1-Ni(1)-Ge(1)#3	99.23(8)	C(7)-N(2)-C(14)	122.6(9)
Ge(1)#2-Ni(1)-Ge(1)#3	114.82(5)	C(7)-N(2)-Ge(1)	122.0(7)
N(2)-Ge(1)-N(1)	96.7(5)	C(14)-N(2)-Ge(1) α	115.0(8)
N(2)-Ge(1)-Ni(1)	130.8(3)	Sum at N(2)	359.6
N(1)-Ge(1)-Ni(1)	131.6(3)		
Sum at Ge(1)	359.1		

Table 6.3. Selected Bond Distances and Angles for **35**

Bond Distances (Å)			
Rh-C(1)	2.056(11)	Rh-Cl	2.400(3)
N(1)-C(1)	1.366(14)	Rh-C(18)	2.140(13)
N(2)-C(1)	1.352(14)	Rh-C(19)	2.113(13)
N(1)-C(2)	1.519(14)	Rh-C(22)	2.251(13)
N(1)-C(5)	1.431(13)	Rh-C(23)	2.205(12)
N(2)-C(15)	1.516(14)	C(18)-C(19)	1.384(19)
N(2)-C(11)	1.436(15)	C(22)-C(23)	1.39(2)
Bond Angles (deg)			
C(1)-Rh-Cl	89.4(3)	C(1)-Rh-C(19)	92.4(4)
N(2)-C(1)-N(1)	117.9(9)	C(1)-Rh-C(18)	91.9(5)
N(1)-C(1)-Rh	121.4(8)	C(18)-Rh-C(23)	82.2(5)
N(2)-C(1)-Rh	120.6(7)	C(19)-Rh-C(22)	80.5(5)
Sum at C(1)	359.9	C(22)-Rh-Cl	92.4(4)
C(1)-N(1)-C(2) *α*	117.2(9)	C(23)-Rh-Cl	91.4(4)
C(1)-N(1)-C(5)	123.3(9)	C(1)-N(2)-C(15) *α*	115.8(9)
C(5)-N(1)-C(2)	118.9(8)	C(11)-N(2)-C(15)	120.3(9)
Sum at N(1)	359.4	C(1)-N(2)-C(11)	123.7(9)
		Sum at N(2)	359.8

Table 6.4. Selected Bond Distances and Angles for **36-(0.5 Toluene)**

Bond Distances (Å)			
Rh(1)-C(1)	2.090(3)	Rh(1)-Cl(1)	2.3539(10)
N(1)-C(1)	1.351(4)	Rh(1)-C(18)	1.876(5)
N(1)-C(2)	1.503(4)	Rh(1)-C(19)	1.899(3)
N(1)-C(5)	1.414(4)	O(1)-C(18)	1.041(5)
N(2)-C(1)	1.349(4)	O(2)-C(19)	1.130(4)
N(2)-C(15)	1.489(4)		
N(2)-C(11)	1.423(4)		
Bond Angles (deg)			
N(2)-C(1)-N(1)	118.9(3)	C(1)-Rh(1)-Cl(1)	87.64(8)
N(1)-C(1)-Rh(1)	121.7(2)	C(19)-Rh(1)-Cl(1)	90.45(12)
N(2)-C(1)-Rh(1)	119.4(2)	C(18)-Rh(1)-C(19)	92.27(17)
Sum at C(1)	360.0	C(18)-Rh(1)-C(1)	89.64(14)
C(1)-N(1)-C(2) *α*	116.3(3)	C(19)-Rh(1)-C(1)	177.91(14)
C(1)-N(1)-C(5)	122.9(3)	C(18)-Rh(1)-Cl(1)	177.24(12)
C(5)-N(1)-C(2)	120.7(2)	C(1)-N(2)-C(15) *α*	116.8(2)
Sum at N(1)	359.9	C(1)-N(2)-C(11)	123.2(2)
		C(11)-N(2)-C(15)	120.0(2)
		Sum at N(2)	360.0

7 Stabilization of Low-Coordinate Metals

I. Introduction

Our preparation and application of N,N'-disubstituted 1,8-DAN ligands led to successful isolation of low-valent, low-coordinate group 14 compounds and even allowed the synthesis of stable carbenes. The work with group 14 elements demonstrated that 1,8-DAN ligands, upon formation of a six-membered metallaheterocycle, offer adequate steric protection of the metal centre, preventing dimerizations or aggregation and that the nitrogen lone-pairs can participate in the stabilization of empty orbitals.[1]

We realized that the key structural features of the 1,8-DAN ligands could be exploited for the stabilization of other coordinatively unsaturated main group metals. Neutral group 13 metals in their +3 oxidation state only possess three anionic ligands. If the ligands are monodentate this leaves the metal electron deficient and Lewis acidic. The group 13 element can attain an octet by coordination of neutral Lewis base ligands, or by π-

[1] See chapters 4 and 5 which present the preparation of stable carbenes and heavier group 14 analogues.

donation from the ligands (if there are no lone-pairs available, there can be hyperconjugation). We speculated that the chelating nature of 1,8-DAN ligands would orient the nitrogen lone-pairs to allow for orbital overlap with the unoccupied orbital of group 13 metals, stabilizing three coordinate species. Additionally, the steric protection afforded by the N-substituents would also provide kinetic stabilization preventing dimerization via bridging ligands.

Boron complexes incorporating unsubstituted 1,8-DAN have been reported, and seemingly exist as three coordinate B species. However, none of the compounds have been structurally characterized and they still possess reactive N-H groups.[2] One aluminum compound containing the disubstituted ligand N,N'-bis(trimethylsilyl)-1,8-DAN was identified as a by-product of a MAO co-catalyzed polymerization reaction, but in this compound the ligand did not assume the desired chelating geometry.[3] "Proton sponge" or N,N,N',N'-tetramethyl-1,8-DAN has been used as a neutral chelating ligand for boron, usually generating cationic salts by displacement of one anionic ligands (hydride or halide).[4] Disilylated 1,8-DAN ligands have been used to form complexes of the heavier group 13 metals (In and Tl) however this work mainly involves the use of metals in their +1 oxidation state.[5]

We therefore decided to prepare 1,8-DAN complexes of group 13 metals, specifically B and Al which are well known for their Lewis acid behavior. This chapter will present our results in preparing some boron and aluminum compounds supported by 1,8-DAN based ligands. We will also present a Zn compound which is structurally analogous to the isolated Al compound.

---

[2] (a) Caserio, Jr., F. F.; Cavallo, J. J.; Wagner, R. I. *J. Org. Chem.* **1961**, *26*, 2157-2158. (b) Chissick, S. S.; Dewar, M. J. S.; Maitlis, P. M. *J. Am. Chem. Soc.* **1961**, *83*, 2708-2711. (c) Maruyama, S.; Kawanishi, Y. *J. Mater. Chem.* **2002**, *12*, 2245-2249. (d) Kaupp, G.; Naimi-Jamal, M. R.; Stepanenko, V. *Chem. Eur. J.* **2003**, *9*, 4156-4160. (e) Goetze, R.; Nöth, H. *J. Organomet. Chem.* **1978**, *145*, 151-166.

[3] Lee, C. H.; La, Y.-H; Park, S. J.; Park, J. W. *Organometallics* **1998**, *17*, 3648-3655.

[4] (a) Keller, P. C.; Rund, J. V. *Inorg. Chem.* **1979**, *18*, 3197-3199. (b) Hartman, J. S.; Shoemaker, J. A. W. *Polyhedron* **2000**, *19*, 165-176. (c) Onak, T.; Rosendo, H.; Siwapinyoyos, G.; Kubo, R.; Liauw, L. *Inorg. Chem.* **1979**, *18*, 2943-2945.

[5] (a) Hellmann, K. W.; Galka, C.; Gade, L. H.; Steiner, A.; Wright, D. S.; Kottke, T.; Stalke, D. *Chem. Commun.* **1998**, 546-550. (b) Hellmann, K. W.; Galka, C. H.; Rüdenauer, I.; Gade, L. H.; Scowen, I. J.; McPartin, M. *Angew. Chem., Int. Ed.* **1998**, *37*, 1948-1951. (c) Gade, L. H.; Galka, C. H.; Hellmann, K. W.; Williams, R. M.; De Cola, L.; Scowen, I. J.; McPartlin, M. *Chem. Eur. J.* **2002**, *8*, 3732-3746.

II. Results

A. Reactions of 1,8-(^{i}PrNH)$_2$C$_{10}$H$_6$ with BH$_3$·L

The equimolar reaction of 1,8-(^{i}PrNH)$_2$C$_{10}$H$_6$ (**4a**) with the borane THF adduct BH$_3$·THF did not lead to hydrogen production, and the NMR spectrum only contained the starting materials. Reactions between proton sponge and diborane B_2H_6 have been reported to be unusually slow and the steric bulk of the ligand was believed to be the reason for the sluggish behaviour.[4a] The ^{i}Pr groups are larger than the Me groups on proton sponge, yet all our previous results did not indicate that the steric bulk would be prohibitive. Perhaps the diamine simply could not displace the THF ligand of the Lewis adduct. We therefore decided to react one equivalent of ligand **4a** with the borane dimethyl sulfide adduct in toluene. Evidence that these reagents reacted was provided by the observed the disappearance of the purple colour of the ligand and the formation of a light pinkish solution. The ^{1}H NMR spectrum of the reaction products showed that the ligand had in fact reacted, but the spectrum clearly indicated the presence of more than one compound. Recrystallization of the product from ether at -25°C gave the colourless compound **37**. The product was characterized by NMR spectroscopy which confirmed the presence of the ligand, but two overlapping septets and four distinct doublets indicated a completely asymmetric environment, where both sides and both faces of the ligand are inequivalent.

Scheme 7.1

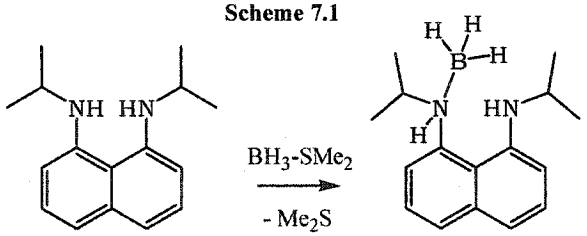

4a **37**

In order to establish the nature of compound **37** we determined the molecular structure by performing and X-ray diffraction study (Table 7.1) of the crystals. The results are illustrated in Figure 7.1 and Table 7.2 contains a list of selected bond lengths and angles. The structure reveals that the ligand has simply functioned as a Lewis base and that **37** is an amine adduct of BH_3 (Scheme 7.1). Only one of the amine groups is bound to the B atom, and this causes the N-C_{naph} bond to rotate in such a way that the borane lies on one side of the naphthalene plane while the ^{i}Pr group lies on the other. The rather long B-N bond of

1.640(3) Å is typical of a dative interaction, implying a Lewis adduct. The boron bound N(1) atom has a pyramidal geometry (sum of all angles for N(1) of 337.97) indicating that it possesses either a proton or a stereochemically active lone-pair. In addition, the ^{i}Pr group on the other N atom (N(2)) is oriented to enable the N lone-pair to participate in intramolecular hydrogen bonding. All of these parameters assure us that the assigned composition of compound **37** is the correct one.

The lack of protonolysis of borane by the diamine ligand was somewhat surprising, however we believed that the other products of the reaction could be boron amido compounds and that compound **37** was in fact only an intermediate in the reaction. Repeating the reaction of an equimolar ratio of the diamine ligand and borane dimethyl sulfide at a higher temperature of 60°C for approximately 12 hours yielded a pale yellow solution. NMR spectroscopy of the product, an off-white solid, revealed the complete conversion of starting material, and a single set of ligand signals suggesting the presence of only one compound assumed to be the anticipated diamidoborane **38**.

Scheme 7.2

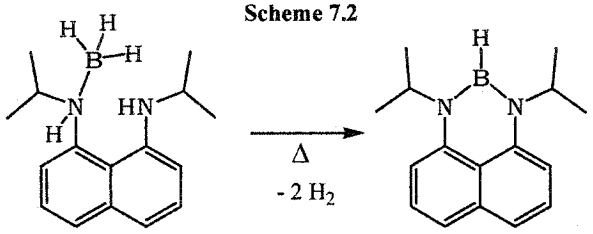

37 **38**

The quadrupolar nature of ^{11}B usually broadens protons signals such that the B-H resonances are not observed. We obtained the ^{11}B decoupled ^{1}H NMR spectrum for compound **38** and indeed observed a slightly broadened singlet integrating for 1 proton at 4.65 ppm which is not visible in the standard non-decoupled ^{1}H NMR spectrum. This observation in combination with the appearance of only one set of resonances for the ^{i}Pr groups indicated a very symmetric environment for the ligand and supports the assignment of **38** being a planar tricoordinate boron species.

An X-ray diffraction study of compound **38** was performed and confirmed the tricoordinate geometry (Table 7.1). The molecular structure is illustrated in Figure 7.2 and Table 7.3 contains a list of selected bond lengths and angles. The most striking feature of the structure is the predicted planar tricoordinate geometry of the B centre. The ligand bite angle

of 121.0(3)° closely approaches the ideal angle of 120° for a perfect six-membered aromatic ring. However the nitrogens are slightly pulled in towards each other, as evinced by the small internal angles at the C_{naph}-N carbons 117.5(2)° for N(1)-C(4)-C(9) and 117.3(2)° for N(2)-C(10)-C(9), resulting in a distorted hexagon. The B-N bond lengths of 1.418(3) and 1.413(3) Å indicate substantial multiple-bond character.[6] The planar geometry with the short B-N bonds seems to substantiate the idea that the diamino ligand is an efficient π-donor and stabilizes the coordinatively unsaturated species.

B. Reaction of 1,8-(^{i}PrNH)$_2$C$_{10}$H$_6$ with AlH$_3$·NMe$_2$Et

Encouraged by the boron results we proceeded to investigate the synthesis of an aluminum analogue of **38**. The reaction of diamine ligand **4a** with one equivalent of an alane-amine adduct (AlH$_3$·NMe$_2$Et) in toluene quickly led to the disappearance of the purple colour for the ligand. The off-white product of the reaction **39** was characterized by NMR spectroscopy and the proton spectrum indicated a new compound containing a ligand which is symmetrically bound to Al with one methine septet but diastereotopic methyls for the ^{i}Pr groups. The presence of signals in addition to those typical for the 1,8-DAN ligand could be assigned to Me$_2$EtN bonded to the aluminum and originating from the starting material.

Scheme 7.3

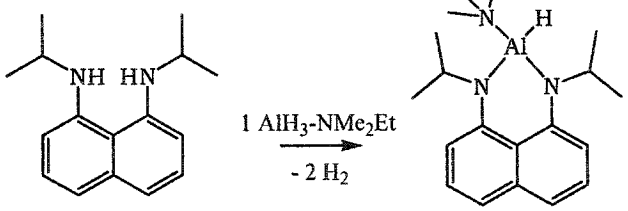

4a **39**

We rationalize the product to be the amine Lewis adduct of the desired diamidoalane. In this case the metal remains in a four coordinate geometry, presumably tetrahedral, which would position the hydride on one side of the ligand plane and the amine on the other. Like in compound **38** the quadrupole nature of Al makes the Al-H signal too broad for detection in the ^{1}H NMR, but unfortunately the aluminum decoupling experiments did not succeed in sharpening the signal enough for it to be observable. The diastereotopic signals for the

[6] L. Weber, E. Dobbert, H-G Stammler, B. Neumann, R. Boese, D. Blaser *Chem. Ber., Recueil* **1997**, *130*, 705-710.

methyls of the ^{i}Pr groups however clearly support the proposed ligand array on a tetrahedral Al centre. Additionally we can conclude that the amine is bound strongly enough to inhibit a fluxional dissociative behaviour, otherwise the diastereotopic signals would be broadened or appear as one average signal.

The reluctance of compound **39** to adopt a planar three coordinate environment suggests that the Al-NMe_2Et interaction is thermodynamically more favourable than π-donation from amido ligands and formation of a three coordinate species. The different orbital sizes for Al (compared to the smaller B) could result in less overlap between the N lone-pairs and the empty orbital. Investigations into possible π bonding between N and heavier group 13 elements[7] have revealed very low rotational barriers for Al-N bonds.[8] These results imply that there is minimal multiple bonding between the two centers.[9] Short Al-N bonds are, more likely, the result of increased ionic character, as opposed to π bonding. In addition to weaker π-donation, the amine functioning as a better Lewis base, than dimethyl sulfide (for B), could also explain the reluctance of the compound to adopt a coordinatively unsaturated geometry.

C. Reaction of 1,8-(^{i}PrNH)$_2$C$_{10}$H$_6$ with AlMe$_3$

The very small size of the hydride ligand in compound **39** clearly offers little steric protection of the Al centre from the Lewis basic amine. Believing that a slight increase in ligand size could push the equilibrium in favour of a three coordinate species we decided to attempt the preparation of an Al methyl derivative. Reacting the same diamine ligand **4a** with trimethyl aluminum in equimolar ratios did not yield the expect product. NMR spectroscopy of the reaction products revealed a mixture comprised of an unidentified diamido compound and some remaining unreacted diamine. Performing the same reaction in a 1:2 ligand to metal ratio produced a crude product whose NMR spectra appeared to be

---

[7] a) For reviews on multiple bonding between heavier main group elements see: Power, P. P. *Chem. Rev.* **1999**, *99*, 3463-3503. b) Power, P. P.; Moezzi, A.; Pestana, D. C.; Petrie, M. A.; Shoner, S. C.; Waggoner, K. M. *Pure & Appl. Chem.* **1991**, *63*, 859-866.

[8] a) Petrie, M. A.; Ruhlandt-Senge, K.; Power, P. P. *Inorg. Chem.* **1993**, *32*, 1135-1141 b) Waggoner, K. M.; Ruhlandt-Senge, K.; Wehmschulte, R. J.; He, X.; Olmstead, M. M.; Power, P. P. *Inorg. Chem.* **1993**, *32*, 2557-2561.

[9] For theoretical calculations on amidoalane compounds see: Kormos, B. L.; Cramer, C. J. *Inorg. Chem.* **2003**, *42*, 6691-6700.

similar to the amido product observed in the 1:1 reaction. Crystallization of the reaction mixture from cold (-35°C) ether gave colourless crystals of compound **40** (Scheme 7.4).

Scheme 7.4

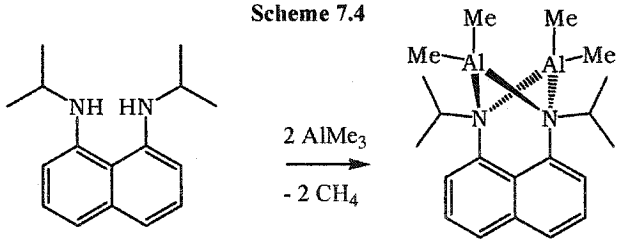

4a **40**

An X-ray diffraction study was performed on the crystals (Table 7.1) and the molecular structure is illustrated in Figure 7.3. Selected bond lengths and angles are listed in Table 7.4. Compound **40** is a bimetallic Al species with each aluminum centre possessing a four-coordinate geometry consisting of two methyl groups, and the two nitrogens of a 1,8-DAN ligand. The two lone-pairs on each of the anionic N are bonded to the two different Al centres. Effectively the ligand serves as two bridging amido groups for two $AlMe_2$ moieties forming a Al_2N_2 metallacycle which is puckered, or butterfly in shape. The butterfly shape positions the two methyls in inequivalent environments, but there are no significant differences in the Al-C bond lengths ranging from 1.954(5) to 1.966(5) Å. All of the Al-N bond lengths are the same within error (from 1.971(4) to 1.982(4) Å) and are consistent with bridging amido species.[10] The ligand plane defined by the naphthalene and the two nitrogens is perpendicular to the Al-Al vector. The "bite angles" (N-Al-N) are equivalent and average out to 80.5° and the two C-Al-C angles differ only very slightly being 115.1(2)° for C(17)-Al(1)-C(18) and 116.2(2)° for C(19)-Al(2)-C(20).

An almost identical compound reported recently $[\mu\text{-}1,8\text{-}C_{10}H_6(NSiMe_3)_2](AlMe_2)_2$,[3] (**DD**) was originally obtained from the attempted alkylation of a titanium 1,8-DAN compound $\{1,8\text{-}C_{10}H_6(NSiMe_3)_2\}TiCl_2$ with two equivalents of $AlMe_3$. Compound **DD** could also be prepared directly from reacting the ligand with 2 equiv of $AlMe_3$. Apart from having different N-substituents, **DD** is basically isostructural with compound **40** with the exception that the "bite angles" are slightly larger (83.0(2)°) causing a minor narrowing of

[10] For instance the Al-N bond lengths for the bridging amido group in $[(Me_2N)_2Al(\mu\text{-}NMe_2)]_2$ are 1.951(2) and 1.979(2) Å in Waggoner, K. M.; Olmstead, M. M.; Power, P. P. *Polyhedron* **1990**, *9*, 257-263.

the C-Al-C angle to 111.1(3)°. Related bimetallic aluminum dimethyl compounds bridged by diamido-PDA ligands were recently reported.[11]

The crystals used for X-ray analysis were used for spectroscopic characterization of **40**, however the ^{1}H NMR appeared more complex than expected and indicated the possibility for there being two different species containing both the diamido ligand and Al methyls. It is unclear at the moment whether the second set of signals is due to some sort of aggregation or fluxional behaviour of **40** or if it is in fact a second compound having co-crystallized with **40**. The spectra display only three distinct peaks for the Al methyls, two of which can be assigned to **40**. At this point the third signal is tentatively assigned to a mononuclear tricoordinate species which is intermixed with the crystals of **40**.

D. Reaction of 1,8-(^{i}PrNH)$_2$C$_{10}$H$_6$ with ZnMe$_2$

The results with AlMe$_3$ showed that a bimetallic species with aluminum dialkyl moieties was a stable product even in the presence of the parent diamine ligand. This surprising lack of reactivity was believed to arise from the tetrahedral geometry of the aluminum centres in compound **40**. The lack of further reactivity could stem from the inability of another amine to coordinate to the aluminum centre inhibiting protonolysis of the methyl group. As a result, further reaction of **40** with diamine is kinetically unfavoured. Similar to aluminum alkyls, zinc alkyls are well-known reagents, often used as alkyl transfer agents. Zn alkyls can also be used as strong bases. The lower coordination number for dialkyl zinc should alleviate some of the steric constraints compared to trialkyl aluminum.

Reacting the diamine ligand **4a** with one equivalent of ZnMe$_2$ did not lead to complete reaction. ^{1}H NMR analysis of the reaction mixture showed the presence of the parent ligand, along with signals indicating a species containing both the 1,8-DAN ligand and Zn methyls. By altering the reaction stoichiometry to two equivalents of ZnMe$_2$ per ligand, complete deprotonation of the ligand was observed. The NMR spectra of the compound **41** display a single set of ligand signals and only one doublet for the methyls of the ^{i}Pr groups integrating for 12 protons. Based on the integration ratios of the ^{1}H NMR and

[11] Bezombes, J.-P.; Gehrhus, B.; Hitchcock, P. B.; Lappert, M. G.; Merle, P. G. *Dalton Trans.* **2003**, 1821-1829.

the reaction stoichiometry the structure of **41** was proposed to be analogous to the aluminum compound **40**.

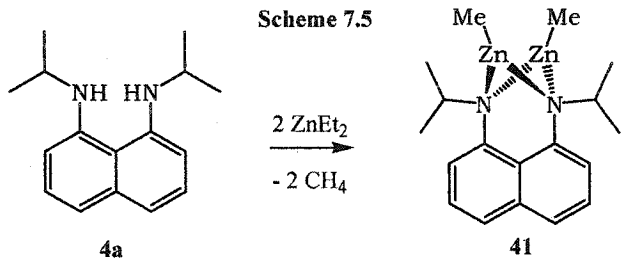

Single crystals of compound **41** suitable for an X-ray diffraction study (Table 7.1) were obtained and the molecular structure is illustrated in Figure 7.4. A list of selected bond lengths and angles is included in Table 7.5. The structure of **41** incorporates two crystallographically unique molecules which are chemically identical. Only one of the molecules will be discussed for the sake of brevity. Like compound **40**, compound **41** is a bimetallic complex where one diamido ligand serves as a side-on bridging unit for two ZnMe moieties. A similar butterfly shaped Zn_2N_2 metallacycle is formed with the two different Zn atoms bonded to each nitrogen of the ligand. One Me group from the starting material is retained on each Zn centre. Other than the planar trigonal geometry of the Zn atoms (sum of angles = 359.96°) the structure is almost identical to that of the aluminum compound **41**.

There are numerous examples of amidozinc compounds, many of which exist as amido bridged species.[12] Examples of related tricoordinate dimeric alkylzinc amides, having the general formula $[AkZnNRR']_2$ have been characterized.[13,14,15] The Zn-N bond lengths in these species range from 2.009 to 2.081 Å, which is in agreement with the bond lengths in compound **41** of 2.035-2.057 Å (Table 7.5). Reaction of a similar chelating diamido ligand (± *trans*-1,2-$(N(H)SiMe_3)_2$-*cyclo*-C_6H_{10}) with two equivalents of dialkylzinc yielded an amido bridged tetrametallic compound instead of an analogous bimetallic species.[16]

---

[12] a) Lappert, M. F.; Power, P. P.; Sanger, A. R.; Srivastava, R. C. *Metal and Metalloid Amides*; Wiley: New York, 1980 b) O'Brien, P. In *Comprehensive Organometallic Chemistry*, 2nd ed.; Wilkinson, G.; Stone, F. G. A.; Abel, E. W., Eds.; Pergamon: Oxford, U.K., 1995, Vol. 3, pp 175-206.
[13] Bell, N. A.; Shearer, H. M. M.; Spencer, C. B. *Acta Cryst.* **1983**, *C39*, 1182-1185.
[14] Walker, D. A.; Woodman, T. J.; Schormann, M.; Hughes, D. L.; Bochmann, M. *Organometallics* **2003**, *22*, 797-803.
[15] a) Westerhausen, M.; Bollwein, T.; Pfitzner, A.; Nilges, T.; Deiseroth, H.-J. *Inorg. Chim. Acta* **2001**, *312*, 239-244 b) Olmstead, M. M.; Grigsby, W. J.; Chacon, D. R.; Hascall, T.; Power, P. P. *Inorg. Chim. Acta* **1996**, *251*, 273-284.
[16] Chakraborty, D.; Chen, E. Y.-X. *Organometallics* **2003**, *22*, 769-774.

III. Conclusion

The ability of 1,8-DAN based ligands to stabilize electronically and coordinatively unsaturated group 13 species was explored by analyzing the products of reactions with N,N'-disubstituted-1,8-DAN and various metal hydrides and alkyls. In the case of boron, the ligand imparted enough steric protection and electronic density to stabilize a three coordinate diamido borane. The aluminum analogue of such a compound could not be prepared, and instead a Lewis adduct of diamidoalane and dimethylethylamine was formed. In the case of Al alkyls, the ligand seems to favour the formation of a bimetallic compound which resisted further reaction with the parent ligand. Similar results were obtained with dialkyl Zn. The formation of such a similar compound using a $ZnMe_2$ instead of $AlMe_3$ insinuates that the bridging ability of diamido 1,8-naphthalene is important when considering the future synthesis of metal complexes. A better understanding for the formation of the bimetallic compounds and their intermediates would be necessary before we can make solid conclusions on the possibilities for making interesting unsaturated group 13 complexes.

Experimental Section

General: All manipulations were carried out in either a nitrogen filled dry box or under nitrogen using standard Schlenk techniques. Reaction solvents were sparged with nitrogen then dried by passage through column of activated alumina using an apparatus purchased from Anhydrous Engineering. Deuterated benzene was purchased from Aldrich Chemical Company and were dried by vacuum transfer from potassium. $BH_3{\cdot}THF$, $BH_3{\cdot}SMe_2$, $AlH_3{\cdot}NMe_2Et$, $AlMe_3$ and $ZnMe_2$ were purchased from Aldrich Chemical Company and used without further purification. ^1H and ^{13}C NMR spectra were run on a Varian Gemini-200, a Bruker 300 MHz or a Bruker 500MHz spectrometer using the residual protons of the deuterated solvent for reference.

Preparation of 1-(BH_3NH^iPr)-8-(NH^iPr)-$C_{10}H_6$, (37)

The diamine (^{i}PrNH)$_2C_{10}H_6$ **4a** (0.21g, 0.87 mmol) was dissolved in approximately 30 ml of toluene in a round bottom flask equipped with a stir bar. To the solution was added dropwise

$BH_3{\cdot}SMe_2$ (0.073g, 0.96 mmol) pre-dissolved in toluene. The solution was stirred for one hour. The volatiles were removed under vacuum and the crude product was crystallized by dissolving in ether and cooling to -25°C. The product was isolated as colourless crystals, quickly washed with hexane and dried under vacuum (0.122g, 0.48 mmol, 55 %).

^{1}H NMR (C_6D_6, 500 MHz): with ^{11}B decoupling δ 10.7 (br, 1H, N*H*), 7.64 (d, 1H, C*H*), 7.38 (d, 1H, C*H*), 7.33 (d, 1H, C*H*), 7.13 (t, 1H, C*H*), 7.08 (t, 1H, C*H*), 6.61 (d, 1H, C*H*), 3.42 (br, 1H ,N*H*), 3.25-3.35 (m, 2H, C*H*Me_2), 2.77 (s br, 3H, B*H*$_3$), 1.41 (d, 3H, C*H*$_3$), 1.10 (d, 3H, C*H*$_3$), 0.84 (d, 3H, C*H*$_3$), 0.54 (d, 3H, C*H*$_3$).

Preparation of HB[1,8-(N^{i}Pr)$C_{10}H_6$], (38)

The diamine (^{i}PrNH)$_2C_{10}H_6$ **4a** (0.40g, 1.65 mmol) was dissolved in approximately 30 ml of toluene and transferred to a Schlenk equipped with a Teflon screw cap. To the solution was added $BH_3{\cdot}SMe_2$ (0.140g, 1.84 mmol) pre-dissolved in toluene. The solution was heated to 60°C overnight. The volatiles were removed under vacuum and the crude product was crystallized by dissolving in hexane and cooling to -25°C. The product was isolated as colourless crystals and dried under vacuum (0.397g, 1.57 mmol, 95 %).

^{1}H NMR (C_6D_6, 500 MHz): with ^{11}B decoupling δ 7.21-7.25 (m, 4H, C*H*), 6.37-6.41 (m, 2H, C*H*), 4.65 (s br, 1H, B*H*), 3.70 (s, 2H, C*H*Me_2), 1.14 (d, 12H, C*H*$_3$).

^{13}C NMR (C_6D_6, 500 MHz): δ 142.2 (*C*), 137.6 (*C*), 127.4 (*C*H), 122.5 (*C*), 118.5 (*C*H), 103.3 (*C*H), 47.1 (*C*HMe_2), 23.2 (*C*H$_3$).

^{11}B NMR (C_6D_6, 500 MHz): with ^{1}H decoupling δ 26.1 (s *B*N_2H)

Preparation of HAl(NMe_2Et)[1,8-(N^{i}Pr)$C_{10}H_6$], (39)

The diamine (^{i}PrNH)$_2C_{10}H_6$ **4a** (0.20g, 0.83 mmol) was dissolved in approximately 30 ml of toluene in a round bottom flask equipped with a stir bar. To the solution was added a 0.5 M toluene solution of $AlH_3{\cdot}NMe_2Et$ (1.65 ml, 0.83 mmol) dropwise. The solution was stirred overnight and turned to a dirty yellow. The volatiles were removed and the product was recrystallized from an ether/toluene solution a -25°C. The product was isolated as small off-white crystals and dried under vacuum (0.14g, 0.41 mmol, 49 %).

^{1}H NMR (C_6D_6, 300 MHz): δ 7.35 (t, 2H, C*H*), 7.23 (dd, 2H, C*H*), 6.70 (d, 2H, C*H*), 3.92 (s, 2H, C*H*Me_2), 2.12 (q, 2H, C*H*$_2$), 1.54 (s, 6H, C*H*$_3$), 1.44 (d, 6H, C*H*$_3$), 1.39 (d, 6H, C*H*$_3$),

0.23 (t, 3H, CH_3). ^{13}C NMR (C_6D_6, 300 MHz): δ 152.9 (*C*), 139.4 (*C*), 126.7 (*C*H), 122.3 (*C*), 116.9 (*C*H), 107.2 (*C*H), 52.2 (CH_2), 49.1 ($CHMe_2$), 42.9 (NCH_3), 25.49 (CH_3), 25.36 (CH_3), 6.6 (*C*H3).

Preparation of [μ-1,8-$C_{10}H_6(N^iPr)_2$]($AlMe_2$)$_2$, (40)

The diamine (^{i}PrNH)$_2C_{10}H_6$ **4a** (0.242g, 1.0 mmol) was dissolved in approximately 15 ml of hexane in a round bottom flask equipped with a stir bar. To the solution was added a 2.0 M hexanes solution of $AlMe_3$ (1.0 ml, 2.0 mmol). The solution was stirred overnight and turned black, then brown.. The volatiles were removed to yield a beige solid. The product was recrystallized from ether at -25°C (0.0174g, 49%).

^{1}H NMR (C_6D_6 200MHz): δ 7.29 (m, 4H), 7.10 (m, 2H), 6.94 (d, 2H), 6.71 (m, 1H), 4.05 (sept, 2H), 3.59 (m, 1H), 1.32 (overlapping d for 12H and a m for approx. 6H), -0.04 (s, 6H), -0.13 (br, 2H), -1.04 (s, 6H).

Preparation of [μ-1,8-$C_{10}H_6(N^iPr)_2$]($ZnMe$)$_2$, (41)

The diamine (^{i}PrNH)$_2C_{10}H_6$ **4a** (0.242g, 1.0 mmol) was dissolved in approximately 10 ml of hexane in a round bottom flask equipped with a stir bar. To the solution was added a 2.0 M toluene solution of $ZnMe_2$ (1.0 ml, 2.0 mmol). The solution was stirred overnight and turned vary dark. The volatiles were removed and the product was recrystallized from pentane at -25°C.

^{1}H NMR (C_6D_6 200MHz): δ 7.20 (m, 4H), 6.53 (m, 2H), 3.54 (sept, 2H), 1.26 (d, 12H), -0.39 (s, 6H).

Structural determinations for 37, 38, 40 and 41:

Single crystals were mounted on thin glass fibres using viscous oil and then cooled to the data collection temperature. Crystal data and details of the measurements are summarized in Table 5.1. Data were collected on a Bruker AX SMART 1k CCD diffractometer using 0.3° ω-scans at 0, 90, and 180° in ϕ. Unit-cell parameters were determined from 60 data frames collected at different sections of the Ewald sphere. Semi-empirical absorption corrections based on equivalent reflections were applied (Blessing, R., *Acta Cryst.*, **1995,** A51, 33-38).

The structures were solved by direct methods, completed with difference Fourier syntheses and refined with full-matrix least-squares procedures based on F^2. All non-hydrogen atoms were refined with anisotropic displacement parameters. All hydrogen atoms were treated as idealized contributions. All scattering factors and anomalous dispersion factors are contained in the SHELXTL 5.1 program library (Sheldrick, G. M., Bruker AXS, Madison, WI, 1997).

Figure 7.1. Thermal ellipsoid plot showing the molecular structure and atom numbering scheme for the borane Lewis adduct **37**. Thermal ellipsoids are drawn at 30% probability.

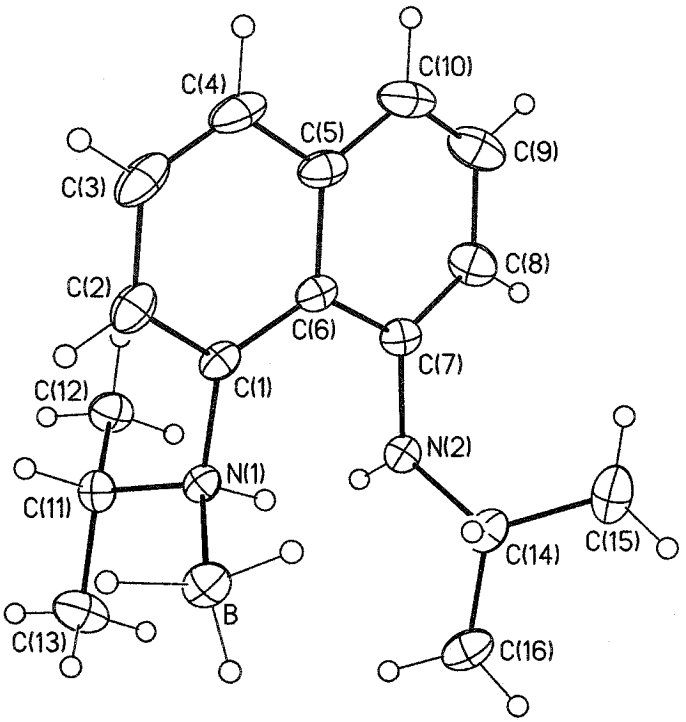

Figure 7.2. Thermal ellipsoid plot showing the molecular structure and atom numbering scheme for the diamido borane **38**. Carbon bound hydrogen atoms have been omitted for clarity. Thermal ellipsoids are drawn at 30% probability.

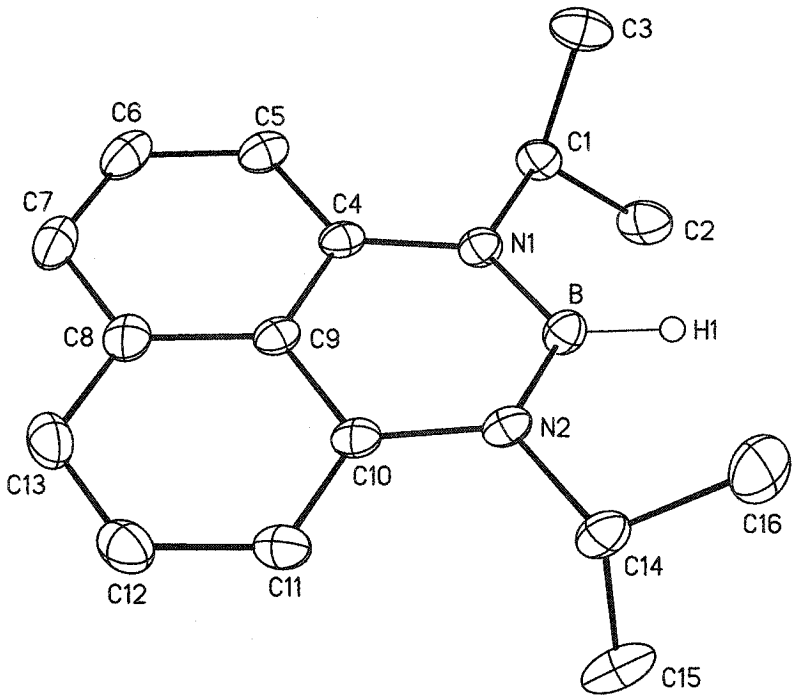

Figure 7.3. Thermal ellipsoid plot showing the molecular structure and atom numbering scheme for the bimetallic aluminum species **40**. Hydrogen atoms have been omitted for clarity. Thermal ellipsoids are drawn at 30% probability.

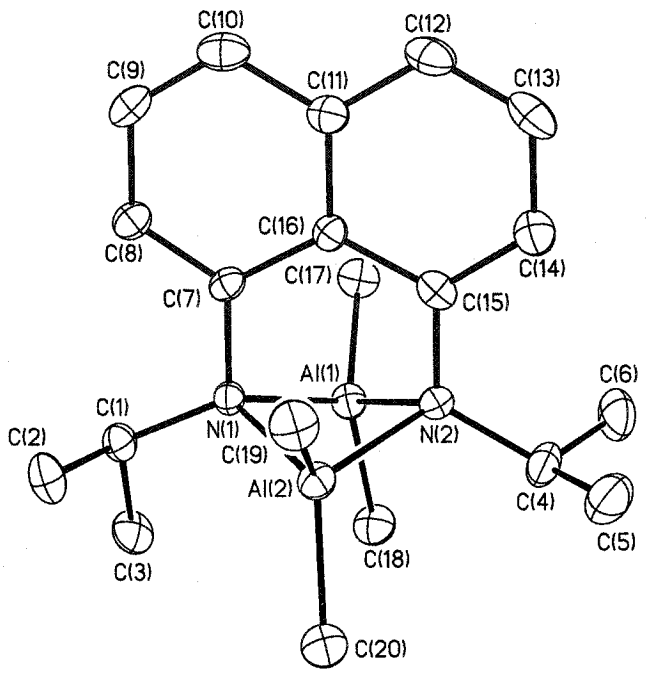

Figure 7.4. Thermal ellipsoid plot showing the molecular structure and atom numbering scheme for one of the two symmetry unique molecules of the bimetallic zinc species **41**. Hydrogen atoms have been omitted for clarity. Thermal ellipsoids are drawn at 30% probability.

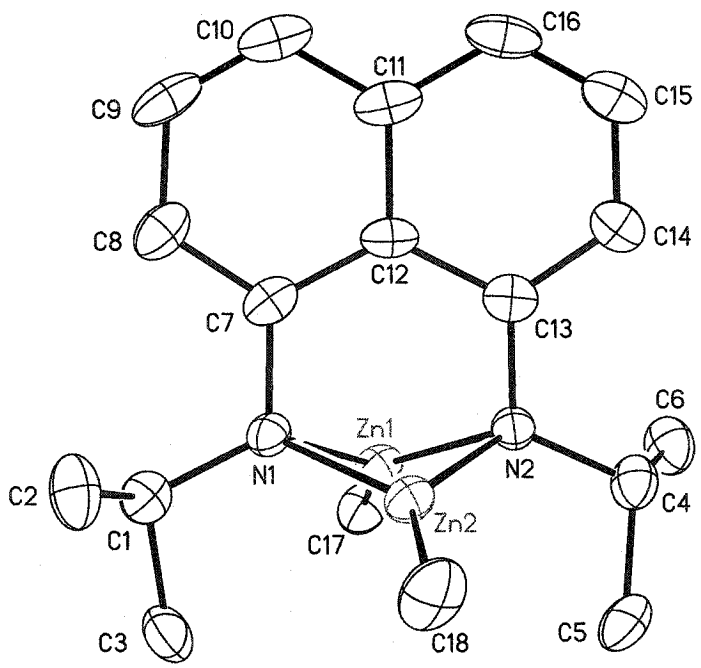

Table 7.1. Selected Crystal Data and Data Collection Parameters for **37**, **38**, **40**, and **41**.

	37	**38**	**40**	**41**
empirical formula	$C_{16}H_{25}BN_2$	$C_{16}H_{21}BN_2$	$C_{20}H_{32}Al_2N_2$	$C_{18}H_{26}N_2Zn_2$
formula weight	256.19	252.16	354.44	401.15
T (K)	203(2)	203(2)	238(2)	238(2)
wavelength (Å)	0.71073	0.71073	0.71073	0.71073
crystal system	Monoclinic	Monoclinic	Triclinic	Monoclinic
space group	C2/c	$P2_1/n$	P-1	P2(1)/c
a (Å)	25.701(4)	9.3317(16)	8.422(3)	15.123(7)
b (Å)	6.6330(10)	8.6413(14)	8.519(3)	9.854(4)
c (Å)	18.679(3)	18.233(3)	14.842(5)	25.144(9)
α (deg)	90	90	86.710(4)	90
β (deg)	94.319(2)	91.065(3)	80.335(4)	92.63(7)
γ (deg)	90	90	78.309(4)	90
V (Å^3)	3175.2(8)	1470.0(4)	1027.6(6)	3743(3)
Z	8	4	2	8
abs coeff (mm^{-1})	0.062	0.066	0.145	2.561
final R indices	R1 = 0.0653	R1 = 0.0798	R1 = 0.0545	R1 = 0.0334
	wR2 = 0.1846	wR2 = 0.1313	wR2 = 0.1381	wR2 = 0.0566

Table 7.2. Selected Bond Distances and Angles for **37**.

Bond Distances (Å)			
B-N(1)	1.640(3)	N(2)-C(7)	1.438(2)
N(1)-C(1)	1.469(2)	N(2)-C(14)	1.502(2)
N(1)-C(11)	1.524(2)		
Bond Angles (deg)			
C(1)-N(1)-B	111.32(14)	C(1)-N(1)-C(11)	111.18(13)
C(11)-N(1)-B	115.47(15)	C(7)-N(2)-C(14)	116.09(15)
Sum at N(1)	337.97		

Table 7.3. Selected Bond Distances and Angles for **38**.

Bond Distances (Å)			
B-N(1)	1.418(3)	B-N(2)	1.413(3)
N(1)-C(4)	1.409(3)	N(2)-C(10)	1.413(3)
N(1)-C(1)	1.492(3)	N(2)-C(14)	1.492(3)
Bond Angles (deg)			
N(2)-B-N(1)	121.0(3)	C(10)-N(2)-B	120.4(2)
C(4)-N(1)-B	120.4(2)	B-N(2)-C(14) α	121.0(2)
B-N(1)-C(1)	120.7(2) α	C(10)-N(2)-C(14)	118.27(19)
C(4)-N(1)-C(1)	118.54(18)	Sum at N(2)	359.67
Sum at N(1)	359.65	N(2)-C(10)-C(9)	117.3(2)
N(1)-C(4)-C(9)	117.5(2)	C(11)-C(10)-N(2)	123.1(2)
C(5)-C(4)-N(1)	123.7(2)		

Table 7.4. Selected Bond Distances and Angles for **40**.

Bond Distances (Å)			
Al(1)-N(1)	1.977(4)	Al(2)-N(1)	1.982(4)
Al(1)-N(2)	1.971(4)	Al(2)-N(2)	1.982(4)
Al(1)-C(17)	1.959(5)	Al(2)-C(19)	1.957(5)
Al(1)-C(18)	1.966(5)	Al(2)-C(20)	1.954(5)
N(1)-C(7)	1.457(5)	N(2)-C(15)	1.437(5)
N(1)-C(1)	1.522(6)	N(2)-C(4)	1.503(6)
Bond Angles (deg)			
N(2)-Al(1)-N(1)	80.73(16)	N(1)-Al(2)-N(2)	80.33(16)
C(17)-Al(1)-C(18)	115.1(2)	C(20)-Al(2)-C(19)	116.2(2)
Al(1)-N(1)-Al(2)	92.00(16)	Al(1)-N(2)-Al(2)	92.17(17)
C(1)-N(1)-Al(1)	122.8(3)	C(4)-N(2)-Al(1)	114.7(3)
C(7)-N(1)-Al(1)	103.3(3)	C(15)-N(2)-Al(1)	106.7(3)
C(7)-N(1)-C(1)	114.2(3)	C(15)-N(2)-C(4)	119.7(4)

Table 7.5. Selected Bond Distances and Angles for **41**.

Bond Distances (Å)			
Zn(1)-N(1)	2.057(4)	Zn(2)-N(1)	2.035(4)
Zn(1)-N(2)	2.036(4)	Zn(2)-N(2)	2.041(4)
Zn(1)-C(17)	1.929(4)	Zn(2)-C(18)	1.939(5)
N(1)-C(7)	1.430(5)	N(2)-C(13)	1.428(5)
N(1)-C(1)	1.477(6)	N(2)-C(4)	1.490(5)
Bond Angles (deg)			
N(2)-Zn(1)-N(1)	80.93(14)	N(1)-Zn(2)-N(2)	81.33(15)
C(17)-Zn(1)-N(1)	138.76(18)	C(18)-Zn(2)-N(1)	138.90(18)
C(17)-Zn(1)-N(2)	140.27(18)	C(18)-Zn(2)-N(2)	139.73(19)
Sum at Zn(1)	359.96	Sum at Zn(2)	359.96
Zn(2)-N(1)-Zn(1)	90.35(15)	Zn(1)-N(2)-Zn(2)	90.77(15)
C(1)-N(1)-Zn(1)	120.3(3)	C(4)-N(2)-Zn(1)	116.0(3)
C(1)-N(1)-Zn(2)	115.9(3)	C(4)-N(2)-Zn(2)	120.2(3)
C(7)-N(1)-Zn(1)	101.6(3)	C(13)-N(2)-Zn(1)	107.5(3)
C(7)-N(1)-Zn(2)	107.1(3)	C(13)-N(2)-Zn(2)	102.0(3)
C(7)-N(1)-C(1)	117.5(4)	C(13)-N(2)-C(4)	116.7(4)

8 Zirconium Guanidinates

I. Introduction

The continuing search for active Ziegler-Natta catalysts has, during the last decade, yielded a variety of highly active non-metallocene catalysts for the polymerization of α-olefins.[1] A central theme of these efforts has been the development of cationic metal alkyl complexes that are sufficiently stable to promote the propagating olefin insertion steps in preference to the deactivating side-reactions of β-hydrogen elimination and chain transfer. Monocyclopentadienyl zirconium (IV) acetamidinate complexes, [(η^5-C_5Me_5){RNC(Me)NR}ZrR'_2] (R = alkyl, R' = alkyl) are among the recent additions to the field of living α-olefin polymerization catalysts.[2, 3] The acetamidinate ligands in these

[1] For selected reviews see: (a) Ittel, S. D.; Johnson, L. K.; Brookhart, M. *Chem. Rev.* **2000**, *100*, 1169 and references therein. (b) Gibson, V. C.; Spitzmesser, S. K. *Chem. Rev.* **2003**, *103*, 283-315 and references therein. (c) Gade, L. H. *Chem. Commun.* **2000**, 173. (d) Volkis,V.; Nelkenbaum, E.; Lisovskii, A.; Hasson, G.; Semiat, R.; Kapon, M.; Botoshansky, M.; Eishen, Y.; Eisen, M. S. *J. Am. Chem. Soc.* **2003**, *125*, 2179. and references therein

[2] (a) Keaton, R. J.; Sita, L. R. *J. Am. Chem. Soc.* **2002**, *124*, 9070-9071. (b) Keaton, R. J.; Koterwas, L. A.; Fettinger, J. C.; Sita, L. R. *J. Am. Chem. Soc.* **2002** *124*, 5932-5933. (c) Jayaratne, K. C.; Sita, L. R. *J. Am. Chem. Soc.* **2001**, *123*, 10754-10755. (d) Keaton, R. J.; Jayaratne, K. C.; Henningsen, D. A.; Koterwas, L. A.; Sita, L. R. *J. Am. Chem. Soc.* **2001**, *123*, 6197-6198. (e) Jayaratne, K. C.; Keaton, R. J.; Henningsen, D. A.;

species are readily modified to yield catalyst precursors that are capable of stereospecific polymerization of "difficult" monomers such as 1,5-hexadiene and vinylcyclohexane.[2d,e]

Like amidinates, N-substituted guanidinate anions $\{RNC(NR'_2)NR\}^-$ are nitrogen-based chelating ligands that can be subjected to rational substituent modifications in order to control the steric and electronic properties of their metal complexes.[4] Guanidinate complexes have been prepared by insertion of carbodiimides into metal amido linkages, proton transfer between guanidines and metal amides/hydrocarbyls and via salt metathesis approaches with lithium guanidinates and metal halides.[4,5,6,7] Complexes of guanidinate ligands are beginning to emerge as interesting species in small molecule activation.[5d,k,l,6a,b,8]

Chart 8.1

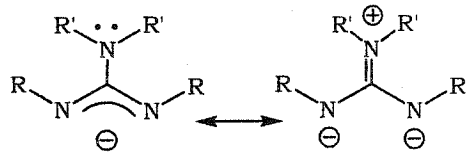

EE

A characteristic feature of guanidinate ligands is the presence of the NR'_2 function that is capable of donating lone pair electron density to the central carbon of the chelate ring thus stabilizing a zwitterionic resonance structure (**EE**, Chart 8.1). This resonance structure leads to a formal negative charge on both nitrogens effectively increasing electron donation

---

Sita, L. R. *J. Am. Chem. Soc.* **2000**, *122*, 10490-10491. (f) Jayaratne, K. C.; Sita, L. R. *J. Am. Chem. Soc.* **2000**, *122*, 958-959.

[3] Related benzamidinate monocyclopentadienyl zirconium (IV) are reported in: (a) Gomez, R.; Green, M. L. H.; Haggitt, J. L. *J. Chem. Soc., Dalton Trans.* **1996**, 939. (b) Gomez, R.; Duchateau, R.; Chernega, A. N.; Teuben, J. N.; Edelmann, F. T.; Green, M. L. H. *J. Organomet. Chem.* **1995**, *491*, 153. (c) Gomez, R.; Duchateau, R.; Chernega, A. N.; Meetsma, A.; Edelmann, F. T.; Teuben, J. H.; Green, M. L. H. *J. Chem. Soc., Dalton Trans.* **1995**, 217-225. (d) Gomez, R.; Green, M. L. H.; Haggitt, J. L. *J. Chem. Soc., Chem. Commun.* **1994**, 2607-2608.

[4] For a recent review of guanidinate complexes see: Bailey, P. J.; Pace, S. *Coord. Chem. Rev.* **2001**, *214*, 91-141.

[5] (a) Foley, S. R.; Yap, G. P. A.; Richeson, D. S. *Inorg. Chem.* **2002**, *41*, 4149. (b) Ong, T.-G.; Wood, D.; Yap, G. P. A.; Richeson, D. S. *Organometallics* **2002**, *21*, 2839. (c) Foley, S. R.; Yap, G. P. A.; Richeson, D. S. *Polyhedron* **2002**, *21*. 619. (d) Ong, T.-G.; Wood, D.; Yap, G. P. A.; Richeson, D. S. *Organometallics* **2002**, *21*, 1. (e) Lu, Z.; Yap, G. P. A.; Richeson, D. S. *Organometallics* **2001**, *20*, 706. (f) Foley, S. R.; Yap, G. P. A.; Richeson, D. S. *J. Chem. Soc., Chem. Commun.* **2000**, 1515. (g) Thirupathi, N.; Yap, G. P. A.; Richeson, D. S. *Organometallics* **2000**, *19*, 2573. (h) Thirupathi, N.; Yap, G. P. A.; Richeson, D. S. *J. Chem. Soc., Chem. Commun.* **1999**, 2483. (i) Wood, D.; Yap, G. P. A.; Richeson, D. S. *Inorg. Chem.* **1999**, *38*, 5788. (j) Bazinet, P.; Wood, D.; Yap, G. P. A.; Richeson, D. S. *Inorg. Chem.* **2003**, *42*, 6225-6229. (k) Ong, T.-G.; Yap, G. P. A.; Richeson, D. S. *Chem. Commun.* **2003**, 2612-2613. (l) Ong, T.-G.; Yap, G. P. A.; Richeson, D. S. *J. Am. Chem. Soc.* **2003**, *125*, 8100-8102.

[6] (a) Mullins, S. M.; Duncan, A. P.; Bergman, R. G.; Arnold, J. *Inorg. Chem.* **2001**, *40*, 6952-6963. (b) Duncan, A. P.; Mullins, S. M.; Arnold, J.; Bergman, R. G. *Organometallics* **2001**, *20*, 1808-1819. (c) Giesbrecht, G. R.; Arnold, J. *J. Chem. Soc., Dalton Trans.* **2001** 923. (d) Giesbrecht, G.R.; Whitener, G. D.; Arnold, J. *Organometallics* **2000**, *19*, 2809-2812. (e) Giesbrecht, G.R.; Shafir, A.; Arnold, J. *J. Chem. Soc.,Dalton Trans.* **1999**, 3601-3604.

[7] Coles, M. P.; Hitchcock, P. B. *J. Chem. Soc., Dalton Trans.* **2001**, 1169.

[8] Okamoto, S.; Livinghouse, T. *Organometallics* **2000**, *19*, 1449.

to the metal and possibly stabilizing cationic metal centres. In order to maximize this effect the NR'_2 centre should be sp^2 hybridized leaving the lone electron pair in a p-orbital that can overlap with the conjugated NCN moiety. In addition, a small dihedral angle between the plane of the CNR'_2 groups and that defined by NCN chelate is necessary for maximum π-donation. These features have been previously noted and recently applied in the synthesis of stable guanidinate-supported cationic metal alkyl complexes.[6b] Some of these compounds have low to moderate activities for ethylene polymerization.

There is considerable potential for related complexes and we have prepared and characterized new mono-pentamethylcyclopentadienyl and bis(trimethylsilyl)cyclopentadienyl zirconium(IV) guanidinate complexes, $Cp^{R1}\{^{i}PrNC(NR'R'')N^{i}Pr\}ZrR_2$ which form the basis for this chapter. In addition to examining the structural characteristics of these compounds in the solid-state we present data on their fluxional behavior in solution. When combined with appropriate co-catalysts, these organozirconium complexes effect the oligomerization of 1-hexene.

II. Results and Discussion

A. Synthesis and Structure of $Cp^{R1}\{^{i}PrNC(NR'R'')N^{i}Pr\}ZrX_2$ Derivatives via Salt Metathesis

Complexes with a combination of guanidinato- and cyclopentadienyl-supporting ligands are directly related to mono(cyclopentadienyl)zirconium amidinato species.[2] Given the tremendous success with amidinates as supporting ligands in α-olefin polymerization we felt that examination of related guanidinate species was necessary. Our efforts in the preparation and investigation of such compounds have revealed two practical routes to the targeted complexes. The guanidinate anion can be introduced into the coordination sphere of Zr(IV) through proton-transfer coupled with hydrocarbon elimination and through salt metathesis reactions using lithium guanidinates.

Mono(cyclopentadienyl)(guanidinato)zirconium dichloride compounds can be prepared by reaction of lithium guanidinates with one equivalent of $Cp^{R1}ZrCl_3$ ($Cp^{R1} = \eta^5$-C_5Me_5 (Cp*) or η^5-1,3-$(Me_3Si)_2C_5H_3$ (Cp'')) yielding the half-sandwich guanidinate

complexes $Cp^{R1}\{^{i}PrNC(NR'R'')N^{i}Pr\}ZrCl_2$ (Scheme 8.1). Complexes **42** , **43** and **44** display similar NMR spectra, which confirmed the presence of a 1:1 ratio of Cp^{R1} and guanidinate ligands, and support the proposed molecular structures. The appearance of a single set of resonances for the ^{i}Pr substituents of the Zr bonded N atoms is indicative of a symmetric and fluxional bidentate interaction. In the absence of a dynamic process that equilibrates the methyl groups of the ^{i}Pr substituents, one would anticipate two equal intensity doublets for these groups.

Scheme 8.1

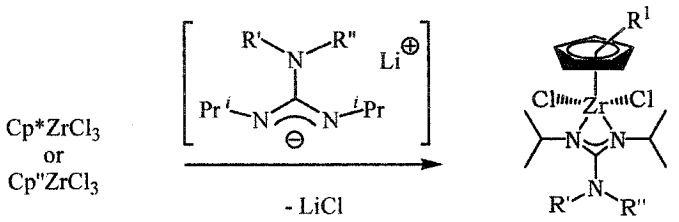

$Cp^* = \eta^5\text{-}Me_5C_5$
$Cp'' = \eta^5\text{-}1,3\text{-}(Me_3Si)_2C_5H_3$

42 Cp^{R1} = Cp", R' = ^{i}Pr, R" = H
43 Cp^{R1} = Cp*, R' = Me
44 Cp^{R1} = Cp*, R' = ^{i}Pr, R" = CH_2Ph

Single-crystal X-ray diffraction analysis of **44** was undertaken in order to confirm the coordination geometry of the metal centre and the connectivity of the ligands for these compounds (Table 8.2). The molecular structure of compound **44** is presented in Figure 8.1 with selected bond distances and angles listed in Table 8.3. Complex **44** displays a metal centre in a distorted four-legged piano stool environment consisting of the Cp* ligand, two *cis*-chlorides, and the two nitrogen atoms of the bidentate guanidinate anion. The restricted bite angle of the guanidinate ligand (59.9(1)°) leads to some distortion from an ideal piano stool arrangement.

The guanidinate ligand exhibits a typical binding mode where the anionic charge seems to be fully delocalized between N(1) and N(2) resulting in identical Zr-N bond lengths of 2.239(4) and 2.243(4) Å and equivalent N-C bond lengths of 1.360(6) and 1.345(6) Å within the chelate ring. A small torsion angle of 35.4° for N(2)-C(27)-N(3)-C(26) indicates that there is potential for participation of the lone electron pair on the planar N(3) centre to become involved in the π-system of the chelate. Some degree of π-bonding between C(27)-N(3) is further suggested by the relatively short bond length of 1.404(5) Å. However comparison of this value with the analogous exocyclic C-N distance (1.373(4) Å)

in the reported compound $Cp\{^{i}PrNC(NMe_2)CN^{i}Pr\}ZrCl_2$ [6b] (**FF**) suggests that resonance structure **DD** is less important for the more electron rich (Cp* vs Cp) compound **44** than it is for **FF** and that the donor ability of the guanidinate ligand is flexible, accommodating the demands of the metal centre.

The molecular structure for the N,N',N''-trisubstituted guanidinato compound **42** was also determined via X-ray crystallography (Table 8.2) and the result is illustrated in Figure 8.2. Table 8.4 contains a list of selected bond lengths and angles. The structural parameters and overall geometry at the Zr centre is very similar to compound **44**. The four-legged piano stool configuration with a symmetrically bound guanidinate and *cis* chlorides are all consistent with compound **44**. The substantially different topology for the bis(trimethyl silyl)cyclopentadienyl ligand (Cp'') compared to the pentamethyl derivative does not seem to influence the geometry at the metal centre significantly. The reduced electron donation from this ligand however has significant impact on the guanidinate-metal interaction. The average Zr-N bond for **42** is 0.04 Å shorter and the exocyclic C-N bond (C(10)-N(3)) shows a 0.046 Å decrease to 1.358(6) Å. This implies a stronger contribution from the lone-pair on N(3) to the π-system of the NCN chelate and this is in fact reflected by a small dihedral angle between the two planes defined by C7-N3-C10 and N1-C10-N2 of 30.3°. Since they possess a single N-substituent, trisubstituted guanidinates have less steric constraints and can more easily achieve a co-planar configuration of the exocyclic nitrogen with the π-system of the NCN chelate, in turn allowing the ligand more flexibility in varying the degree of electron donation to the metal.

Desiring to investigate the potential effects guanidinate ligands could have on the reactivity of Zr complexes we prepared dialkyl derivatives. The dichloride species **42-44** are very good entry points and can be cleanly converted to dialkyls through reaction with alkyllithium or Grignard reagents.

Addition of two equivalents of MeLi to solutions of **43** and **44** generated the desired dimethyl compounds **45** and **46** in good yields (Scheme 8.2). The appearance of Zr-Me moieties in the ^{1}H NMR clearly confirmed the identity of these compounds. Similar to the dichloride starting materials, the isopropyl groups in **45** appear in the ^{1}H NMR spectrum with a single resonance for the methine protons and one doublet for the methyl groups. These

results contrast with the reports of the attempted methylation of $Cp\{^{i}PrNC(NMe_2)CN^{i}Pr\}ZrCl_2$ (**FF**) with MeLi which resulted in a ligand redistribution reaction to generate Cp_2ZrMe_2 and $[Me_2NC(N^{i}Pr)_2]_2ZrMe_2$ while reaction with MeMgCl led to the desired product, $Cp\{^{i}PrNC(NMe_2)CN^{i}Pr\}ZrMe_2$ (**GG**).[6b] In contrast to **45**, the room temperature ^1H NMR spectrum for **46** exhibited a broad signal for the methyls of the ^{i}Pr groups on the chelating nitrogen centres indicating a decreased rate of ligand fluxionality.

Scheme 8.2

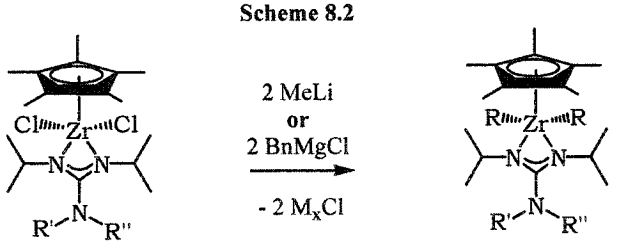

43) R' = R'' = Me
44) R' = ^{i}Pr, R'' = CH_2Ph

45) R = R' = R'' = Me
46) R = Me, R' = ^{i}Pr, R'' = CH_2Ph
47) R = CH_2Ph, R' = ^{i}Pr, R'' = CH_2Ph

The molecular structure of compound **46** was determined by single crystal X-ray diffraction (Table 8.2) and the result of this study is displayed in Figure 8.3. Selected bond distances and angles are provided in Table 8.5. As with the dichloride analogue **44**, the metal centre in **46** is in a distorted four-legged piano stool environment defined by the Cp* ligand, the two nitrogens of the chelating guanidinato ligand and the two Zr-Me groups. Several structural differences between **44** and **46** are noteworthy. Specifically, there is a slight increase in the average Zr-N bond lengths of 0.05Å and a larger difference between the two distances for **46**. Furthermore, **46** displays a longer N(3)-C(27) distance of 1.416(3)Å and a larger torsion angle of 48.3° for N(2)-C(27)-N(3)-C(26). Taken together, these metrical differences suggest there is less interaction between the lone pair on the exocyclic nitrogen and the conjugated NCN chelate ring for **46** compared to **44**. These changes appear to correlate with the decreased electrophilicity of the metal centre when Cl is replaced by Me and support the concept of guanidinate having a flexible ability to donate electrons through resonance structure **EE** (Chart 8.1).

Complex **44** also reacts with two equivalents of $PhCH_2MgCl$ to generate the dibenzyl derivative **47** in a moderate yield (Scheme 8.2). In contrast to **42-46**, compound **47** exhibits thermal instability in solution and slowly decomposes to give unidentified species. We

attribute the slightly lower yield of this product to this observation. Similar to compounds **42-46**, the ^{1}H NMR spectrum for compound **47** displayed signals for Cp* and the guanidinato ligands in an appropriate 1:1 ratio. The methyl groups for the ^{i}Pr substituents on the chelating N-centres appear as a sharp doublet, again indicative of a fluxional species at room temperature. Additionally, the ^{1}H NMR spectrum of **47** displayed resonances for diastereotopic methylene protons of the Zr-CH_2Ph moieties. These appear with a characteristic AB pattern at 2.03 and 2.53 ppm.

Single crystals of **47**, suitable for X-ray diffraction analysis, could be grown from either Et_2O or hexane. The molecular structure of **47** was determined and the results are summarized in Tables 8.2, selected bond lengths and angles are listed in Table 8.6 and Figure 8.4 illustrates the solid-state structure. The observed unit cell contained two crystallographically unique, but chemically equivalent molecules. Both molecules exhibit the same distorted piano stool geometric arrangement of the ligands around the metal centre as seen for compounds **42**, **44** and **46**. The bite angles of the guanidinate ligands and the Zr-N bond lengths are comparable to values obtained for the dimethyl derivative **46**. The structural parameters obtained for **47** indicate undistorted monodentate benzyl groups. The exocyclic N(3)-C(7) bond length of 1.404(4) Å is slightly shorter than the value obtained for the dimethyl analogue **46** suggesting a more electrophilic metal.

B. Synthesis and Structure of $Cp^{R1}\{^iPrNC(NH^iPr)N^iPr\}ZrMe_2$ Derivatives via Proton Transfer

An alternate route for the introduction of guanidinate ligands is through proton-transfer coupled with hydrocarbon elimination. The direct reaction of N,N',N''-triisopropylguanidine and the half-sandwich trialkyl compounds Cp''$ZrMe_3$ or Cp*$ZrMe_3$ proceeds smoothly to generate the desired dialkyl species **48** and **49** (Scheme 8.3). The

Scheme 8.3

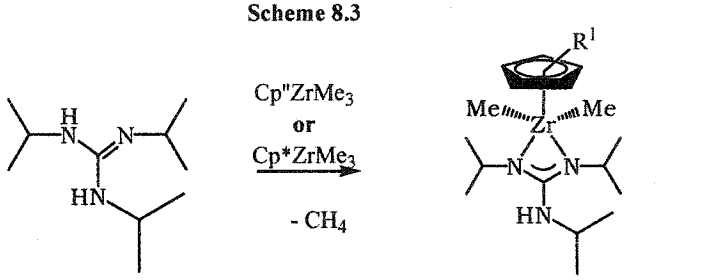

48) Cp^{R1} = Cp*
49) Cp^{R1} = 1,3-$(SiMe_3)_2$Cp

guanidine is singly deprotonated by one of the zirconium methyl groups with elimination of methane. The ^{1}H and ^{13}C NMR spectra for **48** and **49** are similar to the other dimethyl species (**45,46**), and show only one set of resonances for the methyls of the ^{i}Pr groups on the chelating nitrogens. The data supports analogous structures for **48** and **49** with a fluxional ligating interactions.

The molecular structure for the Cp* derivative **48** was determine by X-ray diffraction studies and the results are summarized in Table 8.2 and the structure is illustrated in Figure 8.5. Table 8.7 lists selected bond length and angles for **48**. Compound **49** exhibits similar geometric parameters as the previously discussed complexes. Consistent with a more electron rich metal centre compared to the dichloride analogue **42**, compound **48** displays a slightly longer C(10)-N(3) bond (1.378(5) Å) and longer Zr-N distances (2.246(3) and 2.281(3) Å). The larger torsion angle of 43.4(7)° (compared to 30.3°) is also in line with less electronic contribution from the nitrogen lone-pair.

C. Variable-Temperature ^{1}H NMR of Compounds 46 and 47

Provided that the NR'R" groups are planar and free to rotate, compounds **42-49** each possess a mirror plane in their limiting structures and are, therefore, not chiral. However, due to the asymmetry of these compounds perpendicular to this symmetry plane the magnetic environment above the guanidine ligand plane (NCNZr) is different than the environment below it; therefore, the Me groups of the ^{i}Pr substituents on the metal-bonded nitrogen atoms are diastereotopic and should display unique NMR signals. As indicated in Scheme 8.4, one would expect the static structures of **42-49** to exhibit a pair of doublets for the diastereotopic CH_3 groups (labelled *t* and *b*) and a single multiplet for the associated methine protons. The

Scheme 8.4

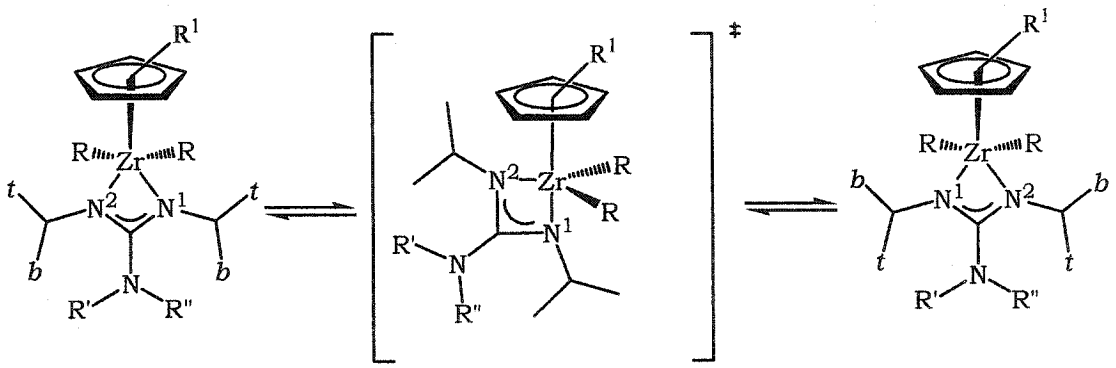

room temperature NMR spectra of compounds **42-49** display only one signal for these groups with an integration value of four equivalent methyl groups. This observation is consistent with a fluxional process that interchanges the *t* and *b* groups and is similar to the configurational exchange that was recently examined for $[\{(Me_2N)C(N^iPr)_2\}_2Zr(CH_2Ph)_2]$ (**CC**).[6b] The recent report of a similar exchange process in monocyclopentadienyl titanium(IV) acetamidinate complexes concluded that exchange occurs through rotation around the internal C_2 axis of the amidinate ligand or "ring-flipping".[9, 10] The proposed transition state for this rearrangement is similar to that shown in Scheme 8.4.

Elucidation of the fluxional processes observed for **42-49** has direct bearing on configurational stability of guanidinate metal complexes and is important for future applications of these complexes. In an effort to address this issue we examined the variable-temperature ^{1}H NMR spectra of compounds **46** and **47**. The broad room temperature ^{1}H NMR signals for the diastereotopic methyl groups of compound **46** resolved into two equal intensity peaks at 285 K and become a sharp doublet at 315 K (Figure 8.6). As expected the related methine signal does broaden upon cooling but remains as a single multiplet down to 280 K. Furthermore, the Zr-Me signal, while shifting slightly downfield at lower temperatures, remains a sharp singlet over this temperature range. The spectral changes

Figure 8.6

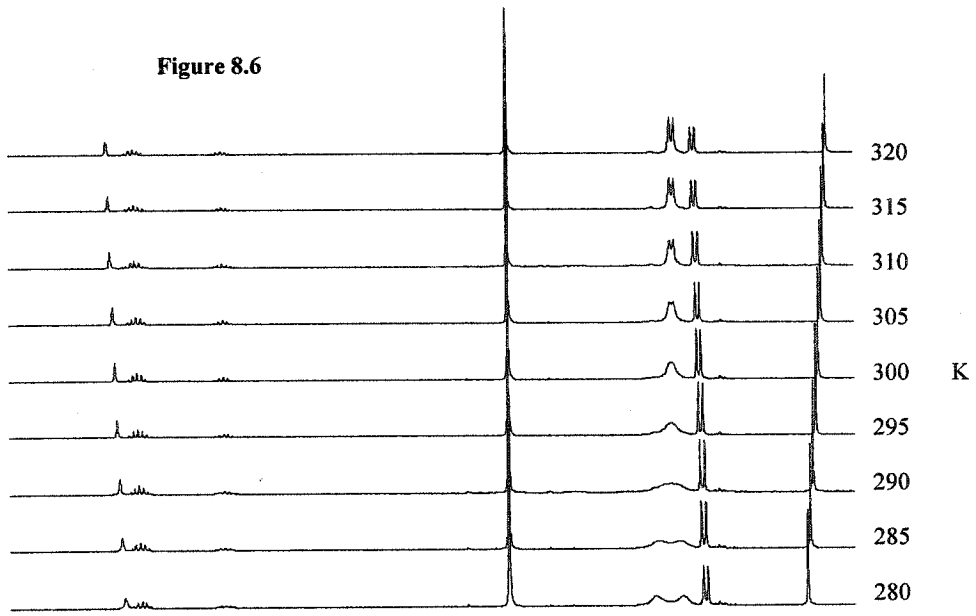

[9] Koterwas, L. A.; Fettinger, J. C.; Sita, L. R. *Organometallics* **1999**, *18*, 4183.
[10] A dissociative mechanism for Ti-benzamidinate fluxionality is proposed in: Stewart, P. J.; Blake, A. J.; Mountford, P. *Organometallics*, **1998**, *17*, 3271.

observed for **46** are consistent with the ring-flipping mechanism of Scheme 8.4. In particular, the observation of single resonances for both the Zr-Me and the methine groups militates against formation of an asymmetric isomer of **46**.

The possibility for exchange of the two hydrocarbyl ligands bonded to Zr, which would also result in averaging of signals, can be addressed through examination of the variable temperature behavior of the NMR signals of **47**. The room temperature ^{1}H NMR of compound **47** is characterized by magnetic equivalence for the ^{i}Pr substituents of the chelating nitrogens and an AB pattern for the diastereotopic protons of the Zr-CH_2Ph groups. Any intra- or inter-molecular exchange between the benzyl groups of **47** should lead to collapse of the AB splitting pattern of the diastereotopic methylene protons into a singlet in the NMR spectrum. At room temperature it is clear that for **47** the exchange process that equilibrates the diastereotopic methyl groups does not involve interconversion of the benzyl groups. Cooling an NMR sample of **47** to 253K led to decoalescence for the methyl signals for the N^{i}Pr groups, which continued to sharpen as the sample was cooled to 223K. The coupling pattern for the Zr-CH_2Ph units does not change over this temperature range. These observations further support a symmetric limiting structure for this species and a fluxional process that does not result in exchange of the hydrocarbyl ligands. Again, these observations support the ring-flipping mechanism of Scheme 8.4 as the origin of configurational change in these compounds.

C. Hexene Oligomerization Experiments

Given the exceptional ability of related half-sandwich Zr acetamidinate compounds to polymerize α-olefins, we screened complexes **44** and **46** as 1-hexene polymerization catalysts. The identity of cocatalyst, solvent and temperature were varied and the results of these efforts are summarized in Table 8.1. Under the conditions presented in Table 8.1, compounds **44** and **46** were only capable of catalyzing the oligomerization of 1-hexene. The activity of these compounds for reaction with hexene did not appear to vary over a period of 20 hours thus ruling out either high initial rates of polymerization or an induction period for this reaction.

The first clear indication that the products of these reactions were of low molecular weight was provided by the ^{1}H and ^{13}C NMR spectra of these materials. In particular, proton

resonances of significant intensity were observed in the olefinic region (4.8-5.4 ppm) for all products reported in Table 8.1 and their ^{13}C NMR spectra display a rich collection of resonances. The presence of signals due to both internal and terminal olefins are present in all oligomerization products. The molecular weights (M_w) for the oligo-1-hexenes in Table 8.1 were determined using the relative integration intensities of the ^1H NMR spectra. These molecular weights represent an oligomerization of between 4 – 9 monomer units. These results suggest that β-hydrogen elimination and reinsertion ("chain walking") is a very significant process in 1-hexene oligomerization with **44** and **46**.

Table 8.1. Summary of Data for 1-hexene oligomerization with compounds **45** and **46**.

Entry	cmpd	Cocatalyst[a]	solvent	T (°C)	[1-hexene] M	[Zr] 10^{-3} M	oligomer yield[c] (g)	M_w[d]
1	**45**	$[Ph_3C][B(C_6F_5)_4]$	C_6H_5Cl	20	2.0	3.9	0.37	nd
2	**46**	MAO[b]	$C_6H_5CH_3$	20	6.4	1.8	0.12	-
3	**46**	$[Ph_3C][B(C_6F_5)_4]$	C_6H_5Cl	20	3.6	3.6	0.12	460
4	**46**	$[Ph_3C][B(C_6F_5)_4]$	$C_6H_5CH_3$	20	3.6	3.6	0.13	407
5	**46**	$[Ph_3C][B(C_6F_5)_4]$	$C_6H_5CH_3$	50	3.6	3.6	0.60	771
6	**46**	$[Ph_3C][B(C_6F_5)_4]$	C_6H_5Cl	50	3.6	3.6	trace	-
7	**46**	$[Ph_3C][B(C_6F_5)_4]$	$C_6H_5CH_3$	50	6.3	1.4	2.64	nd

[a] equimolar ratio with Zr, [b]500 eq/Zr, [c]after 20 hr of reaction, [d]values were obtained from ^1H NMR integration of olefinic *vs.* aliphatic signals

At 20°C there was no apparent effect on 1-hexene oligomerization activity from either solvent or cocatalyst. However, there are clear differences between reactions in toluene and chlorobenzene with a reaction temperature of 50°C (entries 5 and 6). For reactions in toluene an increase in temperature led to increased activity and generated products of higher M_w. In contrast, reactions run at 50°C in chlorobenzene produced an insignificant amount of oligomer. This is particularly interesting given that chlorobenzene is

the preferred solvent for 1-hexene polymerization using monocyclopentadienyl zirconium (IV) acetamidinate catalysts.

D. Model for supported Catalysts

Homogeneous polymerization catalysis has made significant contributions to the understanding of the polymerization process, and the preparation of well-defined single-site catalysts which can be fine-tuned to maximize performance. Nevertheless, heterogeneous catalysts are still the premiere choice for industrial processes due to technological or engineering advantages such as better morphology control, high polymer bulk density and no reactor fouling.[11] Several methods for the "heterogenization" of homogeneous catalysts, such as anchoring to silica pre-treated with MAO or tethering to a solid support, are routinely used. Yet there remains a lack of understanding of the effects the solid support have on the reactivity of the catalysts. Silsesquioxanes have been used as homogenous models for silica-grafted or tethered polymerization catalysts.[12,13,14] We decided to investigate the preparation of silsesquioxane tethered mono(cyclopentadienyl)(guanidinato)zirconium catalysts with the desire to evaluate the feasibility and the potential for "heterogenization" of this class of catalyst.

As highlighted in Chapter 2, our chosen approach was to introduce a guanidine ligand directly onto a closed-cage silsesquioxane which possessed a benzyl bromide function. The tethered tetrasubstituted guanidine, easily obtained via guanylation, reacted smoothly with Cp''$ZrMe_3$ to yield the guanidinato species **50** in quantitative yields. The reaction is analogous to the previously described combination of N,N',N''-triisopropyl guanidine with half-sandwich zirconium trialkyls. The reaction is easily followed by NMR spectroscopy, and the product (**50**) displays the typical signals due to the metal guanidinate moiety, along with the additional signals due to the tethered silsesquioxane. A broad signal for the diastereotopic methyls of the ^{i}Pr groups on Zr bound nitrogens suggests that the ligand-metal

---

[11] Fink, G.; Steinmetz, B.; Zechlin, J.; Przybyla, C.; Tesche, B. *Chem. Rev.* **2000**, *100*, 1377-1390.

[12] For a recent review on using silsesquioxanes as models for heterogeneous supports see Duchateau, R. *Chem. Rev.* **2002**, *102*, 3525-3542 and references therein

[13] For specific examples see: (a) Feher, F. J.; Blanski, R. L. *J. Chem. Soc., Chem. Commun.* **1990**, 1614-1616. (b) Feher, F. J.; Walzer, J. F.; Blanski, R. L. *J. Am. Chem. Soc.* **1991**, *113*, 3618-3619. (c) Liu, J.-C. *Chem. Commun.* **1996**, 1109-1110.(a)

[14] For examples of silsesquioxane tethered fluorenyl ligands see: (a) Severn, J. R.; Duchateau, R.; van Santen, R. A.; Ellis, D. D.; Spek, A. L.; Yap, G. P. A. *Dalton Trans.* **2003**, 2293-2302. (b) Severn, J. R.; Duchateau, R.; van Santen, R. A.; Ellis, D. D.; Spek, A. L. *Organometallics* **2002**, *21*, 4-6.

interaction is also fluxional. Apparently the presence of a very large siloxide cage does not interfere with the structural properties of the mono(cyclopentadienyl)(guanidinato) complex. Investigations into the reactive properties of compound **50** are required to fully assess the impact of the tethered silsesquioxane and will be explored in the future.

Scheme 8.5

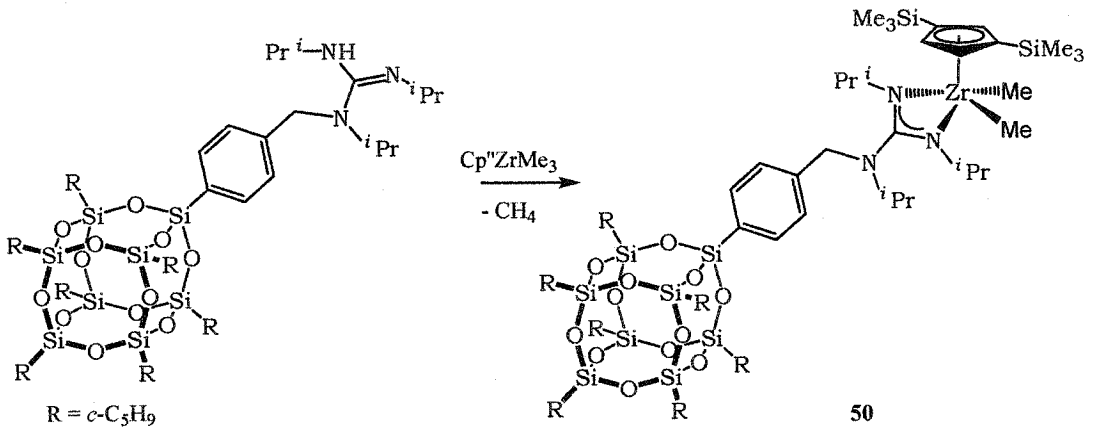

III. Conclusion

A family of half-sandwich guanidinate supported zirconium complexes has been prepared and isolated. Examination of their solid state structures indicates that guanidinate ligands can exhibit flexible electron donor ability through a π-interaction between the exocyclic NR_2 moiety and the NCN chelating group. The guanidinate ligands in these species exhibited dynamic coordination behaviour which we ascribe to a ring-flipping process. Although it appears that the reported Cp* {^{i}PrNC(NR'R")N^{i}Pr}$ZrMe_2$ complexes (**45** and **46**) are active for multiple insertions of 1-hexene to generate oligomers, they are, unlike related acetamidinato complexes, ineffective at polymerizing 1-hexene. We attribute this to a rapid rate of β-elimination and our current efforts are directed to determining the factors responsible for this with the goal of controlling this process for improved catalyst control.

Experimental Section

General Considerations All manipulations were carried out in either a nitrogen filled dry box or under nitrogen using standard Schlenk techniques. Solvents were distilled from Na/K alloy under nitrogen. Deuterated, benzene and toluene were purchased from Aldrich Chemical Company and were dried by vacuum transfer from potassium. ^{1}H and ^{13}C NMR spectra were run on a Varian Gemini-200, a Bruker 300 MHz or a Bruker 500MHz spectrometer using the residual protons of the deuterated solvent for reference. Exceptionally for compounds **49** and **50** NMR spectra were run on Varian Mercury 400 (^{1}H, 400 MHz; ^{13}C, 100.5 MHz) and Varian Indigo 500 (^{29}Si, 100 MHz) Spectrometers. BnMgCl and MeLi were used as received from Aldrich Chemical Company. Cp^*ZrCl_3,[15] $Cp''ZrCl_3$,[16] Cp^*ZrMe_3,[15] $Cp''ZrMe_3$[17] were prepared according to literature procedures.

General Procedure for 1-Hexene Polymerization

In a round bottom flask or a Teflon-sealed Schlenk flask were weighed out the solid precatalysts **46** (0.010g, 18.8 μmol) and cocatalyst $[CPh_3][B(C_6F_5)_4]$ (0.018g, 19.5 μmol). The reaction solvent (toluene or chlorobenzene) was added (2.5 g) and the solution stirred for 10 minutes. For entry 1 (Table 8.1) a 6.7% Al by weight MAO solution (2.1g) and toluene (0.3g) were added to solid precatalyst **45** (0.012g, 28.2 μmol). To the solution was added, all at once, 1-hexene (1.6g, or 6.7g) and the reactions were stirred for 24 hours. In cases where heating was required the Schlenks were taken out of the dry-box and heated using an oil bath. The reactions were quenched by addition of 2.5 ml of methanol and the crude polymer obtained by removal of volatiles *in vacuo*. The polymer was purified by column chromatography using aluminum oxide, and hexanes as eluent. Removal of all volatiles yielded the purified polymers as very viscous liquids.

Preparation of $Cp''[(^{i}PrN)_2C(NH^{i}Pr)]ZrCl_2$, (42)

Dropwise addition of methyllithium (0.9 mL of 1.4 M, 1.26 mmol) to a solution of triisopropylguanidine **5a** (0.233 g, 1.26 mmol) dissolved in about 30 mL of ether produced a colorless reaction mixture that was stirred for 40 min. Solid $Cp''ZrCl_3$ (0.52 g, 1.28 mmol)

---

[15] Wolczanski, P. T.; Bercaw, J. E. *Organometallics* , **1982**, *1*, 793-799.
[16] Winter, C. H.; Zhou, X.-X.; Dobbs, D. A.; Heeg, M. J. *Organometallics* **1991**, *10*, 210-214.
[17] Lancaster, S. J.; Robinson, O. B.; Bochmann, M.; Coles, S. J.; Hursthouse, M. B. *Organometallics* **1995**, *14*, 2456-2462.

was added to this reaction mixture. The solution turned orange/red and eventually became a pale yellow followed by formation of a precipitate. The reaction was stirred overnight, and all volatiles were removed under vacuum. The product was extracted in 40 mL of hexane, which was filtered through a Celite pad, and the volatiles were removed to yield the product as a yellow solid (0.40 g, 58%). The product could then be further purified by recrystallization from diethyl ether at -25 °C.

^{1}H NMR (C_6D_6, 300 MHz): δ 0.38 (s, 18H, Si(CH_3)$_3$), 0.74 (d, 6H, CH(CH_3)$_2$), 1.27 (d, 12H, CH(CH_3)$_2$), 3.38 (sept, 1H, CHMe$_2$), 3.59 (overlapping br, 1H, NH, and sept, 2H, CHMe$_2$), 6.98 (d, 2H, Cp-*H*), 7.13 (t, 1H, Cp-*H*). ^{13}C NMR (C_6D_6, 300 MHz): δ 0.1 (Si(CH_3)$_3$), 23.4 (CH(CH_3)$_2$), 24.0 (CH(CH_3)$_2$), 45.8 (CHMe$_2$), 48.0 (CHMe$_2$), 125.4 (Cp-H), 130.4 (Cp-Si), 131.1 (Cp-H), 162.0 (CN3).

Preparation of Cp*[Me$_2$NC(N^{i}Pr)$_2$]ZrCl$_2$, (43)

In a 100 ml round bottom flask equipped with a magnetic stirrer was added (Me$_2$N)C(N^{i}Pr)$_2$Li·0.5THF[18] (0.400 g, 1.9 mmol) and about 25 ml of ether. To this clear solution was added solid Cp*ZrCl$_3$ (0.637g, 1.9 mmol). The formation of a precipitate and appearance of a yellow colour took place in a matter of minutes. The reaction was stirred overnight. The volatiles were removed under vacuum, 5 ml of hexane was added and removed by vacuum. Approximately 50 ml of hexane was added and the suspension filtered through Celite. The filtrate was collected and all volatiles were removed under vacuum giving a yellow solid product in a 78 % yield (0.702 g, 1.5 mmol). The product can be further purified by crystallization from ether.

^{1}H NMR (300 MHz, C_6D_6): δ 3.50 (*sept*, 2 H, CHMe2), 2.21 (s, 6 H, (CH_3)$_2$N), 2.08 (s, 15 H, Cp(CH_3)$_5$), 1.22 (d, 12 H, CH(CH_3)$_2$). ^{13}C NMR (300 MHz, C_6D_6): δ 171.7 (CN_3), 125.1 (Cp*), 48.5 (CHMe$_2$), 40.3 ((CH_3)$_2$N), 23.9 (CH(CH_3)$_2$), 13.0 (Cp(CH_3)$_5$). $C_{19}H_{35}Cl_2N_3Zr$ C, 48.80; H, 7.54; N, 8.99. Found: C 48.55, H 7.90, N8.89

Preparation of Cp*[PhCH$_2$(^{i}Pr)NC(N^{i}Pr)$_2$]ZrCl$_2$, (44)

In a 100 ml round bottom flask equipped with a magnetic stirrer was added benzylisopropylamine (0.227 g, 1.52 mmol) and about 25 ml of ether. MeLi (1.09 ml, 1.52

[18] Prepared by addition of LiNMe$_2$ to diisopropylcarbodiimide and crystallization out of THF at -25°C.

mmol) was added to the solution and stirred for 45 min. 1,3-Diisopropylcarbodiimide (0.191g, 1.52 mmol) was added and stirred for another 45 min. To the clear solution was added solid Cp^*ZrCl_3 (0.505g, 1.52 mmol). The solution turned pale yellow and formation of a precipitate was observed. The reaction was stirred overnight. The volatiles were removed under vacuum, and the sticky yellow solid was washed with 5 ml of hexanes. Then toluene was added and the suspension was filtered through Celite to yellow a clear yellow filtrate. The volatiles were removed under vacuum and a yellow solid product was obtained (0.650 g, 75% yield). The product can be further purified by crystallization from toluene.

^{1}H NMR (300 MHz, C_6D_6): δ 7.14 (br, 5 H, Ar*H*), 3.93 (s, 2 H, PhCH_2), 3.84 (*sept*, 2 H, C*H*(CH_3)$_2$), 3.32 (*sept*, 1 H, C*H*(CH_3)$_2$), 2.01 (s, 15 H, Cp(CH_3)$_5$), 1.33 (d, 12 H, CH(CH_3)$_2$), 0.86 (d, 6 H, CH(CH_3)$_2$). ^{13}C NMR (300 MHz, C_6D_6): δ 173.8 (*C*N_3), 140.9 (Ar*C*), 128.8 (Ar*C*H), 127.8 (Ar*C*H), 127.6 (Ar*C*H), 125.6 (Cp*), 51.1 (1C, *C*HMe_2) 49.9 (Ph*C*H_2), 48.5 (2C, *C*HMe_2), 25.0 (br, 4C, CH(*C*H_3)$_2$), 21.3 (2C, CH(*C*H_3)$_2$) 13.3 (Cp(*C*H_3)$_5$). $C_{27}H_{43}Cl_2N_3Zr$ Calcd. C, 56.72; H, 7.58; N, 7.35; Found C 56.67, H 7.98, N 7.25.

Preparation of $Cp^*[Me_2NC(N^iPr)_2]ZrMe_2$, (45)

In a 100 ml round bottom flask equipped with a magnetic stirrer was added **43** (0.200 g, 0.43 mmol) and about 15 ml of ether. To this clear solution was added MeLi (0.61 ml, 0.85 mmol). The formation of a white precipitate and disappearance of the yellow colour took place in a matter of minutes. The reaction was stirred overnight. The volatiles were removed under vacuum. Approximately 5-10 ml of hexanes was added and the suspension filtered through Celite. The filtrate was collected and all volatiles were removed under vacuum giving a white solid product in a 82 % yield (0.150 g, 0.35 mmol). The product can be further purified by crystallization from hexane.

^{1}H NMR (300 MHz, C_6D_6): δ 3.45 (*sept*, 2 H, C*H*Me2), 2.38 (s, 6 H, (CH_3)$_2$N), 2.03 (s, 15 H, Cp(CH_3)$_5$), 1.10 (d, 12 H, CH(CH_3)$_2$), 0.35 (s, 6H, Zr(CH_3)$_2$). ^{13}C NMR (300 MHz, C_6D_6): δ 174.4 (*C*N_3), 119.5 (Cp*), 47.7 (*C*HMe_2), 45.5 (Zr(*C*H_3)$_2$), 40.5 ((*C*H_3)$_2$N), 24.8 (CH(*C*H_3)$_2$), 12.2 (Cp(*C*H_3)$_5$).

Preparation of Cp*[PhCH$_2$(^{i}Pr)NC(N^{i}Pr)$_2$]ZrMe$_2$, (46)

In a 100 ml round bottom flask equipped with a magnetic stirrer was added **43** (0.400 g, 0.70 mmol) and about 60 ml of ether. To the suspension was added MeLi (1.0 ml, 1.4 mmol), the solution turned colourless and the formation of a precipitate was observed. The reaction was stirred overnight. The volatiles were removed under vacuum, and the white solid was extracted with about 20 ml of hexanes. The suspension was filtered through Celite and the filtrate collected. The volume was reduced to about 3-4 ml under vacuum and then cooled to –25°C. Colourless crystals of the product were obtain after 1 day, and isolated and dried to give the desired product (0.250 g, 67% yield).

^{1}H NMR (300 MHz, C_6D_6): δ 7.23-7.06 (m, 5 H, Ar*H*), 3.96 (s, 2 H, PhC*H*$_2$), 3.85 (*sept*, 2 H, C*H*(CH$_3$)$_2$), 3.41 (*sept*, 1 H, C*H*(CH$_3$)$_2$), 1.96 (s, 15 H, Cp(C*H*$_3$)$_5$), 1.13 (br, 12 H, CH(C*H*$_3$)$_2$), 0.98 (d, 6 H, CH(C*H*$_3$)$_2$), 0.39 (s, 6H, Zr(CH$_3$)$_2$). ^{13}C NMR (300 MHz, C_6D_6): δ 174.8 (*C*N$_3$), 141.5 (Ar*C*), 128.6 (Ar*C*H), 128.2 (Ar*C*H), 127.3 (Ar*C*H), 119.6 (Cp*), 51.2 (1C, *C*HMe$_2$) 50.2 (Ph*C*H$_2$), 47.8 (2C, *C*HMe$_2$), 47.5 (2C, Zr(*C*H$_3$)$_2$), 25.6 (br, 4C, CH(*C*H$_3$)$_2$), 21.5 (2C, CH(*C*H$_3$)$_2$) 12.3 (Cp(*C*H$_3$)$_5$).

Preparation of Cp*[PhCH$_2$(^{i}Pr)NC(N^{i}Pr)$_2$]Zr(CH$_2$Ph)$_2$, (47)

In a 100 ml round bottom flask equipped with a magnetic stirrer was added **43** (0.560 g, 0.98 mmol) and about 40 ml of ether. To the solution was added BnMgCl (1.0 M ether solution, 1.96 ml, 1.0 mmol), the solution slowly turned brown and the formation of a precipitate was observed. The reaction was stirred overnight. The volatiles were removed under vacuum, and the solid was extracted with about 20 ml of hexanes. The suspension was filtered through Celite and the filtrate collected. The volatiles were removed to yield the desired product (0.298 g, 45%). Further purification of the product can be achieved by re-crystallization from ether or hexane at –25°C. The product crystallizes with ether or hexane in the lattice, which cannot be removed under vacuum. Dissolution of the compound in toluene, followed by drying under vacuum affords the pure desired product.

^{1}H NMR (300 MHz, tol-d_8): δ 7.29 (d, 4 H, Ar*H*), 7.21-7.06 (overlapping t and m, 9 H, Ar*H*), 6.87 (t, 2 H, Ar*H*), 4.04 (s, 2 H, PhC*H*$_2$N), 3.86 (*sept*, 2 H, C*H*(CH$_3$)$_2$), 3.49 (*sept*, 1 H, C*H*(CH$_3$)$_2$), 2.53 (d (*J*=12.3 Hz), 2 H, Zr(C*H*$_2$Ph)$_2$), 2.03 (d (*J*=12.8 Hz), 2 H, Zr(C*H*$_2$Ph)$_2$) 1.86 (s, 15 H, Cp(C*H*$_3$)$_5$), 1.11 (d, 12 H, CH(C*H*$_3$)$_2$), 0.98 (d, 6 H, CH(C*H*$_3$)$_2$). ^{13}C NMR

(300 MHz, tol-d_8): δ 174.8 (CN_3), 151.1 (2C, Ar*C*), 141.4 (1C, Ar*C*), 128.6 (1C, Ar*C*H), 128.4 (2C, Ar*C*H),128.1 (1C, Ar*C*H), 127.9 (2C, Ar*C*H), 127.4 (1C, Ar*C*H), 121.8 (Cp*), 121.5 (2C, Ar*C*H), 78.0 (2C, Zr(CH_2Ph)$_2$), 51.8 (1C, *C*HMe$_2$) 50.7 (br, PhCH_2N), 48.1 (2C, *C*HMe$_2$), 25.5 (4C, CH(CH_3)$_2$), 21.6 (2C, CH(CH_3)$_2$) 12.4 (Cp(CH_3)$_5$).

Preparation of Cp*[(^{i}PrNH)C(N^{i}Pr)$_2$]ZrMe$_2$, (48)

A toluene solution of guanidine **5a** (0.034g, 0.18 mmol) was added to Cp*ZrMe$_3$ (0.050g, 0.18 mmol) dissolved in about 20 mL of toluene. The reaction was allowed to stir at room-temperature overnight. All volatiles were removed under vacuum to leave a white solid that was identified as pure **48** (0.071g, 87%)

^{1}H NMR (300 MHz, C_6D_6): δ 3.49-3.42 (overlapping *sept*, 3 H, C*H*Me2, and br, 1H, N*H*), 2.06 (s, 15 H, Cp(CH_3)$_5$), 1.16 (d, 12 H, CH(CH_3)$_2$), 0.87 (d, 6H, CH(CH_3)$_2$), 0.34 (s, 6H, Zr(CH_3)$_2$). ^{13}C NMR (300 MHz, C_6D_6): δ 166.4 (CN_3), 119.3 (Cp*), 47.1 (2C, *C*HMe$_2$), 46.2 (1C, *C*HMe2), 44.7 (Zr(CH_3)$_2$), 24.4 (2C, CH(CH_3)$_2$), 23.6 (1C, CH(CH_3)$_2$), 12.1 (Cp(CH_3)$_5$).

Preparation of Cp''(^{i}PrN)$_2$C(NH^{i}Pr)ZrMe$_2$, (49).

A toluene solution of guanidine **5a** (0.185g, 1 mmol) was added to Cp''ZrMe$_3$ (0.345g, 1 mmol) dissolved in about 20 mL of toluene. The reaction was allowed to stir at room-temperature overnight. All volatiles were removed under vacuum to leave a white solid that was identified as pure **49** (0.510g, 99%).

^{1}H NMR (C_6D_6, 400 MHz): δ 0.31 (s, 18H, Si(CH_3)$_3$), 0.44 (s, 6H, ZrCH_3) 0.88 (d, 6 H, CH(CH_3)$_2$), 1.18 (d, 12 H, CH(CH_3)$_2$), 3.48 (overlapping br, 1H, N*H*, and sept, 2H, C*H*Me$_2$), 3.58 (sept, 1H, C*H*Me$_2$), 6.72 (d, 2H, Cp*H*), 6.99 (t, 1H, Cp*H*). ^{13}C NMR (C_6D_6, 400 MHz): δ 0.36 (Si(CH_3)$_3$), 24.1 (CH(CH_3)$_2$), 24.5 (CH(CH_3)$_2$), 40.7 (Zr-CH_3), 46.1 (*C*HMe$_2$), 47.1 (*C*HMe$_2$), 121.2 (CH_{Cp}), 124.9 (CSi_{Cp}), 127.6 (CH_{Cp}), 167.3 (CN_3).

Preparation of Cp''[(*c*-C$_5$H$_9$)$_7$Si$_8$O$_{12}$C$_6$H$_4$CH$_2$(^{i}Pr)NC(N^{i}Pr)$_2$]ZrMe$_2$, (50)

In a round bottom flask was dissolved the silsesquioxane tethered guanidine **6d** (0.681g, 0.58 mmol) in toluene. To this solution was added Cp''ZrMe$_3$ (0.200g, 0.58 mmol) pre-dissolved in toluene. The reaction was stirred overnight. All volatiles were removed under vacuum, hexane was added and removed under vacuum and the obtained product was freeze-dried.

The product was obtained as a white powder in a near-quantitative (within exp. error) yield. (0.83g, 95%).

^{1}H NMR (C_6D_6): δ 7.97 (d, 2H, CH_{Bn}), 7.35 (d, 2H, CH_{Bn}), 7.21 (t, 1H, C$H_{Cp''}$), 6.77 (d, 2H, C$H_{Cp''}$), 3.98 (s, 2H, CH_2-Bn), 3.93 (sept, 2H, CHMe$_2$), 3.36 (sept, 1H, CHMe$_2$), 1.40-1.96 (m, 56H, CH_2-cC$_5$H$_9$), 1.26 (br, 12H, CH_3-^{i}Pr), 1.21 (m, 7H, CH-cC$_5$H$_9$), 0.95 (d, 6H, CH_3-^{i}Pr), 0.46 (s, 6H, ZrCH_3), 0.29 (s, 18H, SiCH_3). ^{13}C NMR (C_6D_6): δ 177.3 (CN$_3$), 144.2 (C), 134.7 (CH$_{Bn}$), 132.4 (1C, CH$_{Cp''}$), 131.0 (C), 128.0 (CH$_{Bn}$), 123.6 (C), 119.8 (2C, CH$_{Cp''}$), 52.2 (1C, CHMe$_2$), 50.5 (CH$_2$-Bn), 48.1 (1C, CHMe$_2$), 38.5 (ZrCH$_3$), 27.84, 27.46, 27.35 (CH$_2$-cC$_5$H$_9$), 25.1 (br, CH$_3$-^{i}Pr), 22.75, 22.72 (CH-cC$_5$H$_9$), 21.7 (s, CH_3-^{i}Pr), 0.2 (ZrCH$_3$). ^{29}Si NMR (C_6D_6, 500, d1=8 sec): δ -8.8 (Cp(SiMe$_3$)$_2$) -65.5, -65.9, -78.7 ((≡O)$_3$$SiC_5H_9$, 3:4:1).

Crystal Structure Determination of Compounds 42, 44, 46, 47·hexane and 48.

Suitable crystals were selected, mounted on thin glass fibres using viscous oil and cooled to the data collection temperature. Data were collected on a Bruker AX SMART 1k CCD diffractometer using 0.3° ω-scans at 0, 90, and 180° in ϕ. Unit-cell parameters were determined from 60 data frames collected at different sections of the Ewald sphere. Semi-empirical absorption corrections based on equivalent reflections were applied (Blessing, R., *Acta Cryst.*, **1995,** A51, 33-38).

No symmetry higher than triclinic was evident from the diffraction data **47·hexane**. Systematic absences in the diffraction data and unit-cell parameters were uniquely consistent for the reported space groups for **43**, and **44**. The structures were solved by direct methods, completed with difference Fourier syntheses and refined with full-matrix least-squares procedures based on F^2. A hexane solvent molecule was located co-crystallized in the asymmetric unit of **47·hexane**. All non-hydrogen atoms were refined with anisotropic displacement parameters. All hydrogen atoms were treated as idealized contributions. All scattering factors are contained in the SHEXTL 5.10 program library (Sheldrick, G. M., Bruker AXS, Madison, WI, 1997).

Figure 8.1. Molecular structure and atom numbering scheme for the half-sandwich zirconium guanidinate dichloride, compound **44**. Hydrogen atoms have been omitted for clarity. Thermal ellipsoids are drawn at 30% probability.

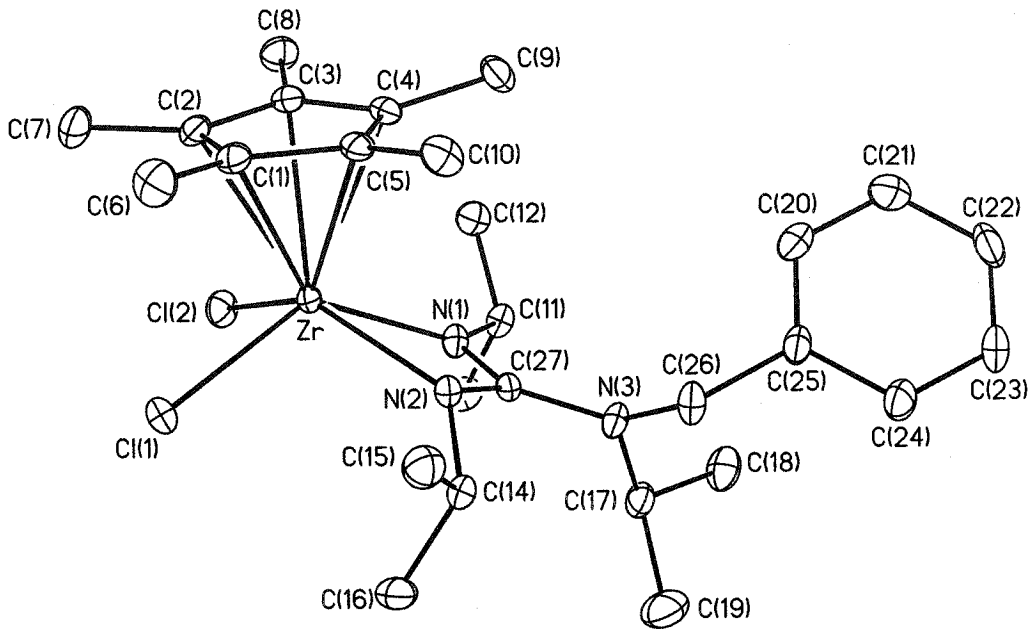

Figure 8.2. Molecular structure and atom numbering scheme for the half-sandwich zirconium guanidinate dichloride, compound **42**. Hydrogen atoms have been omitted for clarity. Thermal ellipsoids are drawn at 30% probability.

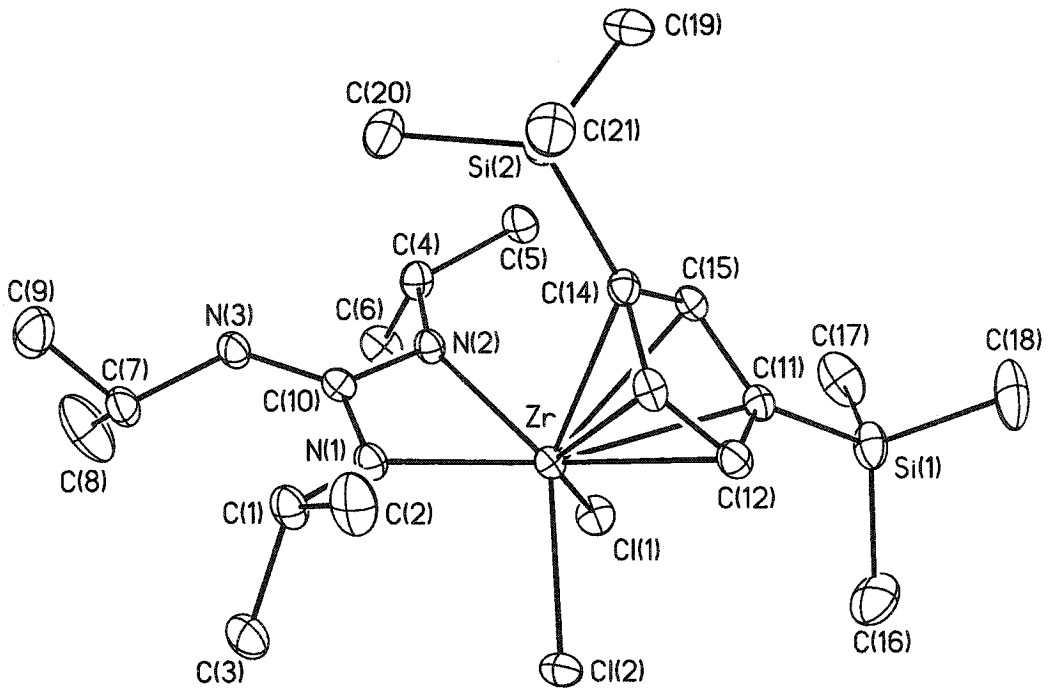

Figure 8.3. Molecular structure and atom numbering scheme for the half-sandwich zirconium guanidinate dimethyl, compound **46**. Hydrogen atoms have been omitted for clarity. Thermal ellipsoids are drawn at 30% probability.

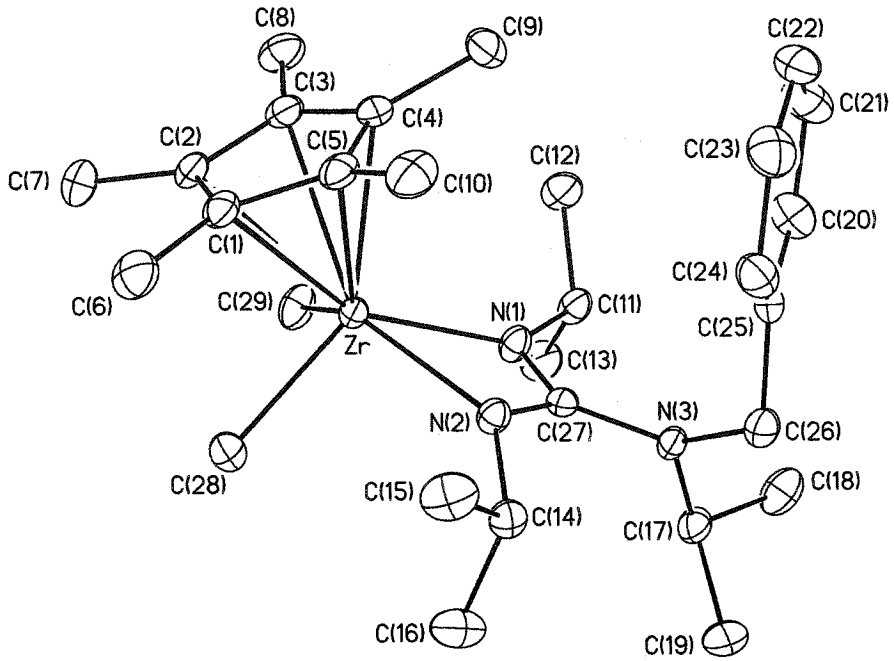

Figure 8.4. Molecular structure showing one of the two symmetry unique molecules of half-sandwich zirconium guanidinate dibenzyl, compound **47·hex**. Hydrogen atoms and hexane have been omitted for clarity. Thermal ellipsoids are drawn at 30% probability.

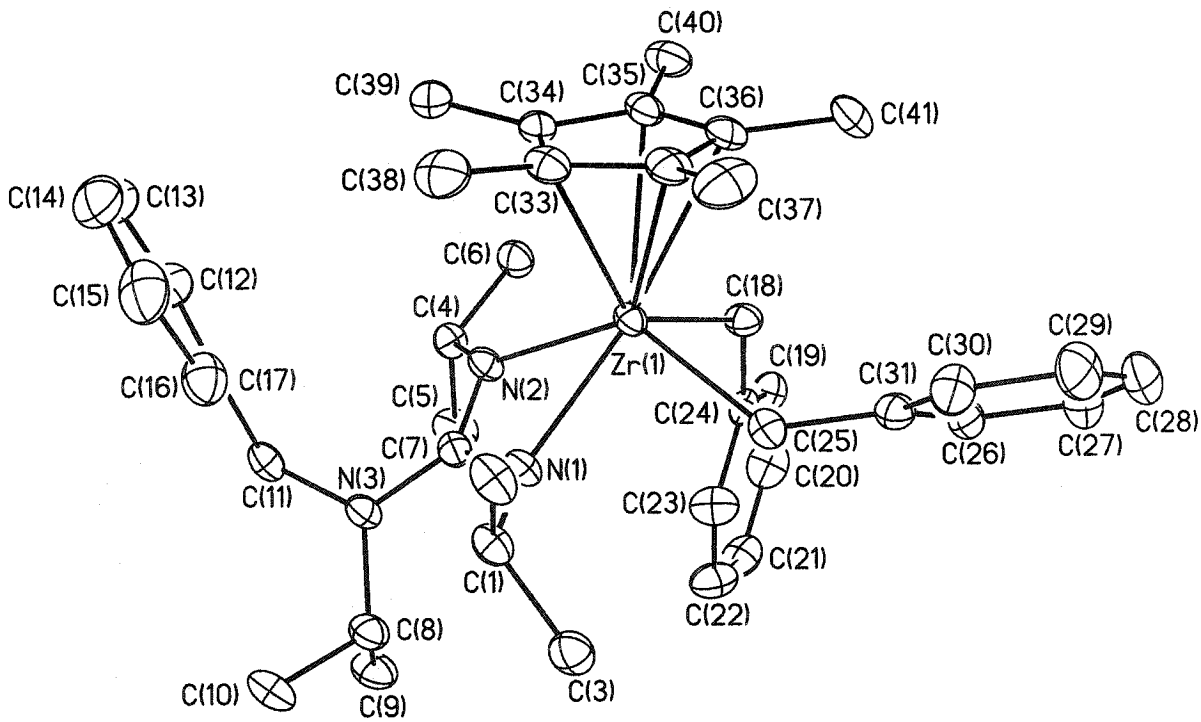

Figure 8.5. Molecular structure and atom numbering scheme for the half-sandwich zirconium guanidinate dimethyl, compound **48**. Hydrogen atoms have been omitted for clarity. Thermal ellipsoids are drawn at 30% probability.

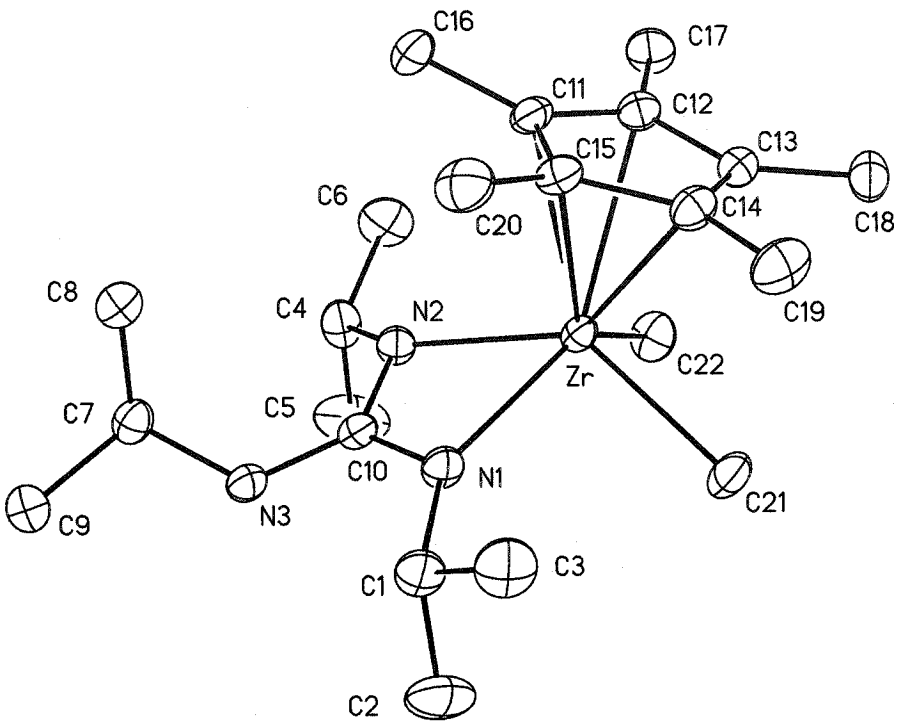

Table 8.2. Selected Crystal Data and Data Collection Parameters for **44, 42, 46, 47** and **48.**

	44	**42**	**46**	**47·(hex)**
empirical formula	$C_{27}H_{43}Cl_2N_3Zr$	$C_{21}H_{43}Cl_2N_3Si_2Zr$	$C_{29}H_{49}N_3Zr$	$C_{47}H_{71}N_3Zr$
formula weight	571.76	555.88	530.93	769.29
T (K)	203(2)	203(2)	203(2)	203(2)
wavelength (Å)	0.71073	0.71073	0.71073	0.71073
crystal system	Monoclinic	Orthorhombic	Monoclinic	Triclinic
space group	$P2_1/c$	Pbca	$P2_1/n$	P-1
a (Å)	9.6952(16)	a = 14.7062(14)	14.470(3)	10.493(3)
b (Å)	15.319(3)	b = 19.0303(19)	11.774(2)	14.760(4)
c (Å)	19.299(3)	c = 20.916(2)	17.590(3)	26.895(7)
α (deg)	90	90	90	89.329(4)
β (deg)	97.216(2)	90	100.727(2)	81.033(3)
γ (deg)	90	90	90	88.792(4)
V (Å^3)	2843.5(8)	5853.6(10)	2944.3(10)	4113.3(17)
Z	4	8	4	4
abs coeff (mm^{-1})	0.594	0.652	0.393	0.303
final R indices	R1 = 0.0540	R1 = 0.0507	R1 = 0.0369	R1 = 0.0548
	wR2 = 0.1454	wR2 = 0.1394	wR2 = 0.0855	wR2 = 0.1278

Table 8.2. Selected Crystal Data and Data Collection Parameters for **44, 42, 46, 47** and **48.**

	48
empirical formula	$C_{22}H_{43}N_3Zr$
formula weight	440.81
T (K)	203(2)
wavelength (Å)	0.71073
crystal system	Orthorhombic
space group	Pna2(1)
a (Å)	a = 17.1184(18)
b (Å)	b = 10.0724(11)
c (Å)	c = 14.5065(15)
α (deg)	90
β (deg)	90
γ (deg)	90
V (Å^3)	2501.3(5)
Z	4
abs coeff (mm^{-1})	0.449
final R indices	R1 = 0.0716
	wR2 = 0.1756

Table 8.3. Selected Bond Distances and Angles for **44.**

	Bond Distances (Å)		
Zr-N(1)	2.243(4)	Zr-Cl(1)	2.4482(12)
Zr-N(2)	2.239(4)	Zr-Cl(2)	2.4685(12)
N(1)-C(27)	1.360(6)	Zr-C(1)	2.577(4)
N(1)-C(11)	1.485(6)	Zr-C(2)	2.518(4)
N(2)-C(27)	1.345(6)	Zr-C(3)	2.538(4)
N(2)-C(14)	1.491(6)	Zr-C(4)	2.540(4)
N(3)-C(27)	1.404(5)	Zr-C(5)	2.556(4)
N(3)-C(26)	1.482(6)		
N(3)-C(17)	1.493(6)		
	Bond Angles (deg)		
N(2)-Zr-N(1)	59.87(14)	N(1)-Zr-C(4)	90.50(14)
N(1)-Zr-Cl(2)	86.24(10)	N(2)-Zr-C(5)	82.50(13)
N(2)-Zr-Cl(1)	93.00(10)	C(14)-N(2)-Zr	136.3(3)
Cl(1)-Zr-Cl(2)	90.52(4)	C(27)-N(2)-Zr	94.5(3)
C(11)-N(1)-Zr	141.1(3)	C(27)-N(2)-C(14)	118.2(4)
C(27)-N(1)-Zr	93.9(3)	Sum of angles at N(2)	349.0
C(27)-N(1)-C(11)	124.1(3)	C(27)-N(3)-C(17)	119.3(4)
Sum of angles at N(1)	359.1	C(27)-N(3)-C(26)	118.0(4)
C(26)-N(3)-C(27)-N(2)	-35.4(6)	C(26)-N(3)-C(17)	119.1(4)
C(17)-N(3)-C(27)-N(1)	-61.7(6)	Sum of angles at N(3)	356.4

Table 8.4. Selected Bond Distances and Angles for **42.**

	Bond Distances (Å)		
Zr-N(1)	2.194(3)	Zr-Cl(1)	2.4348(12)
Zr-N(2)	2.214(4)	Zr-Cl(2)	2.4910(12)
N(1)-C(10)	1.355(6)	Zr-C(11)	2.567(4)
N(1)-C(1)	1.486(5)	Zr-C(12)	2.550(4)
N(2)-C(10)	1.347(5)	Zr-C(13)	2.533(4)
N(2)-C(4)	1.485(5)	Zr-C(14)	2.560(4)
N(3)-C(10)	1.358(6)	Zr-C(15)	2.530(4)
N(3)-C(7)	1.473(6)		
	Bond Angles (deg)		
N(1)-Zr-N(2)	60.44(13)	N(1)-Zr-C(14)	96.85(13)
N(1)-Zr-Cl(2)	87.16(10)	N(2)-Zr-C(14)	85.76(14)
N(2)-Zr-Cl(1)	88.14(10)	C(4)-N(2)-Zr	141.9(3)
Cl(1)-Zr-Cl(2)	90.44(4)	C(10)-N(2)-Zr	94.0(3)
C(1)-N(1)-Zr	141.2(3)	C(10)-N(2)-C(4)	121.4(4)
C(10)-N(1)-Zr	94.6(3)	Sum of angles at N(2)	356.3
C(10)-N(1)-C(1)	123.7(4)	C(10)-N(3)-C(7)	130.8(4)
Sum of angles at N(1)	359.5		

Table 8.5. Selected Bond Distances and Angles for **46**.

	Bond Distances (Å)		
Zr-N(1)	2.271(2)	Zr-C(28)	2.266(3)
Zr-N(2)	2.309(2)	Zr-C(29)	2.291(3)
N(1)-C(27)	1.343(3)	Zr-C(1)	2.589(2)
N(1)-C(11)	1.477(3)	Zr-C(2)	2.597(2)
N(2)-C(27)	1.343(3)	Zr-C(3)	2.571(2)
N(2)-C(14)	1.484(3)	Zr-C(4)	2.531(2)
N(3)-C(27)	1.416(3)	Zr-C(5)	2.552(2)
N(3)-C(26)	1.465(3)		
N(3)-C(17)	1.494(3)		
	Bond Angles (deg)		
N(1)-Zr-N(2)	58.23(7)	N(1)-Zr-C(4)	102.32(8)
N(1)-Zr-C(29)	84.51(9)	N(2)-Zr-C(5)	89.79(8)
C(28)-Zr-N(2)	91.77(9)	C(14)-N(2)-Zr	138.82(16)
C(28)-Zr-C(29)	85.52(12)	C(27)-N(2)-Zr	93.95(14)
C(11)-N(1)-Zr	140.50(15)	C(27)-N(2)-C(14)	120.6(2)
C(27)-N(1)-Zr	95.65(14)	Sum of angles at N(2)	353.37
C(27)-N(1)-C(11)	122.2(2)	C(27)-N(3)-C(17)	120.21(19)
Sum of angles at N(1)	358.35	C(27)-N(3)-C(26)	121.2(2)
		C(26)-N(3)-C(17)	116.4(2)
		Sum of angles at N(3)	357.81

Table 8.6. Selected Bond Distances and Angles for **47·(hex)**.

	Bond Distances (Å)		
Zr(1)-N(1)	2.284(3)	Zr(1)-C(18)	2.306(4)
Zr(1)-N(2)	2.283(3)	Zr(1)-C(25)	2.369(4)
N(1)-C(7)	1.364(4)	Zr(1)-C(32)	2.570(3)
N(1)-C(1)	1.486(4)	Zr(1)-C(33)	2.549(3)
N(2)-C(7)	1.349(4)	Zr(1)-C(34)	2.604(3)
N(2)-C(4)	1.498(4)	Zr(1)-C(35)	2.634(3)
N(3)-C(7)	1.404(4)	Zr(1)-C(36)	2.600(3)
N(3)-C(8)	1.499(4)		
N(3)-C(11)	1.475(5)		
	Bond Angles (deg)		
N(2)-Zr(1)-N(1)	58.67(10)	N(1)-Zr(1)-C(33)	101.39(11)
N(1)-Zr(1)-C(25)	80.49(11)	N(2)-Zr(1)-C(34)	85.28(11)
N(2)-Zr(1)-C(18)	95.11(12)	C(4)-N(2)-Zr(1)	137.1(2)
C(18)-Zr(1)-C(25)	87.07(13)	C(7)-N(2)-Zr(1)	95.4(2)
C(1)-N(1)-Zr(1)	138.7(2)	C(7)-N(2)-C(4)	125.4(3)
C(7)-N(1)-Zr(1)	94.87(19)	Sum of angles at N(2)	347.9
C(7)-N(1)-C(1)	122.7(3)	C(7)-N(3)-C(8)	121.3(3)
Sum of angles at N(1)	356.27	C(7)-N(3)-C(11)	120.5(3)
		C(11)-N(3)-C(8)	117.4(3)
		Sum of angles at N(3)	359.2

Table 8.7. Selected Bond Distances and Angles for **48**.

	Bond Distances (Å)		
Zr-N(1)	2.246(3)	Zr-C(21)	2.305(5)
Zr-N(2)	2.281(3)	Zr-C(22)	2.282(5)
N(1)-C(10)	1.358(6)	Zr-C(11)	2.543(4)
N(1)-C(1)	1.478(6)	Zr-C(12)	2.577(4)
N(2)-C(10)	1.339(5)	Zr-C(13)	2.576(4)
N(2)-C(4)	1.476(6)	Zr-C(14)	2.570(4)
N(3)-C(10)	1.378(5)	Zr-C(15)	2.539(4)
N(3)-C(7)	1.473(6)		
	Bond Angles (deg)		
N(1)-Zr-N(2)	59.27(12)	N(1)-Zr-C(15)	94.49(14)
N(1)-Zr-C(21)	86.65(16)	N(2)-Zr-C(11)	88.49(13)
N(2)-Zr-C(22)	90.89(17)	C(4)-N(2)-Zr	141.0(3)
C(22)-Zr-C(21)	86.5(2)	C(10)-N(2)-Zr	93.7(2)
C(1)-N(1)-Zr	143.7(3)	C(10)-N(2)-C(4)	121.0(3)
C(10)-N(1)-Zr	94.7(2)	Sum of angles at N(2)	355.7
C(10)-N(1)-C(1)	121.6(4)	C(10)-N(3)-C(7)	126.6(4)
Sum of angles at N(1)	360.0	C(7)-N(3)-C(10)-N(2)	-43.4(7)

9 Denouement

The heart and soul of this work deals with the use of dialkyl-1,8-diamidonaphthalene as a ligand for transition and main group elements. To believe that the contents of this work could possibly allow one to make broad conclusions on the use of this class of ligand would be naive. Having spent countless hours contemplating the possible applications of this ligand class has left us with the sense that we have explored but the tip of the iceberg. One can only guess which will be the most significant contributions of diamidonaphthalenes.

Despite the sincere belief that we have only scratched the surface, this ligand has already shown remarkable versatility. Strong bonding interactions are readily formed with a Ta(V) metal centre. Additionally, the geometry of the six-membered metallaheterocycle, which forces the N-substituents close to the metal, produces such steric strain that C-H activation and metallaaziridine formation is always observed. Although the transformation changes the nature of the metal-ligand interaction, the robust nature of the trianionic binding motif demonstrates the capacity of the ligand for making stable metal complexes. Modifying the size and shape of the substituents should provide a means for avoiding further ligand transformations while maximizing the steric impact of the ligand. The work provides

inspiration that 1,8-DAN based ligands could be used to prepare a multitude of early transition metal complexes.

The key structural and electronic features enabling 1,8-DAN based ligands to form strong bonds with early transition metals also renders them ideal for the stabilization of coordinatively unsaturated main group elements. The stabilization of divalent carbon allowed for the preparation of a novel class of stable singlet carbenes. The electron deficient carbon centre is undoubtedly stabilized, at least in part, through π-donation from the N lone-pairs. Formation of a planar six-membered heterocycle comprised exclusively of sp^2-hybridized atoms also permits for some aromatic stabilization. Heavier analogues (Ge, and Sn) of the carbenes were also prepared through the use of 1,8-diamidonaphthalene ligands.

The unique structural and electronic properties of the perimidine based carbenes, and the heavier analogues, makes them interesting ligands in their own right. Preliminary investigations revealed that these species can function as Lewis bases and be used as neutral ligands with late transition metals. The geometric alignment of the N-substituents enforced by the ligand structure positions them very close to the metal centres. This is revealed spectroscopically by the observation of strongly deshielded proton resonances and hindered metal-carbene rotation, and structurally by observing twisting of the germylene ligand upon ligation to a Ni(0) centre.

The stabilizing influences offered by the 1,8-DAN based ligands also allowed for the isolation of a monomeric, tricoordinate diamidoborane. Attempts to extend this chemistry to the heavier group 13 elements did not yield analogous species, but instead yielded the Lewis base adduct of a diamidoalane, and bimetallic aluminum and zinc species. The side-on bridging mode observed for the ligand with both aluminum and zinc reveals a potential additional way in which 1,8-DAN ligands can contribute to the preparation of interesting and novel metal complexes.

Thus far we have mostly used 1,8-DAN based ligands to prepare unusual species. The overall effect this class of ligands has on the reactivity of a metal centre has only been briefly glimpsed. The potential for flexibility in the electron donation to a metal centre will certainly be an important characteristic of these ligands. This flexibility in electron donation is what attracted our attention to guanidinate ligands. We prepared numerous

mono(cyclopentadienyl)guanidinato zirconium species, and through structural studies, confirmed that guanidinates vary their electronic configurations to meet the electrophilic demands of the metal centre. This key electronic property of guanidinate ligands drastically alters the reactivity of half-sandwich zirconium complexes towards polymerization of α-olefins compared to related amidinate analogues.

Chemistry has evolved over the last century to reach a level of sophistication which at times can be intimidating. The broad areas of research are continuously being divided into more specific subgroups and new challenges tend to deal with achieving specificity, selectivity and efficiency. The perpetual search for optimal performance of metal-based catalysts guarantees a key role for ligand design. Amido ligands already form a very large class of ligand and have proven to be extremely versatile. Diamidonaphthalene and guanidinate ligands have only recently been considered as ligand candidates and have shown flashes of tremendous potential. Only the passage of time will reveal the roles these ligands will play in future chemical enterprises.